CHEMOSELECTIVE SYNTHESIS OF FUNCTIONAL PEPTIDE- AND PROTEIN-CONJUGATES FOR INTRACELLULAR APPLICATIONS

Dissertation zur Erlangung des akademischen Grades des

Doktors der Naturwissenschaften (Dr. rer. nat.)

eingereicht im Fachbereich Biologie, Chemie, Pharmazie

der Freien Universität Berlin

vorgelegt von

NICOLE NISCHAN

geboren in Forst/Lausitz

2015

Diese Arbeit wurde im Zeitraum vom 1.11.2010 bis zum 31.12.2014 unter der Leitung von Prof. Dr. Christian P. R. Hackenberger am Institut für Chemie und Biochemie sowie am FMP Berlin Buch angefertigt.

1. Gutachter: Prof. Dr. Christian P. R. Hackenberger

2. Gutachter: Prof. Dr. Volker Haucke

Disputation am 27.4.2015

Declaration

Herewith I declare that I have prepared this dissertation myself and without the help of any impermissible resources. All citations are marked as such. The present thesis has neither been accepted in any previous doctorate degree procedure nor has it been evaluated as insufficient.

Berlin, January 29th 2015

Nicole Nischan

The work of this dissertation so far resulted in the following publications, talks and posters:

Publications

1) Nicole Nischan*, Alokta Chakrabarti*, Remigiusz A. Serwa, Petra H. Bovee-Geurts, Roland Brock, Christian R. Hackenberger.
*shared contribution
Angew. Chem. Int. Ed. **2013,** *52*, 11920-11924.
Stabilization of Peptides for Intracellular Applications by Phosphoramidate-Linked Polyethylene Glycol Chains.

Also published as:

Angew. Chem. **2013**, *125,* 12138-12142.
Stabilisierung von Peptiden für intrazelluläre Anwendungen mit Phosphoramidat-verzweigten Polyethylenglycol-Ketten.

2) Nicole Nischan, Christian P. R. Hackenberger.
J. Org. Chem. **2014,** *79*, 10727-10733.
Site-specific PEGylation of Proteins: Recent Developments.

3) Nicole Nischan*, Henry D. Herce*, Francesco Natale, Nina Bohlke, Nediljko Budisa, M. Cristina Cardoso, Christian P. R. Hackenberger.
**shared contribution*
Angew. Chem. Int. Ed. **2014,** to be anounced. DOI: 10.1002/anie.201410006
Covalent Attachment of Cyclic TAT Peptides to GFP Results in Protein Delivery into Live Cells with Immediate Bioavailability.

Also published as:

Angew. Chem. **2014,** to be anounced. DOI: 10.1002/ange.201410006
Kovalente Verknüpfung cyclischer TAT-Peptide mit GFP resultiert in der direkten Aufnahme in lebende Zellen mit sofortiger biologischer Verfügbarkeit.

Talks

1) Nicole Nischan, Wiebke Stahlschmidt, Volker Haucke, Alokta Chakrabarti, Roland Brock, Christian P. R. Hackenberger. 2. Berliner Chemie Symposium, Berlin 3. April **2012**.
   Chemoselective Reactions of Azido-Polypeptides by the Staudinger-Phosphite Reaction.
2) Nicole Nischan, Christian P. R. Hackenberger. FMP Winterschool 2014, Berlin 15th to 17th January **2014**.
   Functionalization of Polypeptides and Proteins for Biologic Applications Using Chemoselective Reactions.
3) Nicole Nischan, Christian P. R. Hackenberger. Falling Walls Lab 2014, Berlin 8th to 9th November **2014**.
   Breaking the Wall of Protein Drug Delivery.

Posters

1) Thresen Mathew*, Nicole Nischan*, Verena Börsch, Wiebke Stahlschmidt, Volker Haucke, Christian P. R. Hackenberger. 10th German Peptide Symposium, Berlin 7.-10. March **2011**.
   Chemoselective Glycosylation and Lipidation of Polypeptides by the Staudinger-Phosphite Reaction.
   *shared contribution
2) Nicole Nischan, Wiebke Stahlschmidt, Volker Haucke, Christian P. R. Hackenberger. 1st Berliner Chemie Symposium, Berlin 7. April **2011**
   Chemoselective Lipidation of Polypeptides by the Staudinger-Phosphite Reaction
3) Nicole Nischan, Wiebke Stahlschmidt, Volker Haucke, Christian P. R. Hackenberger. 2nd external Doctoral Student's workshop (SFB 765), Rheinsberg 21.-23. September **2011**.
   Chemoselective Synthesis of Alkylated Peptides by the Staudinger-Phosphite Reaction: Targeted Inhibition of Clathrin-Mediated Endocytosis.
4) Nicole Nischan, Wiebke Stahlschmidt, Volker Haucke, Christian P. R. Hackenberger. The Münster Symposium on Cooperative Effects in Chemistry 2012, Münster 4. Mai **2012**.
   Chemoselective Lipidation of Azido-Polypeptides by the Staudinger-Phosphite-Reaction: Inhibition of Clathrin-Mediated Endocytosis.
5) Nicole Nischan, Remigiusz A. Serwa, Wiebke Stahlschmidt, Alokta Chakrabarti, Roland Brock, Volker Haucke, Christian P. R. Hackenberger. EMBL Chemical Biology 2012, Heidelberg 26.-29. September **2012**.

The Staudinger Phosphite Reaction – A Versatile Tool for the Chemoselective PEGylation and Lipidation of Bioactive Peptides.

6) Nicole Nischan*, Wiebke Stahlschmidt*, Volker Haucke, Christian P. R. Hackenberger. 2. International Symposium of the collaborative Research Center (SFB) 765 "Multivalency in chemistry and Biochemistry, Berlin 18.-19. October **2012**.
Inhibition of Clathrin Mediated Endocytosis by Lipidated Multivalent EPS15-Peptides.
*shared contribution

7) Nicole Nischan, Wiebke Stahlschmidt, Volker Haucke, Christian P. R. Hackenberger. 1st combined external doctoral students workshop Graduate Schools SFB 765 and 858, Rheinsberg 6.-8. March **2013**.
Inhibition of Clathrin Mediated Endocytosis by Multialent EPS15-Peptides Modified by Staudinger-Phosphite-Lipidation.

8) Nicole Nischan, Alokta Chakrabarti, Remigiusz A. Serwa, Petra H. Bovee-Geurts, Roland Brock, Christian P. R. Hackenberger. Sciensation 2013 – the 15th joint PhD Retreat of the MDC and FMP, Kremmen 29.-31. August **2013**
Stabilization of Peptides for Intracellular Applications by branched Phosphoramidate-Linked PEG chains.

9) Nicole Nischan, Alokta Chakrabarti, Remigiusz A. Serwa, Petra H. Bovee-Geurts, Roland Brock, Christian P. R. Hackenberger. 247th ACS National Meeting, Dallas, TX, US 16.-20. März **2014**.
Stabilization of Peptides for Intracellular Applications by branched Phosphoramidate-Linked PEG chains.
*Poster selected for special session (SciMix)

10) Nicole Nischan, Wiebke Stahlschmidt, Volker Haucke, Christian P. R. Hackenberger. 247th ACS National Meeting, Dallas, TX, US 16.-20. März **2014**.
Inhibition of Clathrin Mediated Endocytosis by Multivalent EPS15-Peptides Lipidated via Staudinger-Phosphite-Reaction.

11) Nicole Nischan*, Henry D. Herce*, Dominik Schumacker*, Francesco Natale, Heinrich Leonardt, M. Cristina Cardoso, Christian P. R. Hackenberger. Bioorthogonal Chemistry - Meeting of the Division of Biochemistry, Berlin 16.-18. Juli **2014**.
Enhancing Cellular Uptake of Functional Proteins by Chemoselective Conjugation to Cell Penetrating Peptides.
*Poster prize award

Acknowledgments

First and foremost I want to thank my supervisor Prof. Dr. Christian P. R. Hackenberger for giving me the chance to work on my dissertation in his group and trusting me with the responsible of so many fascinating interdisciplinary projects. I want to thank him for being my mentor, for his never-ending trust, patience, advice and support and most importantly for encouraging me to explore new venues.
I also want to thank my second supervisor Prof. Dr. Volker Haucke for his scientific advice, encouragement and support during my thesis and in planning my career.
I am grateful to all of my collaboration partners from a variety of scientific fields for letting me discover new perspectives which not only promoted the success of the projects but also made me appreciate interdisciplinary work immensely. In this context I want to thank: Prof. Dr. Roland Brock and MSc. Alokta Chakrabarti, especially for having me as an intern and introducing me to image analysis; Prof. Dr. Volker Haucke and Dr. Wiebke Stahlschmidt for teaching me the basics of cell culture and fluorescence microscopy; Prof. Dr. Cristina M. Cardoso, Dr. Henry D. Herce and Dr. Francesco Natale for explaining me the unexplainable transduction mechanism; Prof. Dr. Heinrich Leonardt for his advice; Prof. Dr. Nediljko Budisa and MSc Nina Bohlke for solving for me the genetic code; Dr. Marina Rubini for sharing her knowledge about erythropoietin with me; Prof. Dr. Rainer Haag, Dr. Rahul Tyagi and Dr. Indah Nahiri for the interesting discussions.
I want to thank the former and present members of the AG Hackenberger for the good working atmosphere, for sharing ideas and constructive discussions: Dr. Remigiusz A. Serw, Dr. Verena Börsch, Dr. Thresen Matthew, Dr. Malgorzata Broncel, Dr. Xiaoman Liu, Dr. Ina Wilkening, Dr. Divya Agrawal, Dr. Michaela Mühlberg, Dr. Robert Valleé, Dr. Paul Maikut, M. Sc. Simon Reiske, Dipl.-Ing. (FH) Lukas Artner, M. Sc. Jordi Bertran-Vicente, M. Sc. Oliver Reimann, M. Sc. Andrew Grimes, Dr. Vera Martos, Dr. Stefan Reinke, Dr. Olaia Nieto-Garcia, Dr. Marcie Jaffee, M. Sc. Kristina Sieberz, M. Sc. Maria Glanz, M. Sc. Tom Sauer, M. Sc. Simon Klenk, M. Sc. Dominik Schumacher.
My thanks also for the excellent administrative support to Katta Wittig, Katharina Tebel and Marianne Dreissigacker; for technical support, thanks to Dagmar Krause.
Also I want to thank all of my students for teaching me, especially my interns Sam Fernandez and Rita Nassim.
It takes a village to raise a child, and a good department to do good science, I want to thank both members of the organic chemistry department at Freie Universität and the chemical biology department at FMP. Especially, I want to mention: Achim Wiedekind, the AG Koksch, Dr. Andreas Schäfer & his team, Dr. Andreas Springer & his team, Dr. Thomas Lehmann, the team of Chemikalienausgabe, Dr. Peter Schmieder, Heike Nikolenko, Karl Südow, Dr. Sabine Abel, Heike Stephanowitz.

I want to thank the graduate schools of the FMP and of SFB765 as well as the women foundation for funding of conference presentations and seminars.
Last but not least, I have to thank the people that supported me in every possible way outside of the lab. My family: Kathrin Michel, Christian Michel, Dominique Nischan, Marie Thérésè Nischan, “Opa” Alfred Bischof und “Oma” Ilse Nischan. My friends: Dipl.-Chem. Gregor Koch, Dipl-Chem. Johanna Fröhlich, Michaela Lebsa. And of course, Kfir Lapid.

Abbreviations

AcOH	acetic acid
Alloc	allyloxycarbonyl-
AU	absorbance units
CuAAC	Copper(I)-catalyzed azide-alkyne cycloaddition
DAPI	4',6-diamidin-2-phenylindol
2,5-DHAP	2,5-dihydroxyacetone phosphate
DIC	diisopropylcarbodiimide
DIPEA	*N*,*N*-diisopropylethylamine
DMEM	Dulbecco's modified eagle medium
DMF	dimethylformamide
DTT	dithiothreitol
EDTA	ethylenediaminetetraacetic acid
EPO	erythropoietin
ESI-MS	electrospray ionization mass spectrometry
EtOAc	ethyl acetate
Fmoc	fluorenylmethyloxycarbonyl-
GSH	glutathione reduced
GSSG	glutathione oxidized
HATU	1-[bis(dimethylamino)methylene]-1*H*-1,2,3-triazolo[4,5-b]pyridinium 3-oxid hexafluorophosphate
HBTU	*N*,*N*,*N*',*N*'-Tetramethyl-*O*-(1*H*-benzotriazol-1-yl)uronium hexafluorophosphate
HEPES	2-[4-(2-hydroxyethyl)piperazin-1-yl]ethanesulfonic acid
HOBt	1-hydroxybenzotriazole
HPLC	high-performance liquid chromatography
MALDI	matrix-assisted laser desorption/ionization
MeCN	acetonitrile
MeSPh	thioanisol
NMM	4-methylmorpholine 4-oxide
OAll	Allyloxy-
pAzF	*para*-azidophenylalanine
PEG	polyethylene glycol
PBS	phosphate buffered saline
Rf	retention factor

RP	reversed phase (silica C18)
SDS-PAGE	sodium dodecylsulfate-polyacrylamide gel electrophoresis
SPPS	solid phase peptide synthesis
TFA	trifluoroacetic acid
THPTA	tris(3-hydroxypropyl triazolylmethyl)amine
TIS	triisopropylsilane
UPLC	ultra performance liquid chromatography
UV	ultraviolet

Table of Contents

1 INTRODUCTION

1.1 Motivation: Peptides and Proteins as Tools and Therapeutics

Peptides and proteins are attractive targets and probes for biological and pharmaceutical research due to their unique biological activity, high potency and biocompatibility.[1] In 2013, 48 out of the 200 worldwide top selling drugs were based on proteins, the majority being insulin drugs and monoclonal antibodies.[2] Nevertheless, their application *in cellulo* and *in vivo* is still facing several challenges. One issue is limited stability due to degradation, aggregation, limited solubility, proteolysis, glomerular filtration and antigenic response.[3] Also, the cellular wall displays a commonly impenetrable barrier for peptides and proteins due to their high molecular weight and hydrophilicity; therefore, cytosolic targets stayed out of reach so far. These limitations are challenged by a variety of efforts that aim on one hand at stabilizing peptides and proteins, on the other hand at developing intracellular delivery and targeting approaches. In this context, PEGylation, lipidation and cell penetrating peptides are modifications of high interest and constitute the first focus of this work. Specifically, the requirement for developing these important improvements of the pharmaceutical application of peptide and protein drugs is to develop methods to get access to selectively and site specifically modified proteins. In order to do so, scientists needed to explore methodologies beyond traditional methods of protein expression and organic peptide synthesis. These novel methodologies are referred to by the term “bioconjugation” and form the second focus of this work.

1.2 Bioconjugation

Modifying biopolymers such as proteins with a function of choice by covalent linkage (Figure 1) is usually referred to as bioconjugation and is of utmost importance for research and therapy.[4] By now, a broad range of methodologies is available which all come with their advantages and disadvantages and should be chosen according to the target protein.[5]

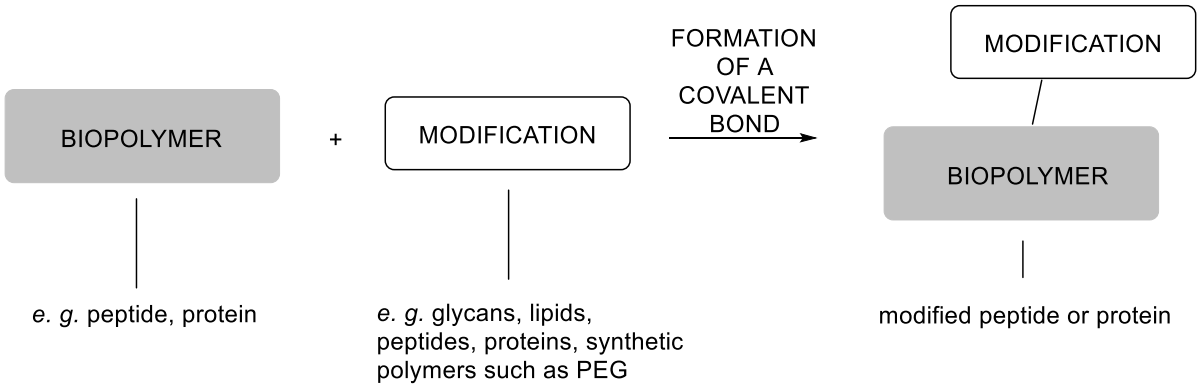

Figure 1. The concept of bioconjugation describes the formation of a covalent bond between a biopolymer such as a protein a modification of choice.

Traditionally, bioconjugation was done by addressing the side chains of the canonical amino acids (AA) of polypeptides. The required starting materials, peptides, can be accessed by organic synthesis methods like solid phase peptide synthesis (SPPS) (see 1.2.1.1). Alternatively, peptides and proteins can be prepared biochemically *via* expression of a target gene (see 1.2.1.2). These polypeptides are usually conjugated with organic synthetic reagents, which contain the modification of choice, by targeting nucleophilic side chains of natural amino acids that are present in the polypeptide of choice, *e. g.* free cysteins (see 1.2.1.3). Notably, because usually several nucleophiles are present in a protein, multiple conjugation is a common challenge of these strategies, leading to heterogeneous conjugate mixtures.

Two major findings caused a paradigm shift in the field of bioconjugation that enabled the site-selective synthesis of homogeneous conjugates: (i) Methods were developed to introduce non-canonical amino acids, most noteworthy selective pressure incorporation (see 1.2.2.1) and genetical code engineering (see 1.2.2.2). (ii) The concept of chemoselective or even bioorthogonal reactions that do not cross-react with any other functionality allows the site-selective modification of proteins without protecting groups and regardless of the AA sequence (see 1.3). Together, these two findings are combined in a two-step protocol for bioconjugation: (i) introduction of the unnatural functionality and (ii) installation of the modification of choice *via* a chemoselective reaction.

1.2.1 Bioconjugation *via* Canonical Amino Acids

1.2.1.1 Solid Phase Peptide Synthesis (SPPS)

Oligo- and Polypeptides can be built up by organic synthesis *via* subsequent amide bond formation[6] of side chain protected[7] amino acids. Most commonly, solid phase peptide synthesis (SPPS) is used for that, in which the polypeptide backbone is built up amino acid by amino acid from the solid support-.[8] In contrast to the biosynthesis of proteins, which assembles polypeptides from the N- to the C-terminus, SPPS is performed in the direction from C-terminus to N-terminus to avoid racemization *via* the formation of aspartimide. The immobilization of the peptide on the solid support allows the removal of reagents and side products of each reaction step by simple filtration, which enables the conduction of SPPS in an automated fashion, making various peptides with a sequence of choice readily accessible.

Specifically, a peptide is assembled *via* SPPS in four steps. First, the starting amino acid building block, which is N-terminal protected, is immobilized on the solid support. Second, the N-terminal protecting group is removed. Third, the next amino acid building block, that is N-terminal protected, is coupled to the free N-terminus of the first amino acid *via* ester activation.[9] The second and third steps are repeated until the peptide sequence of choice is assembled. Finally, the fourth step consists of the deprotection of the N-terminus and, simultaneously, the removal of the amino acid side chain protecting groups and the cleavage from the solid support.

In designing the used amino acid building blocks, it is important that the amino acid side chain protecting groups are stable to the deprotection conditions used to remove the N-terminal protecting group; in other words, the protecting groups have to be orthogonal to each other.[10] A commonly used N-terminal protecting group is Fmoc[11] which can be cleaved with non-nucleophilic base but is stable to acidic conditions.[12] Consequently, in Fmoc-strategy, the amino acid side chain protecting groups need to be stable to base but can be cleavable at acidic conditions. An example of the synthesis of a dipeptide *via* Fmoc strategy on a Wang resin is shown in Scheme 1.

The major drawback of SPPS is the occurrence of truncation products. With elongating sequence of a peptide, an increasing percentage of the peptide molecules becomes inaccessible for the further coupling of amino acids. Not only does this truncation decrease the overall yield of peptide product up to the point of not being able to synthesize the full sequence at all, moreover, the separation of the resulting product mixture often displays a considerable challenge. Every chemical modification made on a peptide potentially adds to these problems. In general, the yields of peptides accessed *via* SPPS drop with the length of the sequence, but usually, sequences of 10-40 amino acids can be accessed by SPPS.

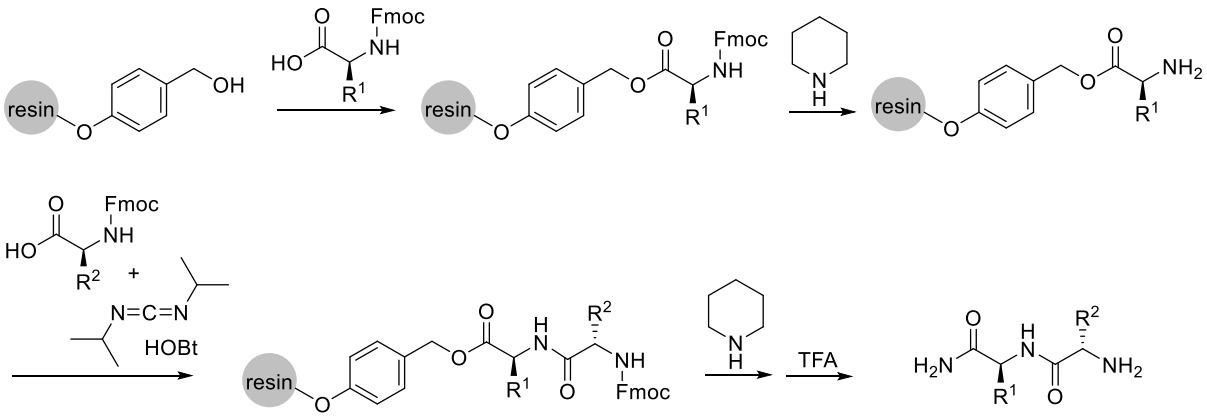

Scheme 1. Synthesis of a dipeptide *via* Fmoc-strategy on a Wang resin.

1.2.1.2 Gene Expression

Full length proteins can be accessed by exploiting protein biosynthesis in bacteria, yeast or mammalian cell culture *via* overexpression of a target protein.

Protein biosynthesis naturally consists of three steps:[13] first, the sequence of triplet codons is transcribed from the DNA to messenger RNA (mRNA) in the nucleus. Second, after transport of the mRNA to the cytosol, this information is translated into the corresponding amino acid sequence at the ribosomes (Figure 2 A), by recruiting the respective tRNA that is specific for the codon that it binds while being specifically loaded with an amino acid by aminoacyl-tRNA synthetases (aaRS) (Figure 2 B). Third, proteins can be modified after translation by so called post translational modifications (PTM) in order to modify their function.

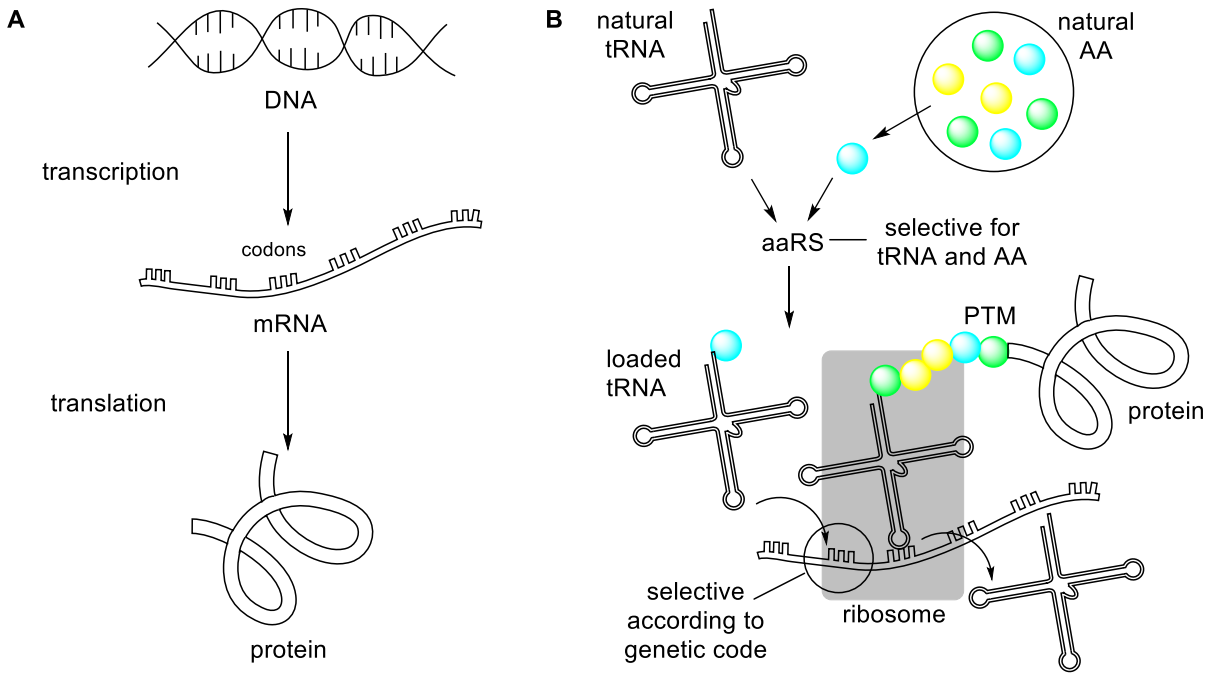

Figure 2. Natural protein biosynthesis. (A) Protein biosynthesis. (B) Translation at the ribosomes in detail.

1.2.1.3 Bioconjugation Reactions Targeting Canonical Amino Acids

Proteins and polypeptides can be functionalized in a straightforward fashion by addressing nucleophilic amino acid side chains such as lysine *via* reagents functionalized electrophiles such as succinimides, sulfonyl chlorides or isothiocyanates.[14] Notably, these strategies often lead to heterogeneous mixtures; the N-terminus can be modified also under the same conditions, which together can hamper the potency and function of the protein. More selective modification is possible by addressing C-terminus, N-terminus, or rare amino acids such as cysteine, tyrosine and tryptophan. In addition, selectivity can be induced by directing ligands.[14]

1.2.1.4 Semisynthesis

The chemoselective reaction of C-terminal thioesters and N-terminal cysteins followed by a *S*,*N*-acyl shift is employed to form a native peptide bond between two polypeptide fragments and is termed native chemical ligation (Scheme 2).[15,16] The two linked polypeptides can be both fully synthetic. In semisynthesis, one polypeptide is from organic synthetic origin, the other from a biosynthetic source. This is achieved introducing a recombinant C-terminal intein to the target protein, which allows the formation of a C-terminal thioester and subsequent ligation to a synthetic polypeptide. This strategy is referred to as expressed protein ligation.[17]

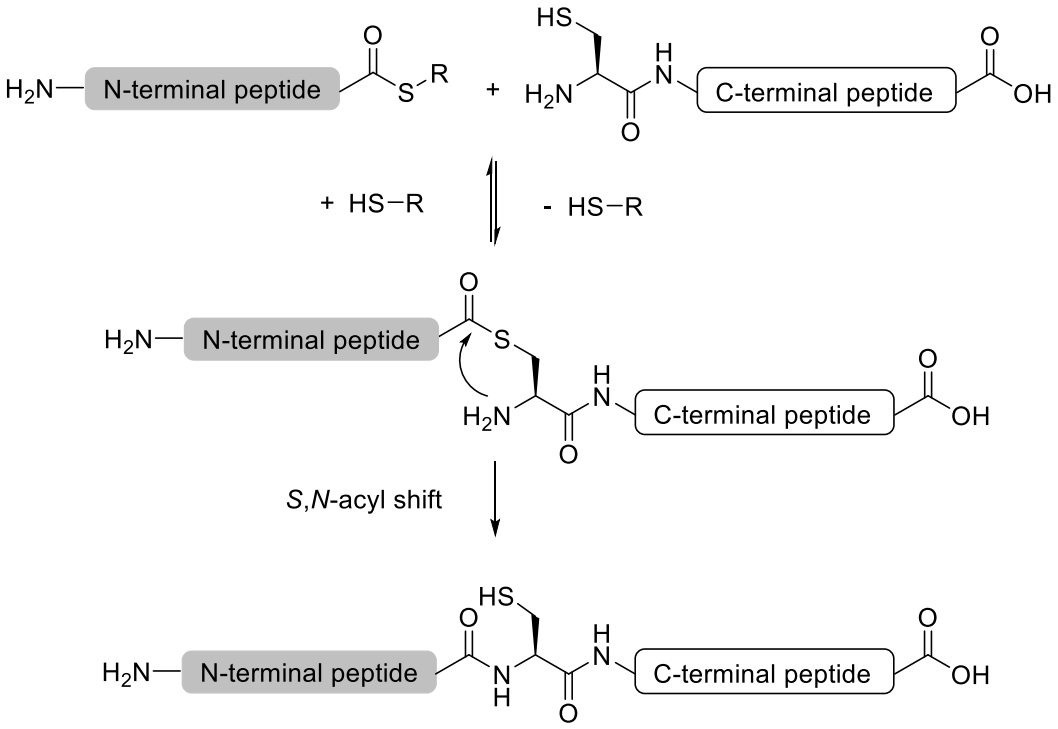

Scheme 2. The chemoselective reaction of a C-terminal thioester and an N-terminal cysteins containing peptide is followed by an irreversible *S*,*N*-acyl shift.[16]

Using multiple ligation steps, even full length proteins can be synthesized including the site specific incorporation of post-translational modifications.[18] Most importantly, these post-translational modifications are not restricted to natural ones allowing for pharmaceutically relevant functionalizations. Along these lines, the laboratory of Kochendorfer achieved to synthesize a full length, homogeneous and site-specifically PEGylated erythropoietin.[19]

The toolbox of peptide and protein ligations is continuously expanded by employing non-canonical thiol containing amino acids on the N-terminal part of the C-terminal ligation partner in combination with post-ligation desulfuration protocols.[16] In addition, continuous efforts are put into identifying new chemoselective reactions for the formation of native peptide bonds,[16,20] established examples include the traceless Staudinger ligation.[21,22]

Alternative to chemical ligations, enzymes can also be employed for the ligation of an expressed protein and a synthetic peptide fragment. An emerging technique is to employ Sortase A, a transpeptidase that ligates a peptide to an expressed protein required that the peptide contains a specific recognition sequence.[23,24]

1.2.2 Bioconjugation *via* Non-canonical Amino Acids

The venue to a more rational design of protein conjugates is opened by novel technologies for the incorporation of non-canonical amino acids to proteins that can then be addressed chemoselectively. This chemoselective bioconjugation offers full control over the site of modification regardless of the amino acids present in the protein and gives access to defined conjugates.

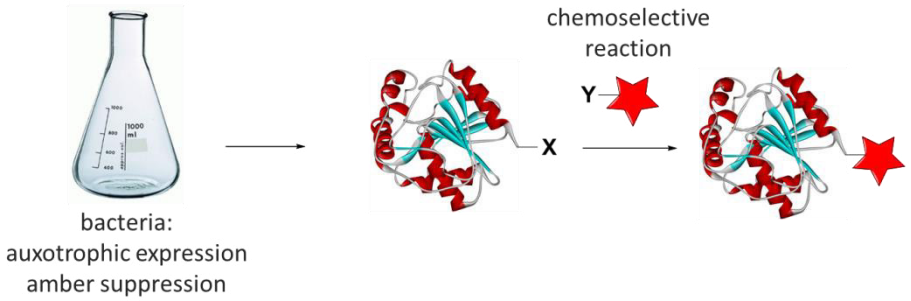

Figure 3. Two-step protocol of chemoselective bioconjugation. Left: incorporation of non-canonical amino acids into proteins by microorganisms. Middle: the expressed protein carries a reaction handle that can be modified chemoselectively. Right: the bioconjugation product is homogeneous and has a defined structure.[16]

SPPS offers many options to introduce non-canonical amino acids to peptides and to modify their side chains selectively, *e. g.* with fluorophores. However, the incorporation of non-canonical amino acids to full length proteins marks a challenge.

This chapter is focusing on methods to introduce non-canonical amino acids into proteins. These methods exploit protein biosynthesis but try to reprogram it. As mentioned before, tRNA and aaRS can be considered the gatekeepers of the genetic code because of their specificity both for loaded amino acid and the codon that is recognized, therefore, amino acid and codon selection are the target for manipulation. Selective pressure incorporation capitalizes on an induced promiscuity of aaRS for the loaded amino acid, genetic code engineering assigns codons that so far have not been used and programs an additional amino acid.

1.2.2.1 Selective Pressure Incorporation

Selective pressure incorporation (SPI) exploits the small window of promiscuity of an aaRS and substitutes one canonical amino acid with a non-canonical one which fits the binding pocket of the aaRS tolerably. For this, the organism needs to be auxotrophic for the replaced amino acid, *i. e.* being unable to synthesize it. The non-canonical substitute is added to the growth media of the culture and needs to be recognized by the now substrate lacking aaRS in order to be loaded to the corresponding tRNA (Figure 4).

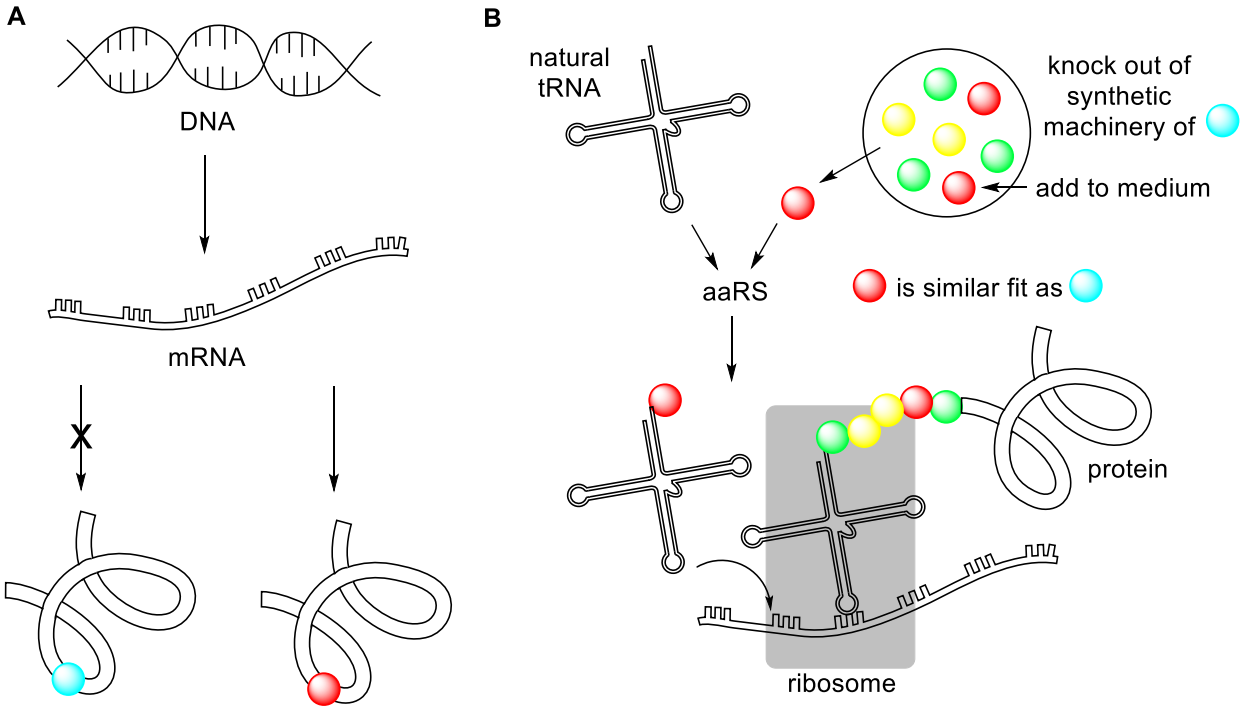

Figure 4. Selective pressure incorporation (A) DNA sequence and transcription is unaltered (B) translation is modified by substitution of canonical for non-canonical amino acid.

Using SPI, many non-canonical amino acids have been incorporated.[25] For instance methionine (**1**) analogues are frequently incorporated (Figure 5), *e. g.* homopropargylalanine (**2**), azidohomoalanine (**3**) or homoallylglycine (**4**).[26] Those could be successfully introduced by increasing

the concentration of the methionine-tRNA synthetase (MetRS) by coexpression in the *E. coli* met auxotroph CAG18491. Homopropargylglycine (**2**) and others can also be introduced as a Leucine substitute by using the T252Y mutant LeuRS with increased promiscuity in *E.coli* under overexpression conditions.[27]

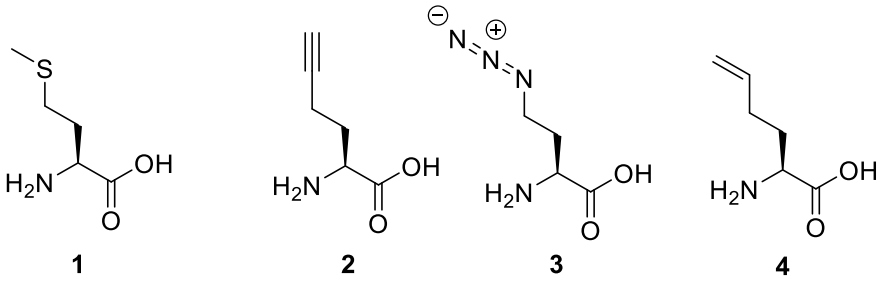

Figure 5. Methionine (**1**) and its analogues: homopropargylglycine (**2**), azidohomoalanine (**3**), homoallylglycine (**4**).

The incorporation of phenylalanine (Phe, **5**) analoga was achieved by using a bacterial PheRS from *E. coli* with reduced substrate specificity due to a mutation in the binding pocket (Ala294→Gly294).[28] The tolerance of this PheRS was further increased by the Tirrell laboratory *via* directed mutation of the active site (Thr251→Gly251); coexpression of the redesigned PheRS in *E. coli* lead to the incorporation of several Phe analoga to dihydrofolate reductase could be demonstrated, including *p*-iodophenylalanine (**6**), *p*-acetylenephenylalanine (**7**) and *p*-azidophenylalanine (**8**) (Figure 6).[29]

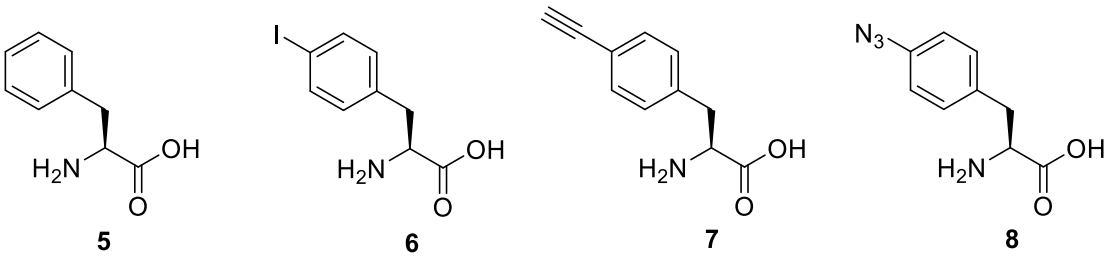

Figure 6. Phenylalanine (**5**) and its analogues: *p*-iodophenylalanine (**6**), *p*-acetylenephenylalanine (**7**) and *p*-azidophenylalanine (**8**).

SPI is a proteome wide approach, which means that the non-canonical amino acid is introduced in every protein of the organism which in turn can lead to compromised activity of the enzyme machinery, cultures grow usually slower. Another notable problem is residual amino acid that is incorporated quicker and leads to inhomogeneous protein products. An advantages is that non-canonical amino acids can be introduced at various positions while the protein is produced at good

yields. In fact, the simultaneous incorporation of three non-canonical amino acids could be demonstrated in a polyauxotrophic *E. coli* strain.[30]

1.2.2.2 Expansion of the Genetical Code

In brief, the method of genetic code expansion programs an additional tRNA – aaRS pair into an organism and by that allows for the incorporation of a non-canonical amino acid in addition to the already present ones.[25,31]

The genetic code translates codons, *i. e.* triplets of nucleotides, into their corresponding amino acids. With four different nucleotides at hand, 64 codons are possible; however, the 20 amino acids are assigned to only 61 codons, which are called sense codons. The three unassigned ones, which are referred to as nonsense codons, do not bind to a corresponding tRNA but to a release factor instead that results in the truncation of protein expression which is why they are referred to as stop codon.

It was found that the binding of the release factors to the amber stop codon (mRNA: UAG, DNA: TAG) can be suppressed *in vitro* by adding a chemically acetylated tRNA that has the ability to bind the stop codon due to a modified anticodon loop region. This technique allowed among others the introduction of *p*-fluorophenylalanine[32] and *p*-iodophenylalanine (**6**)[33] to proteins. This principle of assigning a 21st, *i.e.* non-canonical, amino acid to a stop codon was accomplished *in vivo* by the Schultz laboratory which required the development of an orthogonal tRNA – aaRS pair (Figure 7). Accordingly, they started from a tyrosyl tRNA/TyrRS pair from the archaebacterium of *Methanococcus jannaschii*, and (i) modified the tRNA's anticodon loop region to bind the amber stop codon and (ii) mutated the binding pocket of the corresponding Tyr-RS starting with random mutations followed by several rounds of positive and negative selection in order to load the non-canonical amino acid *O*-methyl-L-tyrosine specifically, which was demonstrated by expression of dihydrofolate reductase.[34] Using a similar approach, also other amino acids like *p*-azidophenylalanine (**8**)[35] could be incorporated to proteins site-specifically.

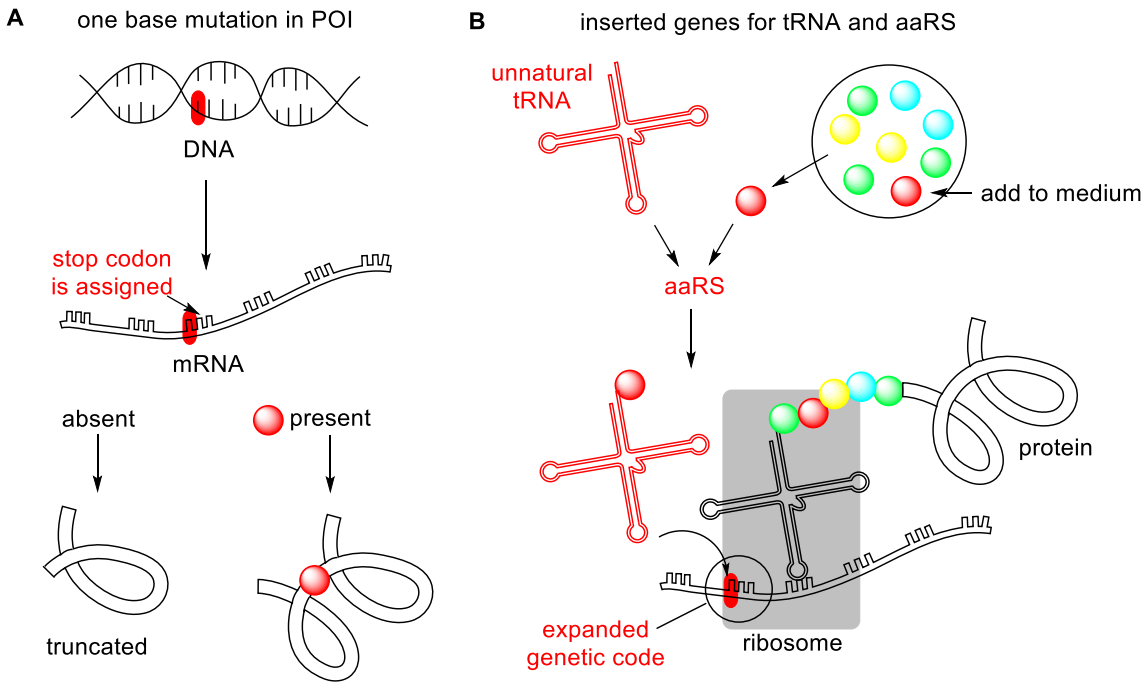

Figure 7. Genetical code expansion. (A) A stop codon is encoded in DNA; during translation, truncation competes with the incorporation of the non-canonical amino acid. (B) The translation is modified by an additional tRNA-aaRS pair that recognizes the stop codon and incorporates the non-canonical amino acid.

Later on, this method was demonstrated by the Schultz group also in eukaryotes, i.e. the yeast strain *Saccharomyces cerevisiae*. Using a similar approach of genetic selection based on a tRNA synthetase from *E. coli* TyrRS, they evolved several synthetases to incorporate various tyrosine (**9**) analogues including *p*-iodophenylalanine (**6**), *p*-azidophenylalanine (**8**), *p*-acetylphenylalanine (**10**) and *p*-benzoylphenylalanine (**11**) (Figure 8).[36] In fact, this principle of amber suppression is also used in nature, albeit it is very rare. Specifically, the methanogeneous bacterium *Methanosarcina barkeri* was found to introduce the amino acid pyrrolysine at the amber stop codon as a 21st amino acid.[37,38] Starting from this finding, an orthogonal pyrrolysyl-tRNA synthetase (PylRS) was developed for the incorporation of lysine analogues into proteins.[39-41] This strategy is applied regularly and the variety of lysine analogues is increasing constantly.[42]

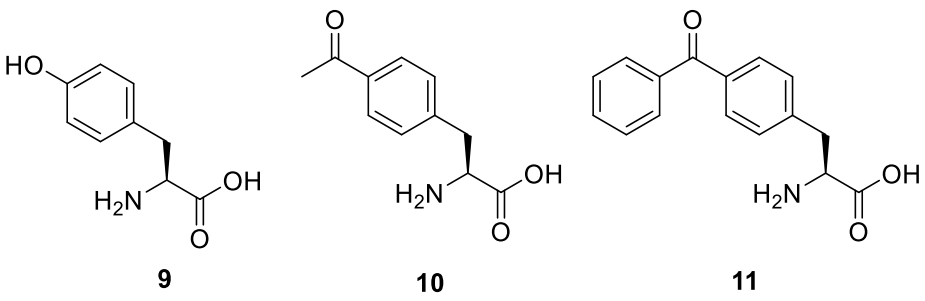

Figure 8. Tyrosine (**9**) analogues *p*-acetylphenylalanine (**10**) and *p*-benzoylphenylalanine (**11**).

By now, a wide range of amino acids could be incorporated site specifically into proteins by this approach, they all require an orthogonal tRNA-aaRS pair that is specific for the respective non-canonical amino acid.[31,43]

The major advantages of genetical code engineering are that first, no canonical amino acid has to be abdicated, and second, non-canonical amino acids with side chains more bulky than those of canonical ones can be incorporated even though they have no similarity to any canonical amino acid. On the other hand, the non-canonical amino acid has to be recognized by the orthogonal aaRS, which usually makes elaborate mutations of its binding pocket necessary.

The general fidelity of the culture is high, because the non-canonical amino acid is only introduced to the target protein and not proteome-wide. A considerable challenge is the competition of the release factors and of the newly programmed tRNA for the binding to the mRNA stop codon, leading to truncated products. In addition, overreading of the stop codon is observed and the resulting deletion product cannot be separated from the target protein. These issues can lead to truncation products and in that case result in low yields and therefore always have to be taken into account.

Constant efforts are invested to broaden the tool box of engineering and expanding the genetic code.[44] Chin and coworkers combined a modified ribosome that catalyzes the translation of several quadruplet codons with a reassigned amber codon for incorporating two different non-canonical amino acids to calmodulin.[41] Also the simultaneous encoding of non-canonical amino acids to the amber and the ochre stop codon has been demonstrated.[45] Budisa and coworkers realized the combination of selective pressure incorporation of two non-canonical AA with genetical code expansion *in vivo*.[44]

1.3 Chemoselective Reactions

Proteins naturally contain a large set of functional groups *e. g.* amines, thiols, disulfides, benzyl groups, alcohols. This makes high demands on any chemical reaction that aims to site-specifically modify a full length protein. The transformation has to be high-yielding without side reactions at conditions that allow maintaining a proteins tertiary structure and ergo its function, which means the reaction has to proceed at physiological conditions with respect to pH and temperature and, most importantly, without any protecting groups. In synthetic organic chemistry, Kolb, Finn and Sharpless defined such reactions as Click-reactions.[46] Reactions that fulfil those requirements in a complex context such as proteins and other biomolecules are also referred to as chemoselective reactions and are of utmost importance for bioconjugation. If they proceed with good kinetics in a living system, e.g. a cell, they are even bioorthogonal, which means that none of the reaction partners crossreacts with any present biomolecule, a concept that has been introduced by Bertozzi.[47,48]

In the last decade, several chemoselective reactions have been identified which has been reviewed extensively.[49,50] A comparison with regard to the kinetics can be found here.[51] Even several heavy metal catalyzed reactions like palladium cross couplings could be conducted *in vivo*.[52]

Examples for reactions that could have been demonstrated repeatedly *in vivo* include the Diels-Alder reaction with inverse electron demand[53] of tetrazines (**12**) and strained alkenes or alkynes such as norbornene (**13**),[54] cyclopropene[55,56] (**14**) and tranccyclooctene[57] (**15**) (Scheme 3 A) and the photoinduced cycloaddition of alkenes (**16**) and tetrazoles[58-61] (**17**) (Scheme 3 B), the traceless Staudinger ligation[21,22] (see 1.3.2.1) and the strain promoted Huisgen reaction of azides and cyclooctynes (see 1.3.1.2).

Azides play a distinguished role in chemoselective bioconjugation, on the one hand because their stability and small size enabled to develop several ways to incorporate them into proteins (see 1.2.2), on the other hand because numerous ways have been described to address them selectively. Specifically, Staudinger- and Huisgen[62]-type reactions play an eminent role in chemoselective reactions, especially for bioconjugation, which is why these reactions will be discussed in detail.

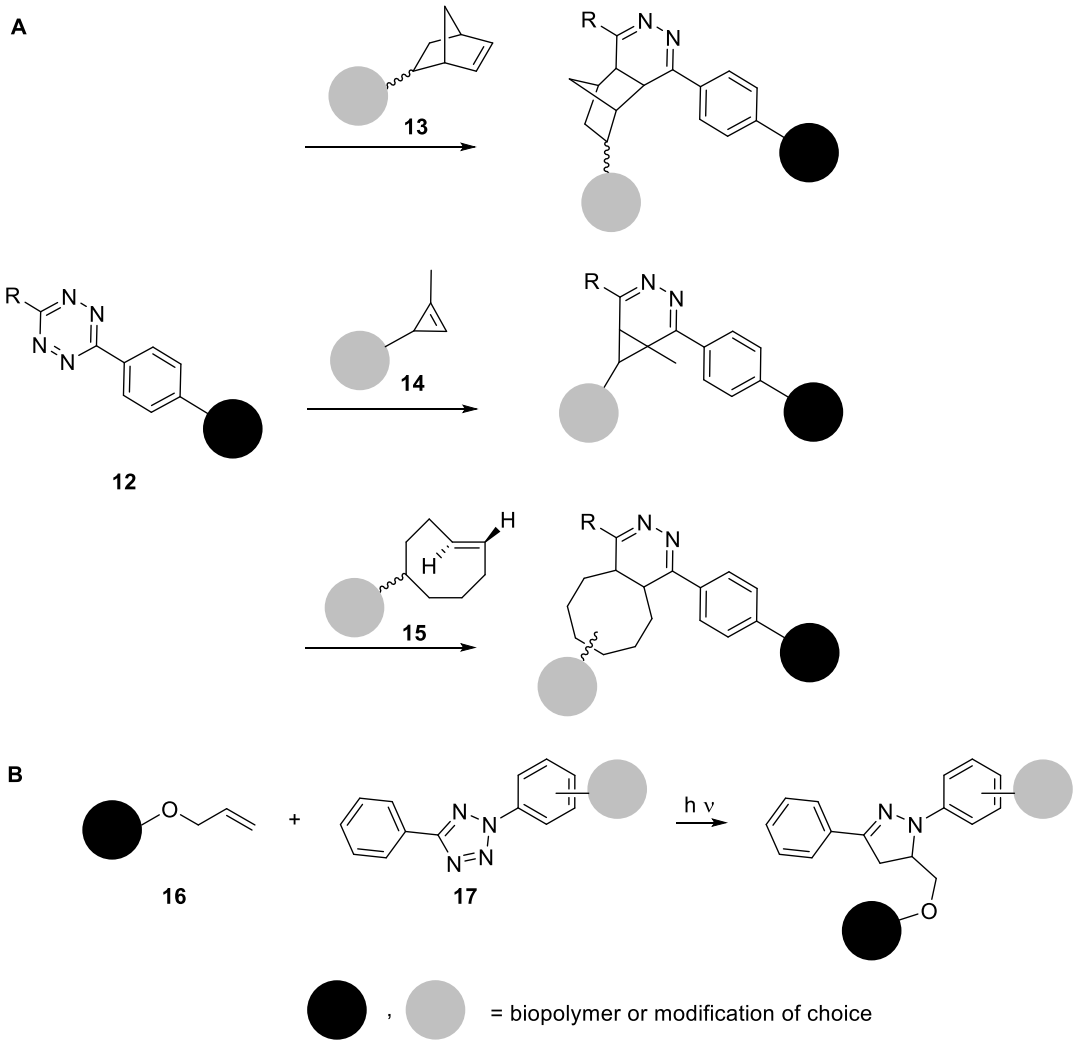

Scheme 3. Chemoselective reactions that are applicable *in vivo*. (A) Diels-Alder reaction wit inverse electron demand of tetrazines (**12**) and norbornene (**13**), cyclopropene (**14**) or tranccyclooctene (**15**). (B) Photoinduced cycloaddition of alkenes (**16**) and tetrazoles (**17**).

1.3.1 Huisgen-Type Reactions[62]

Discovered by Arthur Michael in 1893,[63] the formation of 1*H*-1,2,3-triazoles from azides and alkynes under elevated temperatures was taken up in the 1960ies by Rolf Huisgen and put into context of 1,3-dipolar cycloaddition of several 1,3-dipoles such as azides with dipolarophiles such as alkynes (Scheme 4 A).[64]

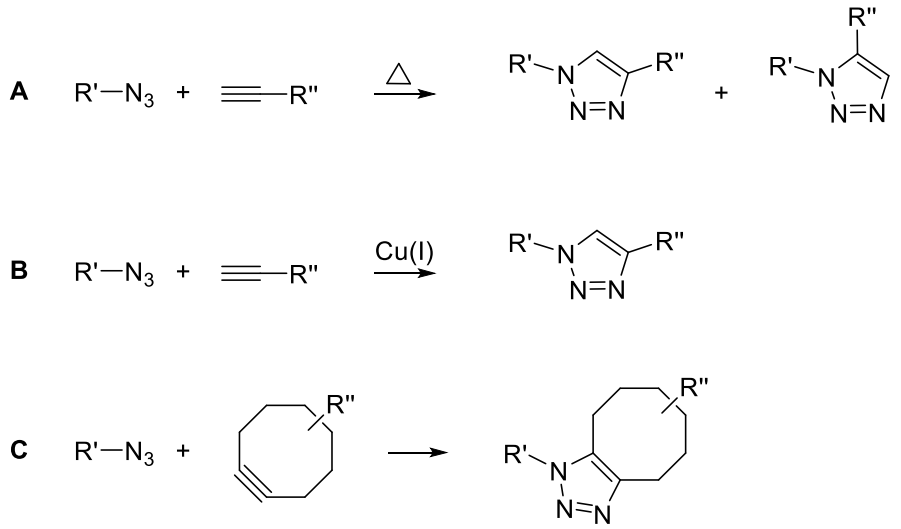

Scheme 4. Huisgen-type reactions of azides and alkynes. (A) Thermal 1,3-dipolar cycloaddition. (B) Copper catalyzed azide-alkyne cycloaddition (CuAAC). (C) Strain promoted azide-alkyne cycloaddition (SPAAC).

1.3.1.1 Copper Catalyzed Azide-Alkyne Cycloaddition (CuAAC)

Another 40 years later, the laboratories of Sharpless[65] and Meldal[66] made the significant discovery that the reaction of azides and terminal alkynes can be catalyzed by Copper(I) to proceed in water at room temperature to give regioselectively 1,4-substituated 1*H*-1,2,3-triazoles (Scheme 4 B). In the following years, this so-called copper catalyzed azide-alkyne cycloaddition (CuAAC) was extensively employed in bioconjugation and in even *in vivo* labelling.[52,67] One requirement for this was of course the incorporation of azides and alkynes into proteins, as described above. Another important step was the development of copper chelating ligands to accelerate the reaction and stabilize the copper from oxidation such as bipyridine[68] or tris(triazolylmethyl)amine ligands (Figure 9), *e. g.* Tris[(1-benzyl-1*H*-1,2,3-triazol-4-yl)methyl]amine (TBTA, **18**).[69] Modifications of the latter are THPTA (**19**) with increased water solubility for the bioconjugation of proteins[70] and BTTAA (**20**) which has reduced toxicity for experiments on and even in cells.[71,72]

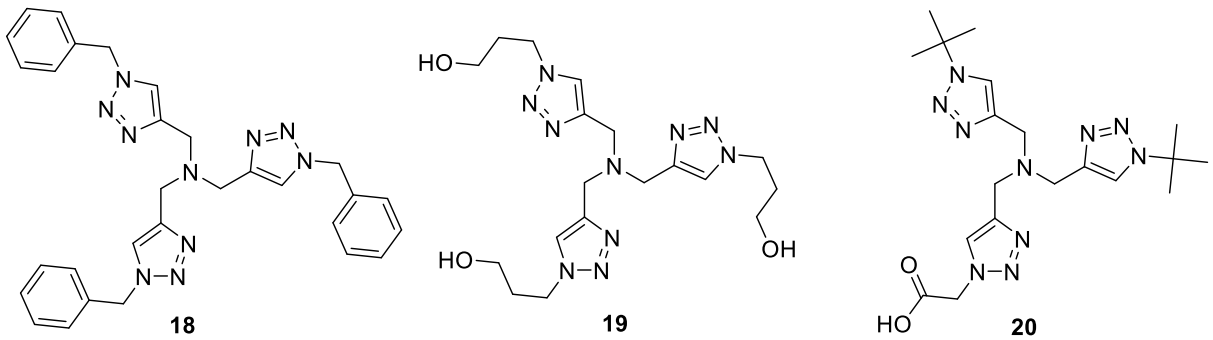

Figure 9. Tris(triazolylmethyl)amine-based ligands applied in CuAAC for bioconjugation: tris[(1-benzyl-1*H*-1,2,3-triazol-4-yl)methyl]amine (TBTA) (**18**), tris[(3-hydroxypropyl-1*H*-1,2,3-triazol-4-yl)methyl]amine (THPTA) (**19**) and [([bis((1-*tert*-butyl-1*H*-1,2,3-triazol-4-yl)methyl)amino]methyl)-1*H*-1,2,3-triazol-1-yl]acetic acid BTTAA (**20**).

The mechanism of CuAAC (Scheme 5) is hypothesized to proceed *via* (i) the formation of a π-complex of Cu(I) and alkyne (ii) upon abstraction of a proton and addition of a second copper species, this π-complex is transformed to a σ-complex, i.e. copper acetylide (iii) the azide is coordinated to the π-bound copper species, forming the acetylide-azide-copper complex, which induces the N3-C4 bond formation of the triazole (iv) the N1-C5 bond is formed upon expulsion of the second copper species (v) finally, exchange of the first copper for a proton yields the 1,4-substituted 1*H*-1,2,3-triazole product.[73] Initially, the formation of the acetylide-azide-copper complex was believed to proceed *via* the formation of a monomeric copper acetylide complex,[65] however evidence accumulated that at least two copper atoms are involved in the cycloaddition steps[67] which is supported also by experiments of the laboratory of Fokin which recently lead to the proposal of an updated mechanism.[73]

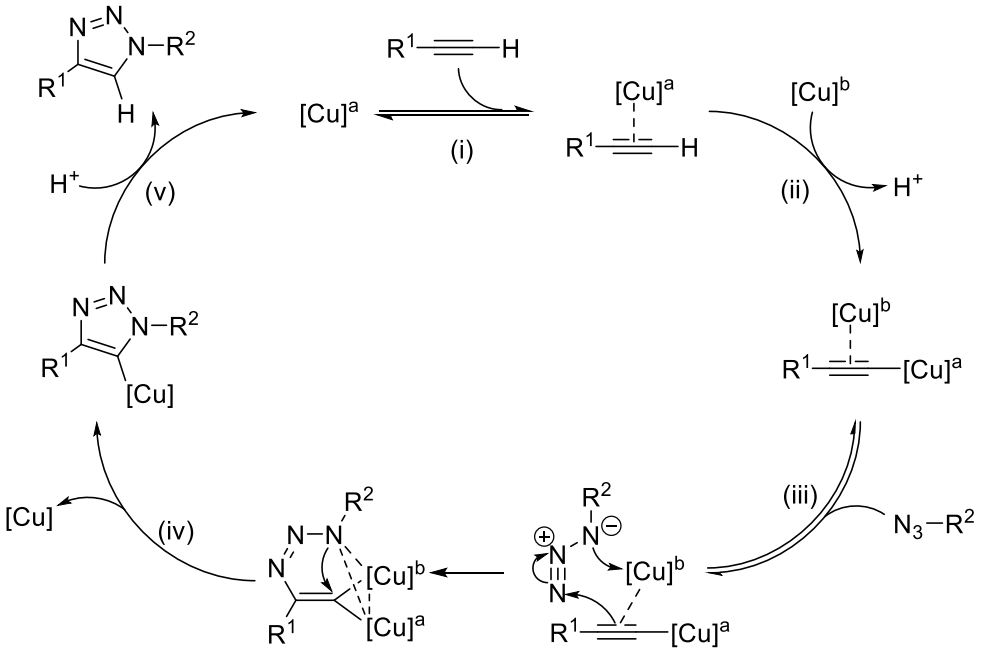

Scheme 5. Hypothesized mechanism of CuAAC.[73]

Interestingly, ruthenium(I) catalyzes also the cycloaddition of azides and alkynes, albeit with reverse regioselectivity yielding 1,5-substituted 1*H*-1,2,3-triazoles.[74,75] The reaction tolerates both terminal and internal alkynes, supporting that it does not proceed *via* a metal acetylide; the regioselectivity of the reaction is controlled by a ruthenacycle intermediate in which the alkynes' sterically less demanding carbon is bound to the azides' terminal nitrogen.[76]

1.3.1.2 Strain Promoted Azide-Alkyne Cycloaddition (SPAAC)

To address azides with alkynes without the need of a potential toxic metal catalyst, researchers explored other strategies to the formation of 1,4-1*H*-1,2,3-triazoles. One successful example lowers

the activation energy by increasing the energy of the alkyne with a straining cyclic backbone (Scheme 4 C). This so-called strain-promoted alkyne-azide cycloaddition (SPAAC) was first demonstrated as the reaction of azides and cyclooctynes in 2004.[77] Since, the reaction rates were increased by modifying the backbone of the cyclooctyne: mono- and difluorocyclooctyne (MOFO, DIFO),[78,79] dimethoxazacyclooctyne (DIMAC),[80] bisarylazacyclooctynone (BARAC);[81] commercially available derivatives include bycyclo[6.1.0]nonyne (BCN),[82] dibenzocyclooctyne (DIBO)[83] and dibenzoazacyclootyne (DIBAC).[84] A More hydrophilic BCN derivative that allowes increased signal to noise ratio in cell surface labelling was reported recently.[85] Notably, a major occurring side reaction of strained cyclooctynes is the addition to thiols, *e. g.* at the side chains of cysteins, which can however be circumvented by alkylating those before bioconjugation.[86]

1.3.2 Staudinger-Type Reactions

The Staudinger reaction, also known as Staudinger reduction, is the synthesis of primary amines from azides (Scheme 6).[87] It is a mild reduction in which first the azide **21** is target of a nucleophilic attack of the phosphine **22**, forming a phosphazid (**23**), followed by the formation on a four-membered ring (**24**), which is opened upon expulsion of molecular nitrogen, resulting in an iminophosphorane/aza-ylide intermediate (**25**). Finally, the P-N- bond of the iminophosphorane is cleaved by hydrolysis, yielding in a primary amine (**26**) and phosphinoxide (**27**).

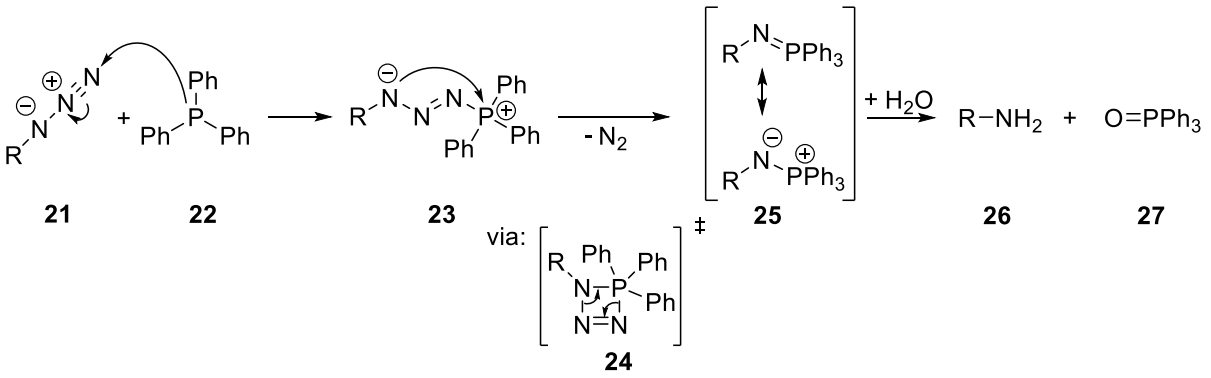

Scheme 6. Mechanism of Staudinger reaction.

The reaction of azides and phosphorous(III) compounds tolerates the presence of a variety of functional groups, moreover, it can be conducted in water at room temperature with high yields, making it a potential chemoselective reaction.[88] This chemoselectivity was capitalized on for developing selective ligation reactions by developing strategies to avoid hydrolysis of the P-N-bond of the iminophosphorane by intercepting it intramolecularly. In this context, several chemoselective

Staudinger-type bioconjugation methods were developed which found widespread application in chemical biology.[88,89]

1.3.2.1 Staudinger Ligations

The so-called Staudinger ligation was initially developed for cell surface glycan labelling.[90] The azide component (**28**) reacts with a phosphite that contains an electrophilic trap (**29**) which allows the formation of an amide instead of an amine (**30**) (Scheme 7). The reaction proceeds like the Staudinger reaction to an iminophosphorane **31**, which instead of hydrolyzing is undergoing intramolecular cyclization to compound **32** with subsequent hydrolysis to conjugate **33** which undergoes cycloreversion to form the ligation product **30** (Scheme 7).[88]

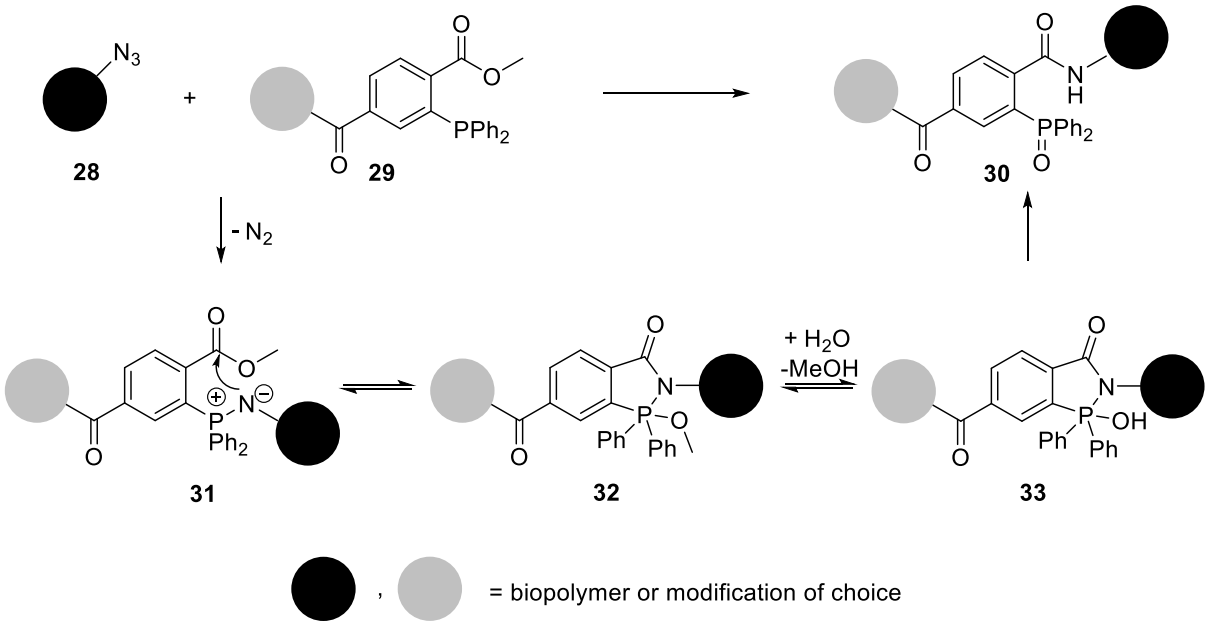

Scheme 7. Staudinger ligation and its mechanism.

The development of a traceless variant of the Staudinger ligation[88,89] was achieved by the laboratories of Bertozzi[21] and Raines[22] and was demonstrated for the ligation of peptides[91] as well as for the ligation of a dipeptide to an N-terminal azide of a protein.[92] Similar to native chemical ligation, the C-terminal protein ligation fragment is functionalized as a thioester (**34**), which is at the same time trans-thioesterified and functionalized with a phosphine by using the reagent *ortho*-2-(diphenylphosphine)phenol (**35**) (Scheme 8). The resulting phosphinothioester (**36**) reacts with the azide fragment to form the iminophosphorane (**37**) which intramolecularly reacts to an amidophosphonium salt (**38**) which is finally hydrolyzed to yield the ligation (**39**) product with a native amide bond (Scheme 8).[93]

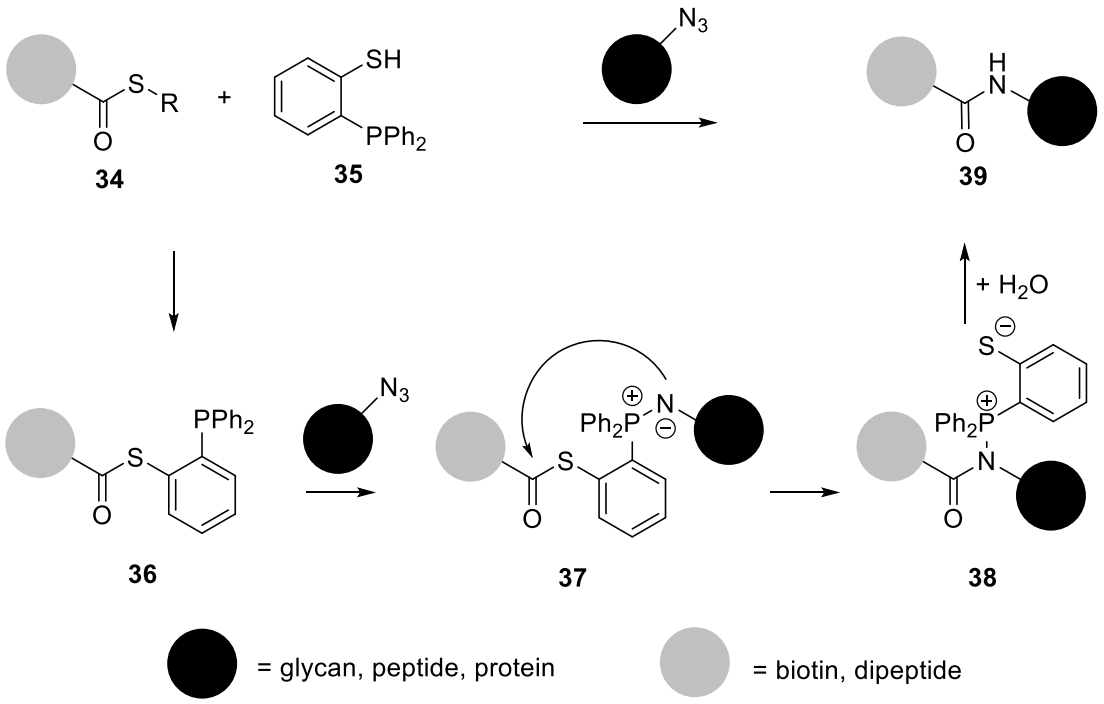

Scheme 8. Traceless Staudinger ligation and its mechanism.[93]

Staudinger Ligation intercepts the cleavage of the P-N bond of the iminophosphorane intramolecularly, thus forming an alternative covalent bond. In contrast, alternative reagents such as phosphites can avoid the cleavage of the P-N bond altogether.[94] The first example of this Staudinger phosphite reaction reports the formation of a stable phosphoramidate bond from phenylazide and trimethylphosphite.[95]

1.3.2.2 Staudinger Phosphite Reaction

The Staudinger phosphite reaction of aryl-azides (**40**) and phosphites (**41**) proceeds analogously to the Staudinger reduction *via* a phosphazide (**42**) to a phosphorimidate (**43**) which undergoes hydrolysis to the reaction product, a phosphoramidate (**44**) (Figure 10 A). The hydrolysis of the phosphorimidate (**43**) was first assumed to proceed *via* an Arbuzov-type rearrangement (Figure 10 B1).[96] However it was found by experiments in ^{18}O-labelled water that more than one pathway exist next to each other, depending on the pH[97] as well as on the substituents on the phosphorous atom.[98] Specifically, ^{18}O-labelling experiments revealed that at a pH of higher than 5, ^{18}O is incorporated at the phosphorous atom to increased extent, which supports the hypothesis of a nucleophilic attack of a water molecule at the phosphorous atom (Figure 10 B(2).); in contrast, at pHs lower than 5, ^{18}O was incorporated only to a minor extent, suggesting a nucleophilic attack on an α-carbon of the alkoxy-substituents instead, which is in accordance to the Arbuzov-type rearrangement (Figure 10 B(1)). Notably, the latter suggested S_N2 attack is favored for electrophilic sp^3-hybridised carbons, however, benzyl groups were

found to be extremely good leaving groups in this reaction, which suggests rather an S_N1 reaction *via* a carbocation (Figure 10 B(3)).[98,99]

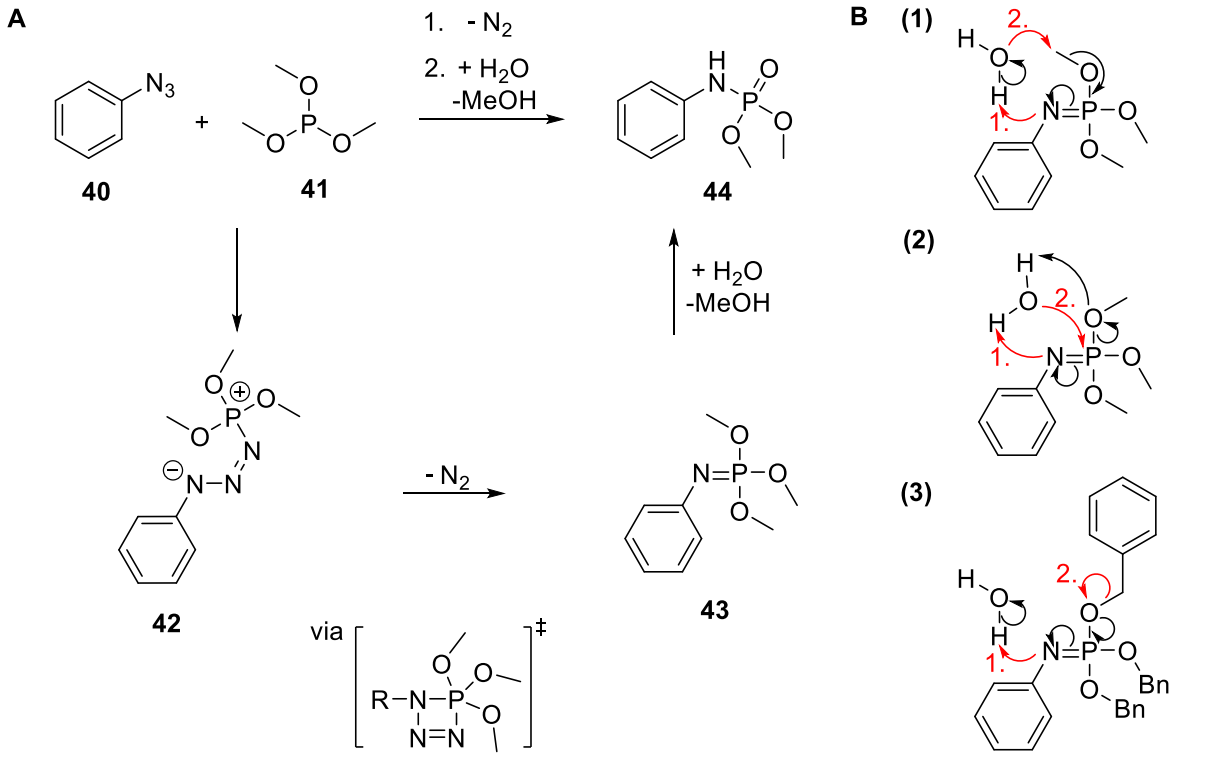

Figure 10. Staudinger phosphite reaction. (A) Staudinger phosphite reaction and its mechanism. (B) Competing mechanisms for the hydrolysis of phosphorimidates, which after protonation of the nitrogen atom proceed *via* (1) Arbuzov-type rearrangement, (2) Nucleophilic attack of water at the phosphorous atom, or (3) loss of a stable leaving group *e. g.* a benzylcation.

Work conducted in the laboratory of Hackenberger identified the Staudinger phosphite reaction of aryl azides as a chemoselective reaction and demonstrated its utility for bioconjugation by the modification of peptides and proteins, including PEGylation, glycosylation and biotinylation.[98,100-103] The key feature of the Staudinger phosphite bioconjugation is that two functionalities can be incorporated in one reaction, using symmetrical substituted phosphites (Scheme 9 A). This is an advantage when several functionalities are beneficial, for instance in PEGylation (see 1.4.1). In order to expand the Staudinger phosphite reaction to the incorporation of only one functionality, Böhrsch *et al.* screened for different unsymmetrical phosphites and identified benzyl-substituents at the phosphite as the better leaving groups during hydrolysis of the phosphorimidate in contrast to alkyl groups (Scheme 9 B).[98] Further investigation of different leaving groups showed that at during hydrolysis of the phosphorimidate, pyridyl-substituents have similar good leaving propensities as a benzyl-substituents, but the corresponding phosphites are more stable to hydrolysis themselves and therefore easier to handle.[104]

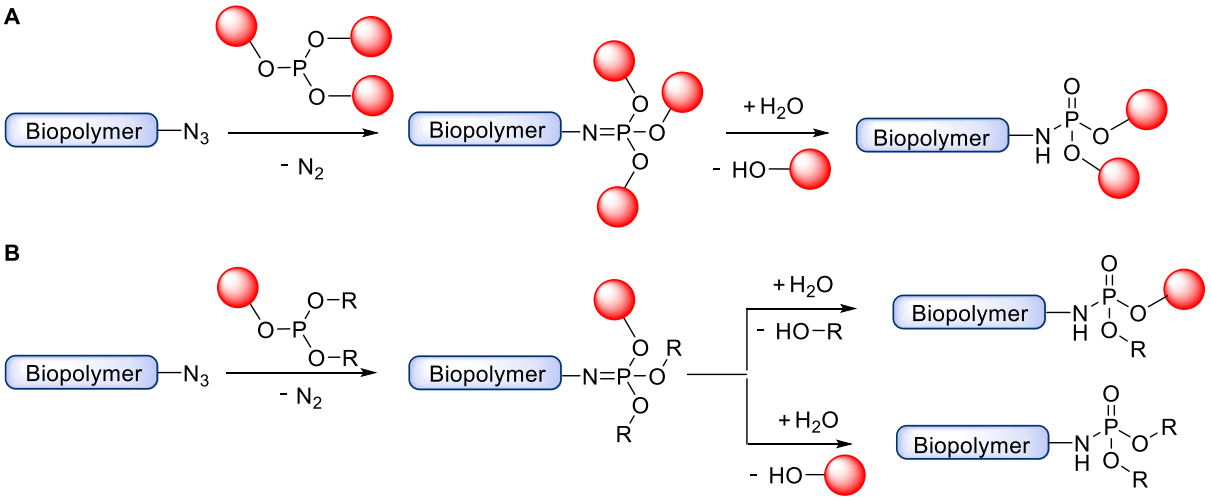

Scheme 9. Staudinger phosphite reaction for bioconjugation. (A) Symmetrical substituted phosphites lead to double modified bioconjugates. (B) Unsymmetrical phosphites lead to single modified bioconjugates, unmodified biopolymers occur as a side reaction.

Most interestingly, the use of phosphites with light cleavable substituents offers access to phosphorylated amino acids on peptides or proteins at a moment of choice. The generation of phospho-tyrosine analogue on proteins has been demonstrated.[102] Peptides site-specifically containing phospho-lysine can be synthesized using this approach, which is a powerful tool for studying the biological relevance of phospho-lysine.[105]

Recently, a tandem Staudinger Huisgen reaction was demonstrated by Valleé *et al.* which enables to conjugate selectively two entities that are both functionalized by an azide.[106,107] It uses borane protected alkyne phosphonites that react with the first azido compound in a CuAAC, the resulting triazolylphosphonite is borane-deprotected to react with the second azido compound in a Staudinger type reaction to yield triazolylphosphonamidates.

1.4 Pharmaceutical Relevant Modifications

1.4.1 PEGylation

This chapter was published as a synopsis (69 references) in the following journal:

Nicole Nischan, Christian P. R. Hackenberger

"Site-specific PEGylation of Proteins: Recent Developments"

J. Org. Chem. **2014**, *79*, 10727-10733.

Publication Date (Web): October 21, 2014

The original article is available at: http://dx.doi.org/10.1021/jo502136n

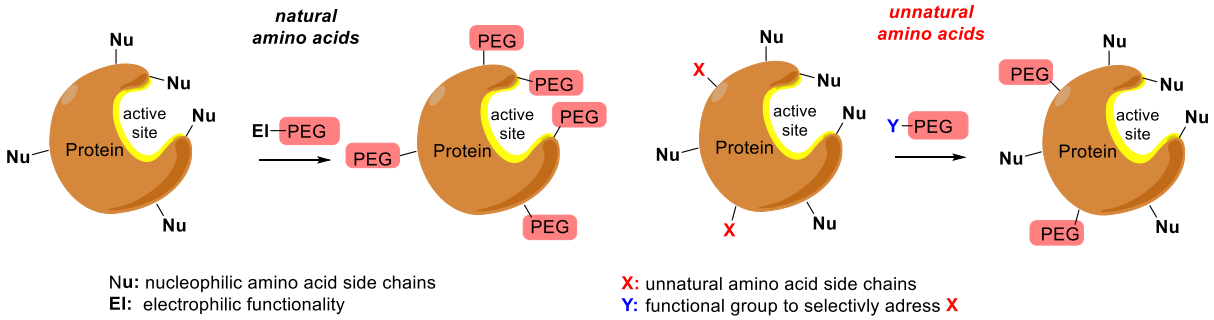

Figure 11. Technologies for the PEGylation of proteins addressing natural (left) or unnatural (right) amino acids.

Abstract

The attachment of linear polyethylene glycol (PEG) to peptides and proteins for their stabilization for *in vivo* applications is a milestone in pharmaceutical research and protein – drug development. However, conventional methods often lead to heterogeneous PEGylation mixtures with reduced protein activity. Current synthetic efforts aim to provide site-specific approaches by chemoselective targeting of canonical and non-canonical amino acids and to improve the PEG architecture. This synopsis highlights recent work in this area, which also resulted in improved pharmacokinetics of peptide and protein therapeutics.

Summary of content

This synopsis highlights the importance of chemoselective bioconjugation for PEGylated therapeutic proteins.

The introduction contains an overview about the relevance of attaching macromolecules to apply peptides and proteins *in vivo* before focusing on PEGylation in detail. The latter is discussed thereafter with respect to advantages, disadvantages and challenges. The effects of PEGylation on the protein of

choice are reviewd, including the structural and pharmacokinetic effects as well as the influence of size and shape, *i. e.* branching, of the PEG-reagent.

In the following, this synopsis discusses traditional random PEGylation technologies that have been used for the first FDA-approved PEGylated protein drugs, but also the region-selective approaches that target canonical amino acids. Main part of the synopsis reviews specific chemoselective PEGylation reactions such as CuAAC, SPAAC and Staudinger reactions that could only be accessed for bioconjugation by implementing non-canonical amino acids *via* amber suppression or selective pressure incorporation techniques.

Responsibility Assignment.

Both Christian P. R. Hackenberger and the author decided which content to include, and wrote and processed the manuscript. Therein, Christian P. R. Hackenberger took a guiding role. The author revised the manuscript accordingly, and designed graphics.

1.4.2 Lipidation

Lipidation, *i. e.* the attachment of hydrophobic moieties, is an important way to control cell signaling and subcellular protein trafficking.[108,109] Important posttranslational lipidations include fatty acetylations[109] like *N*-myristoylation (**45**) and *S*-palmitoylation (**46**) and prenylations such as *S*-farnesylation (**47**) and *S*-geranlygeranylation (**48**) (Figure 12), all of them are controlled by transferring enzymes.[110]

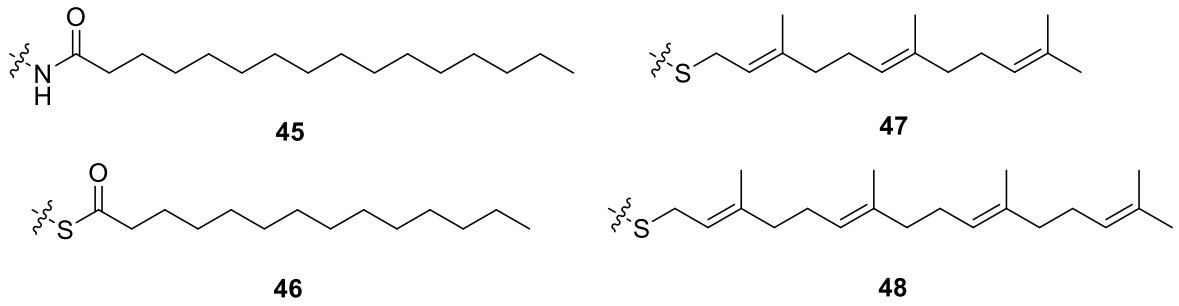

Figure 12. Important posttranslational lipidations: *N*-myristoylation (**45**), *S*-palmitoylation (**46**), *S*-farnesylation (**47**) and *S*-geranlygeranylation (**48**).

Most interesting, the localization of a protein depends on the number and character of the attached lipid. While one acyl or prenyl group commonly leads to reversible binding to membranes, the addition of a second binding motif such as another prenyl or acyl moiety or a basic entity results in membrane anchoring.[109,110] Lipidation of a peptide or protein allows targeting them to a lipid bilayer, stabilizing their structure for enhanced activity[111,112] and increasing their *in vivo* lifetime.[113,114] These benefits make lipidation an attractive functionality in drug design and delivery. One example is Insulin Detemir, an acylated insulin analogue (Levemir®, Novo Nordisk), that has been approved as a long acting insulin drug for the treatment of *diabetes mellitus*.[115]

In addition, the lipidation of peptides can result in amphiphilic molecules that have the ability to self-assemble to micellar structures at low concentrations.[116-118] This micellar organization of lipidated peptides supports their cellular uptake.[119]

Synthetic access to site-specifically lipidated peptides *via* SPPS methods is established whereas the Lipidation is often performed *via* in solution couplings.[120] Site-specific lipidated proteins are accessed employing semisynthetic approaches. Therein, a synthetic lipidated peptide is either coupled *via* a maleimide to a C-terminal thiol of the expressed protein part, or is used in expressed protein ligation *via* a C-terminal cysteine.[121] The application of chemoselective reactions to the lipidation of proteins is rarely reported which pinpoints the need to expand the lipidation toolbox for bioconjugation. The

impact of bioorthogonal lipidation is demonstrated by the laboratory of Lin, who report the control of intracellular GFP-membrane association by lipidation *via* photoinduced aryltetrazole-alkene cycloaddition.[58]

1.4.3 Cell penetrating peptides

Cell penetrating peptides (CPPs) mediate the intracellular transport of cargo that cannot enter cells on its own.[122] In fact, there are many molecules that have a high therapeutic potential and cannot enter cells. One example are peptides and proteins which are usually hydrophilic and far bigger than 500 Da and therefore, according to Lipinski's rule of five, have been considered as non-druggable for a long time. In this context, CPPs have become an indispensable covalent and noncovalent carrier for the drug delivery of peptides and proteins and siRNA.[123-125]

Approaches that traditionally are used to deliver a cargo without the need of its chemical modification in research include electroporation and microinjection. It was found that also certain amphipathic peptides can be used for the intracellular delivery of peptides and proteins by forming non-covalent complexes.[123] Recently, the use of endosomolytic peptide reagents has been reported for the efficient transport of proteins into cells.[126] Specifically, enhanced green fluorescent protein (EGFP) could be delivered to HeLa, Neuro-2a and HDF cells at concentrations of 10 µM EGFP and 5 µM endosomolytic reagent in 1 h, after which 95 to 99 % of the cells survived. The endosomolytic reagent consisted of a fluorophore-labelled dimer of the CPP TAT. While all of these approaches are convenient with regard to synthetic effort, their application *in vivo* is limited. The challenges of non-covalently bound CPP for cargo delivery *in vivo* include the premature disassembly of CPP-cargo-complex as well as the transport of matrix components instead of the cargo.

In contrast, covalent delivery approaches offer the advantage of selective delivery in a complex environment. One possible method is the fusion of the cargo to a protein transduction domain (PTD) that triggers uptake of the cargo into endosomes and later lysosomes.[122,127,128]

1.4.3.1 Arginine-Rich CPPs

Uptake into the cytosol of cells is possible by arginine rich peptides such as the TAT-peptide.[129] Most interestingly, the uptake of the TAT-peptide and other arginine rich CPPs such as octa-arginine proceeds both into the cytoplasm and into the nucleus; the type of uptake corresponding to this characteristic uptake-pattern (Figure 13 C) is termed transduction.[130]

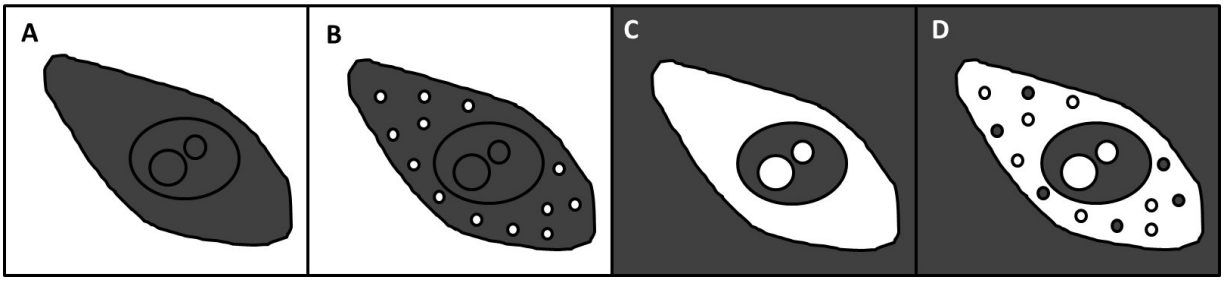

Figure 13. Localization observed before (A) and after (B-D) incubation of cells with fluorophore-labelled TAT-peptide for 1 h. (A) Addition of TAT to the medium. (B) Uptake *via* endocytosis, the peptide is present both in the medium and in the endocytic vesicles. (C) Uptake *via* transduction, the peptide is present in the cytosol and nuclear compartments. (D) Coexistence of endocytosis and transduction.

1.4.3.2 Mechanism of Uptake

The mechanism of this uptake is under ongoing debate.[122] There is strong evidence for micropinocytosis but also for caveolae dependent endocytosis and CME.[122] However, this hypothesis offers little explanation for the fact that arginine rich CPPs can reach the cytosol without being degraded, which could be demonstrated by the application of a mass spectrometry protocol that analyzes the peptides taken up *via* a mass-tag-approach.[131] In addition, it was found that arginine rich CPPs strongly induce negative membrane curvature,[132] whereas micropinocytosis depends on the formation of positive membrane curvature. Moreover, fluorophore-labelled TAT-peptide still showed rapid cellular uptake in experiments conducted at 4°C, at which temperature energy dependent pathways are suppressed.[127] Likewise, the TAT-peptide was readily taken up in the presence of inhibitors or under conditions of knock down of different endocytosis pathways.[127]

Most interestingly, D-isomers of the arginine rich CPPS exhibit also rapid uptake.[133] Guanidinium groups on dendrons were able to transport PNA into HeLa cells.[134] A detailed structure-activity study of the cellular uptake of TAT and polyarginines identified several influencing factors. Uptake increases with the number of arginines and decreases with loss of positive charge.[133] Synthetic guanidinium-peptoids lead to even more rapid uptake, which increased with the length of the spacer between guanidinium group and peptoid backbone.[133] These observations suggested that the uptake depends on the charge and especially the presence of guanidinium groups. Experiments in large unilamellar show that the uptake of arginine rich peptides correlates with the content of anionic phospholipids.[135] A physical, receptor independent mechanism was suggested, such as the formation of pores similarly to antimicrobial peptides. However, the absence of the resulting toxic leakage in the case of arginine rich CPPs did not support this model, which lead to the hypothesis of a transient pore[136,137] or the formation of inverted micells.[135,138] Both of these models include a step of coordination of the peptide by amphiphilic molecules of the lipid bilayer that contain negative charged groups such as phosphates, sulfates or carboxylates.[139] Alternatively, the binding to glycosaminoglycans is discussed.[140] A recent

study including *in vitro* and *in silico* experiments claims that carboxylates are the crucial binding partners and constitute - in combination with the membrane pH gradient - the driving force for the uptake of arginine rich CPPs.[138] This claim is supported by several facts: (i) carboxylates form far more stable hydrogen bonds with guanidinium groups than with ammonium groups, which explains the preference of arginines over lysines. (ii) A higher pH increases the concentration of deprotonated carboxylic acids and favors the formation of inverted micelles. (iii) The slightly lower pH inside cells explains the directed transport of CPPs into cells, because a higher portion of the carboxylic acids are protonated in an intracellular environment. This was proven by the migration of CPPs from one buffer to another passing a hydrophobic phase. (iv) The preincubation of cells with fatty acids increased transduction. In fact, the strong increase of cellular uptake even of proteins by using pyrenebutyrate, the deprotonated form of a very hydrophobic carboxylic acid, can be explained by this.[141,142]

It can be concluded that CPPs are taken up *via* different coexisting pathways, including endocytosis and transduction, with essentially different fates for the polypeptide and its cargo.[143] Endocytosis will lead to degradation of the polypeptide, while transduction offers direct access to the cytosol. Which pathway is followed to which extent depends on the concentration of the conjugate, the size of the cargo, and the metabolism of the cell.[122]

1.4.3.3 Pharmaceutical Applications of CPPs

Cell penetrating peptides are used for a broad range of therapeutic applications[125] wherein they are employed covalently or noncovalently[123] as well as in the combination with liposomes.[112,113] While amphipathic CPPs show severe cytotoxic effects due to causing membrane leakage, arginine rich peptides such as TAT have only mild effects.[144,145] Moreover, the cytotoxicity is dose dependent and decreases with the size of the attached cargo.[146,147]

A remaining challenge is the delivery of proteins. For *ex vivo* applications, invasive procedures like electroporation and microinjection are feasible[148] as well as noncovalent additives like endosomolytic agents.[126] For *in vivo* applications, covalent delivery is promising. However, due to their size, proteins depend on active cellular uptake mechanisms like receptor mediated endocytosis, which leads to endosomal trapping and subsequent lysosomal digestion.[148] Although cytosolic targets stay out of reach for covalently modified proteins so far, there is a high motivation for developing these strategies. One potential application are cell-penetrating antibodies for addressing intracellular targets with high specificity.[149]

2 OBJECTIVE

Chemoselective reactions are powerful tools to bind two biological entities covalently *in vitro* or *in vivo*. Ongoing efforts are invested in their identification, examining the extent of their bioorthogonality and demonstrating their utility by proof-of-principle experiments. However, these studies constitute only the first step on the way to harness the benefits of chemoselective reactions outside of the chemistry lab. In the second step, the scope of applicability of a reaction has to be explored by actually employing it to answer biological questions and solving problems that remained an unbreakable barrier before. Hence, it is necessary to work across the borders of disciplines. One important application of chemoselective reactions is site-selective bioconjugation, which empowers the scientist with unprecedented control and choice of the structures of the bioconjugate. These rationally designed bioconjugates are precious tools in chemical biology to study the importance of the site of a variety of modifications. In addition, defined bioconjugates have a high potential for pharmaceutical applications.

The aim of this work is to demonstrate the utility of chemoselective reactions for answering biological questions and presenting solutions for overcoming present borders in drug delivery. In particular, a variety of pharmaceutically relevant moieties, including PEGylation, lipidation and cell penetrating peptides, shall be conjugated to peptides and proteins to promote their applicability in an *in vivo* context. In doing so, two major problems of peptides and proteins in research and pharma shall be addressed: (i) their limited stability due to degradation, antigenic response and renal filtration, (ii) their inability to cross the cellular membrane.

GOAL 1 – STABILIZATION OF PEPTIDES AND PROTEINS *VIA* PEGYLATION

Project 1: PEGylation of peptides to stabilize them for intracellular applications.

Although PEGylation is well known to enhance residence half-life of polypeptides in serum, limited attention was paid to the effect of PEGylation in cells. This study aims to probe the effect of attaching branched PEG-modifications of varying length to peptides with respect to intracellular stability, activity, and distribution. The PEGylation will be performed by Staudinger phosphite reaction, because it allows accessing a phosphoramidate-linked branched PEG-modification by starting from simple linear PEG-reagents of low expense.

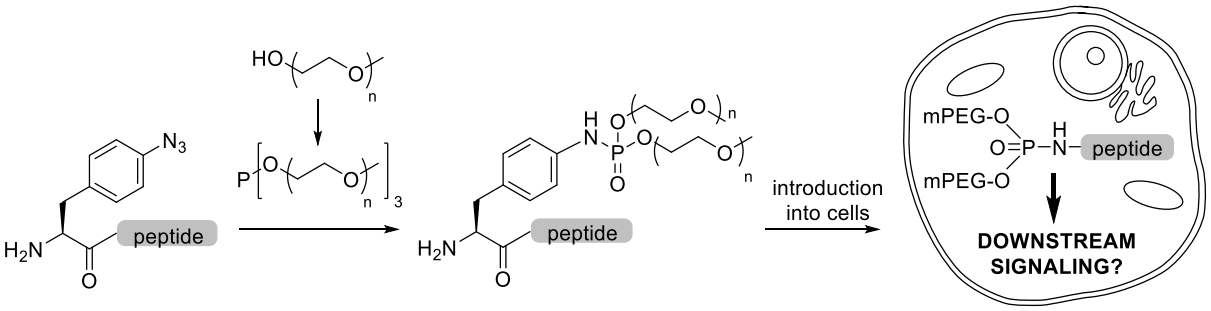

Figure 14. PEGylation of peptides to stabilize them for activating intracellular pathways.

Project 2: PEGylation of erythropoietin for improved activity.

So far, recombinant erythropoietin for therapeutic applications is synthesized in mammalian or insect cell culture which offers good yields but only limited control over the glycosylation pattern, which can hamper activity. This study aims to combine the high yields of expression systems with the control of side-chain modifications by incorporating non-canonical amino acids and addressing them with chemoselective reactions. Side-chain modification of choice is PEGylation due to its being non-toxic, non-antigenic and highly stable *in vivo*.[150] Specifically, PEGylation will be performed by Staudinger phosphite reaction to incorporate branched PEG-chains, which shield the surface of a protein more effectively due to the so-called "umbrella-effect."[151-154] Notably, EPO represents a very demanding target in the context of bioconjugation because it has a strong disposition to aggregate without any stabilizing modifications such as glycans or PEG. Therefore, it is difficult to handle in comparison to other proteins.

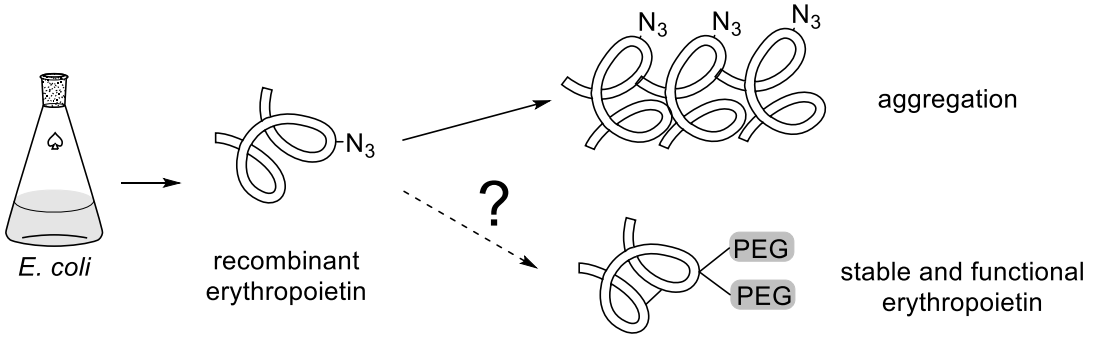

Figure 15. PEGylation strategies for stabilizing erythropoietin in solution.

Project 3: PEGylation of unimolecular liposomes.

While liposomes are an established drug-delivery system, their non-covalent composition can be problematic due to disassembly.[155] Therefore, unimolecular liposomes consisting of dendritic polymeric core-shell architectures represent a promising drug delivery vehicle with high pharmaceutical potential.[155] For simplicity, the outer hydrophilic layer of unimolecular liposomes often consists of linear PEG-chains, but they are not always sufficient for covering the surface of the carrier

entirely. In this work, we want to introduce branched PEG-modifications by the Staudinger phosphite reaction and test their impact on the solubility and the loading capacities of unimolecular liposomes.

GOAL 2 – PROMOTING PEPTIDES AND PROTEINS TO CROSS THE CELLULAR MEMBRANE

Project 4: Lipidation of peptides for localization at and crossing of the cellular membrane.

Lipidation is an important posttranslational modification for the control of the sub-cellular localization of polypeptides. Here, we aim to establish a chemoselective Staudinger-type lipidation strategy and demonstrate its structural versatility at the example of peptides that present multivalently motifs binding a central connector protein in CME. Because of lipidation, we propose that these peptides can cross and localize at the membrane in order to prevent the connector proteins inducing the assembly of clathrin coated pits and thereby inhibiting CME.

Project 5: Conjugation of cyclic CPPs for protein delivery to the cytosol.

The covalent attachment of arginine-rich cell-penetrating peptides is an established strategy to transport small cargo into the cytoplasm and nucleus of cells in a non-endocytic fashion *via* a mechanism referred to as transduction.[122] However, the mode of uptake is dependent on the size of the cargo. Big cargoes such as proteins are taken up in endocytic vesicles where they are trapped and subjected to degradation.[156] Recent work showed that cyclization of arginine-rich CPPs can greatly enhance the transduction efficiency.[157] In this study, we want to test whether the conjugation of one or several cyclic CPPs allows the transport of full-length proteins to the cytosol of living cells (Figure 16).

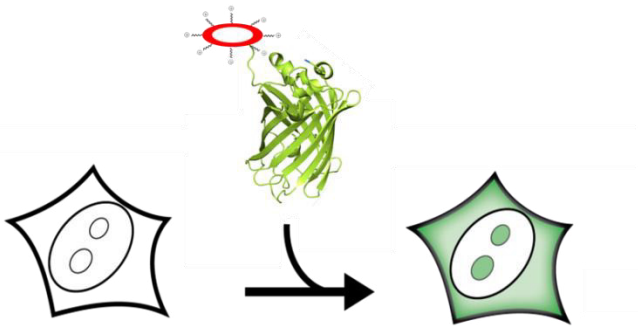

Figure 16. Covalent attachment of cyclic CPPs to proteins to enable their cellular uptake.

3 RESULTS AND DISCUSSION

3.1 Staudinger Phosphite PEGylation of Peptides for their Stabilization for Intracellular Applications

This chapter was published in the following journal:

Nicole Nischan, Alokta Chakrabarti, Remigiusz A. Serwa, Petra H. M. Bovee-Geurts, Roland Brock, Christian P. R. Hackenberger

"Stabilization of Peptides for Intracellular Applications by Phosphoramidate-Linked Polyethylene Glycol Chains"

Angew. Chem. Int. Ed. **2013**, *52*, 11920-11924. / *Angew. Chem.* **2013**, *125*, 12138–12142.

Publication Date (Web): August 22, 2013

The original article is available at: http://dx.doi.org/10.1002/anie.201303467

http://dx.doi.org/10.1002/ange.201303467

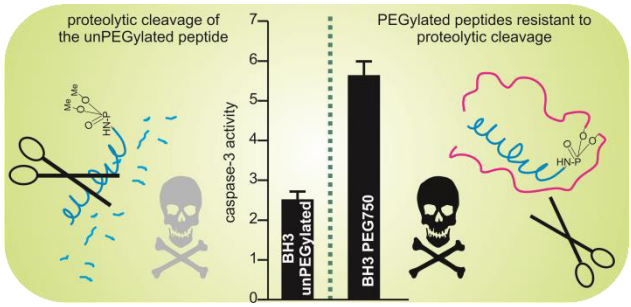

Figure 17. PEGylation stabilizes pro-apoptotic peptides against proteolysis which promotes activation of apoptosis.

Abstract

PEG intracellularly! Although long known to enhance residence half-life of peptides in serum and lysates, the effect of PEGylation on biological probes in cells has received only limited attention. Here it is shown that phosphoramidate-linked PEGylated proapoptotic peptides display a dramatically increased stability in Jurkat cell lysate and a homogenous intracellular distribution as well as high apoptotic activity after introduction into cells.

Responsibility assignment

The design of the project was provided by Christian P. R. Hackenberger and Roland Brock. Remigiusz A. Serwa performed initial reagent synthesis, peptide synthesis and conjugation experiments. The author synthesized reagents, evaluated alternative routes for the synthesis, PEGylation and isolation of peptide-probes and control peptides and studied the in-solution behavior of the peptides with dynamic light scattering. Petra H. M. Bovee-Geurts verified the concentration and fluorescence of all conjugates prior to intracellular experiments. Alokta Chakrabarti performed fluorescence correlation spectroscopy to quantify the stability of the peptides in cell lysate, studied the change of the intracellular distribution of the peptides over time and evaluated the peptides potency to trigger apoptosis by a caspase-3 assay.

Summary of content

While PEGylation of peptides and proteins is an established strategy for their stabilization for *in serum* applications and its pharmacokinetic effects are well studied, little to no information is available for the effects of PEGylation in cells. This can be attributed to the fact that peptides and proteins by themselves cannot pass the cellular membrane and reach the cytosol. To achieve this transport, delivering strategies like cell-penetrating peptides can be applied, however they are limited to small cargo. In contrast, PEGylation traditionally adds significantly to the proteins molecular weight. This complexity is the reason why the potential of PEGylation for intracellular application was unknown so far.

The goal of this study was to probe the impact of PEGylation of peptides in intracellular applications. Specifically, we tested medium-sized oligo- and polyethylene glycol chains, adding only 0.4, 1.5 or 4.0 kDa to the molecular weight of the peptide of choice. As a proof of concept, we chose a peptide derived from the BH3 domain of the proapoptotic BID protein which would allow us to take induction of apoptosis as a read-out. The chosen peptide sequence is usually undergoing proteolysis quickly which prevents it from actually activating apoptosis and was therefore considered a good target peptide.

Fluorophore-labelled BH3-peptides as well as mutated controls (mBH3) carrying an azide as orthogonal handle were synthesized using SPPS. PEGylation was performed using the Staudinger phosphite reaction which has the advantage that it creates a phosphoramidate-branching point, resulting in a peptide conjugated to a branched PEG. PEGylation of the peptides on the solid support did not allow isolation of the products. In contrast, taking advantage of the chemoselectivity of the reaction and performing the reaction in TRIS-buffer lead to minor side-product formation. PEGylated peptides could

be purified in one preparative HPLC step. The PEGylated peptides were identified by ESI-MS, purity was supported by analytical LC-UV.

Dynamic light scattering indicated that all PEGylated BH3-peptides are predominantly present as monomers at a concentration of 1 mM PBS buffer, which ensures that differences in observed intracellular effects are attributed to molecular, not supramolecular behavior of the probes.

The stability of the PEGylated peptides against proteases was tested with fluorescence correlation spectroscopy in Jurkat cell lysates. PEGylation lead to an increase of the half-life of the peptides of factors 1.5, 11 and 57 for attaching 0.4, 1.5 and 4.0 kDa branched PEGs, respectively. Addition of high concentration of proteinase K lead to complete degradation of all peptides, demonstrating that PEGylation inhibits, but not completely impedes accessibility of the peptide to proteases.

The PEGylated peptides retained a homogenous cytoplasmic distribution over a time of 6 h, as demonstrated by confocal fluorescence microscopy.

Finally, the ability of the PEGylated BH3-peptides to activate the intracellular pathway apoptosis was tested *via* a caspase-3 assay. It was found that PEGylation leads to a significant concentration-dependent increase of intracellular activity, while increasing the molecular weight of the peptide only by a factor of 1.5 compared to the unPEGylated peptide.

These results demonstrate the potential of phosphoramidate-linked PEGylated peptides for the selective targeting of intracellular biological pathways, which is of significant pharmaceutical importance.

Outlook

While this study demonstrates the power of using stabilized peptides in cells, these peptides have been delivered to cells *via* electroporation. To exploit the potential of PEGylated peptides for intracellular *in vivo* applications, other delivery strategies need to be exploited, *e. g.* cell penetrating peptides.

3.2 Staudinger Phosphite PEGylation of Erythropoietin for Improved Activity

3.2.1 Introduction of Erythropoietin as Drug Target

Erythropoietin (EPO) is a cytokine that stimulates erythropoiesis, *i. e.* the formation of red blood cells, and has been applied for renal failure related anemia for about 30 years.[158] Human EPO is a glycoprotein of 34 kDa which contains two disulfide bridges and four glycosylations (Uniprot Code P01588). These glycans consist of one branched O-glucoside and three branched N-glucosides with a certain degree of micro-heterogeneity and are essential for solubility as well as for stabilizing the protein against chemical and thermal denaturation, and proteolysis.[159]

The central problem of the biosynthesis of recombinant EPO is the heterogeneity of the sugars depending on the eukaryotic system used for the expression of the EPO gene. Recombinant EPO drug-derivatives on the market are accessed from expression in mammalian and insect cell cultures. The first expression of a recombinant EPO with similar glycosylation pattern and activity as the human form was realized in Chinese hamster ovary cells.[160,161] While expression of EPO in yeast is feasible, it results in very heterogeneous glycosylation patterns with a high degree of hypermannosylation which can evoke an immunogenic reaction. In contrast, expression in bacteria offers access to high amounts of unglycosylated EPO that is prone to aggregation after the recovery from inclusion bodies.

Homogenously glycosylated EPO can be accessed using sequential native chemical ligation (NCL).[162] NCL of synthetic peptides containing *N*-levulinyllysine, followed by covalent attachment of branched PEG containing polymers, enabled the total synthesis of an EPO that showed superior hematopoietic activity compared to the native protein.[19] Recently, the laboratory of Danishefsky succeeded in the total synthesis of an EPO-derivative that is homogeneously glycosylated at the wild-type positions.[163,164] This synthetic strategy opens the venue to attaching glycans that represent the wild-type structures and to deciphering the correlation of glycans and activity.

3.2.2 Outline of the Project

To this end, recombinant EPO for therapeutic purposes is synthesized in mammalian or insect cell culture. These techniques offer good yields but only limited control on the glycosylation pattern, which can hamper activity. On the other hand, sequential ligations achieve full control over the glycosylation pattern of EPO and even allow the introduction of synthetic polymers. However, only small amounts

of protein can be isolated *via* this rout. Here, we aim to combine the high yields of bacterial expression systems with the control of side-chain modifications *via* incorporating non-canonical amino acids and addressing them with chemoselective reactions.

Instead of using glycosylation for the stabilization of EPO in solution, we decided to use PEG, as PEGylation is known to be non-toxic and non-antigenic and leads to high stability *in vivo*.[150] Specifically, for increased stability we aim to incorporate branched PEG-chains, which shield the surface of a protein more effectively due to the so-called "umbrella-effect."[151-154] The synthesis of branched PEG-reagents can be challenging and the corresponding derivatives are usually expensive.[165] These difficulties were overcome in the Hackenberger laboratory by a two-step protocol for the conjugation of branched phosphoramidate-linked PEG-chains to peptides and proteins, in which the PEG-reagent is synthesized neat from inexpensive linear PEG-monomethyl ether and can be applied without purification in the second step, a Staudinger phosphite reaction.[101,103,166,167] This Staudinger phosphite PEGylation technology allows to the non-canonical amino acid *para*-azidophenylalanine (pAP) chemoselectively and therefore gives control over the PEGylation site. The latter has been shown to have significant influence on the pharmacokinetics of therapeutical proteins at the example of human growth hormone.[168]

Notably, EPO represents a very demanding target in the context of bioconjugation because it has a strong disposition to aggregate without any stabilizing modifications such as glycans or PEG and is therefore difficult to handle in comparison to other proteins.

3.2.3 Responsibility Assignment.

The design of the project was provided by Marina Rubini and Christian P. R. Hackenberger, the former of which is a group leader at Universität Konstanz. Marina Rubini developed a biosynthetic expression route for recombinant pAP-containing EPO. The author supplied PEG-phosphite, performed Staudinger phosphite reactions before refolding and developed protocols to evaluate the conversion of the reaction. Marina Rubini performed Staudinger phosphite reaction after refolding and purification of the PEGylated EPO products.

3.2.4 Results and Discussion

3.2.4.1 Expression of *para*-Azidophenylalanine Containing EPO-Mutants

The synthesis of pAP containing EPO mutants was designed and carried out by the laboratory of Marina Rubini. Briefly, the expression was performed in *E.coli* using genetical code engineering based on a

method developed in the Schultz laboratory, which employs an evolved tyrosyl tRNA/TyrRS pair from *Methanococcus jannaschii* to incorporate pAP at the position of an amber stop codon.[34,35] Two EPO mutants were successfully expressed containing pAP at either position 24 (**EPO p24 pAP**) or 38 (**EPO p38 pAP**), purified and sent to the Hackenberger laboratory in denaturing conditions to maintain the protein in solution.

3.2.4.2 Synthetic Route 1

After expression of recombinant EPO in *E.coli*, the formation of functional PEG-EPO-conjugates requires two steps: (i) refolding, which includes the formation of two disulfide bonds, (ii) PEGylation. The PEGylation generally needs to be performed with an excess of PEG-reagent that has to be removed after the reaction *via* dialysis or size-exclusion chromatography. The refolding of a protein is usually conducted at high dilution and is followed by concentration via dialysis. Based on the assumption that excess of PEG-reagent is not interfering in the refolding procedure, we expected that performing PEGylation followed by refolding would allow using only one purification step of dialysis for maximal recovery of PEGylated EPO (Scheme 10).

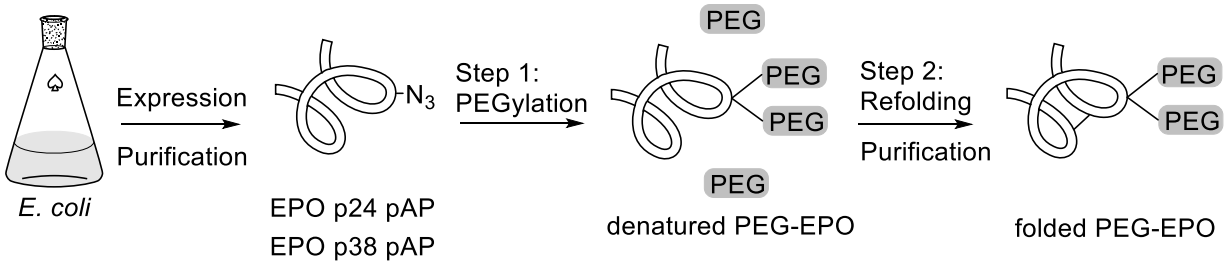

Scheme 10. Synthetic route 1. PEGylation of the EPO-mutants is followed by refolding, only one purification step is needed.

Having the two EPO mutants **EPO p24 pAP** and **EPO p38 pAP** in hand, we performed Staudinger phosphite PEGylation - as reported before – in Tris buffer at pH8 and 30 °C for 72 h,[101,103,166,167] with the difference that denaturing buffer was present in addition. PEG-phosphites contained either short PEG-chains of a molecular weight of 200 Da (**PEG200**) or medium PEG-chains of 750 Da (**PEG750**) and were added to the reaction mixture with either 10- or 100 fold excess.

To analyze the conversion of the PEGylation of proteins, mass spectrometry is the method of choice because it provides the exact mass of the protein, although the polydispersity of the PEG-molecules clearly marks a challenge in analysis.[169] In fact, in spite of various efforts to improve the sample preparation, it was not possible to detect any protein signal with standard mass spectrometry methods including MALDI- and ESI. This can be explained by the fact that EPO and PEG each are difficult to analyze with mass methods. In addition, the reaction sample contains high concentration of excess of

PEG-reagent as well as guanidinium hydrochloride, both of which have to be removed prior to analysis. However, to identify a feasible desalting protocol is challenging because the removal of guanidinium hydrochloride induces the aggregation of EPO. The desalting protocols that were tried included chromatography on FPLC, dialysis and precipitation in acetone, none of which led to the detection of any protein. An external partner was asked to analyze the samples *via* ESI, which lead to a similar result. Finally, the PEGylation reaction was directly followed by refolding according to a protocol supplied by Marina Rubini. However, concentration of the refolding solution was impossible due to aggregation of protein. Separation of protein aggregates *via* centrifugation was not successful. Using the desalting protocols described above, no protein could be detected using MALDI-MS or SDS-PAGE.
Considering the challenges in reaction work up, fractions of the reaction solutions were directly applied in SDS-PAGE. While high salt concentrations are not advisable in SDS-PAGE because they can change the running behavior and lead to artifacts, SDS-PAGE offers information whether protein present. Indeed, all reactions showed bands in the gel that can correspond to expressed EPO albeit the bands were very blotchy (Figure 18 B) which made it impossible to draw conclusions as to whether the proteins carry a modification of 0.4 or 1.5 kDa, respectively. For a qualitative conclusion, the gel was subjected to Western Blot analysis (Figure 18 C). Interestingly, incubation with a commercial antibody against the methoxy group of PEG (anti-PEG-B-47) stains all reactions that contained PEG750 phosphite in a region of 20 kDa that corresponds to covalently or non-covalently PEGylated EPO and in the low molecular range that can correspond to excess phosphite. In contrast, none of the reactions containing PEG200 phosphite shows any signal. This suggests that, in order to be detected by this antibody, the PEG monomethylether has to contain more than four PEG-units.
In the following, a thorough screen for strategies to desalt the protein was undertaken with the goal to facilitate accurate analysis *via* SDS-PAGE. This was done using the mutant **EPO p24 pAP**. In contrast to previous attempt to desalt, every procedure was done very quickly to minimize interaction time of desalted EPO with membranes or column materials. In addition, the aim was not complete desalting but just the reduction of the salt content to 100 mM, which is compatible with SDS-PAGE conditions.
One strategy to reduce the concentration of salt employed micro bio-spin columns P-30, a size exclusion chromatography system, which did not result in a protein band in SDS-PAGE (Figure 19 B, lane 1). Alternatively, Zip Tip®s containing either C18 or C4 reversed phase material for the desalting of peptides and proteins were used according to the provided instructions, however, no protein band could be detected (Figure 19 B, lane 2 and 3). In addition, spin filters with a cutoff of 3 kDa were used with 0.1 % SDS in 100 mM Tris buffer to avoid aggregation of EPO and spun down only once, likewise, no protein was detected (Figure 19 B, lane 4). Finally, a size exclusion material Sephadex G25 was used to elute the protein and retain the salts. Two bed sizes were tried, 200 µL and 500 µL with a dead

volume of 70 and 200 µL, respectively. The smaller bed of 200 µL resulted in a clear protein band, while with the 500 µL bed no protein could be detected (Figure 19 B, lane 5 and 6), supposedly due to the increased interaction area of protein and stationary phase.

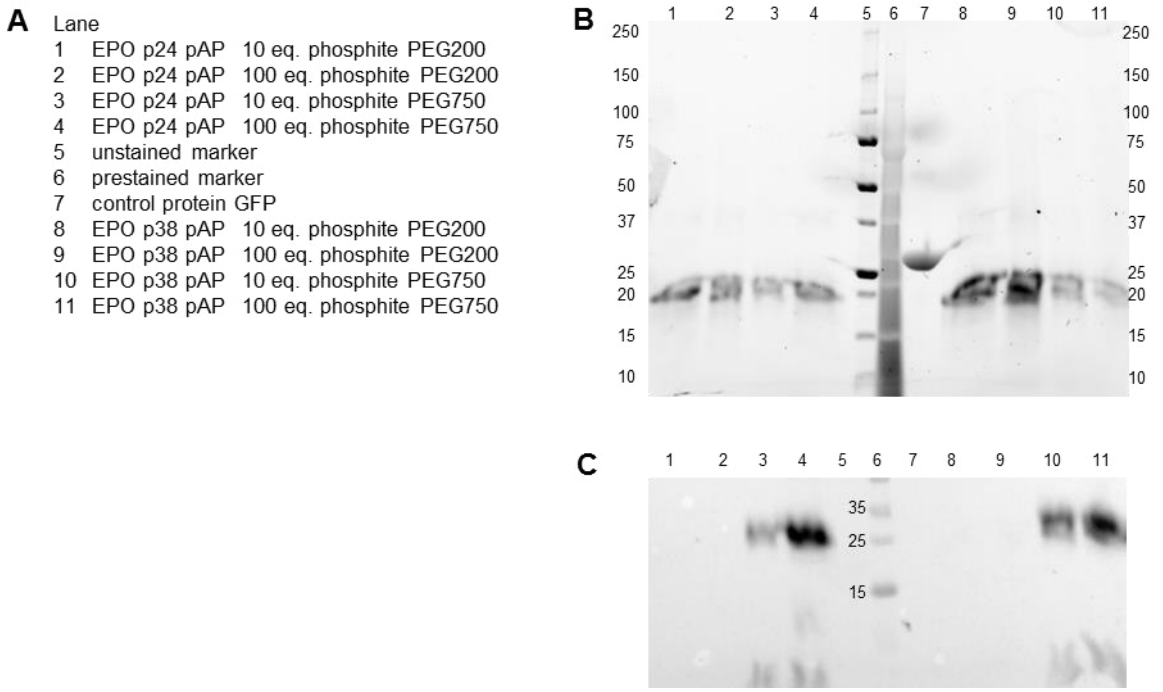

Figure 18. Direct SDS-PAGE and Western Blot of EPO mutants incubated with PEG200 and PEG750 phosphite. (A) Legend. (B) SDS-PAGE. C The corresponding Western blot against anti-PEG-B-47 only stains lanes of reactions containing PEG750 phosphite.

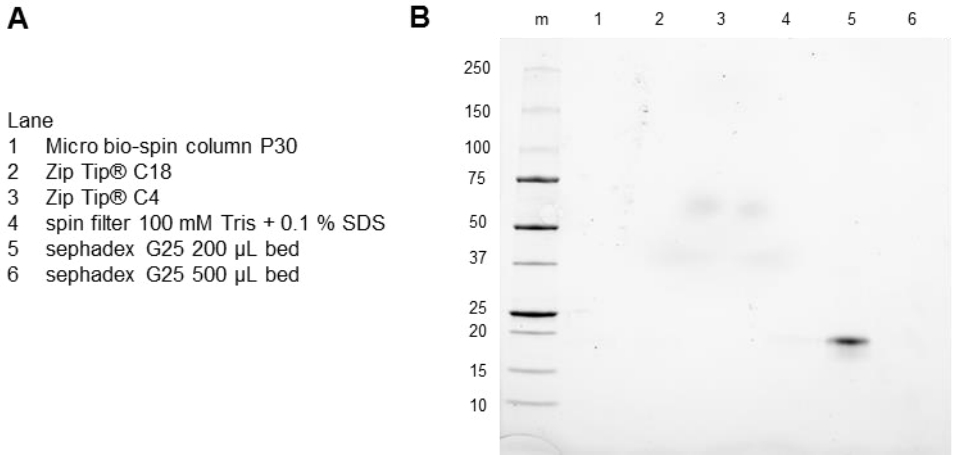

Figure 19. Screening of different protocols to decrease salt concentration in EPO samples. (A) Legend. (B) SDS-PAGE.

With this salt removal protocol in hand, the PEGylation reaction of both **EPO p24 pAP** and **EPO p38 pAP** were analyzed by SDS-PAGE and Western blot against anti-PEG-B-47 (Figure 20). First, **EPO p24 pAP** was incubated with or without different amounts of PEG750 phosphite, followed by filtration over

Sephadex and immediate loading to the SDS-gel (Figure 20 A lane 1-3). In order to visualize a small band shift of 1.5 kDa, the reaction mixtures and unreacted protein were mixed (Figure 20 A, Lane 4 and 5). While all entries show similar intensities in the UV, which accounts for the reproducibility of the work-up procedure of **EPO p24 pAP**, no band-shift could be detected. Western blot analysis of this gel results in weak bands for only those entries that contain PEG-phosphite (Figure 20 B). Interestingly, if the band pattern of the pre-stained markers and the protein-bands of entries 1 and 2 is transferred from the SDS-gel onto the corresponding Western blot, the position of the protein bands is empty (Figure 20 C). Clearly, the Western blot signal is shifted. From this observation it follows that the reaction of EPO-mutant and PEG-phosphite results in a product of shifted mass, and that the conversion of this reaction is very low.

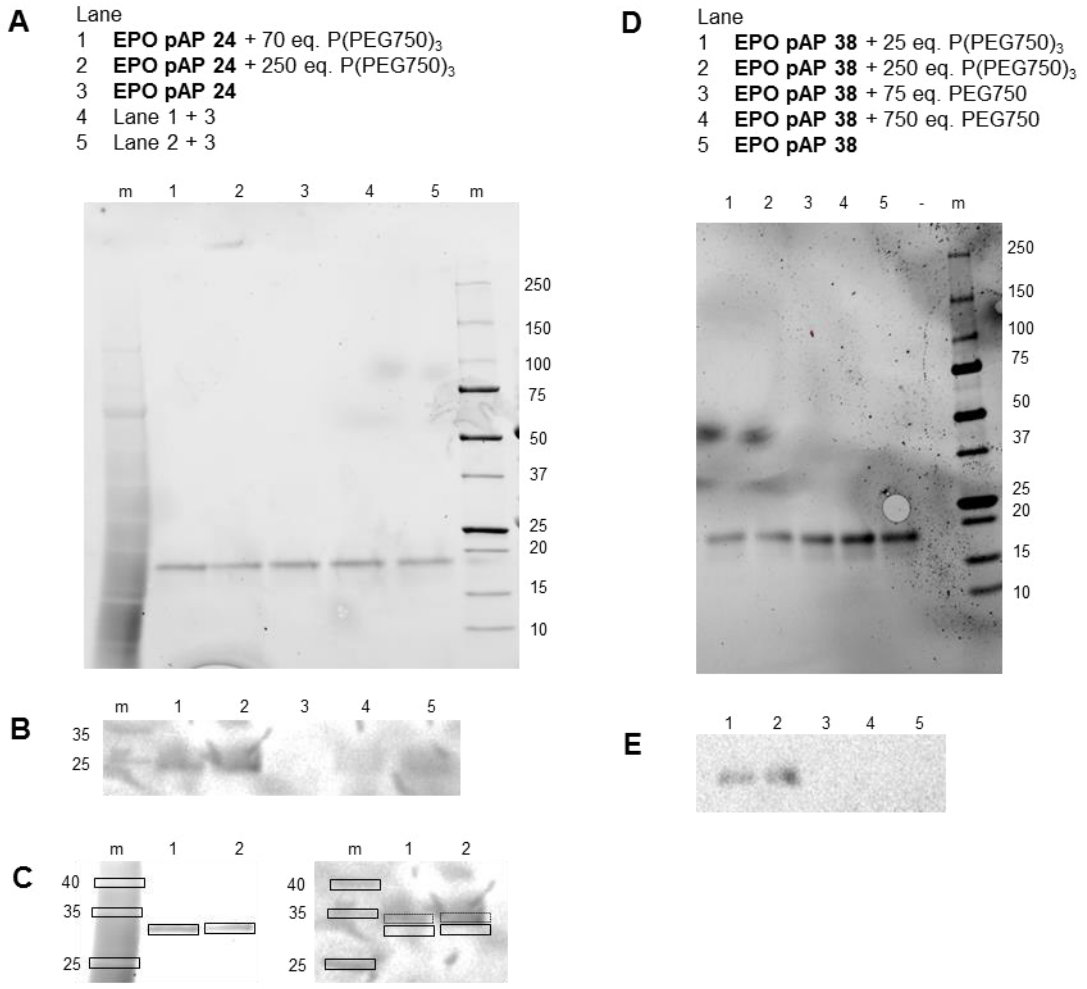

Figure 20. SDS-PAGE and Western Blot of EPO mutants incubated with PEG200 and PEG750-phosphite after reduction of salt content. (A) SDS-PAGE of **EPO p24 pAP**. (B) Corresponding Western blot. (C) Side-by side comparison of SDS-PAGE of A and Western blot of B, which reveals that the respective bands are shifted. (D) SDS-PAGE of **EPO p38 pAP**. (E) Corresponding Western blot, which demonstrates that a covalent linkage is formed between EPO-mutant and PEG-phosphite.

To test whether the PEG750-phosphite and EPO-mutants can form non-covalent bonds, **EPO pAP 38** was either treated with PEG750-phosphite or with an equivalent amount of PEG750-alcohol followed by analysis as described above. Although the reaction samples contained the same amounts of protein, the bands resulting from **EPO pAP 38** show differences in intensity which is in contrast to the gel of **EPO p24 pAP** (Figure 20 A and D). The Western blot results in bands only for those samples that contained phosphite (Figure 20 E, which supports that, upon incubation of EPO-mutants and PEG-phosphites, a covalent linkage is formed.

In summary, performing Staudinger phosphite PEGylation of EPO-mutants in denaturing buffer leads to PEG-EPO-conjugates, albeit with very low conversions. Supposedly, the latter is caused by either high concentrations of guanidinium hydrochloride and nucleophiles such as mercaptoethanol. Previously, the Staudinger phosphite reaction had not been performed under these conditions. To which extent these reagents influence the reaction by nucleophilic attack at intermediates or even at the phosphoramidate product is an interesting question to study. For the present goal, conjugating PEG-phosphites to EPO-mutants, we concluded that an alternate strategy needs to be explored.

3.2.4.3 Synthetic Route 2

Accordingly, we sought to establish an improved refolding protocol for the EPO mutants that would allow subsequent PEGylation with minimal loss due to aggregation (Scheme 11). As the expertise for this is in the group of Marina Rubini, the project from here on was transferred to that group and is still in progress.

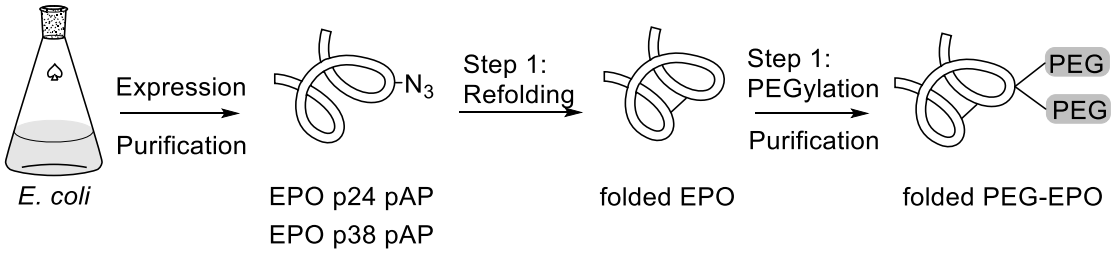

Scheme 11. Synthetic Route 2. PEGylation of EPO-mutants is performed after refolding.

3.2.5 Conclusions and Outlook

Staudinger phosphite PEGylation of pAP containing unfolded EPO-mutants was successful in denaturing conditions, albeit with low yields. To improve conversion, PEGylation should be done under not denaturing conditions and without β-mercaptoethanol after improved refolding. Once PEG-EPO

can be isolated in sufficient amounts, the conjugates will be evaluated for their activity using for instance the colony forming units assay.

3.3 Staudinger Phosphite PEGylation for the Synthesis of Unimolecular Liposomes

3.3.1 Introduction to Unimolecular Liposomes

While liposomes, whose self-assembly is driven by non-covalent interactions, are an established and popular drug-delivery system, temperature or pressure can lead to their disassembly; therefore, unimolecular liposomes consisting of dendritic polymeric core-shell architectures represent a promising drug delivery vehicle with high pharmaceutical potential (Figure 21).[155] Advantages of unimolecular liposomes are their defined size and that they tolerate both hydrophilic and hydrophobic cargo.

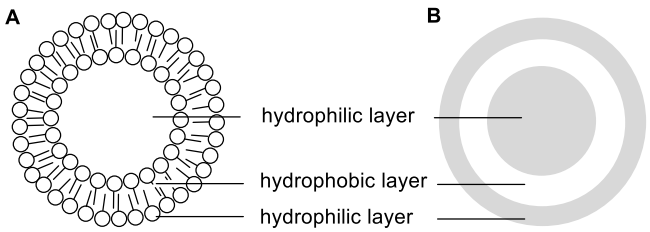

Figure 21. Composition of Liposomes. (A) Conventional liposomes are assembled from amphiphilic molecules. (B) Similarly, a unimolecular liposome consists of one molecule with a hydrophilic core (grey center) that is enclosed by one hydrophobic layer (white shell) and one hydrophilic layer (grey shell).

One of these unimolecular delivery systems are core-multi-shell (CMS) nanotransporters that consist of a hyperbranched polyglycerol core (hPG, Figure 22) surrounded by one layer of C18-alkyl-chains and one layer of monomethoxy PEG.[155] It was demonstrated that these CMS can be loaded with both hydrophilic and hydrophobic cargoes[170-172] while having no influence on cell viability.[173]

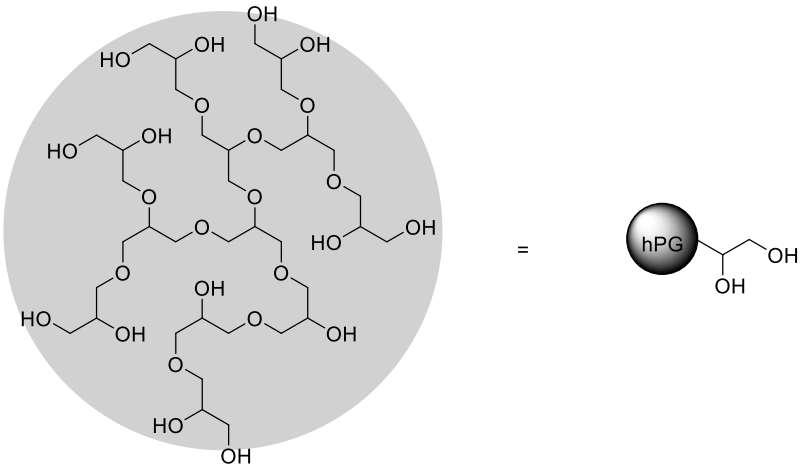

Figure 22. Basis of the structure of the polyglycerol core of CMS.

3.3.2 Outline of the Project

So far, the outer hydrophilic layer of CMSs consisted of linear PEG-chains. Due to the dendritic architecture, linear PEG-chains are not always sufficient for covering the surface of the CMS enough to grand solubility. In this work, we want to test the impact of branched PEG-reagents on the solubility and loading capacities of CMS nanocarriers.

Specifically, we aim to simplify the synthetic protocol to construct such CMS nanocarriers. After coupling hPGs *via* amide or ester bond with a lipophilic linker that contains an aromatic azide, we will employ Staudinger phosphite PEGylation to attach a PEGylated phosphoramidate branching point (Scheme 12). The resulting PEGylated CMS architectures will be compared to previously reported CMS with regard to their solubility as well as their loading capacity in encapsulation studies.

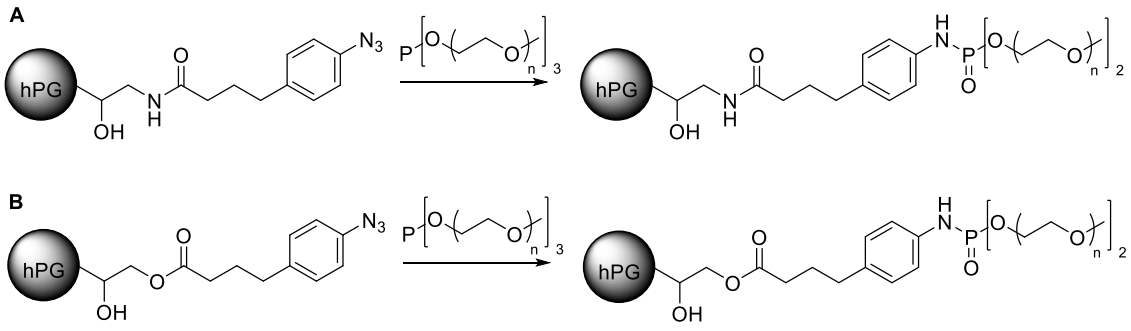

Scheme 12. Synthesis Outline for CMS PEGylated *via* a phosphoramidate branching point. (A) Amide linkage. (B) Ester linkage.

3.3.3 Responsibility Assignment

The design of the project was provided by Rainer Haag and Christian P. R. Hackenberger. Rahul Tyagi and Indah Nurita were responsible for synthesis and upscaling of the ester or amide coupled hPGs. The author supplied PEG-phosphite, performed Staudinger phosphite reaction and developed a protocol for the workup of the PEGylated hPG. Peter Schmieder performed NMR-experiments of the final polymer.

3.3.4 Results and Discussion

An initial test reaction was performed with an hPG modified to 70 % with the lipophilic linker *via* amide bound (**hPG1**). The PEGylation reaction was conducted on a 15 mg scale of polymer with PEG200-phosphite and the conversion was followed by IR and phosphorous NMR (Scheme 13). Removal of PEG200-phosphite was possible *via* dialysis against chloroform. In contrast to the starting material **hPG1**, the resulting product **PEG200-hPG1** was water soluble which is why no longer PEG-phosphites were explored. Notably, characterization of the product was challenging. Due to prominent signals of hPG and PEG ^{1}H- and ^{13}C-NMR-spectra, no conclusion could be drawn as to the ratio of the signals. Accordingly, the product was only supported by IR and ^{31}P-NMR spectra.

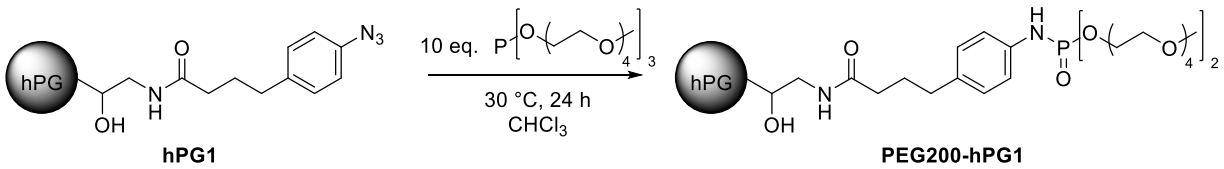

Scheme 13. Test reaction for the PEGylation of hPGs using **hPG1** and PEG200-phosphite.

In order to do a proper characterization and loading experiments with the hPGs, bigger amounts of material needed to be supplied which is why scaling up was the next step. Interestingly, the synthesis of the modified hPGs at bigger scale leads to solubility problems. To this end, only an hPG modified to 35 % *via* ester linkage with the azido linker (**hPG2**) could be synthesized by the Haag laboratory in bigger scale. Accordingly, the developed PEGylation protocol was applied to **hPG2** at tenfold scale in chloroform (150 mg, Scheme 14). The reaction was successful as followed by ^{31}P-NMR, however, dialysis against chloroform did not achieve the separation of excess PEG-reagent, nor did dichloromethane or EtOAc. Successful removal of excess PEG-phosphite was achieved by hydrolysis in 0.05 % TFA followed by dialysis against water. With this protocol, **PEG200-hPG2** could be purified using

solely water and small amounts of TFA with very high recovery. The resulting product was characterized by ^{1}H- and ^{31}P-NMR as well as heteronuclear coupling experiments in order verify that the PEG-chains are linked covalently to the hPG.

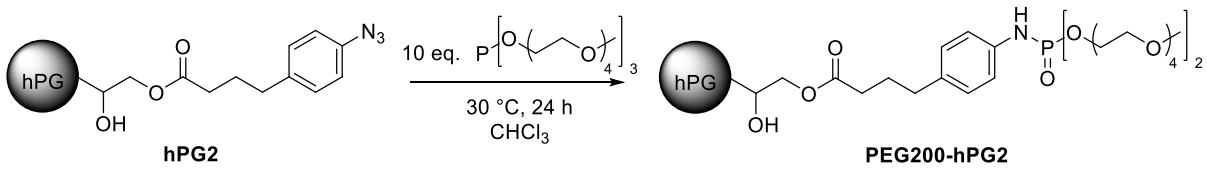

hPG2 PEG200-hPG2

Scheme 14. Scaled-up reaction for the PEGylation of hPGs using **hPG1** and PEG200-phosphite.

Heteronuclear coupling experiments were performed by Peter Schmieder. ^{1}H-^{31}P-hetronuclear multiple bond correlation (HMBC) spectroscopy of **PEG200-hPG2** shows several couplings of the single phosphorous atom (Figure 23). There is a correlation between the phosphorous and the protons at positions 11 and 12 *via* either three or four bonds which demonstrates the covalent linkage to the PEG-chains. In addition, the phosphorous atom couples with the proton at the nitrogen *via* two bonds, and with the proton at position 5 *via* a rarely observed "W"-type coupling over five bonds.

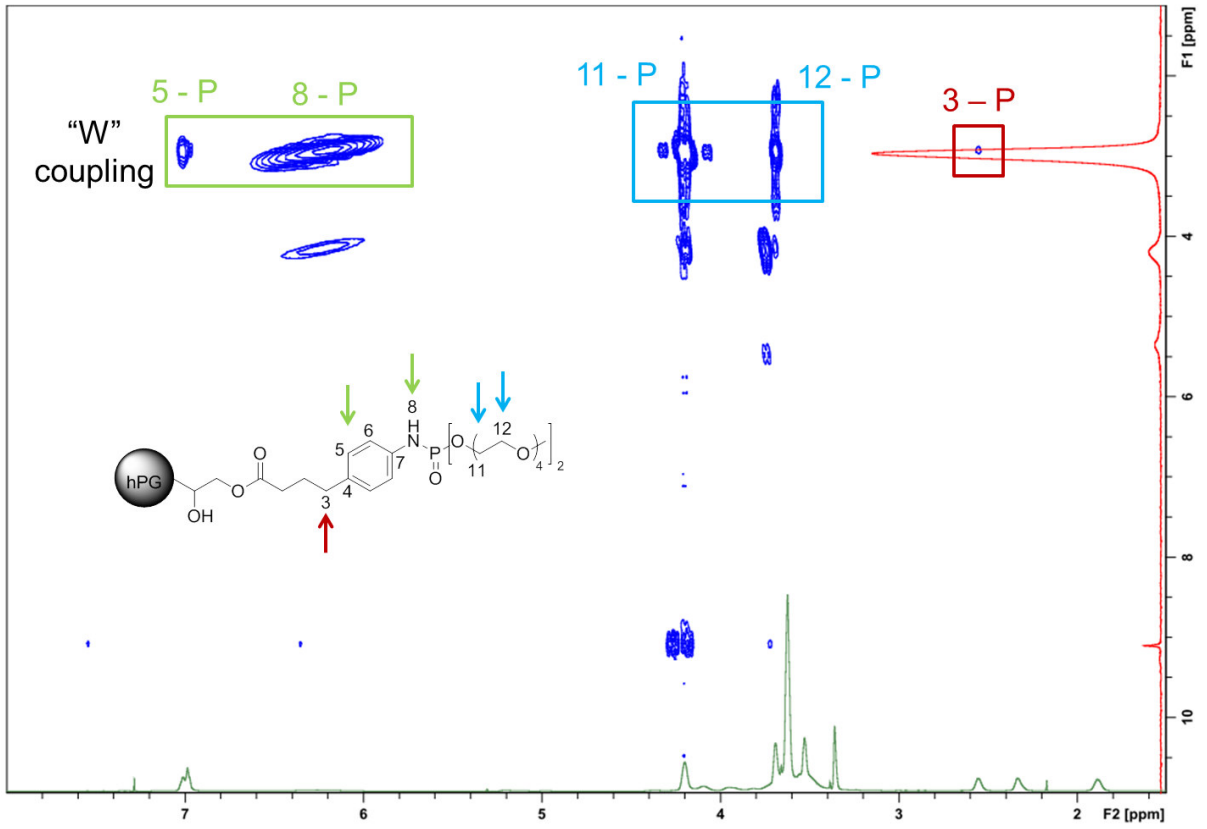

Figure 23. ^{1}H-^{31}P-HMBC of **PEG200-hPG2**. The single phosphorous atom shows correlations both to the PEG-protons as well as the protons on the aryl-linker.

These observations confirm the formation of a covalent bond between PEG-chains and **hPG2** *via* a phosphoramidate branching point. Still, all NMR spectra reveal the presence of small but considerable amounts of impurities that could not be identified at this point.

3.3.5 Conclusions and Outlook

CMS nanocarriers could be successfully solubilized in water by attaching two PEG-chains of only four PEG-units to the functional groups on the surface, which was achieved by using Staudinger phosphite reaction. Due to this complete water solubility, the reaction mixture could be sufficiently purified from excess of PEG-reagent by dialysis against double distilled water. To this end, this protocol was demonstrated at a CMS of 10 kDa molar weight that had been functionalized (35 %) *via* ester linkage with a lipophilic aryl-azido linker. The resulting product was characterized using heteronuclear NMR.
In the future, the developed procedure will be applied to synthesize a library of CMS nanocarriers by varying (i) the functionalization degree, (ii) the attachment of the azide-linker: amide versus ester linkage. The resulting PEGylated CMS will be evaluated for their loading properties.

3.4 Lipidation

3.4.1 Introduction to Clathrin-Mediated Endocytosis

Endocytosis is crucial for the uptake of nutrients and for the regulation of the lipid and protein content of the plasma membrane of a cell.[174] One type of endocytosis is triggered exclusively by membrane-exposed receptor binding to their substrates, which is therefore referred to receptor-mediated endocytosis. The observation that this uptake is exclusively taking place *via* clathrin coated vesicles also termed this type clathrin mediated endocytosis (CME).[175,176] In the complex network of assembling proteins, the adaptor protein complex 2 (AP2) is one of the two major hub proteins next to clathrin triskelia.[177] Essentially, CME starts by membrane bound receptors binding to their extracellular substrates, which induces the recruitment of coat proteins such as AP2 and clathrin to assemble clathrin coated vesicles.[178] Binding of dynamin facilitates fission of the vesicle from the membrane followed by dis-assembly of the coat proteins (Figure 24).[178]

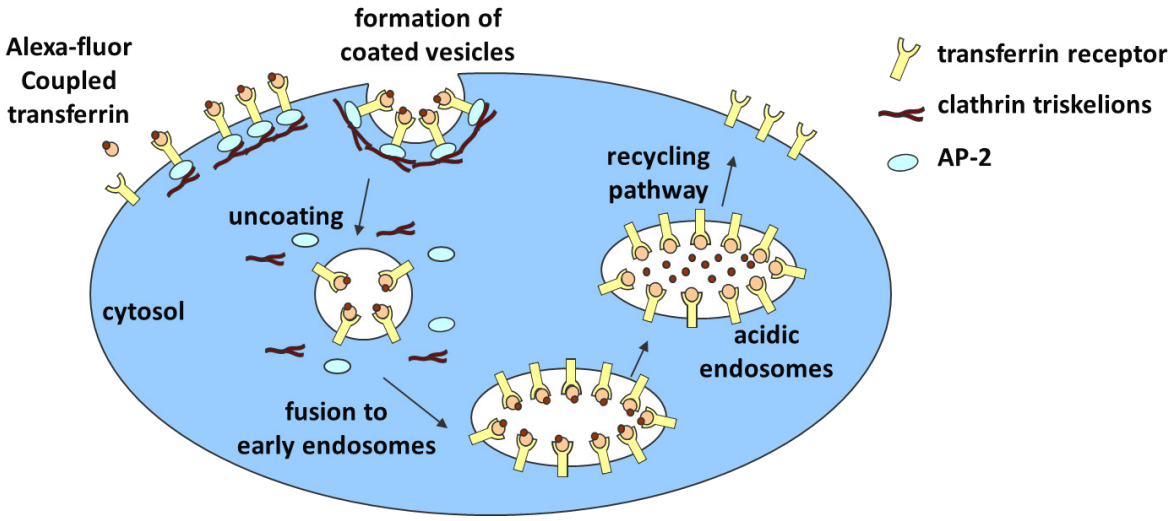

Figure 24. A cell undergoing CME exemplified by the uptake of transferrin by the transferrin receptor, which is harnessed for a well-established assay for the quantification of CME.

To study the function of clathrin, a tool for acute perturbance is ideal as side-effects and compensations would be circumvented with comparison to knock-out or knock-down experiments. Such an acute inhibitor of clathrin binding was presented by Kleist *et al*. in the form of Pitstop®, a small molecule inhibitor that has been identified by library screenings and optimizing lead hits.[179,180] With this tool in hand, other roles of clathrin next to being a connector protein in CME could be studied.[181] In fact, clathrin plays also a role in the formation of the cytoskeleton, in intracellular transport, and

during mitosis.[182] Therefore, inhibiting clathrins function leads to many side effects besides to stopping CME. In order to selectively inhibit CME without perturbing other intracellular events, AP2 displays another potential target.

The alpha-ear of AP2 is known to interact with many other proteins during the formation of clathrin coated pits. One of these binding partners is the COOH-terminal domain of EPS15 protein[183,184] that is discussed to bind *via* repeating peptide motifs such as DPF or DFNXF to the alpha ear of AP2,[185] which is supported by binding studies.[177]

3.4.2 Outline of this Project

The first goal of this project is to design lipidated peptides that can cross and localize at the cellular membrane, with particular stress on developing different lipidation architectures. These peptides carry several repeats of motifs that are reported to interact with the alpha appendage of AP2, and should by binding to this protein disturb clathrin coated pit assembly and thereby inhibit CME (Figure 25).

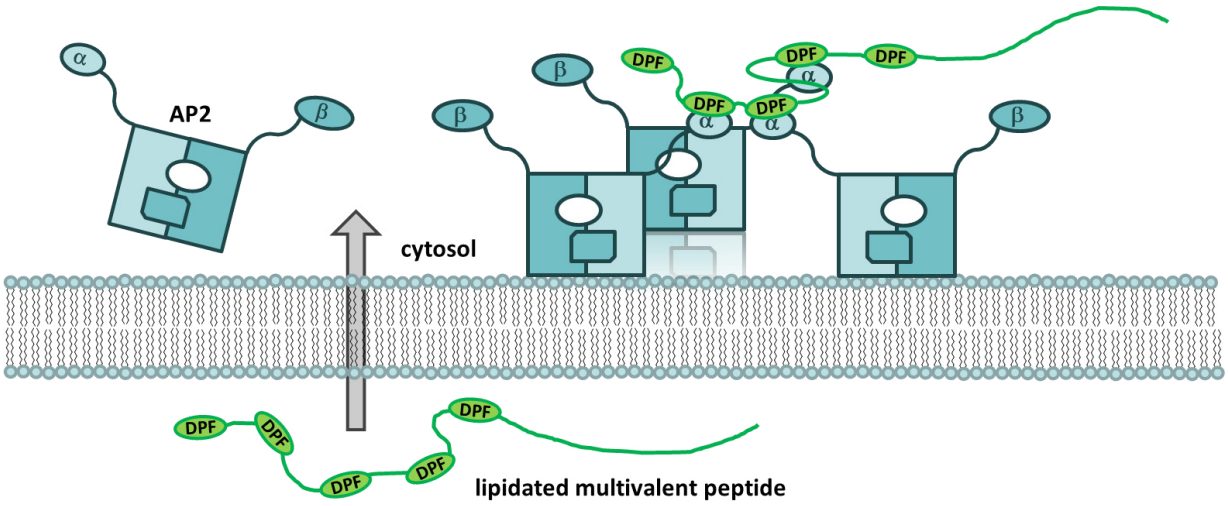

Figure 25. Lipidation promotes cellular uptake and membrane localization of peptides which present DPF binding motifs in a multivalent fashion and bind the α-appendage of AP2, thereby perturbing the formation of clathrin coated pits and inhibiting CME.

3.4.3 Responsibility Assignment.

The design of the project was provided by Volker Haucke and Christian P. R. Hackenberger. Wiebke Stahlschmidt performed the majority of transferrin uptakes. The author was responsible for the design and synthesis of the mono- and dilipidated peptides and performed transferrin uptakes.

3.4.4 Results and Discussion.

The most straightforward way to synthesize lipidated peptides *via* SPPS is the coupling of a fatty acid to the N-terminus. Experiments performed before the work shown here employed the coupling of a stearic acid to the N-terminus of a multivalent peptide sequence derived from the EPS15-protein that contains several DPF-amino acid motifs to perturb CME.[186] This lipidated peptide lead to a specific and concentration dependent Inhibition of CME. However, a change of membrane integrity was observed which suggests side effects. In this work, it was aimed (i) to establish a novel lipidation strategy by Staudinger phosphite reaction and (ii) to synthesis different lipidated peptides an test their effect on CME.

3.4.4.1 Monolipidation

Following previous conducted experiments, a synthetic route to yield mono-lipidated peptides *via* Staudinger phosphite reaction was designed. In order to transfer only one modification of choice, here an alkyl chain, to the peptide of choice, unsymmetrical phosphites were used.[98] Staudinger phosphite reaction of aryl azides and unsymmetrical phosphites leads to two different phosphoramidate products. A screening of different oxy-substituents on the phosphite revealed that benzyl-substituents next to the function of choice result in a favorable ration of mono-functionalized to non-functionalized phosphoramidate product.[98] Recently, it was found that during Staudinger phosphite reaction pyridyl-substituents lead to similar product ratios as benzyl-substituents, with the major advantage that the phosphites are comparatively stable to hydrolysis.[104] Therefore, it is possible to purify the phosphites using silica column chromatography and store them for several months under argon at -20 °C.

One special focus of this study is the influence of different lipid lengths on the inhibition of CME, which is why several unsymmetrical phosphites were synthesized that carry as lipid chain either a linear decyl-, tetradecyl- or octadecyl-chain and as leaving groups pyridyl-substituents (**52**, **53** and **54**, respectively; Scheme 15 A). The phosphites were synthesized by subsequently substituting chloride substituents of phosphorous trichloride (**49**) against amine- and finally oxygen-substituents.[187] Specifically, starting from phosphorous trichloride (**49**), first one chloro-substituent was exchanged against a secondary amine to yield in *N*,*N*-diisopropyl-phosphoramidous dichloride (**50**). Subsequently, the next two chloro-atoms were substituted against pyridylmethyl-groups to give the phosphoramidate **51** with a yield of 55 % (Scheme 15 A). Finally, the amine substituent was exchanged against the alkyl-alcohol of choice to yield in decyl-phosphite **52**, tetradecyl-phosphite **53** and octadecyl-phosphite **54** with moderate yields in high purity. The compounds were characterized by ^{1}H-, ^{13}C- and ^{31}P-NMR as well as with high resolution MS.

To determine the influence of the leaving group, it was also tried to synthesize an octadecyl-phosphite with benzyl-leaving groups (**56**, Scheme 15 B). In contrast to the pyridyl-phosphites, column purification lead to hydrolysis which is why phosphite **56** was used without further purification in the following steps.

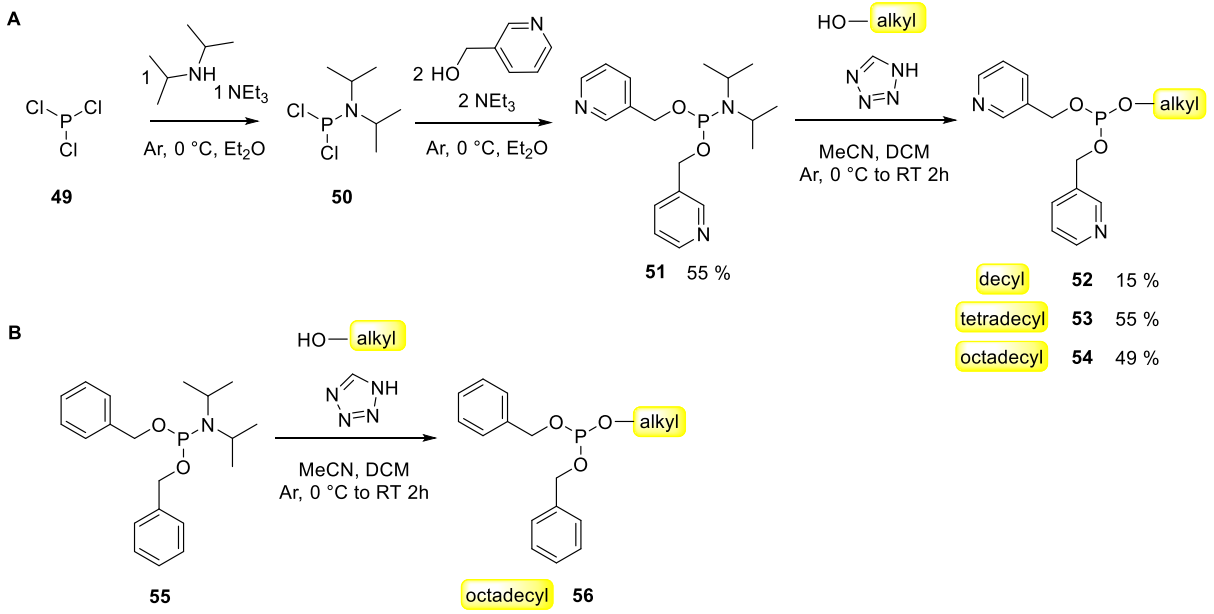

Scheme 15. Synthesis of unsymmetrical substituted phosphites. (A) Starting from phosphorous trichloride (**49**), one chloro substituent is exchanged against a secondary amine to yield in *N*,*N*-diisopropyl-phosphoramidous dichloride (**50**). Substitution of the next two chloro-atoms against pyridylmethylalcohol yields in the phosphoramidite **51**, followed by introduction of the alkylalcohol resulting in the unsymmetrical substituted phosphites **52**, **53** and **54**. (B) Synthesis of octadecyl-dibenzylphosphite **56**.

With the alkyl-phosphites **52**, **53** and **54** in hand, lipidated peptides **57**, **58** and **59** could be synthesized using Staudinger phosphite reaction. For this, an EPS15 derived peptide sequence as used in preliminary studies was synthesized using SPPS on a rink amide resin (Figure 26 A). Azido benzoic acid was coupled to the N-terminus followed by incubation of the resin with 5 equivalents of phosphite **52**, **53** or **54** in DMF, acidic deprotection and semi-preparative HPLC. Notably, no starting material was observed and the lipidated and non-lipidated products could be readily separated (Figure 26 B). Based on the yields of both main products and side products **60**, it can be concluded that the selectivity of Staudinger phosphite reaction using the pyridyl-leaving group is good (5 : 1) to very good (10 : 1) (Figure 26 C). The overall peptide yields are very good, taken into account that this is a 30 amino acid peptide after preparative HPLC.

Notably, this synthetic approach does not require to be performed on the solid support. Due to the remarkable stability of the lipid-pyridyl-phosphoramidate peptides to TFA-cleavage conditions, here it was performed on the solid support which minimized purification steps for maximal yields.

This procedure was also applied to octadecyl-benzyl-phosphite (**56**). However, the resulting phosphoramidate was not stable to TFA-conditions, only the reduced azide could be detected. Accordingly, the azido-peptide **61** was purified using HPLC followed by reaction with the phosphite **56** in solution (Scheme 16). Due to the low solubility of peptide and phosphite, the reaction had to be performed in DMSO, followed by DMSO removal and purification *via* HPLC, which afforded the octadecyl-benzyl-phosphoramidate modified peptide **62** with a yield of 31 %.

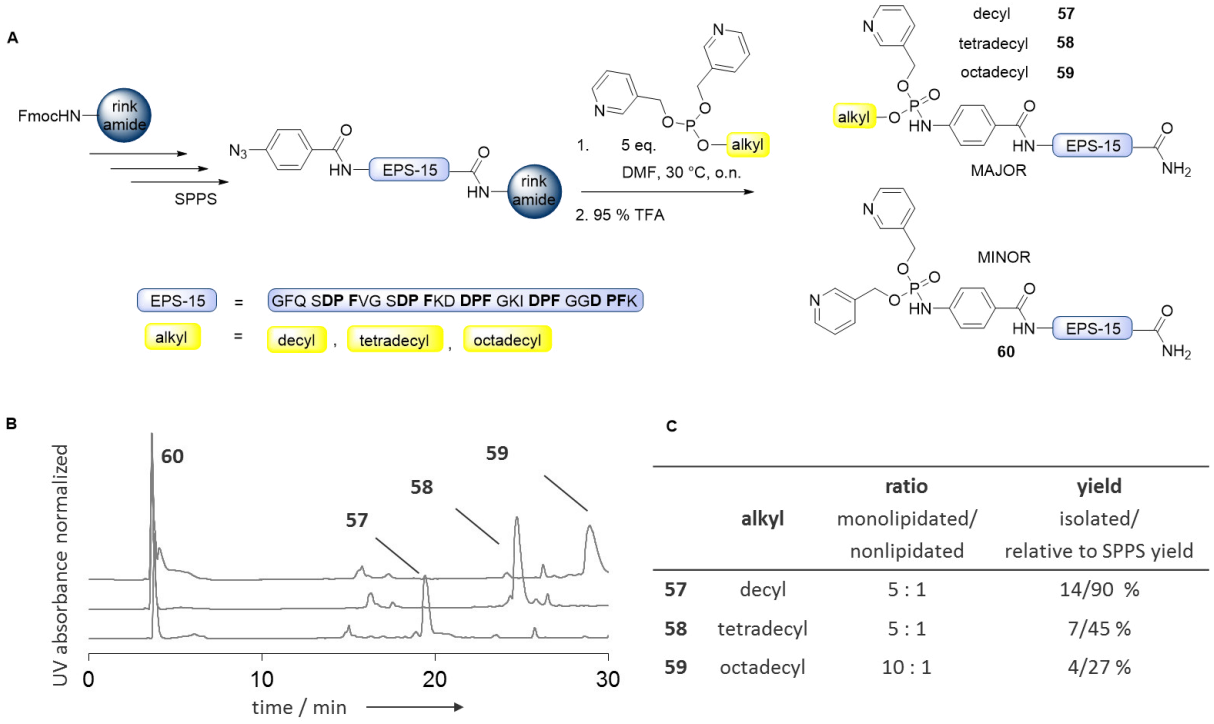

	alkyl	ratio monolipidated/ nonlipidated	yield isolated/ relative to SPPS yield
57	decyl	5 : 1	14/90 %
58	tetradecyl	5 : 1	7/45 %
59	octadecyl	10 : 1	4/27 %

Figure 26. Synthesis of monolipidated multivalent peptides. (A) Azido-peptides presenting several DPF-amino acid motifs were synthesized by SPPS and Staudinger phosphite reaction was performed with different phosphites on the solid support followed by TFA cleavage to yield in a monolipidated product and a non-lipidated side-product. (B) Product and side-product of Staudinger phosphite reaction could be readily purified using reversed phase HPLC. (C) The ratio of product and side-product of Staudinger phosphite reaction was determined based on the yield. The selectivity was good to very good. Total yields of the lipidated peptides were very good taking into account the yield of the SPPS.

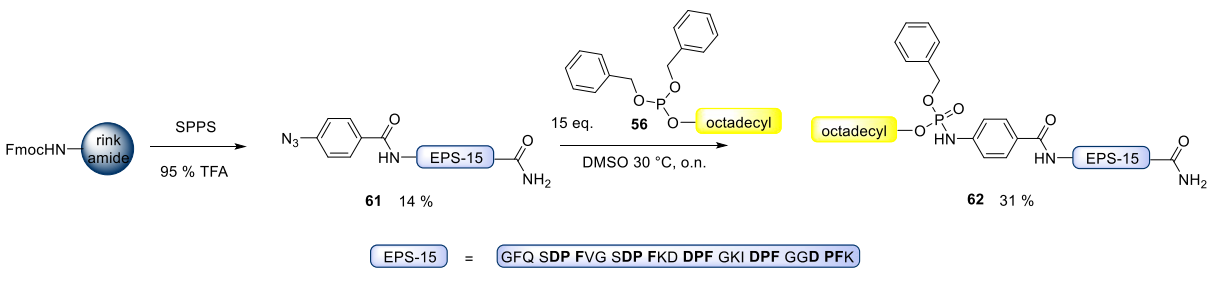

Scheme 16. Synthesis of octadecyl-benzyl-phosphoramidate (**62**) in solution.

These monolipidated EPS15 peptides were evaluated on their potential as CME inhibitors via a transferrin uptake assay (Figure 27), performed by Wiebke Stahlschmidt. Therein, human cervical cancer cells (HeLa) were starved and pre-incubated with the peptide probes for 60 min, followed by 15 min of transferrin uptake with Alexa-labelled transferrin. Afterwards, cells were fixed, mounted and analyzed by epifluorescence microscopy. The sum of fluorescence intensity is proportional to the amount of transferrin taken up. Uptakes performed at peptide concentrations of 10 and 20 µM suggest a correlation between the length of lipid and inhibition of CME (Figure 27 C). Incubation with the decyl-pyridyl-modified peptide (**57**) had no influence, whereas the tetradecyl-pyridyl-peptide (**58**) shows about 10 % and octadecyl-pyridyl-peptide (**58**) about 30 % of reduction of transferrin uptake. However, transferrin uptake with the octadecyl-pyridyl-peptide at higher concentration did not show an increase of inhibition, suggesting non-specific interactions.

Notably, incubation with the octadecyl-benzyl-peptide (**58**) lead to essentially similar results as the incubation with the octadecyl-pyridyl-peptide (**62**).

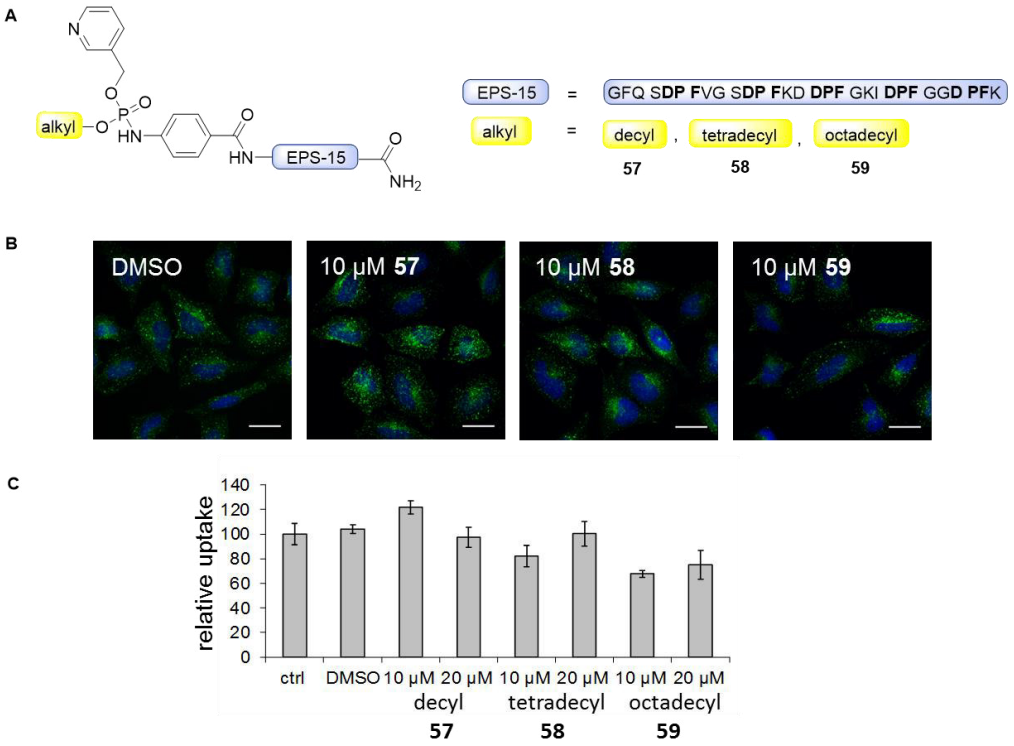

Figure 27. Transferrin uptake of monolipidated multivalent peptides, performed by Wiebke Stahlschmidt. (A) Structure of the tested monolipidated peptides. Three different alkyl lengths were investigated. (B) Representative epifluorescense microscopy pictures of cells after 1h pre-incubation with peptides and 15 min of transferrin uptake. Showing DAPI-stain (blue) and Transferrin (green), scale bar 20 µm. (C) Relative quantification of transferrin uptake of cells after incubation with the respective monolipidated peptides at different concentrations.

3.4.4.2 Study with Fluorescent Peptides

In order to verify the assumption that the lipidation of peptides facilitates their cellular uptake and localization at the cellular membrane, we also designed fluorophore-labelled peptides. As the N-terminus of the peptides is carrying the lipid modification, carboxyfluorescein, which is a cost-efficient and FDA approved dye,[188] was introduced at the C-terminus of the peptides. For this, following a protocol developed by Roland Brock,[189] carboxyfluorescein was loaded on the resin before building up the peptide sequence *via* SPPS (Scheme 17 A). After the synthesis of the peptide on the solid support, one of two different lipid modifications was introduced. First, an octadecyl-pyridylmethyl phosphoramidate was attached to the EPS15-peptide to yield in **63** (Scheme 17 B). Second, a stearic acid was coupled *via* amide bond to the N-terminus to yield in **65**, which corresponds to the stearic acid coupled EPS15-peptide (**64**) used in the preliminary studies[186] (Scheme 17 C).

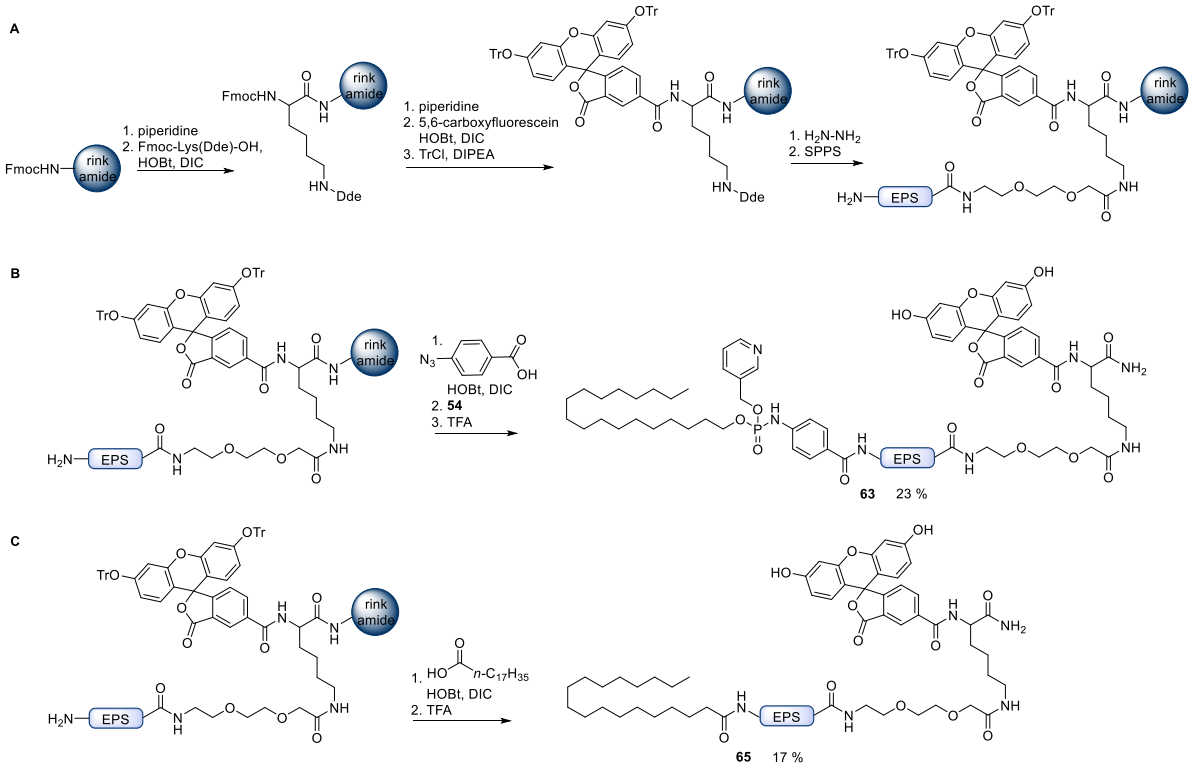

Scheme 17. Synthesis of C-terminally fluorophore labelled control peptides. (A) Loading of a rink amide resin with carboxyfluorescein according to a protocol demonstrated by Brock.[189] Trityl-protection of the hydroxyl groups of the carboxyfluorescein followed by removal of an orthogonally protected lysine side chain allow subsequent SPPS. (B) Synthesis of the fluorescein labelled monolipidated phosphoramidate modified EPS-peptide (**63**). (C) Synthesis of the fluorescein labelled stearic acid coupled EPS-peptide (**65**).

With these two fluorescent variants of the two best inhibitor candidates in hand (Figure 28 A-D), we first compared the inhibition of CME of the unlabeled to that of the labelled peptide. The two stearic acid coupled peptides (**64**, **65**) both showed inhibition of about 90 %, whereas the two octadecyl-

pyridylmethyl-phosphoramidate modified peptides **59** and **63** showed 20 to 30 % of inhibition. This supports that the addition of a fluorophore does not significantly change the behavior of the peptides. During microscopy analysis of these transferrin uptakes, carboxyfluorescein was also imaged both for the stearic acid coupled peptide (**65**, Figure 28 E) and the phosphoramidate peptide (**59**, Figure 28 F). Both peptides accumulate at the cell membrane and are present in the cytosol and at the Golgi apparatus.

Finally, the peptides **59**, **63**, **64** and **65** were analyzed by dynamic light scattering in PBS buffer, revealing that all cells are present as micellar structures at concentrations of 20 µM, which offers an explanation to the question, how these peptides can penetrate the cellular membrane. It can be concluded that the monovalent octadecyl-peptides are taken up by the cells and are localized at similar parts of the cell. Therefore, different effects in clathrin mediated endocytosis cannot be attributed to the localization of the peptides.

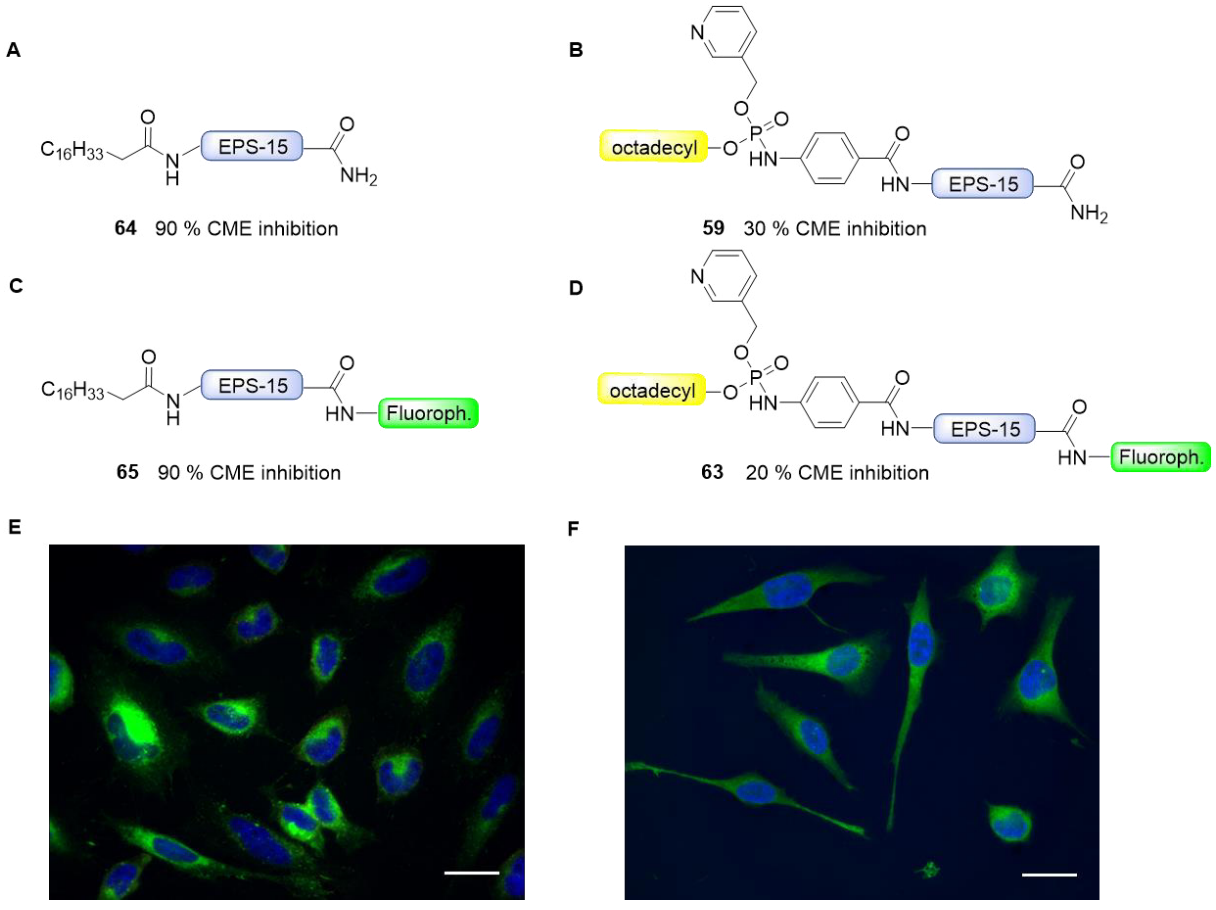

Figure 28. (A-D) Selected peptides and the maximal observed inhibition of transferrin uptake. (A) Stearic acid coupled EPS peptide (**64**). (B) Octadecyl phosphoramidate modified EPS peptide (**59**). (C) Stearic acid coupled EPS peptide labelled with fluorescein (**65**). D Octadecyl phosphoramidate modified EPS peptide labelled with fluorescein (**63**). (E-F) Representative epifluorescense microscopy pictures of cells after 1h preincubation with peptides and 15 min transferrin uptake. Showing DAPI stain (blue) and fluorescein (green), scale bar 20 µm. (E) Stearic acid coupled EPS peptide labelled with fluorescein (**65**). Uptake performed by Wiebke Stahlschmidt. (F) Octadecyl phosphoramidate modified EPS peptide (**63**) labelled with fluorescein.

3.4.4.3 Dilipidation

Next to the length of the alkyl-chain, the influence of the number of attached lipid chains on the performance of the peptides was investigated. Therefore, symmetrical phosphites were synthesized according to literature procedures,[190] tris(octadecyl)phosphite was accessed commercially. Dilipidated peptides were synthesized by SPPS followed by Staudinger phosphite reaction on the solid support and subsequent acidic cleavage (Figure 29 A). The resulting peptides were very hydrophobic, bis(octadecyl)phosphoramidate EPS peptide (**68**) was not soluble at all. Decyl- and Tetradecyl modified peptides **66** and **67** were soluble and could be purified on a reversed phase C4-HPLC material in good yields. Transferrin uptake assays with these peptides were performed by Wiebke Stahlschmidt and revealed no effect of the peptides (Figure 29 B). Supposedly, the peptides' affinity for the cellular membrane is too high making them not dynamic enough. Regardless, the chemical protocol presented here allows the straight forward synthesis of dilipidated molecules for the presentation of a modification of choice on a lipid bilayer.

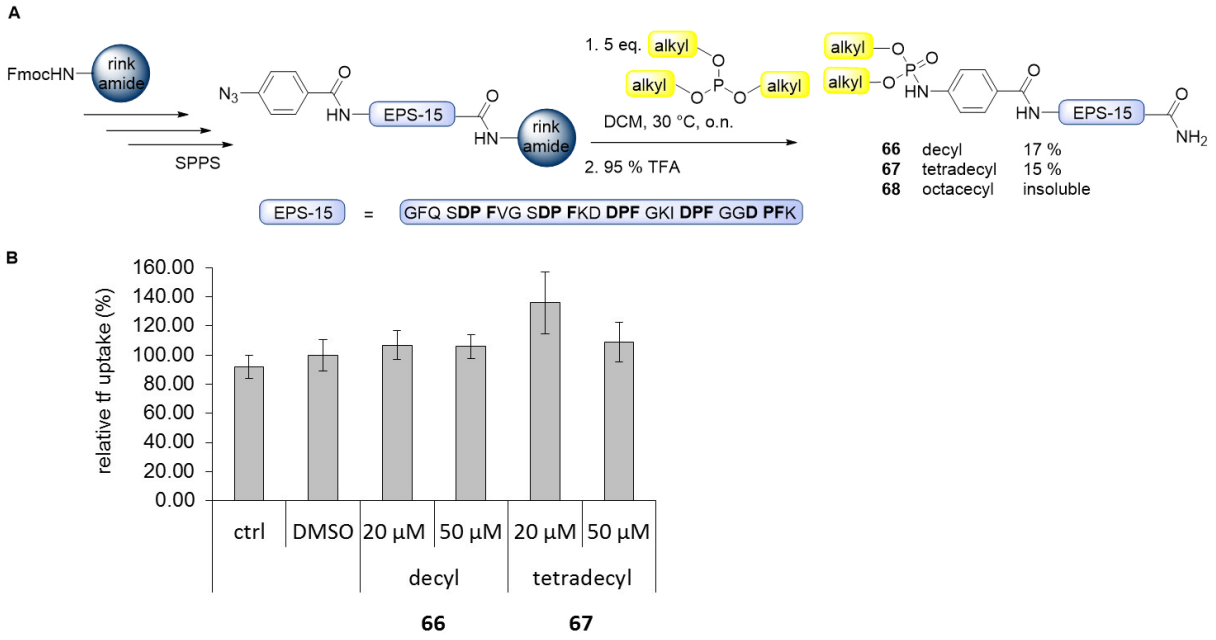

Figure 29. Synthesis and transferrin uptake of dilipidated multivalent peptides. (A) Azido-peptides presenting several DPF-amino acid motifs were synthesized by SPPS. Staudinger phosphite reaction was performed with different symmetrical phosphites on the solid support followed by TFA-cleavage to yield in dilipidated peptides. (B) Transferrin uptake of dilipidated multivalent peptides was performed by Wiebke Stahlschmidt.

3.4.4.4 Bivalent Amphiphysin Peptides.

Whereas the binding constants reported for EPS15-derived DPF-peptides are rather weak, amphiphysin derived FxDNF motifs are stronger binders of the AP2 α-appendage, as demonstrated with isothermal titration calorimetry.[177] Several attempts to synthesize a linear bivalent peptide

carrying this motif failed or gave too many truncation products during SPPS (Scheme 18 A and B). Therefore, an alternative strategy for the bivalent presentation of the FxDNF motifs was created. After an orthogonal sidechain-protected lysine building-block was attached to the resin for final modifications, a branching point was installed followed by the introduction of PEG linkers for flexibility. Subsequently, the two peptide motifs were built up simultaneously *via* SPPS (Scheme 18 C). Finally, the orthogonal protecting group was removed and an aryl azide was introduced followed by Staudinger phosphite reaction in order to incorporate an octadecyl-chain. Two bivalent peptides could be isolated (Scheme 18 C). However, none of them led to inhibition of CME.

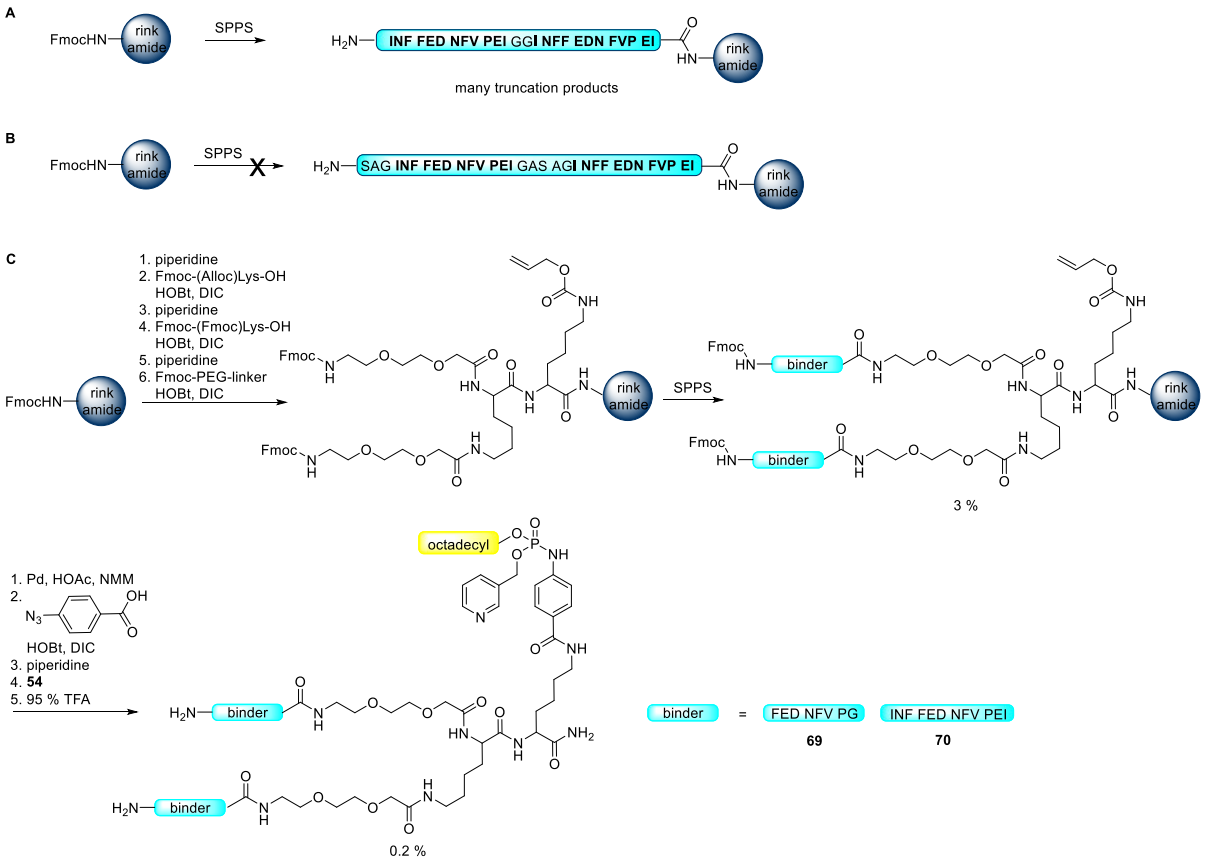

Scheme 18. Synthesis of peptides presenting a strong binder bivalently. (A) SPPS of a bivalent linear peptide with short GG spacer was successful but yielded in many truncation products. (B) After increase of the length of the spacer, no target peptide could be detected by HPLC-MS. (C) Bivalent peptides were synthesized by introducing a branching point on the solid support followed by SPPS to build up two peptide motifs simultaneously. Subsequently, the orthogonal Alloc-protecting group at a lysine side chain was removed followed by introduction of an aryl azide and Staudinger phosphite reaction to yield in monolipidated bivalent peptides.

3.4.5 Summary and Outlook.

The lipidation of aryl-azido polypeptides *via* Staudinger phosphites was developed and demonstrated at a versatility of structures, varying both the leaving- and the alkyl-group. The stability of the alkyl-

pyridyl- or bisalkyl-phosphoramidates against TFA-cleavage conditions allows a straightforward synthesis of mono- and dilipidated peptides with high yields. Finally, bivalent peptides were synthesized by installing a branching point on the solid support.

All peptide probes were tested as potential inhibitors of CME, octadecyl-pyridyl-phosphoramidate modified EPS15-peptide showed the highest inhibition with 30 %. This peptide was compared to stearic acid coupled EPS15-peptide and fluorescein modified equivalents. All of these peptides form micellar structures as shown via DLS measurements and are taken up into cells where they are present at the membrane, in the cytosol and at the Golgi.

The Staudinger phosphite lipidation is a powerful method to lipidate a molecule of choice as azides are easily and regularly incorporated. Specifically, dilipidation should be evaluated on its ability to present a function of choice on lipid bilayers such as cells or liposomes.

3.5 Covalent Attachment of Cyclic TAT Peptides to GFP Results in Protein Delivery into Live Cells with Immediate Bioavailability

This chapter was published in the following journal:

Nicole Nischan, Henry D. Herce, Francesco Natale, Nina Bohlke, Nediljko Budisa, M. Cristina Cardoso, Christian P. R. Hackenberger

"Covalent Attachment of Cyclic TAT Peptides to GFP Results in Protein Delivery into Live Cells with Immediate Bioavailability"

Angew. Chem. Int. Ed. **2015**, to be announced / *Angew. Chem.* **2015**, to be announced.

Publication Date (Web): December 17th, 2014

The original article is available at: http://dx.doi.org/10.1002/anie.201410006, http://dx.doi.org/10.1002/ange.201410006

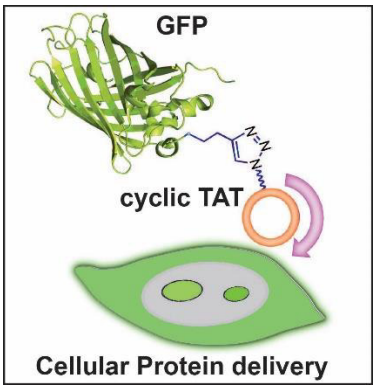

Figure 30. Conjugation of cyclic TAT to GFP results in efficient transduction into live cells.

Abstract

Knocking on the cellular door! Conjugation of cyclic cell penetrating peptides (CPPs) to full-length GFP by CuAAC enables direct protein transport into the cell. Our findings reveal that the cyclic CPP-GFP conjugates are internalized into live cells with immediate bioavailability in the cytosol and the nucleus, whereas linear CPP-analogues are not efficient for GFP transduction. This technology expands the application of cyclic CPPs to the efficient transport of functional full-length proteins into live cells.

Responsibility assignment

The design of the project was provided by Christian P. R. Hackenberger and M. Cristiana Cardoso. The author developed and scaled up a protocol to synthetically access various conjugatable TAT-Peptides,

evaluated their applicability in protein conjugation, optimized the GFP-CPP conjugation to full conversion, developed a purification protocol for maximal protein-conjugate recovery, synthesized a linear TAT-GFP conjugate as control and evaluated the impact of the CPP-conjugation on the photophysical properties of GFP. Henry D. Herce performed all cellular uptake experiments and microscopy, this includes uptakes of different proteins, protein-conjugates and peptides at different concentrations, experiments to explore the mechanism of uptake and collecting a movie demonstrating motility and cell cycle viability. Francesco Natale conducted Fluorescence Recovery after Photobleaching experiments and quantified the intracellular concentration of GFP. Nina Bohlke and was responsible for expressing the auxotroph GFP mutant and Nediljko Budisa contributed the concept for this.

Summary of content

The covalent attachment of arginine-rich cell-penetrating peptides (CPPs) such as the TAT-Peptide or polyarginine is an established strategy to transport small cargo into the cytoplasm and nucleus of cells in a non-endocytic fashion *via* a mechanism referred to as transduction.[122] However, the mode of uptake is dependent of the size of the cargo, big cargoes such as proteins are taken up in endocytic vesicles were they are trapped and subjected to degradation.[156] In fact, early reports observed cytosolic delivery of a polyarginine-GFP-fusion,[191] but later these results were revealed to be fixation artifacts,[192] which is why in general only those results are considered to be reliable that have been acquired using life cell microscopy.[122]

Non-covalent approaches for intracellular protein delivery use the physical disruption of the plasma membrane *via* electroporation or microinjection or the addition of delivering additives.[126,141,142] Although subjecting cells to considerable stress these approaches are very attractive for *ex vivo* application because they are readily applicable for any protein. Currently, methods for the cytosolic delivery of proteins *in vivo* are lacking. A covalent delivery method for proteins would be very promising for pharmaceutical applications.

Based on recent work, in which the laboratory of Cardoso has shown that the transduction efficiency of arginine-rich CPPs can be greatly enhanced by their cyclization,[157] we aimed here to test whether the conjugation of cyclic CPPs allows the transport of functional, full-length proteins to the cytosol of living cells. As a proof of concept we chose GFP as both cargo and fluorophore, while its fluorescence is also proof of correct folding.

We accessed site-specific cyclic conjugates of a cyclic TAT and GFP by applying the chemoselective CuAAC.[65,66,70,73] The use of chemoselective techniques is essential for conjugation site, in addition, cyclic CPPs cannot be introduced *via* standard biosynthesis. Therefore, a GFP mutant containing a

homopropargyl glycine at the N-terminus was obtained by auxotrophic expression in *E. coli*.[25,31] Also, different cyclic TAT-Peptides, containing alternating L- and D-amino acids for maximum uptake efficiency,[157] were synthesized carrying either a peptide- or an oligoethylene-spacer with either azidobenzoic acid or azidobutanoic acid as orthogonal handle. Therein, orthogonal protecting groups at Lys and Glu were used for the cyclization of the peptide on the solid support. Having both alkyne-GFP and cyclic azido-CPPs at hand, CuAAC was performed. Albeit optimization efforts, cyclic CPPs with a peptide spacer did not lead to full conversion, several strategies to separate conjugated and unconjugated GFP failed. On the contrary, the cyclic CPP with an oligoethylene spacer lead to full conversion at optimized conditions, a purification protocol for high recovery using dialysis was developed and the product was characterized *via* MALDI-MS. A linear TAT-GFP could be synthesized and isolated in a similar fashion and was used as control to resemble a TAT-GFP fusion protein. Comparison of UV absorption and fluorescence spectra of both conjugated and unconjugated GFP demonstrated that the photo-physical properties of GFP are not changed by conjugation highly charged cyclic TAT.

With unconjugated GFP and GFP conjugated to either linear or cyclic TAT-peptide, cellular uptake experiments were performed in human cervical cancer cells (HeLa). Unconjugated GFP did not enter or bind the cellular membrane at a concentration of 150 µM. Co-incubation of unconjugated GFP and linear TAT-peptide lead to the same result for GFP, while the TAT-Peptide could readily transduce cells. GFP conjugated to linear TAT-peptide did bind to the cellular membrane, transduction was not ovserved at 50 and 100 µM, at 150 µM, 1 % of the cells was transduced. In contrast, GFP conjugated to cyclic TAT-peptide did transduce into the majority of cells at 50 and 100 µM, at 150 µM, 84 % of the cells were transduced.

This data shows that the increase of transduction efficiency caused by the structural modification of cyclization of arginine rich peptides also allows the transduction of full-length functional proteins. Cytosolic delivery of GFP was supported by fluorescence recovery after photobleaching experiments. Incubation of cells at 4 °C or in the presence of a micropinocytosis inhibitor also lead to efficient transduction of cells, which supports that transduction is the mode of uptake. The general morphology of the cells and the fact that the cells continue to move and undergo mitotic division indicates that the uptake of cTAT-GFP is well tolerated and does not interfere with integrity and metabolism of the cells. Taken together, our findings represent the first efficient delivery of full-length functional proteins to the cytosol of living cells *via* a covalent strategy. While for therapeutic applications the efficiency of uptake still has to be improved for to facilitate protein delivery at lower concentrations and also under growth conditions, our findings demonstrate that this covalent approach is a venue promising to pursue.

Outlook

Strategies envisioned to improve the transduction efficiency include the coupling of multiple CPPs to a single protein and the exploration of other CPPs such as cyclic R10.[157] So far, it has been tried to synthesize a conjugatable cyclic R10, however, although cyclization was successful, it was impossible to attach a linker supposedly due to the steric hindrance of bulky Pbf-protecting groups of the arginine side chains.

The multiple conjugation of CPPs to GFP was attempted *via* using double or triple auxotroph GFP mutants accessed similarly as described above an conjugating them with cyclic TAT peptides by CuAAC. Surprisingly, although equivalents of reactants were chosen according to alkyne number, the conversion was very low. After a reaction time of 72 h, the major signal in MALDI was corresponding to the starting material independent of mutant or CPP; double or triple modification could not be detected at all (Table 1).

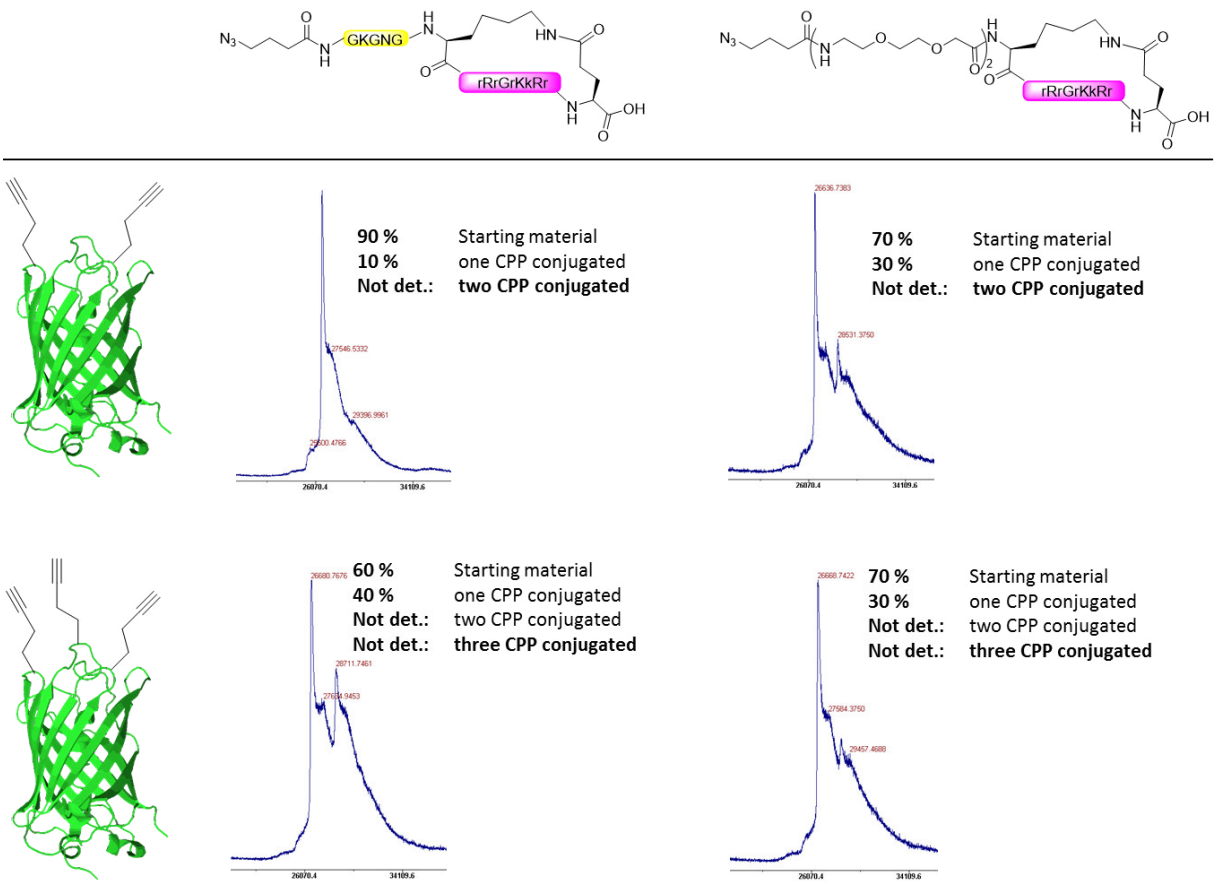

Table 1. CuAAC of bivalent and trivalent alkyne-GFP mutants reacted with cyclic TAT peptides containing either a peptide- (left) or and oligoethylene glycol-spacer. MALDI-MS shows low conversion for all reactions. Reaction conditions: 10 µM protein, 420 µM azide (14 eq. per alkyne), 170 µM Cu (5 eq. per alkyne), 8 °C, 72 h. Conditions: 6 µM protein, 420 µM azide (23 eq. per alkyne), 170 µM Cu (9 eq. per alkyne), 8 °C, 72 h (bottom)

In order to test whether these low conversions can be attributed to the bulkiness of the cyclic CPPs, we next probed the conjugation or the triple GFP mutant with small azido peptides that resemble the linker and that were available. While the conversions where slightly better than for the cyclic CPPs, they were still insufficient. Only traces of double modified GFP could be detected, no signal corresponding to triple modified GFP could be detected (Table 2).

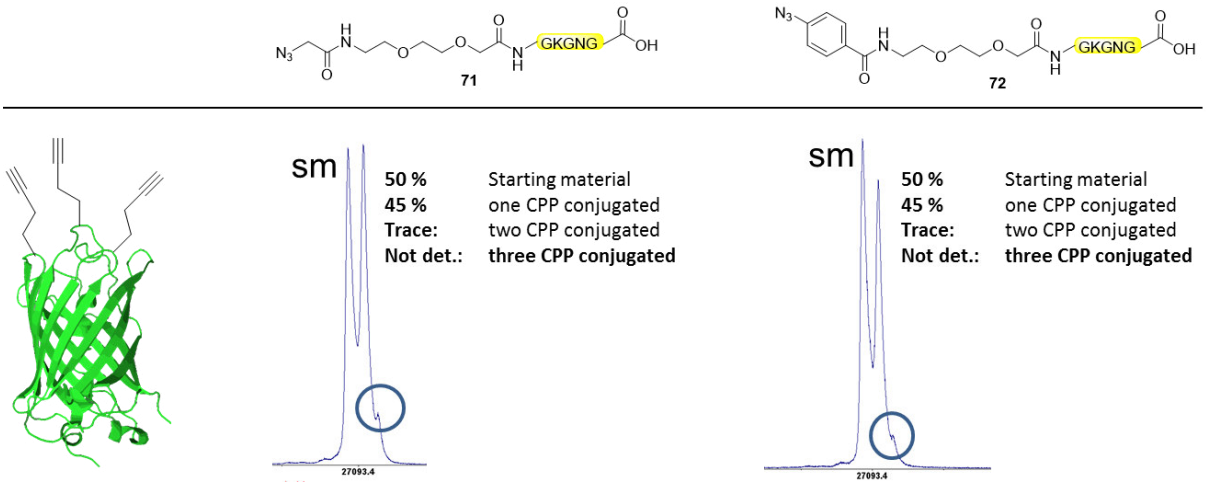

Table 2. CuAAC of trivalent alkyne-GFP mutant reacted with small azido-peptides **71** and **72**. MALDI-MS shows low conversion for both reactions. Reaction conditions: 14 µM protein, 420 µM azide (10 eq.), 170 µM Cu (4 eq.), 15 °C, 16 h.

To conclude, alkyne groups in the double or triple mutant GFP used were not accessible for efficient conjugation with peptides *via* CuAAC. Accordingly other mutants, alternative conjugation chemistries or a preassembly of the cyclic CPPs should be explored.

4 SUMMARY AND OUTLOOK

This work demonstrates the utility of chemoselective reactions for the bioconjugation of pharmaceutically relevant modifications to peptides and proteins for promoting their delivery. Specifically, PEGylation, Lipidation and Cell Penetrating Peptides were conjugated to peptides or proteins in order to (i) increase their stability against proteolysis, (ii) promote their solubility and (iii) facilitate their cellular uptake.

Project 1: PEGylation of peptides to stabilize them for intracellular applications.[167]

In this study, the impact of phosphoramidate-branched PEGylation was probed for its impact on intracellular distribution and the activity of proapoptotic peptides. Although PEGylation is well known to enhance residence half-life of polypeptides in serum, limited attention was paid to the effect of PEGylation in cells so far. Even with short branched PEG chains of a total mass of 1.5 and 4 kDa, the stabilization against proteolysis in Jurkat cell lysate was significantly increased by a factor of 11 and 57, respectively. Most importantly, PEGylation with a weight increase of only 1.5 kDa was sufficient to increase the peptides' intracellular apoptosis inducing activity significantly and in a concentration dependent manner. The attachment of longer PEG chains did not increase activity. These results demonstrate the potential of phosphoramidate-linked PEGylated peptides for the selective targeting of intracellular biological pathways, which is of significant pharmaceutical importance.

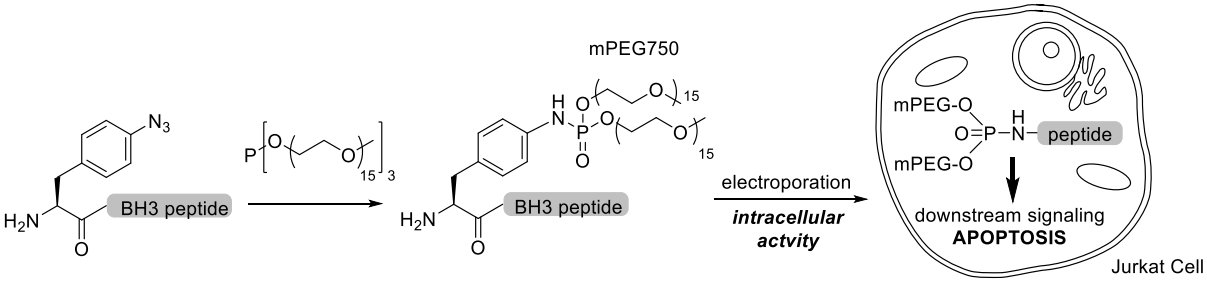

Figure 31. PEGylation of peptides for the intracellular downstream activation of apoptosis.

Project 2: PEGylation of erythropoietin for improved activity.

Staudinger phosphite PEGylation of pAP containing unfolded EPO-mutants succeeded under denaturing conditions, albeit with very low yields. This was demonstrated by a SDS-PAGE and Western blot against a PEG-specific antibody. To improve conversion, PEGylation will be performed under not denaturing conditions after improved refolding. Once PEG-EPO can be isolated in sufficient amounts, the conjugates will be evaluated for their activity using for instance colony assays.

Project 3: PEGylation of unimolecular liposomes.

Unimolecular liposomes such as CMS nanocarriers are a drug delivery vehicle with high pharmaceutical potential.[155] The outer hydrophilic layer of CMS usually consists of linear PEG-chains which are not

always leading to sufficient solubility. In this work, two PEG-chains of only four PEG-units each were attached to CMS nanocarriers by Staudinger phosphite reaction, which led to complete solubility in water. Unbound PEG-reagent could be removed efficiently by acidic hydrolysis followed by dialysis against double distilled water. To this end, this synthesis and work up was scaled up for the PEGylation of a CMS of 10 kDa molar weight that had been functionalized to 35 % *via* ester linkage with a lipophilic aryl-azido linker. The PEGylated CMS was characterized using heteronuclear NMR-experiments. In the future, the developed PEGylation protocol will be applied to other CMSs that vary in loading or linker attachment. The resulting PEGylated CMS nanocarriers will be evaluated for their loading properties.

Project 4: Lipidation of peptides for localization at and crossing of the cellular membrane.

The lipidation of aryl-azido polypeptides *via* Staudinger phosphites was developed and demonstrated at a versatility of structures, varying both the leaving- and the lipid-group. The stability of the phosphoramidates against TFA-cleavage conditions allowed a straightforward synthesis of mono- and dilipidated peptides with high yields. Finally, bivalent peptides were synthesized by installing a branching point on the solid support.

All peptide probes were tested as potential inhibitors of CME, octadecyl-pyridyl-phosphoramidate modified EPS15-peptide showed the highest inhibition with 30 %. The peptides are taken up into cells, supposedly due to the formation of micellar structures, which they form according to DLS-measurements.

Project 5: Conjugation of cyclic CPPs for protein delivery to the cytosol.[193]

Here it was demonstrated that the conjugation of the cyclic CPP TAT by a CuAAC gives access to full-length, folded and functional GFP-conjugates, which are taken up *via* transduction by live cells with immediate cytosolic availability. Azido-CPPs were synthesized by SPPS which included the use of orthogonal protecting groups for cyclization. Alkyne-GFP was synthesized in an auxotroph *E. coli* system. To achieve full conversions in the CuAAC of cyclic TAT and GFP, a PEG-linker was essential while a peptide linker was not sufficient. Functionality of the conjugates was proven by UV- and fluorescence spectroscopy. While the conjugation of a linear TAT to GFP did not induce its transduction, attachment of a cyclic TAT enabled the transduction of GFP to the majority of cells at 50, 100 and 150 µM concentration under serum reduced conditions. While the uptake efficiency needs to be improved to further increase protein uptake also under growth conditions and for therapeutic applications, for instance by coupling of multiple CPPs or combining this covalent approach with *e. g.* liposomes, these results demonstrate an unprecedented, efficient, and direct intracellular cytosolic delivery of a folded full-length functional protein by a covalent approach.

5 ZUSAMMENFASSUNG UND AUSBLICK

Diese Arbeit behandelt die Anwendung chemoselektiver Reaktionen auf die Biokonjugation von Peptiden und Proteinen mit pharmazeutisch relevanten Modifikationen. Im Speziellen wurden die PEGylierung, die Lipidierung und das Konjugieren von zellpenetrierenden Peptiden untersucht um Peptide und Proteine (i) gegen Proteolyse zu stabilisieren, (ii) ihre Löslichkeit zu erhöhen und (iii) um ihre zelluläre Aufnahme zu ermöglichen.

Projekt 1: Stabilisierung von Peptiden für intrazelluläre Anwendungen mittels PEGylierung.[167]

Obwohl die PEGylierung von Polypeptiden ein etabliertes Mittel für die Erhöhung ihrer Plasmahalbwertszeit ist, wurde dem Einfluss der PEGylierung auf die Stabilität von Peptiden in Zellen bis jetzt nur wenig Aufmerksamkeit zu Teil. In diesem Projekt wurde der Einfluss von Phosphoramidat-verzweigter PEG-Ketten auf die intrazelluläre Verteilung und die Aktivität proapoptotischer Peptide untersucht. Selbst kurze verzweigte PEG-Ketten mit einer Gesamtmasse von 1.5 und 4 kDa erhöhten die proteolytische Stabilität der Peptide in Jurkat Zelllysat signifikant um einen Faktor von 11 bzw. 57; dabei blieb die homogene zytoplasmatische Verteilung der Peptide erhalten. Eine N-terminale PEGylierung von einem Gewicht von 1.5 kDa war ausreichend um die intrazelluläre proapoptotische Aktivität der Peptide signifikant und konzentrationsabhänging zu erhöhen. Die Verwendung längerer PEG-Ketten führte nicht zu einer Aktivitätserhöhung. Diese Ergebnisse verdeutlichen das Potential Phosphoramidat-verzweigter PEGylierter Polypeptide für die selektive Aktivierung intrazellulärer Signalübertragungswege mit pharmazeutischer Relevanz.

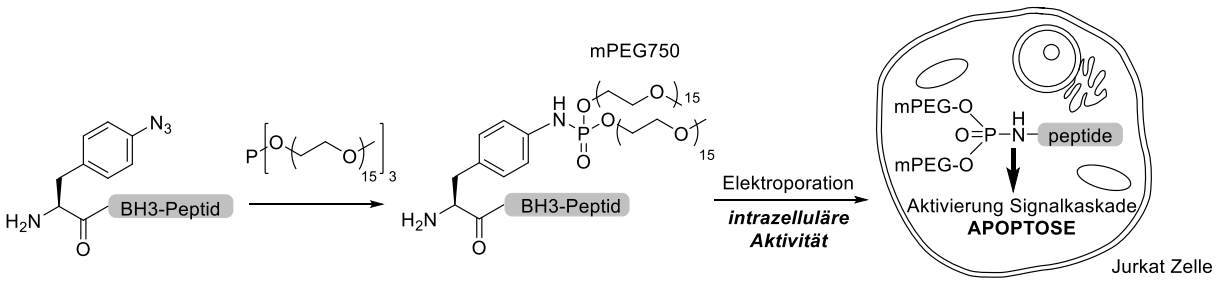

Figure 32. PEGylierung von Peptiden für die intrazelluläre Aktivierung von Apoptose.

Projekt 2: PEGylation von Erythropoietin für verbesserte Aktivität.

pAP-enthaltende EPO-Mutanten wurden mittels Staudinger Phosphit Reaktion unter denaturierenden Bedingungen PEGyliert, jedoch mit sehr geringem Umsatz, was mittels SDS-PAGE und Western Blot mit einem PEG-spezifischen Antikörper nachgewiesen wurde. Zur Verbesserung des Umsatzes wird die PEGylierung unter nativen Bedingungen in unmittelbarer Folge nach einer optimierten Rückfaltung erprobt werden. Nach erfolgreicher Isolierung hinreichender Mengen von PEG-EPO werden diese Konjugate auf ihre Aktivität mittels Kolonieassays untersucht werden.

Projekt 3: PEGylierung von unimolekularen Liposomen.

Unimolekulare Liposomen, wie z. B. CMS Nanocarrier, sind Transportwerkzeuge mit hohem pharmazeutischen Potential.[155] Die äußere hydrophile Schicht von CMSs besteht dabei normalerweise aus linearen PEG-ketten, was nicht immer zu ausreichender Löslichkeit führt. In dieser Arbeit konnten CMS durch das Anbringen von Phosphoramidat-verzweigten PEG-Ketten von jeweils nur vier Monomeren vollständig wasserlöslich gemacht werden. Ungebundene PEG-Reagenzien konnten effizient durch säurekatalysierte Hydrolyse gefolgt von Dialyse gegen destilliertes Wasser entfernt werden. Das beschriebene Verfahren ist auf Ansätze von 150 mg CMS anwendbar und wurde am Beispiel von der PEGylierung eines CMS demonstriert, welches eine molare Masse von 10 kDa aufwies und an 35 % seiner Endgruppen über eine Esterbindung mit einem lipophilen Azidolinker funktionalisiert worden war. Der PEGylierte CMS wurde mittels heteronuklearen NMR-Experimenten charakterisiert. Das hier etablierte PEGylierungsprotokoll soll in Zukunft auf CMS mit anderem Funktionalisierungsgrad und alternativer Linkerverbindung angewendet werden. Die resultierenden PEGylierten CMS Nanocarrier werden dann auf ihre Beladungseigenschaften untersucht werden.

Projekt 4: Lipidierung von Peptiden für deren Lokalisation und Membranpermeation.

Die Lipidierung von Arylazidopolypeptiden mittels Staudinger-Phoshitreaktion wurde entwickelt und anhand vielfacher Strukturen demonstriert, wobei sowohl die Abgangs- als auch die Lipidgruppe modifiziert wurden. Die hohe Stabilität der Phosphoramidate gegen TFA-Bedingungen ermöglicht die direkte Synthese von mono- und dilipidierten Peptiden mit hohen Ausbeuten. Außerdem wurden bivalente Peptide mithilfe einer Verzweigung an der Festphase synthetisiert.

Alle Peptide wurden als potentielle Inhibitoren von CME untersucht. Octadecyl-pyridyl-phosphoramidat-modifiziertes EPS15-Peptid zeigte mit 30 % die höchste Inhibition. Die Peptide werden in Zellen aufgenommen, vermutlich aufgrund von Mizellenbildung, was durch DLS-Messung gestützt wird.

Projekt 5: Konjugation zyklisierter zell-penetrierender CPPs an Proteine resultiert in deren Transduktion von Lebenden Zellen.[193]

Hier wurde gezeigt, dass die Konjugation des zyklisierten CPPs TAT an GFP mittels CuAAC zu ganzen, gefalteten, funktionalen GFP-Konjugaten führt, welche von lebenden Zellen mit sofortiger zytosolischer Verfügbarkeit mittels Transduktion aufgenommen werden. Azido-CPPs wurden mittels SPPS synthetisiert, wobei orthogonale Schutzgruppen für die Zyklisierung verwendet wurden. Alkin-GFP wurde mittels eines auxotrophen Stamms von *E. coli* synthetisiert. Voller Umsatz der CuAAC von zyklisiertem TAT und GFP konnte nur unter Verwendung eines PEG-Linkers erreicht werden, ein Peptidlinker war hingegen nicht ausreichend. Während die Konjugation eines linearen TATs an GFP nicht zur Transduktion führte, bewirkte ein zyklisiertes TAT die Transdukion von GFP in den Großteil

aller Zellen bei einer Konzentration von 50, 100 und 150 µM unter serumfreien Bedingungen. Wenngleich die Aufnahmeeffizienz unter Wachstumsbedingungen erhöht werden muss, zum Beispiel durch mehrfaches Konjugieren zyklisierter CPPs, zeigen diese Resultate eine nicht zuvor dagewesene Transduktionseffizienz von ganzen, gefalteten, funktionalen Proteinen mittels eines kovalenten Ansatzes.

6 EXPERIMENTAL PART

6.1 Materials and Methods

Reagents and solvents, unless stated otherwise, were commercially available as reagent grade or HPLC grade and did not require further purification. Amino acids and resins were purchased from IRIS Biotech GmbH (Germany) or Novabiochem (Merck KGaA, Germany).
Azides, phosphite precursors and symmetrical phosphites were either commercial or prepared according to the literature.

Flash chromatography was performed on silica gel (Acros Silicagel 60 A, 0.035-0.070 mm). TLC was performed on aluminium-backed silica plates (60 mash F254, 0.2 mm, Merck), which were analyzed *via* UV or developed using potassium permanganate solution.

Nuclear Magnetic Resonance ^{1}H-NMR, ^{13}C-NMR and ^{31}P-NMR spectra were recorded on a Bruker AV300 in deuterated solvent. The chemical shifts are reported relative to the residual solvent peak as a standard in ppm.

SPPS Peptides were synthesized with an Activo-P11 Peptide Synthesizer (Activotec SPP Ltd., UK) or ABI 433A Peptide Synthesizer (Applied Biosystems, Inc., USA) *via* standard Fmoc-based conditions with HOBt/HBTU/DIPEA activation and piperidine Fmoc deprotection in DMF.

Preparative HPLC purification of the peptides was performed on a JASCO LC-2000 Plus system (JASCO, Inc., Easton, Maryland, USA) using a reversed phase C18 column (Kromasil material) or reversed phase C4 column (Jupiter, Phenomenex Inc., Torrance, CA, USA) at a constant flow of 16 mL/min) using water and acetonitrile with 0.1% TFA) applying an optimized gradient using a Smartline Manager 5000 with interface module, two Smartline Pump 1000 HPLC pumps, a 6-port-3-channel injection valve with 1.0 mL loop, a UV detector (UV-2077) and a high pressure gradient mixer (All Knauer, Berlin, Germany). Alternatively a Gilson® PLC 2020 Personal Purification System (Gilson Inc., Middleton, WI, USA) including a Nucleodur column (VP 250/32 C18 HTec 5µm) by Macherey-Nagel was used at a flow rate of 30 mL/min.

LC UV purity was determined by either HPLC-UV or UPLC-UV system:

HPLC-UV was measured at 220 nm on a system consisting of a Waters 600S controller, a Waters 616 pump, a Waters 717plus autosampler and a Waters 2489 UV/Visible detector operated with Empower 2 software (all Waters Corporation, US) using a C18-column (Eclipse, Agilent Technologies, US, 100 Å, 5 µm, 4.6 mm x 250 mm) at constant flow of 1.0 mL/min with 5 min 10 % and then a gradient over 30 min of 10 % to 100 % MeCN in water with 0.1 % TFA unless stated otherwise.

UPLC-UV was measured at 220 nm on an Acquity UPLC H-Class operated with Empower 3 software (all Waters Corporation, US) on a C18-column (Acquity UPLC BEH C18, 1.7 µm, 2.1 mm x 50 mm) at constant flow of 0.6 mL/min with 0.5 min 10 % and then a gradient over 15 min of 10 % to 95 % MeCN in water with 0.1 % TFA unless stated otherwise.

ESI-MS was measured on one of the following systems:

Agilent 6210 ToF LC-MS system (Agilent Technologies, US) at constant flow of 0.2 mL/min with water and MeCN containing 0.1 % TFA to give high resolution mass spectra.

LCT Premier Micromass Technologies System coupled to a Waters Acquity UPLC at constant flow of 0.2 mL/min with water and MeCN containing 0.1 % formic acid with phosphoric acid as lockmass; the data was processed using Mass Lynx Software (all Waters Corporation, US) to give high resolution mass spectra.

Waters 3100 mass detector after a Waters HPLC-UV or UPLC-UV system (all Waters Corporation, US) as stated above *via* direct injection at constant flow of 0.6 mL/min with water and MeCN containing 0.1 % TFA to give low resolution mass spectra.

MALDI was measured on an AB SCIEX TOF/TOF 5800 (Applied Biosystems, Inc., USA) using 2,5-DHAP matrix and dried droplet sample preparation.

2,5-DHAP matrix was prepared by dissolving 7.6 mg of 2,5-DHAP in 375 µL ethanol and adding 125 µL of an 18 mg/mL aqueous solution of diammonium hydrogen citrate.

For sample preparation 2 µL of protein solution were precipitated in 8 µL cold acetone, the solvent was removed and the resulting pellet dissolved in 2 µL of double distilled water, which were mixed with 2 µL of 2% TFA and 2 µL of 2,5-DHAP matrix solution until chrystallization started. 1 µL of this suspension was deposed on a ground steel target and left to dry prior to measuring.

6.2 Staudinger Phosphite PEGylation of Erythropoietin for Improved Activity

Erythropoietin mutants created by Dr. Marina Rubini. Erythropoietin (EPO) mutants containing *para*-azidophenylalanine (pAzF) at position 24 or 38 (**EPO p24 pAP** and **EPO p38 pAP**) were expressed in the laboratory of Dr. Marina Rubini and send in denaturing buffer consisting of 10 mM mercaptoethanol, 5 mM imidazole, 20 mM Tris buffer at pH8, 3 M guanidiniumchloride. The EPO stocks contained **EPO p24 pAP** at a concentration of 15 µM and **EPO p38 pAP** at a concentration of 37 µM, as determined by measuring the absorbance at 280 nm on a nanodrop ND1000 and estimating the extinction coefficient to be Ɛ(280 nm) = 22430 M^{-1} cm^{-1} at reduced conditions based on tyrosines, tryptophanes and free cysteins.

Staudinger Phosphite PEGylation of EPO mutants.

Reaction at 100 % denaturing conditions: A solution of PEG200- or PEG750-phosphite in 500 µL of protein stock was shaken at 1000 turns per minute at 30 °C for 72 h.

Reaction at 50 % denaturing conditions: A solution of PEG200- or PEG750- phosphite or alcohol in 100 µL 100 mM Tris buffer (pH 8.2 at 30 °C) was added to 100 µL of protein stock, followed by shaking at 1000 turns per minute at 30 °C for 72 h.

Refolding of EPO.

The refolding buffer consists of 20 mM Tris-HCl, 0.5 M arginine hydrochloride, 1 mM GSH and 0.3 mM GSSG at pH 8.5. EPO solution in denaturing conditions is diluted 1/200 in refolding buffer and cooled at 4 °C overnight, followed by concentration using ultracentrifugation.

Desalting procedures evaluated for EPO desalting.

Procedures evaluated for desalting EPO samples included different reverse phase silica materials, centrifugal spin filters and size exclusion material. The feasibility of the protocols was estimated by SDS-PAGE (10 well with 30 µL pockets).

Reversed phase. Zip Tip® (Merck Millipore) containing C18 and C4 material were used. 10 µL sample were loaded by pipetting up and down 10 times, followed by washing with double distilled water containing 0.1 % TFA five times and elution with 3 µL of 50 % of MeCN in water containing 0.1 % TFA. For pH-control, 7 µL of 100 mM Tris buffer (pH 8.2) were added and used for analysis by SDS-PAGE.

Centrifugal spin filters. 30 µL of protein sample were diluted with 430 µL of SDS running buffer (0.1 % SDS in 100 mM Tris) and concentrated with centrifugal filters (Amicon Ultra 0.5 mL 3K MWCO regenerated cellulose, Merck Millipore, Merck KGaA, Germany). 10 µL sample were taken for analysis by SDS-PAGE.

Size exclusion material. Sephadex G25 material was swollen in 100 mM Tris buffer (pH 8.2), bed sizes of 200 µL or 500 µL were loaded in centrifugal frits, solvent was removed and based on the dead volume, the beds were loaded with either 70 µL or 200 µL of protein sample and spinned down. From the eluted fraction, 10 µL of sample were taken for analysis by SDS-PAGE.

SDS-PAGE

SDS-PAGE analysis was done on Mini Protean® TGX Stain-Free™ precast gels by Bio Rad (Bio-Rad Laboratories Inc., USA), 4-20 %, either with 15 well comb and 15 µL pockets or 10 well comb and 30 µL pockets using as eluent 1 % SDS running buffer consisting of 0.25 M Tris and 1.92 M glycine. Loading samples were taken by mixing 10 µL of protein solution with 3.5 µL of 4 x SDS with mercaptobromphenol by vortex followed by spinning down, heating to 95 °C for 5 minutes and spinning down again. Electrophoresis was carried out at 250 V for 25 minutes followed by imaging with a Bio Rad imager after gel activation for 2 minutes.

Western Blot

SDS-gel as described above was transferred to a nitrocellulose membrane in transfer buffer of 10 % ethanol in a buffer containing 0.25 M Tris and 1.92 M glycine at 250 mA for 1 h. After successful transfer was verified with prestained markers, non-specific binding was blocked by incubation with 3 % of milk powder in 10 mL PBS overnight. The membrane was washed with PBS, incubated with 10 mL PBS 3 times for 5 minutes followed by incubation with 10 µL of 0.5 mg/mL anti PEG antibody (PEG-B-47, rabbit monoclonal IgG purchased by epitomics®, abcam®, UK) in 10 mL PBS for 60 min. After washing the membrane with PBS and incubation with 10 mL PBS 3 times for 5 minutes, the membrane was incubated with 5 µL of 0.5 mg/mL anti rabbit antibody (ab97051, goat anti rabbit IgG H&L (HRP) in 10 mL PBS containing 3 % milkpowder. Finally, the membrane was washed with PBS, incubated with 10 mL PBS 3 times for 5 minutes and analyzed by adding 1 mL of each component of WesternBright Chemilumineszenz Substrate for Film, and imaging immediately.

6.3 Staudinger Phosphite PEGylation for the Synthesis of Unimolecular Liposomes

Infrared (IR) spectroscopy was performed on a Tensor 27 instrument (Bruker, Bruker Corporation, Billerica, MA, USA).

hPGs as provided by the group of Rainer Haag.

hPG1. Unmodified: MW = 10 kDa, 70 % functionalized, amide linkage, total MW = 17 kDa, approximately 28 azide functionalities per molecule.

hPG2. Unmodified: MW = 10 kDa, 35 % functionalized, ester linkage, total MW = 13.5 kDa, approximately 14 azide functionalities per molecule.

PEGylation of hPG1, small scale

hPG1 (15 mg, 0.025 mmol of azide) were dissolved in 0.8 mL $CHCl_3$ and added to 0.25 mmol of PEG200 or PEG750-phosphite (10 eq.). The mixture was shaken at 600 turns per minute at 30 °C. After 24 h, conversion was complete according to IR. The product was diluted in $CHCl_3$ and dialyzed against $CHCl_3$ using a Spectra-Por® 2 Dialysis Membrane with 12 kDa to 14 kDa molecular weight cut off (Spectrum Laboratories Inc., USA), which afforded **PEG200-hPG1**.

^{31}P-NMR (300 MHz, $CDCl_3$): δ [ppm]= 9.

IR (KBr) selected signal: ν = 2053 cm^{-1}, which is characteristic for azide groups, is present in **hPG1**, but absent in **PEG200-hPG1**.

PEGylation of hPG2, big scale

hPG2 (150 mg, 0.16 mmol of azide) were dissolved in 5 mL $CDCl_3$ and added to 1.6 mmol of PEG200 phosphite (1.00 g, 10 eq.), the mixture was stirred at 30 °C for 24 h. After removal of the solvent under reduced pressure, 50 mL of water containing 0.05 % TFA were added and stirred for 72 h. Solvent was removed under reduced pressure and the product was dialyzed against double distilled water using Spectra-Por® 2 Dialysis Membrane with 12 kD to 14 kD molecular weight cut off (Spectrum Laboratories Inc., USA) which afforded 180 mg (86 %) of the **PEG200-hPG2**.

^{1}H-NMR (600 MHz, $CDCl_3$): δ [ppm]= 6.96-7.03 (m, 4 H, $C_{AR}\underline{H}$), 6.45-6-05 (b, 1H, N$\underline{H}$), 4.20 (s, 4H, P-O-$C\underline{H}_2$-CH_2), 3.45-3.75 (m, 38 H), 3.56 (s, 4H), 2.55 (b, 2H, C-$C\underline{H}_2$-C), 2.34 (b, 2H, C-$C\underline{H}_2$-C), 1,88 (b, 2H, C-$C\underline{H}_2$-C). **^{31}P-NMR** (600 MHz, $CDCl_3$): δ [ppm]= 3.

6.4 Lipidation

6.4.1 Synthesis of Unsymmetrical Phosphites

Bis(pyridyl)-*N*,*N*-diisopropylphosphoramidite (51)

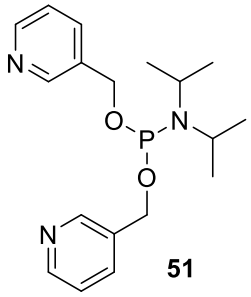

51

Protocol. Modified from the synthesis of other phosphoramidites.[194] Under argon atmosphere, 1,1-dichloro-*N*,*N*-diisopropylphosphinamine (**50**; 1.810 g; 8.96 mmol) was suspended in dry Et_2O and brought to 0 °C. A solution of pyridine-3-methanol (1.73 mL; 1.96 g; 17.92 mmol; 2.0 eq.) and Et_3N (2.48 mL; 1.81 g; 17.92 mmol; 2.0 eq.) in dry Et_2O (15 mL) was added drop wise within 10 min. The reaction was stirred to reach RT overnight. The resulting precipitate was removed *via* filtration and washed twice with Et_2O (20 mL). The filtrate was concentrated under reduced pressure and the crude product was purified *via* column chromatography over silica using EtOAc/Et_3N/*n*-hexanes 3:1:7 (Rf = 0.19) to yield in bis(pyridyl)-*N*,*N*-diisopropylphosphoramidite (**51**) as colorless oil (1.698 g; 4.89 mmol; 55 %).

Chemical formula = $C_{18}H_{26}N_3O_2P$; molar mass M = 347.39 g/mol.

^{1}H-NMR (300 MHz, $CDCl_3$): δ [ppm]= 8.47 (s, 2H, $C_{AR}\underline{H}$), 8.39 (d, $^3J_{H,H}$= 5.0 Hz, 2H, $C_{AR}\underline{H}$), 7.54 (d, $^3J_{H,H}$= 7.9 Hz, 2H, $C_{AR}\underline{H}$), 7.13 (dd, $^3J_{H,H\ 1}$= 4.8 Hz, $^3J_{H,H\ 2}$= 7.8 Hz, 2H, $C_{AR}\underline{H}$), 4.54-4.69 (m, 4H, O-C$\underline{H}_2$-C_{AR}), 3.50-3.63 (m, 2H, N-C$\underline{H}$), 1.08 (d, $^3J_{H,H}$= 6.8 Hz, 12H, CH-C$\underline{H}_3$). **^{13}C-NMR** (300 MHz, $CDCl_3$): δ [ppm]= 148.8 (2C, $\underline{C}_{AR}$H), 148.6 (2C, $\underline{C}_{AR}$H), 134.7 (2C, $\underline{C}_{AR}$H), 134.6 (d, $^3J_{C,P}$= 7.4 Hz, 2C, $\underline{C}_{AR}$C), 123.2 (2C, $\underline{C}_{AR}$H), 63.1 (d, $^2J_{C,P}$= 18.6 Hz, 2C, O-$\underline{C}H_2$-C_{AR}), 43.1 (d, $^2J_{C,P}$= 12.3 Hz, 2C, N-$\underline{C}$H), 24.6 (d, $^3J_{C,P}$= 7.3 Hz, 4C, CH-$\underline{C}H_3$). **^{31}P-NMR** (300 MHz, $CDCl_3$): δ [ppm] = 149.

ESI-MS (positive mode): m/z (found) $[M+H]^+$ = 348.1824, m/z (calculated) $[M+H]^+$ = 348.1835.

Decyl-bis(pyridin-3-ylmethyl)phosphite (**52**)

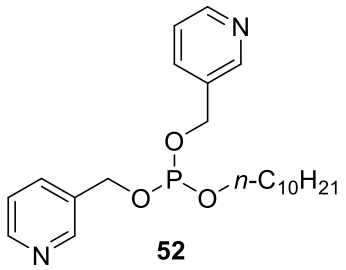

52

Protocol. Under argon atmosphere, dry decanol (0.158 g, 1.0 mmol) was suspended in a solution of tetrazole (1.56 mL, 0.7 mmol, 0.7 eq., 0.45 M in MeCN) in a 1:1 mixture of dry DCM and dry MeCN (10 mL) and brought to 0 °C. To this, a solution of dipyridyl-*N*,*N*-diisopropylphosphoramidite (**51**; 1.0 mmol) in dry MeCN (5 mL) was added. The solution was stirred vigorously for 1 h at 0 °C and 2 h at RT. Then, dry Et_2O was added (20 mL) and the insoluble material was removed by filtration. Solvents where removed under reduced pressure. The residue was purified *via* column chromatography over silica with 1% Et_3N in Et_2O (Rf = 0.33) to yield decyl bis(pyridin-3-ylmethyl) phosphite (**52**) as colourless liquid (61 mg; 0.15 mmol; 15 %) in good purity.

Chemical formula = $C_{22}H_{33}N_2O_3P$, M = 404.48 g/mol.

^{1}H-NMR (300 MHz, CD_3CN): δ [ppm] = 8.54 (s, 2H, $C_{AR}\underline{H}$), 8.49 (d, $^3J_{H,H}$= 4.6 Hz, 2H, $C_{AR}\underline{H}$), 7.69 (d, $^3J_{H,H}$= 7.9 Hz, 2H, $C_{AR}\underline{H}$), 7.31 (dd, $^3J_{H,H\,1}$= 4.8 Hz, $^3J_{H,H\,2}$= 7.8 Hz, 2H, $C_{AR}\underline{H}$), 4.89 (d, $^3J_{H,P}$= 7.9 Hz, 4H, O-$C\underline{H}_2$-C_{AR}), 3.77-3.84 (m, 2H, O-$C\underline{H}_2$-CH_2), 1.50-1.57 (m, 2H, O-CH_2-$C\underline{H}_2$), 1.20-1.35 (m, 14H, CH_2-$C\underline{H}_2$-CH_2), 0.87 (t, $^3J_{H,H}$= 6.6 Hz, 3H, CH_2-$C\underline{H}_3$). **^{13}C-NMR** (300 MHz, CD_3CN): δ [ppm] = 150.4 (2C, $\underline{C}_{AR}H$), 150.3 (2C, $\underline{C}_{AR}H$), 136.5 (2C, $\underline{C}_{AR}H$), 135.4 (d, $^3J_{C,P}$= 4.7 Hz, 2C, $\underline{C}_{AR}C$), 124.8 (2C, $\underline{C}_{AR}C$), 64.3 (d, $^2J_{C,P}$= 11.9 Hz, 1C, P-O-$\underline{C}H_2$-CH_2-), 62.9 (d, $^2J_{C,P}$= 10.3 Hz, 2C, P-O-$\underline{C}H_2$-C_{AR}), 33.1 (1C, -CH_2-$\underline{C}H_2$-CH_2-), 32.2 (d, $^3J_{C,P}$= 5.2 Hz, 1C, P-O-CH_2-$\underline{C}H_2$-), 30.7 (*b*, 2C, -CH_2-$\underline{C}H_2$-CH_2-), 30.5 (1C, -CH_2-$\underline{C}H_2$-CH_2-), 30.4 (1C, -CH_2-$\underline{C}H_2$-CH_2-), 26.9 (1C, -CH_2-$\underline{C}H_2$-CH_2-), 23.8 (1C, -CH_2-$\underline{C}H_2$-CH_3), 14.9 (1C, -CH_2-$\underline{C}H_3$). **^{31}P-NMR** (300 MHz, CD_3CN): δ [ppm] = 140. **ESI-MS** (positive mode, MeCN): m/z (found) $[M+H]^+$ = 405.2297, m/z (calculated) $[M+H]^+$ = 405.2307.

Tetradecyl-bis(pyridin-3-ylmethyl)phosphite (**53**)

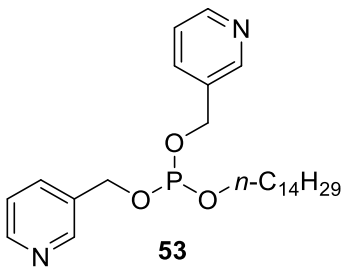

53

Procedure. Under argon atmosphere, dried tetradecanol (0.214 g; 1.00 mmol) was suspended in a solution of tetrazole (1.56 mL, 0.70 mmol, 0.7 eq., 0.45 M in MeCN) in a 1:1 mixture of dry DCM and dry MeCN (10 mL) and brought to 0 °C. To this, a solution of dipyridyl *N*,*N*-diisopropylphosphoramidite

(**51**; 0.347 g, 1.00 mmol, 1 eq.) in dry MeCN (5 mL) was added. The solution was stirred vigorously for 1 h at 0 °C and 5 h at RT and the completion of the reaction was confirmed *via* TLC (1% NEt_3 in Et_2O). Then, dry Et_2O was added (20 mL) and the insoluble material was removed by filtration. Solvents where removed under reduced pressure. The residue was purified *via* column chromatography over silica with 1% Et_3N in Et_2O (Rf = 0.33) to yield tetradecyl bis(pyridin-3-ylmethyl) (**53**) phosphite as white solid (0.254 g; 0.55 mmol; yield 55 %) in good purity.

Chemical formula = $C_{26}H_{41}N_2O_3P$, M = 460.59 g/mol.

^{1}H-NMR (300 MHz, CD_3CN): δ [ppm] = 8.54 (s, 2H, $C_{AR}\underline{H}$), 8.49 (d, $^3J_{H,H}$= 4.7 Hz, 2H, $C_{AR}\underline{H}$), 7.68 (d, $^3J_{H,H}$= 7.8 Hz, 2H, $C_{AR}\underline{H}$), 7.29 (dd, $^3J_{H,H\,1}$= 4.7 Hz, $^3J_{H,H\,2}$= 7.8 Hz, 2H, $C_{AR}\underline{H}$), 4.88 (d, $^3J_{H,P}$= 7.8 Hz, 4H, O-$C\underline{H}_2$-C_{AR}), 3.77-3.84 (m, 2H, O-$C\underline{H}_2$-CH_2), 1.50-1.59 (m, 2H, O-CH_2-$C\underline{H}_2$), 1.20-1.35 (m, 22H, CH_2-$C\underline{H}_2$-CH_2), 0.86 (t, $^3J_{H,H}$= 6.5 Hz, 3H, CH_2-$C\underline{H}_3$). **^{13}C-NMR** (300 MHz, CD_3CN): δ [ppm] = 150.5 (2C, $\underline{C}_{AR}H$), 150.3 (2C, $\underline{C}_{AR}H$), 136.5 (2C, $\underline{C}_{AR}H$), 135.4 (d, $^3J_{C,P}$= 4.8 Hz, 2C, $\underline{C}_{AR}C$), 124.8 (2C, $\underline{C}_{AR}C$), 64.4 (d, $^2J_{C,P}$= 12.0 Hz, 1C, P-O-$\underline{C}H_2$-CH_2-), 63.0 (d, $^2J_{C,P}$= 10.2 Hz, 2C, P-O-$\underline{C}H_2$-C_{AR}), 33.2 (1C, -CH_2-$\underline{C}H_2$-CH_2-), 32.3 (d, $^3J_{C,P}$= 5.2 Hz, 1C, P-O-CH_2-$\underline{C}H_2$-), 31.0 (1C, -CH_2-$\underline{C}H_2$-CH_2-), 31.0 (1C, -CH_2-$\underline{C}H_2$-CH_2-), 30.9 (*b*, 2C, -CH_2-$\underline{C}H_2$-CH_2-), 30.9 (1C, -CH_2-$\underline{C}H_2$-CH_2-), 30.8 (1C, -CH_2-$\underline{C}H_2$-CH_2-), 30.6 (1C, -CH_2-$\underline{C}H_2$-CH_2-), 30.5 (1C, -CH_2-$\underline{C}H_2$-CH_2-), 27.0 (1C, -CH_2-$\underline{C}H_2$-CH_2-), 23.9 (1C, -CH_2-$\underline{C}H_2$-CH_3), 15.0 (1C, -CH_2-$\underline{C}H_3$). **^{31}P-NMR** (300 MHz, CD_3CN): δ [ppm] = 139.

ESI-MS (positive mode, MeCN): m/z (found) $[M+H]^+$ = 461.2943, m/z (calculated) $[M+H]^+$ = 461.2933.

Octadecyl-bis(pyridin-3-ylmethyl)phosphite (**54**)

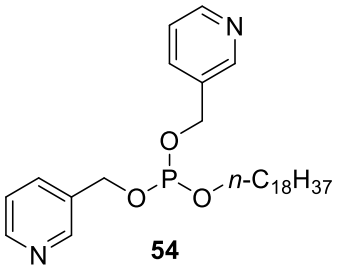

54

Procedure. Under argon atmosphere, dried octadecanol (0.271 g; 1.00 mmol) was suspended in a solution of tetrazole (1.56 mL, 0.70 mmol, 0.7 eq., 0.45 M in MeCN) in a mixture of 11 mL dry DCM and 8 mL dry MeCN and brought to 0 °C. A solution of dipyridyl *N*,*N*-diisopropylphosphoramidite (**51**; 0.347 g, 1.00 mmol, 1.0 eq.) in 5 mL dry MeCN was added. The solution was stirred vigorously for 1 h at 0 °C and 5 h at RT and the completion of the reaction was confirmed *via* TLC (1% NEt_3 in Et_2O). Then, dry Et_2O was added (20 mL) and the insoluble material was removed by filtration. Solvents where removed under reduced pressure. The residue was purified *via* column chromatography over silica with 1% Et_3N in Et_2O (Rf = 0.27) to yield octadecyl bis(pyridin-3-ylmethyl) phosphite (**54**; 0.253 g; 0.49 mmol; yield 49 %) in good purity.

Chemical formula = $C_{30}H_{49}N_2O_3P$, M = 516.70 g/mol.

^{1}H-NMR (300 MHz, CD_3CN): δ [ppm] = 8.53 (s, 2H, $C_{AR}\underline{H}$), 8.49 (d, $^{3}J_{H,H}$= 4.8 Hz, 2H, $C_{AR}\underline{H}$), 7.70 (d, $^{3}J_{H,H}$= 8.2 Hz, 2H, $C_{AR}\underline{H}$), 7.31 (dd, $^{3}J_{H,H\,1}$= 4.9 Hz, $^{3}J_{H,H\,2}$= 7.8 Hz, 2H, $C_{AR}\underline{H}$), 4.89 (d, $^{3}J_{H,P}$= 7.9 Hz, 4H, O-$C\underline{H}_2$-C_{AR}), 3.77-3.84 (m, 2H, O-$C\underline{H}_2$-CH_2), 1.50-1.59 (m, 2H, O-CH_2-$C\underline{H}_2$), 1.20-1.35 (m, 30H, CH_2-$C\underline{H}_2$-CH_2), 0.87 (t, $^{3}J_{H,H}$= 6.6 Hz, 3H, CH_2-$C\underline{H}_3$). **^{13}C-NMR** (300 MHz, CD_3CN): δ [ppm] = 150.5 (2C, $\underline{C}_{AR}H$), 150.3 (2C, $\underline{C}_{AR}H$), 136.5 (2C, $\underline{C}_{AR}H$), 135.4 (d, $^{3}J_{C,P}$= 4.7 Hz, 2C, $\underline{C}_{AR}C$), 124.8 (2C, $\underline{C}_{AR}C$), 64.3 (d, $^{2}J_{C,P}$= 12.1 Hz, 1C, P-O-$\underline{C}H_2$-CH_2-), 62.9 (d, $^{2}J_{C,P}$= 10.3 Hz, 2C, P-O-$\underline{C}H_2$-C_{AR}), 33.1 (1C, -CH_2-$\underline{C}H_2$-CH_2-), 32.3 (d, $^{3}J_{C,P}$= 5.2 Hz, 1C, P-O-CH_2-$\underline{C}H_2$-), 30.8 (*b*, 8C, -CH_2-$\underline{C}H_2$-CH_2-), 30.8 (1C, -CH_2-$\underline{C}H_2$-CH_2-), 30.7 (1C, -CH_2-$\underline{C}H_2$-CH_2-), 30.7 (1C, -CH_2-$\underline{C}H_2$-CH_2-), 30.5 (1C, -CH_2-$\underline{C}H_2$-CH_2-), 30.3 (1C, -CH_2-$\underline{C}H_2$-CH_2-), 27.0 (1C, -CH_2-$\underline{C}H_2$-CH_2-), 23.9 (1C, -CH_2-$\underline{C}H_2$-CH_3), 15.0 (1C, -CH_2-$\underline{C}H_3$). **^{31}P-NMR** (300 MHz, CD_3CN): δ [ppm] = 140.

ESI-MS (positive mode, MeCN): m/z (found) $[M+H]^+$ = 517.3540, m/z (calculated) $[M+H]^+$ = 517.3559.

Octadecyl-dibenzyl-phosphite (**56**)

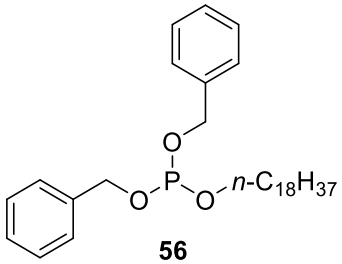

56

Procedure. Under argon atmosphere, dried octadecanol (0.500 g; 1.85 mmol; 1.05 eq.) was suspended in a solution of tetrazole (2.74 mL; 1.23 mmol; 0.7 eq.; 0.45 M in MeCN) in 30 mL dry DCM and brought to 0 °C. Dibenzyl-*N*,*N*-diisopropylphosphoramidite (**55**; 0.58 mL; 1.76 mmol; 1.0 eq.) was added. The solution was stirred vigorously for 30 min at 0 °C and 1 h at RT. The solvent was removed under reduced pressure and the solid residue was extracted three times with Et_2O (6 mL, 2 mL, 2 mL). Combined extracts were concentrated under reduced pressure to yield octadecyl-dibenzyl-phosphite (**56**) as colorless solid (0.832 g) in low purity.

Chemical formula = $C_{32}H_{51}O_3P$, M = 514.70 g/mol.

^{1}H-NMR (400 MHz, C_6D_6): δ [ppm] = 7.00-7.35 (m, 10H, $C_{AR}\underline{H}$), 4.87 (d, $^{2}J_{H,P}$= 8.0 Hz, 4H, O-$C\underline{H}_2$-C_{AR}), 3.82 (m, 2H, O-$C\underline{H}_2$-CH_2), 1.55 (quint, $^{3}J_{H,H}$= 8.0 Hz, 2H, O-CH_2-$C\underline{H}_2$), 1.20-1.45 (m, 30H, CH_2-$C\underline{H}_2$-CH_2), 0.92 (t, $^{3}J_{H,H}$= 8.0 Hz, 3H, CH_2-$C\underline{H}_3$). **^{31}P-NMR** (400 MHz, C_6D_6): δ [ppm] = 140.

6.4.2 Synthesis of Mono-Lipidated EPS15-Peptides

Azidobenzoic acetylated EPS15-peptide (61)

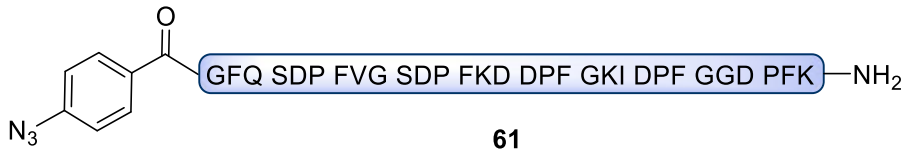

61

Procedure. After loading Rink Amide AM Resin (0.1 mmol; 0.71 mmol/g) with Boc protected Fmoc-lysine manually, the peptide was synthesized *via* SPPS using Fmoc-chemistry with HOBt/HBTU/DIPEA in NMP on an Applied Biosystem synthesizer, followed by coupling *para*-azidobenzoic acid to the N-terminus manually (10 eq., 1h, RT, HOBt and DIC in DMF). One half of the batch (0.05 mmol) was used for reactions on the solid support. The other part of the batch of azidopeptide (0.05 mmol) was cleaved from the solid support (2 h in 2 mL cleavage cocktail of 95 % TFA, 2 % TIS, 2 % DTT, 1 % MeSPh), precipitated in cold ether and purified by semi-preparative HPLC (10 to 60 % of MeCN in Water, containing 0.1 % TFA on RP-C18 column) to yield peptide **61** in a white trifluoroacetate (25.48 mg; 6.80 µmol; yield 14 %) in good purity.

Molar mass (peptide) = 3.40 kDa; molar mass (TFA_3 salt) = 3.75 kDa.

ESI-MS (positive mode): m/z (found) = 1135.5252 $[M+3H]^{3+}$ (calculated m/z = 1135.5269).

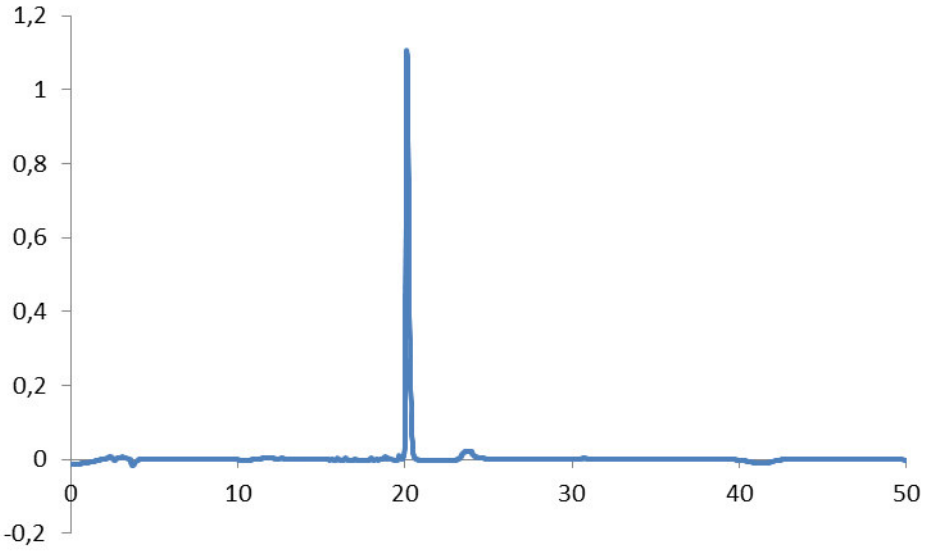

Figure 33. HPLC-UV chromatogram of azidobenzoic acetylated EPS15-peptide (**61**).

Decyl-pyridyl-phosphoramidate-EPS15-peptide (57)

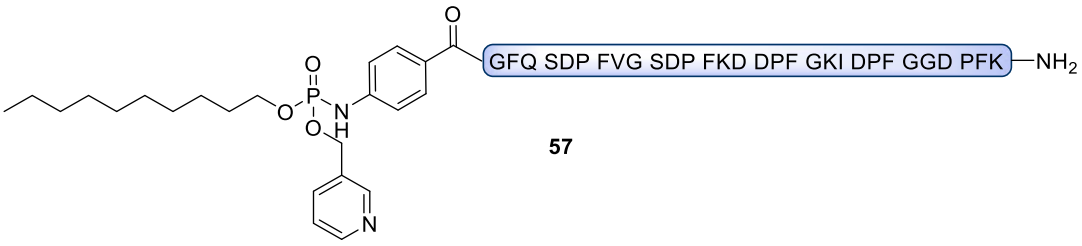

57

Procedure. Solid support bound azidobenzoic acetylated EPS15-peptide (0.005 mmol) was incubated with decyl dipyridyl phosphite (**52**; 5 eq.; 0.025 mmol) in DMF (0.5 mL) at 30 °C overnight, followed by cleavage from the solid support (2 h; RT; 95 % TFA; 2 % TIS; 2 % DTT; 1 % PhSMe) and precipitation in cold ether. Purification by preparative HPLC (20 to 45 % of MeCN in water containing 0.1 % TFA on RP-C18 column) yielded the peptide **57** as white trifluoroacetate in good purity (2.27 mg; 0.56 µmol; yield 11 % (in relation to loading of the resin) or 83 % (taking into account the yield of 14 % of the azidopeptide).

Molar mass (peptide) = 3.69 kDa; molar mass (TFA_3 salt) = 4.03 kDa.

ESI-MS (positive mode): m/z (found) = 923.1918 $[M+4H]^{4+}$ (calculated m/z = 923.1908).

Side-product. The non-lipidated side-product **58** was isolated as well (0.44 mg; 0.11 µmol; yield 2 % (in relation to loading of the resin) or 16 % (taking into account the yield of 14 % of the azidopeptide). Molar mass (peptide) = 3.64 kDa; molar mass (TFA_3 salt) = 3.98 kDa.

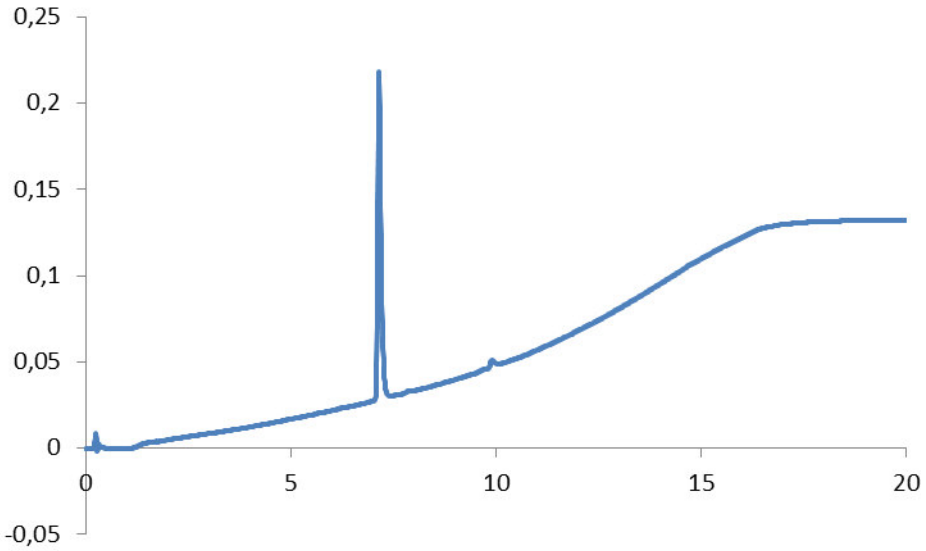

Figure 34. UPLC-UV chromatogram of decyl-pyridyl-phosphoramidate-EPS15-peptide (**57**).

Tetradecyl-pyridyl-phosphoramidate-EPS15-peptide (58)

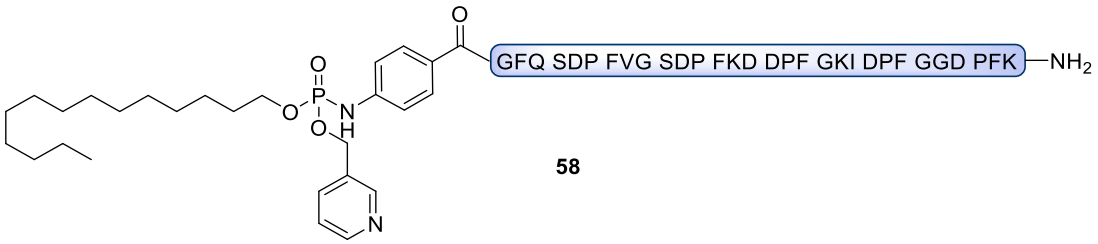

58

Procedure. Solid support bound azidobenzoic acetylated EPS15-peptide (0.005 mmol) was incubated with tetradecyl dipyridyl phosphite (**53**; 5 eq.; 0.025 mmol) in DMF (0.5 mL) at 30 °C overnight, followed by cleavage from the solid support (2 h; RT; 95 % TFA; 2 % TIS; 2 % DTT; 1 % PhSMe) and precipitation in cold ether. Purification by preparative HPLC (25 to 50 % of MeCN in water containing 0.1 % TFA on RP-C18 column) yielded the peptide **58** as white trifluoroacetate in good purity (1.35 mg; 0.31 µmol; yield 6 % (in relation to loading of the resin) or 45 % (taking into account the yield of 14 % of the azidopeptide).

Molar mass (peptide) = 3.75 kDa; molar mass (TFA_3 salt) = 4.09 kDa.

ESI-MS (positive mode): m/z = 1249.2715 $[M+3H]^{3+}$ (calculated m/z = 1249.2726).

Side-product. The non-lipidated byproduct **60** was isolated as well (0.51 mg; 0.13 µmol; yield 3 % (in relation to loading of the resin) or 19 % (taking into account the yield of 14 % of the azidopeptide). Molar mass (peptide) = 3.64 kDa; molar mass (TFA_3 salt) = 3.98 kDa.

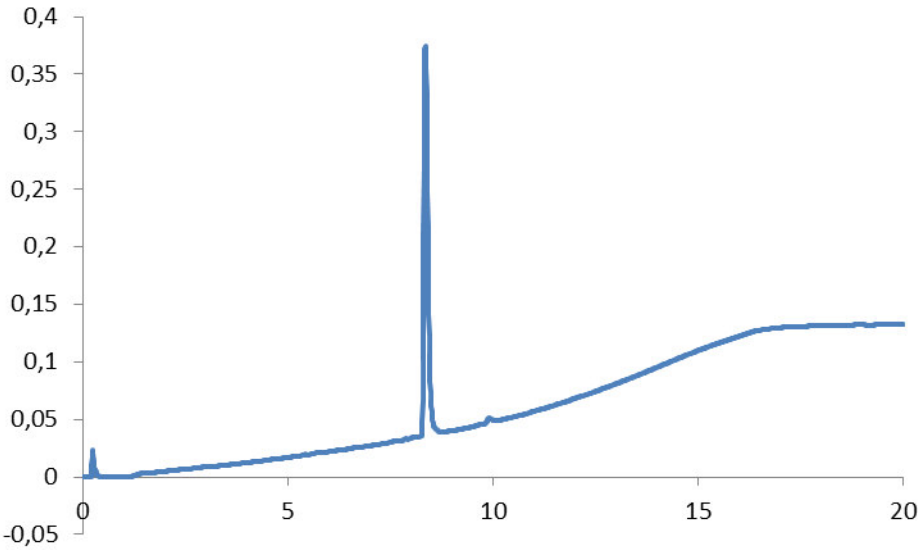

Figure 35. UPLC-UV chromatogram of tetradecyl-pyridyl-phosphoramidate-EPS15-peptide (**58**).

Octadecyl-pyridyl-phosphoramidate-EPS15-peptide (59)

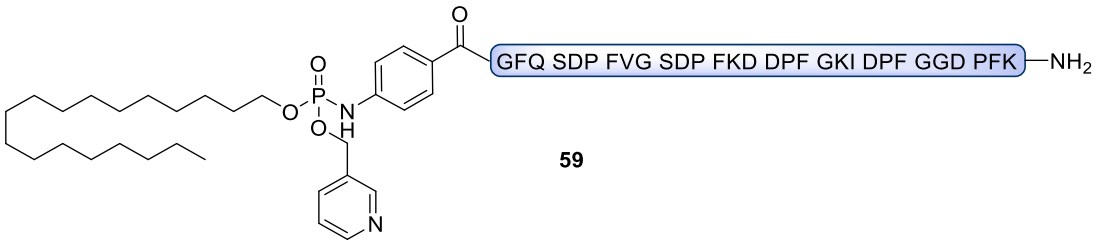

59

Procedure. Solid support bound azidobenzoic acetylated EPS15-peptide (0.005 mmol) was incubated with octadecyl dipyridyl phosphite (**54**; 5 eq.; 0.025 mmol) in DMF (0.5 mL) at 30 °C overnight, followed by cleavage from the solid support (2 h; RT; 95 % TFA; 2 % TIS; 2 % DTT; 1 % PhSMe) and precipitation in cold ether. Purification by preparative HPLC (30 to 55 % of MeCN in water containing 0.1 % TFA on RP-C18 column) yielded the peptide **59** as white trifluoroacetate in good purity (0.75 mg; 0.18 µmol; yield 4 % (in relation to loading of the resin) or 27 % (taking into account the yield of 14 % of the azidopeptide).

Molar mass (peptide) = 3.80 kDa; molar mass (TFA_3 salt) = 4.15 kDa.

ESI-MS (positive mode): m/z = 951.2200 $[M+3H]^{3+}$ (calculated m/z = 951.2221).

Side-product. The non-lipidated byproduct **60** was isolated as well (0.24 mg; 0.06 µmol; yield 1 % (in relation to loading of the resin) or 9 % (taking into account the yield of 14 % of the azidopeptide). Molar mass (peptide) = 3.64 kDa; molar mass (TFA_3 salt) = 3.98 kDa.

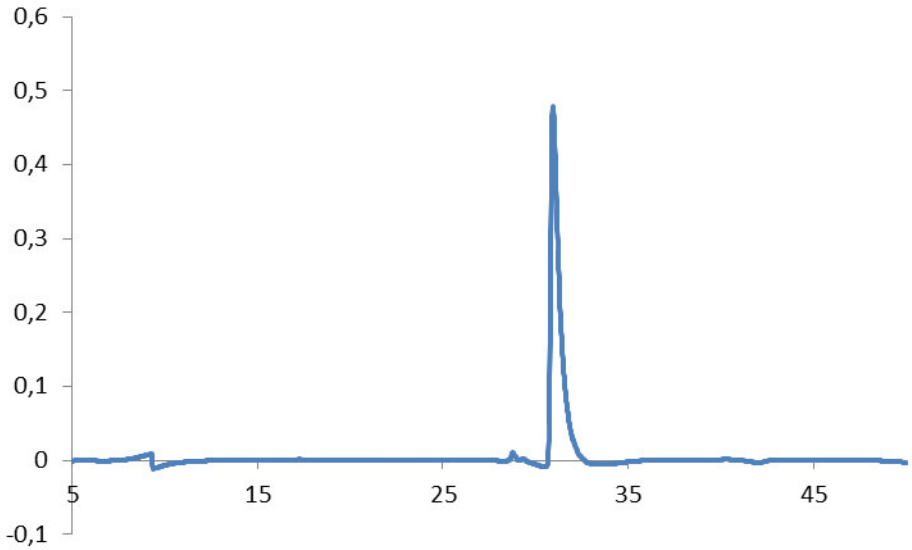

Figure 36. HPLC-UV chromatogram of octadecyl-pyridyl-phosphoramidate-EPS15-peptide (**59**).

Octadecyl-benzyl-phosphoramidate-EPS15-peptide (62)

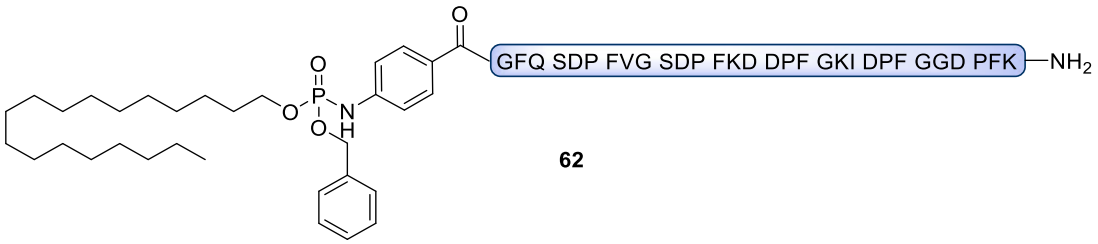

62

Procedure. To a solution of azidobenzoic acetylated EPS15-peptide (**61**; 6.00 mg; 1.6 µmol) in 700 µL dry DMSO octadecyl dibenzylphosphite (**56**; 12 mg; 24 µmol; 15 eq.) was added and shaken at 1200 turns per minute for 16 h at 30 °C. To remove the DMSO, the solution was added to 70 mL of double distilled water followed by loading on a Sep Pak® Vac 12cc (2 g) C18 cartridge (Waters Corporation, US) and subsequent elution with 1:1 MeCN : water containing 0.1 % TFA and concentration *via* lyophyliization. Purification by preparative HPLC (60 to 100 % of MeCN in water containing 0.1 % TFA on RP-C4 column, retention time 14.7-15.1 min) yielded the peptide **62** as white trifluoroacetate in good purity (2.04 mg; 0.49 µmol; yield 31 %).

Molar mass (peptide) = 3.80 kDa; molar mass (TFA_3 salt) = 4.15 kDa.

ESI-MS (positive mode): m/z = 1267.6267 $[M+3H]^{3+}$ (calculated m/z = 1267.6284).

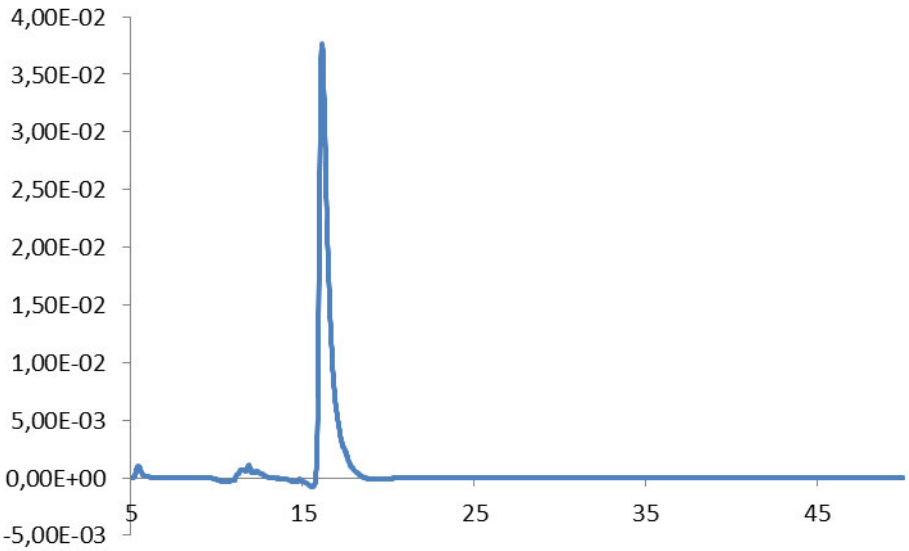

Figure 37. HPLC-UV chromatogram of octadecyl-benzyl-phosphoramidate-EPS15-peptide (**62**) on a C4 column with a gradient from 60 % to 100 % of MeCN in water containing 0.1 % TFA.

6.4.3 Synthesis of Fluorescein-Labelled EPS15-Peptides

Fluorescein labelled EPS15-peptide

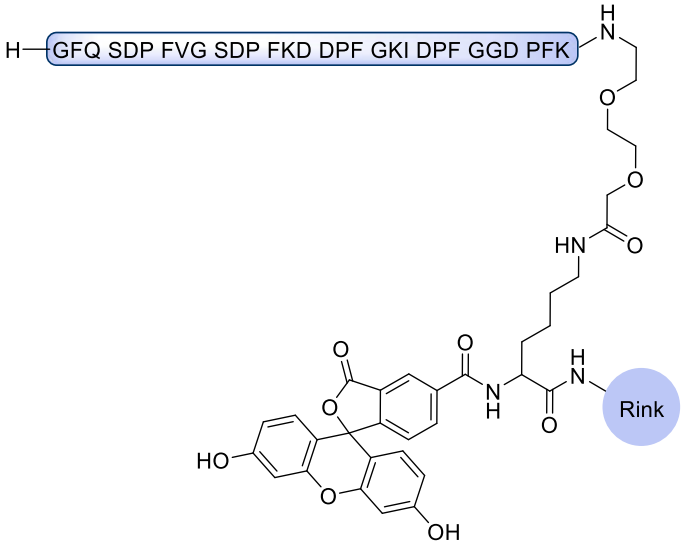

Procedure. After loading a Rink Amide resin (0.1 mmol) was with Fmoc-Lys-(Dde), Fmoc was deprotected and carboxyfluorescein was coupled to the amine. The hydroxylgroups of the carboxyfluorescein were protected with trityl groups. Subsequently, the Dde-group was removed using hydrazine and a short PEG-linker (Fmoc-O2Oc-OH) was coupled to the amine. This modified resin was then applied to SPPS on an Applied Biosystems peptide synthesizer using 10 equivalents of Fmoc-amino acid as well as HOBt/HBTU and DIPEA as coupling reagents in each step. The resin was washed, dried and stored until further use. Formation of product was confirmed *via* testcleavage (2 h; RT; 95 % TFA; 2 % TIS; 2 % DTT; 1 % PhSMe) followed by ESI-MS.

Molar mass (peptide) = 3.89 kDa; molar mass (TFA_4 salt) = 4.35 kDa.

ESI-MS (positive mode): m/z = 973.8 $[M+4H]^{4+}$ (calculated m/z = 973.4), 1297.9 $[M+3H]^{3+}$ (calculated m/z = 1297.6), 1946.6 $[M+2H]^{2+}$ (calculated m/z = 1945.9).

Fluorescein labelled octadecyl-pyridyl-phosphoramidate-EPS15-peptide (63)

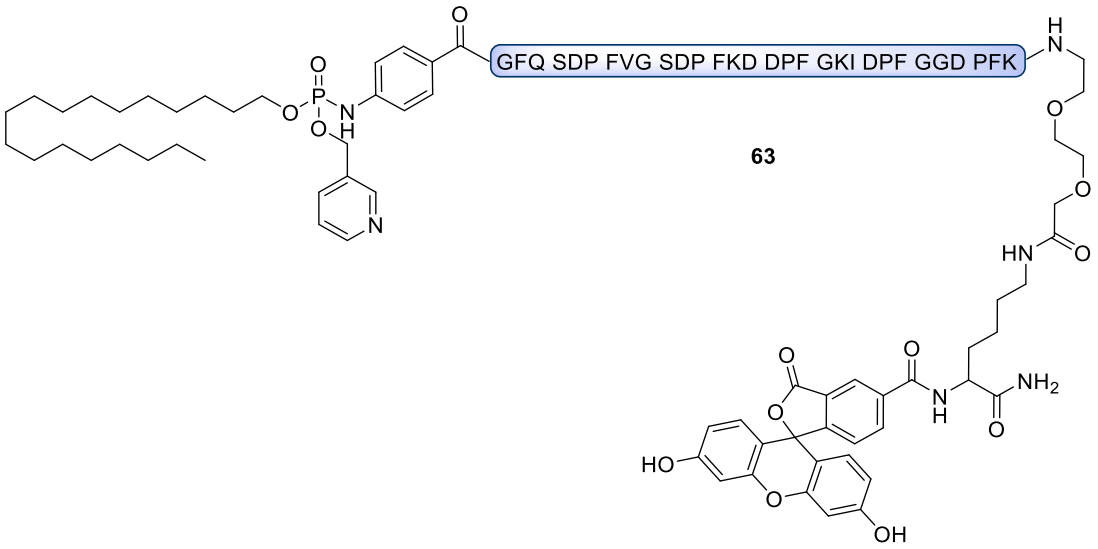

Procedure. Solid support bound fluorescein labelled EPS15-peptide (0.01 mmol) was coupled with azidobenzoic acid (10 eq., HOBt, DIC in DMF 2h RT) followed by incubation with octadecyl dipyridyl phosphite (**59**; 10 eq.; 0.10 mmol) in 0.5 mL DMF at 30 °C overnight. The peptide was cleaved from the solid support (2 h; RT; 95 % TFA; 2 % TIS; 2 % DTT; 1 % PhSMe) and precipitated in cold ether. Purification by preparative HPLC (60 to 100 % of MeCN in water containing 0.1 % TFA on RP-C4 column) yielded the peptide **63** as yellow trifluoroacetate in good purity (10.80 mg; 2.26 µmol; yield 23 %).

Molar mass (peptide) = 4.43 kDa; molar mass (TFA_3 salt) = 4.77 kDa.

ESI-MS (positive mode): m/z = 1109.2 $[M+3H]^{3+}$ (calculated m/z = 1109.0).

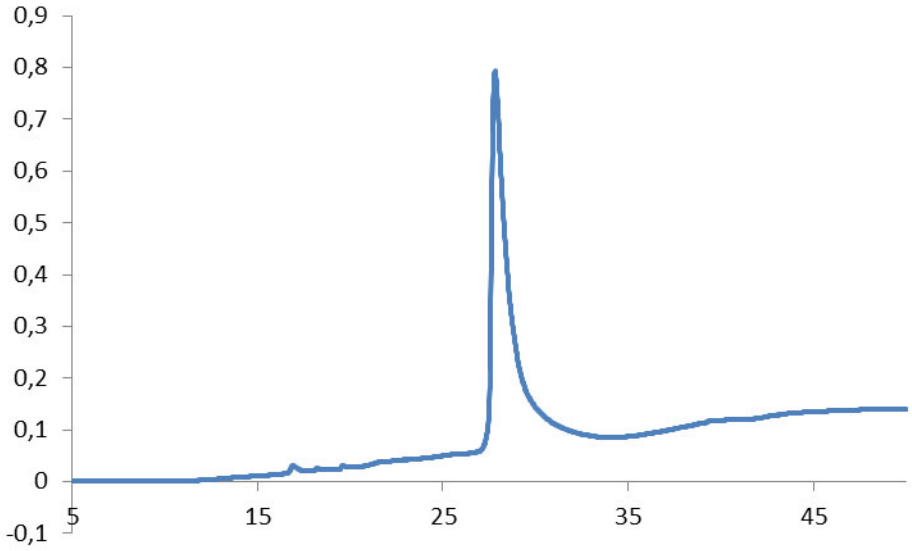

Figure 38. HPLC-UV chromatogram of fluorescein labelled octadecyl-pyridyl-phosphoramidate-EPS15-peptide (**63**) on a C4-column.

Stearic acid coupled EPS15-azidopeptide (64)

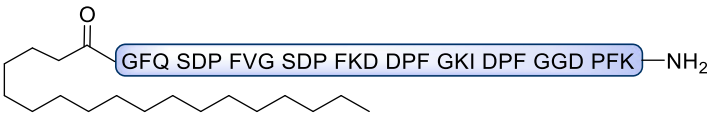

64

Procedure. Rink Amide AM Resin (0.1 mmol; 0.71 mmol/g) was loaded with Fmoc-lysine (Boc protected) and applied to SPPS using Fmoc-couplingS with HOBt/HBTU/DIPEA in NMP on a Applied Biosystem synthesizer. To a portion of that resin (0.02 mmol), stearic acid was coupled (10 eq., HOBt and DIC in DMF, 2 h, RT) followed by washing, drying and cleavage from the solid support (2 h; RT; 95 % TFA; 2 % TIS; 2 % DTT; 1 % PhSMe). Purification by semi-preparative HPLC (60 to 100 % of MeCN in water, containing 0.1 % TFA on RP-C4 column) yielded the peptide **64** as white trifluoroacetate in good purity (13.73 mg; 3.55 µmol; yield 18 %).

Molar mass (peptide) = 3.52 kDa; molar mass (TFA_3 salt) = 3.87 kDa.

ESI-MS (positive mode): m/z = 1175.9398 $[M+3H]^{3+}$ (calculated m/z = 1175.9380).

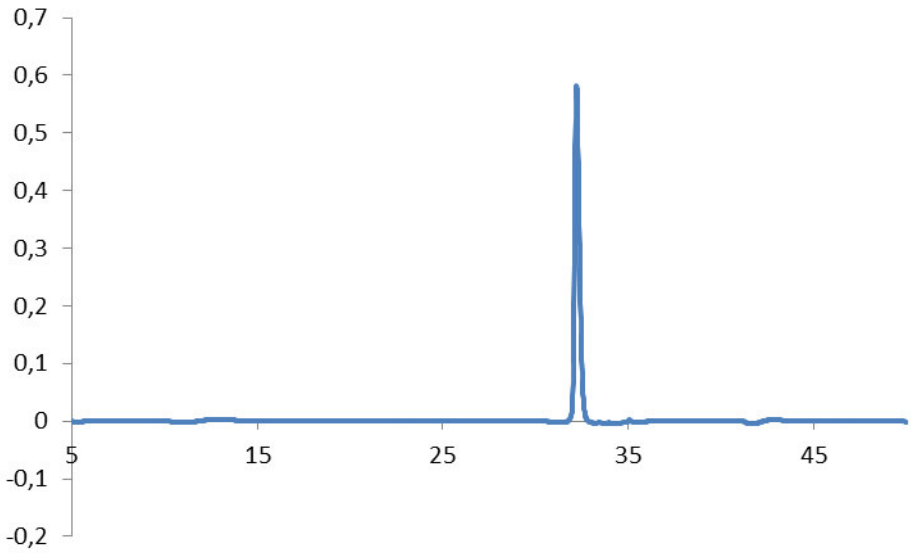

Figure 39. HPLC-UV chromatogram of stearic acid coupled EPS15-azidopeptide (**64**).

Fluorescein labelled stearic acid coupled EPS15-peptide (65)

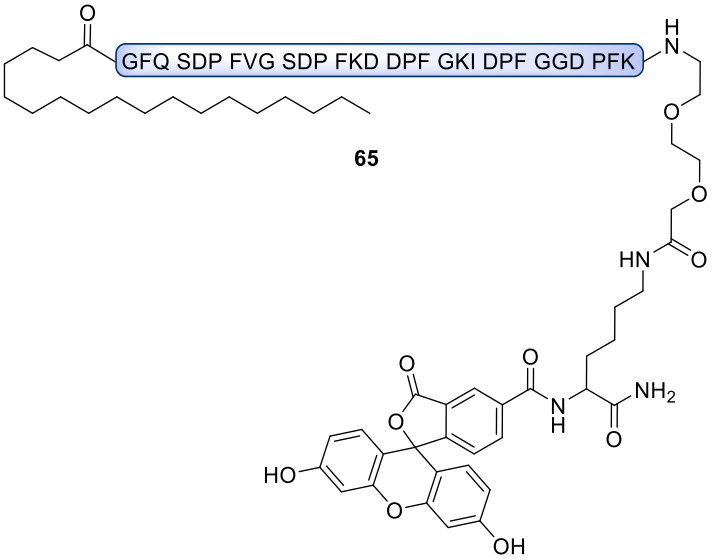

Procedure. Solid support bound fluorescein labelled EPS15-peptide (0.005 mmol) was coupled with stearic acid (20 eq., HOBt and DIC in DMF, 2 h, RT) followed by washing, drying and cleavage from the solid support (2 h; RT; 95 % TFA; 2 % TIS; 2 % DTT; 1 % PhSMe). Purification by semi-preparative HPLC (60 to 100 % of MeCN in water, containing 0.1 % TFA on RP-C18 column) yielded the peptide **65** as a yellow trifluoroacetate in good purity (3.89 mg; 0.86 µmol; yield 17 %).

Molar mass (peptide) = 4.16 kDa; molar mass (TFA_3 salt) = 4.50 kDa.

ESI-MS (positive mode): m/z = 1040.0079 $[M+4H]^{4+}$ (calculated m/z = 1040.0096).

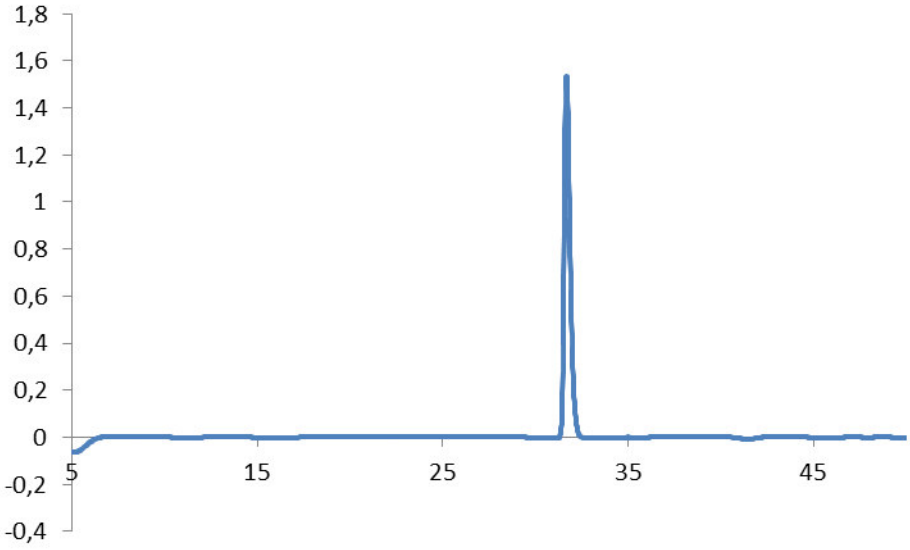

Figure 40. HPLC-UV chromatogram of fluorescein labelled stearic acid coupled EPS15-peptide (**65**).

6.4.4 Synthesis of Bis-Lipidated EPS15-Peptides

Bis(decyl)-phosphoramidate-EPS15-peptide (66)

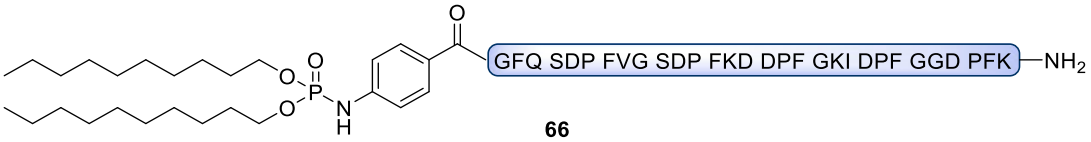

66

Procedure. Solid support bound azidobenzoic acetylated EPS15-peptide (0.01 mmol) was incubated with tris(decyl) phosphite (20.1 mg; 0.04 mmol; 4 eq.) in 1 mL DCM at 30 °C for 20 h, followed by cleavage from the solid support (2 h; RT; 95 % TFA; 2 % TIS; 2 % DTT; 1 % PhSMe) and precipitation in cold ether. Purification by preparative HPLC (10 min 50 %, then gradient of 50 % to 100 % of MeCN in water containing 0.1 % TFA on RP-C4 column; retention time 19 to 22 min) yielded the peptide **66** as white trifluoroacetate in good purity (7.01 mg; 1.72 µmol; yield 17 %).

Molar mass (peptide) = 3.74 kDa; molar mass (TFA_3 salt) = 4.08 kDa.

ESI-MS (positive mode): m/z (found) = 1246.9507 $[M+3H]^{3+}$ (calculated m/z = 1246.9565).

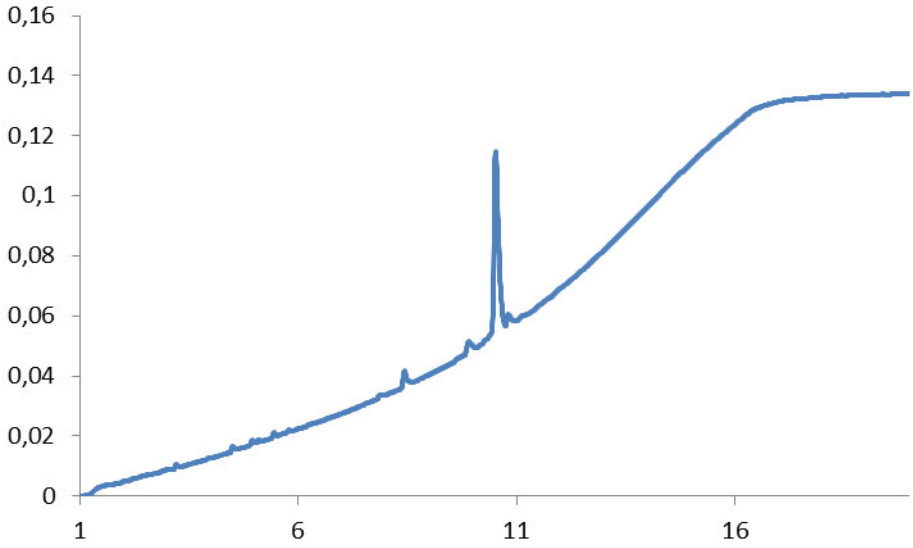

Figure 41. UPLC-UV chromatogram of bis(decyl)-phosphoramidate-EPS15-peptide (**66**).

Bis(tetradecyl)-phosphoramidate-EPS15-peptide (67)

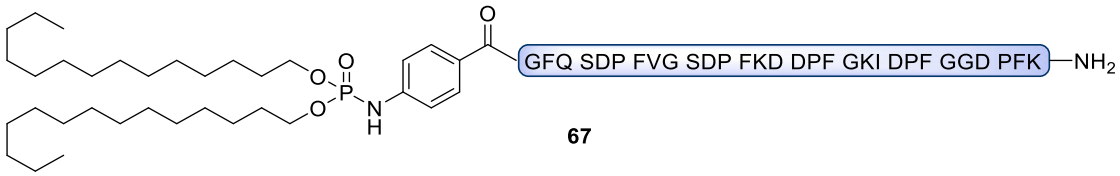

67

Procedure. Solid support bound azidobenzoic acetylated EPS15-peptide (0.01 mmol) was incubated with tris(tetradecyl) phosphite (70 mg; 0.10 mmol; 10 eq.) in 1.5 mL DCM at 30 °C for 20 h, followed by cleavage from the solid support (2 h; RT; 95 % TFA; 2 % TIS; 2 % DTT; 1 % PhSMe) and precipitation

in cold ether. Purification by preparative HPLC (10 min 50 %, then gradient of 50 % to 100 % of MeCN in water containing 0.1 % TFA on RP-C4 column; retention time 33 min) yielded the peptide **67** as white trifluoroacetate in good purity (6.09 mg; 1.45 µmol; yield 15 %).

Molar mass (peptide) = 3.85 kDa; molar mass (TFA_3 salt) = 4.19 kDa.

ESI-MS (positive mode): m/z (found) = 1284.2994 $[M+3H]^{3+}$ (calculated m/z = 1284.3316)

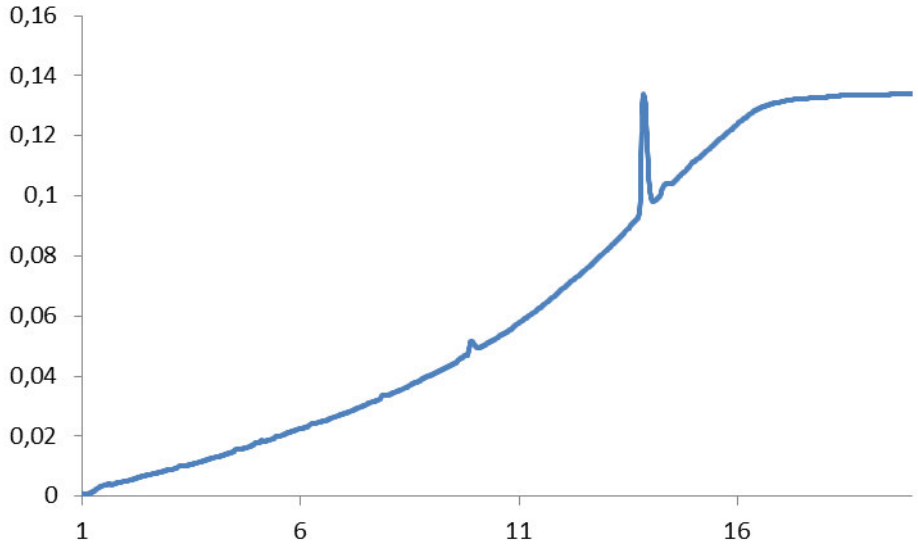

Figure 42. UPLC-UV chromatogram of bis(tetradecyl)-phosphoramidate-EPS15-peptide (**67**).

6.4.5 Synthesis of Lipidated FXDNF-Peptides

Octadecyl-pyridyl-phosphoramidate bivalent FEDNFVPG peptide (69)

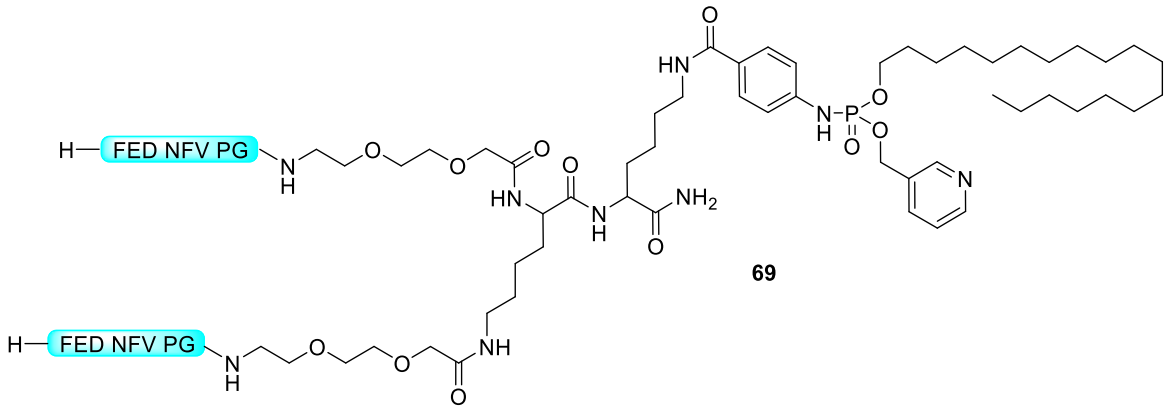

Procedure. After loading Nova PEG Rink Amide AM Resin LL (0.05 mmol; 0.23 mmol/g) with Alloc protected Fmoc-lysine followed by capping (pyridine:Ac_2O 9:1; 30 min; RT), Fmoc was removed to add Fmoc protected Fmoc-lysine as branching unit. The resin was applied to SPPS using Fmoc-chemistry with HOBt/HBTU/DIPEA double couplings in NMP on an Applied Biosystem synthesizer to simultaneously construct the two peptide handles starting with a PEG linker and leaving N-terminal

Fmoc on. The Alloc protecting group was removed using $Pd(PPh_3)_4$ (110 mg; 0.09 mmol; 1.8 eq.) in a mixture of $CHCl_3$/AcOH/NMM in a ratio of 37/2/1 for two hours at room temperature under Argon bubble mixture. To remove the Palladium catalyst afterwards, it was additionally washed with 0.2 M DIPEA in DMF. *Para*-azidobenzoic acid was coupled to the lysine side chain (10 eq.; HOBt and DIC in DMF; 1h; RT), Fmoch removed and the peptide was washed, dried and stored until further use. A part of the batch of azidopeptide (0.03 mmol) was incubated with octadecyl dipyridyl phosphite (**59**; 104 mg; 0.20 mmol; 6.7 eq.) in 2 mL DMF for 24 h, followed by cleavage from the solid support (2 h; RT; 95 % TFA; 2 % TIS; 2 % DTT; 1 % PhSMe) and precipitation in cold ether. Purification by preparative HPLC (50 to 60 % of MeCN in water containing 0.1 % TFA on RP-C4 column) yielded the peptide **69** as white trifluoroacetate in good purity (2.14 mg; 0.77 µmol; yield 3 %).

Molar mass (peptide) = 2.92 kDa; molar mass (TFA_2 salt) = 3.14 kDa.

ESI-MS (positive mode): m/z (found) = 973.1 $[M+3H]^{3+}$ (calculated m/z = 973.2), 1459.3 $[M+2H]^{2+}$ (calculated m/z = 1459.2), 1945.7 $[2M+3H]^{3+}$ (calculated m/z = 1945.3).

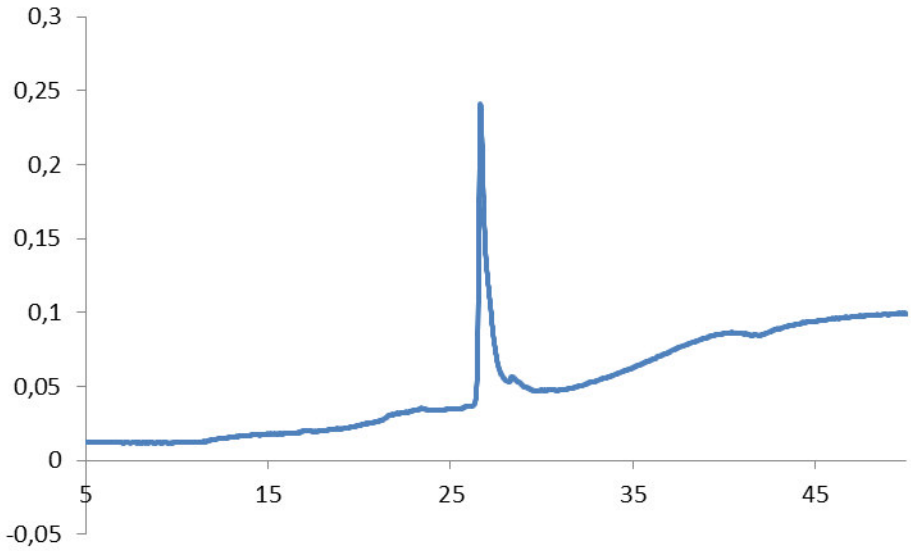

Figure 43. HPLC-UV chromatogram of octadecyl-pyridyl-phosphoramidate bivalent FEDNFVPG peptide (**69**).

Octadecyl-pyridyl-phosphoramidate bivalent INFFEDNFVPEIG peptide (70)

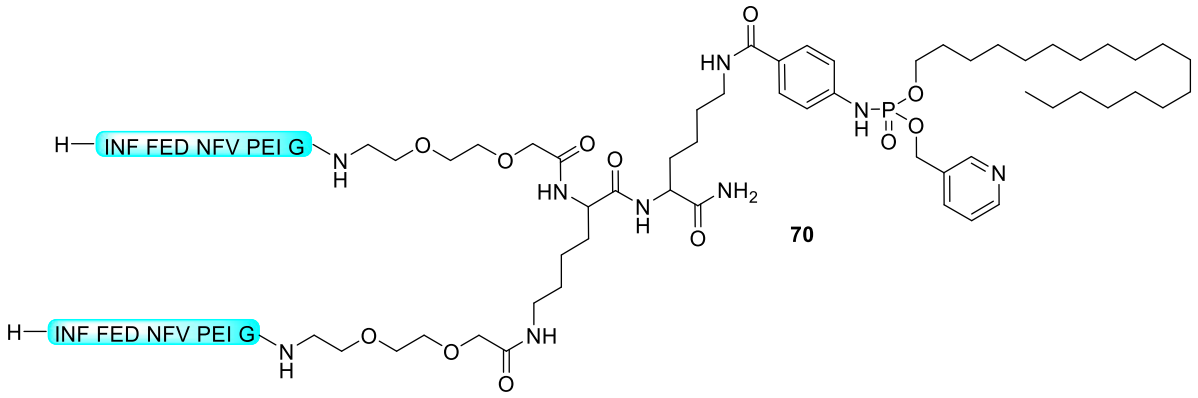

Procedure. After loading Nova PEG Rink Amide AM Resin LL (0.05 mmol; 0.23 mmol/g) with Alloc protected Fmoc-lysine followed by capping (pyridine:Ac_2O 9:1; 30 min; RT), Fmoc was removed to add Fmoc protected Fmoc-lysine as branching unit. The resin was applied to SPPS using Fmoc-chemistry with HOBt/HBTU/DIPEA double couplings in NMP on an Applied Biosystem synthesizer to simultaneously construct the two peptide handles starting with a PEG linker and leaving N-terminal Fmoc on. The Alloc protecting group was removed using $Pd(PPh_3)_4$ (110 mg; 0.09 mmol; 1.8 eq.) in a mixture of $CHCl_3$/AcOH/NMM in a ratio of 37/2/1 for two hours at room temperature under Argon bubble mixture. To remove the Palladium catalyst afterwards, it was additionally washed with 0.2 M DIPEA in DMF. *Para*-azidobenzoic acid was coupled to the lysine side chain (10 eq.; HOBt and DIC in DMF; 1h; RT), Fmoc was removed and the peptide was washed, dried and stored until further use. A part of the batch of azidopeptide (0.03 mmol) was incubated with octadecyl dipyridyl phosphite (**59**; 104 mg; 0.20 mmol; 6.7 eq.) in 2 mL DMF for 24 h, followed by cleavage from the solid support (2 h; RT; 95 % TFA; 2 % TIS; 2 % DTT; 1 % PhSMe) and precipitation in cold ether. Purification by preparative HPLC (50 to 60 % of MeCN in water containing 0.1 % TFA on RP-C4 column) yielded the peptide **70** as white trifluoroacetate in good purity (0.26 mg; 0.06 µmol; yield 0.2 %).

Molar mass (peptide) = 4.15 kDa; molar mass (TFA_2 salt) = 4.38 kDa.

ESI-MS (positive mode): m/z (found) = 1384.2 $[M+3H]^{3+}$ (calculated m/z = 1384.0).

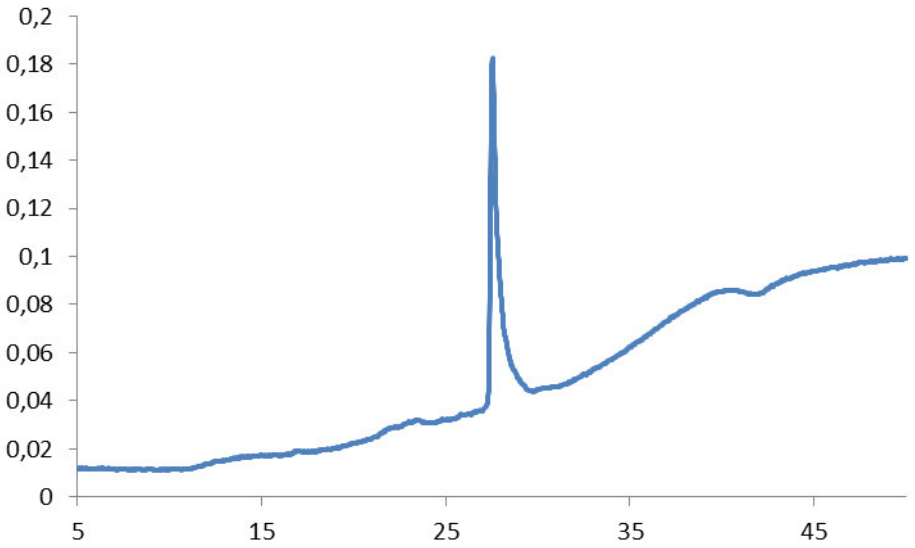

Figure 44. HPLC-UV chromatogram of octadecyl-pyridyl-phosphoramidate bivalent INFFEDNFVPEIG peptide (**70**).

6.4.6 Dynamic Light Scattering

DLS-measurements were performed on a Malvern Instruments Zetasizer nano ZS (Malvern Instruments Ltd., Worcestershire, UK) with a backscatter detection angle of 173° at a temperature of 25 °C using a 4 mW 632.8 nm HeNe laser. Each measurement was conducted at a concentration of 20 µM of EPS-peptide in PBS buffer at least three times. The size distribution by intensity was calculated by the software based on the correlation functions using the Multiple Narrow Modes algorithm consisting of a non-negative least squares fit.[195] This size distribution by intensity was converted to a distribution by volume employing the Mie theory.[196]

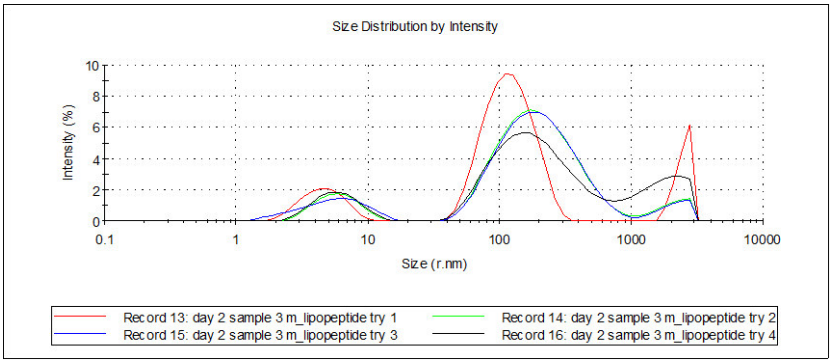

Figure 45. Size distribution of octadecyl-pyridyl-phosphoramidate-EPS15-peptide (**59**).

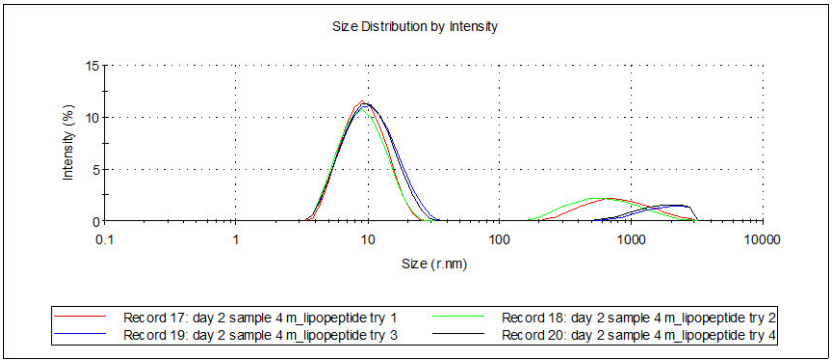

Figure 46. Size distribution of fluorescein labelled octadecyl-pyridyl-phosphoramidate-EPS15-peptide (**63**).

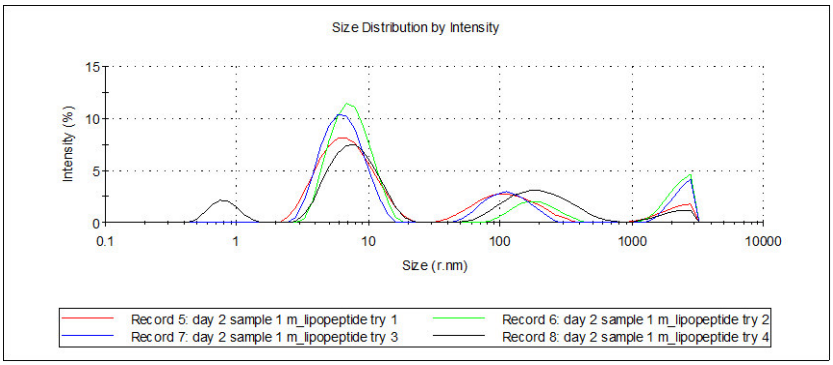

Figure 47. Size distribution of stearic acid coupled EPS15-azidopeptide (**64**).

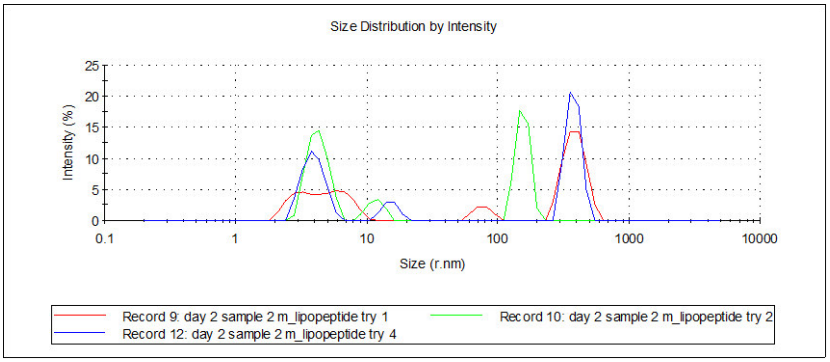

Figure 48. Size distribution of fluorescein labelled stearic acid coupled EPS15-peptide (**65**).

6.4.7 Cell Culture Experiments

Transferrin Uptake Assay. HeLa cells were split on matrigel/collagen coated coverslips in 24 well plates and incubated at 37 °C overnight. The next day, 70 % confluent cells were washed with PBS and starved in fetal bovine serum free DMEM for 1 h, followed by incubation with the candidate peptides at a concentration as indigated in fetal bovine serum free DMEM for 1 h. Transferrin uptake was carried out at the same concentration of candidate peptide with 20 µg/mL of Alexa568 coupled transferrin

(Invitrogen, USA) in fetal bovine serum free DMEM for 15 min at 37 °C. Afterwards the cells were washed with ice-cold PBS containing 10 mM $MgCl_2$ three times. Finally, the cells were fixed using 4 % *para* -formaldehyde and 4 % sucrose as osmotic stabilizer in PBS in the dark for 15 min and mounted to microscopic slides using Shandon Immu-Mount containing DAPI stain. Cells were imaged on an epifluorescence microscope (Nikon corporation, Japan) using the DAPI channel for the nuclei, the TxRed channel for Alexa568 coupled transferrin and the GFP channel in case of carboxyfluorescein. Data was analyzed using ImageJ (open scource). Per entry, at least 100 cells were imaged.

6.5 Covalent Attachment of Cyclic TAT Peptides to GFP Results in Protein Delivery into Live Cells with Immediate Bioavailability

6.5.1 Model Peptides for Studying Multiple CPP-GFP Conjugation

Fmoc-Glycine loaded Wang resin (127 mg; 0.1 mmol; 0.79 mmol/g) was applied to SPPS using double couplings with HOBt/HBTU/DIPEA in NMP on the Applied Biosystem synthesizer (sequence = GKGN). The resin was washed thoroughly and dried (total weight 160.4 mg).

Peptide with PEGlinker and Azidoglycine (71)

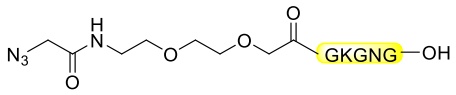

71

Wang resin bound peptide (40.1 mg; 0.025 mmol) was swollen in CH_2Cl_2 and consecutively, a PEGlinker (1x 10 eq., 2h; 1x 5 eq., o.n., RT, HOBt and DIC in DMF) and azidoglycine (10 eq., 2h, RT, HOBt and DIC in DMF) were coupled to the N-Terminus. After washing and drying, the peptide was cleaved from the solid support (2 h in 2 ml of mixture 95 % TFA, 2 % TIS, 2 % DTT, 1 % MeSPh) and purified by semi-preparative HPLC (0 to 100 % of MeCN in Water, containing 0,1 % TFA on RP-C18 column) to yield the peptide **71** as a white trifluoroacetate (7.90 mg; 10.22 µmol; yield 40.9 %; molar mass (peptide) = 0.66 kDa; molar mass (TFA_1 salt) = 0.77 kDa) in good purity. HRMS: m/z: 660.3078 $[M+H]^+$ (calcd. m/z: 660.3065; Δ 2.0 ppm).

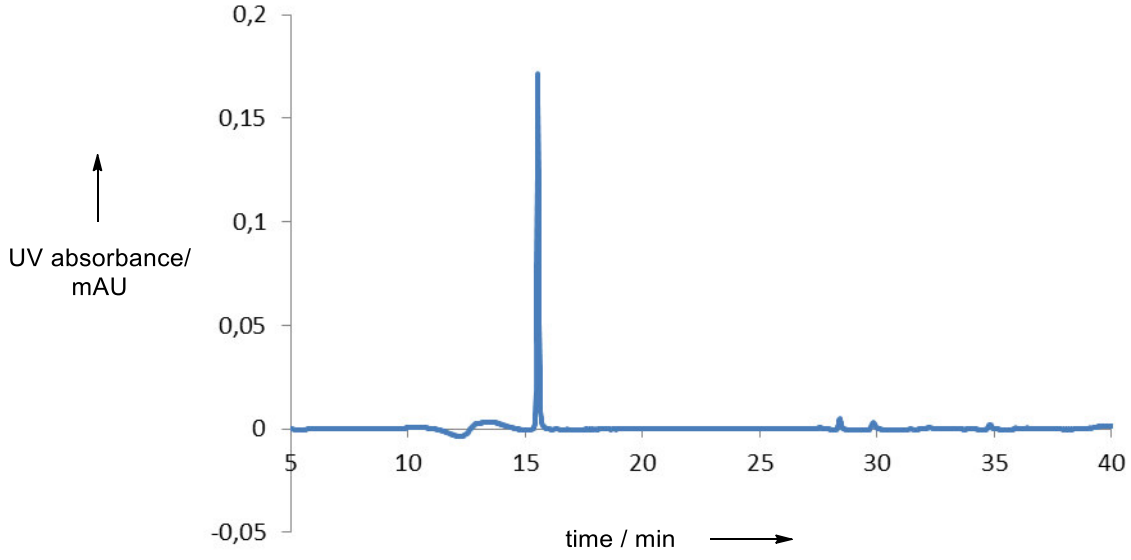

Figure 49. HPLC-UV-chromatogram of isolated **71** using a gradient of 0 % to 100 % MeCN in water (with 0.1 % TFA).

Peptide with PEGlinker and *para*-Azidobenzoic acid (72)

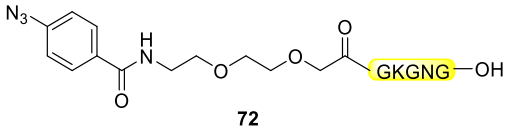

72

Wang resin bound peptide (40.1 mg; 0.025 mmol) was swollen in CH_2Cl_2 and consecutively, a PEGlinker (1x 10 eq. 2h, 1x 5 eq. o.n., RT, HOBt and DIC in DMF) and *para*-azidobenzoic acid (10 eq., 2h, RT, HOBt and DIC in DMF) were coupled to the N-Terminus. After washing and drying, the peptide was cleaved from the solid support (2 h in 2 ml of mixture 95 % TFA, 2 % TIS, 2 % DTT, 1 % MeSPh) and purified by semi-preparative HPLC (0 to 100 % of MeCN in Water, containing 0,1 % TFA on RP-C18 column) to yield the peptide **72** as a white trifluoroacetate (7.74 mg; 9.27 µmol; yield 37.1 %; molar mass (peptide) = 0.72 kDa; molar mass (TFA_1 salt) = 0.84 kDa) in good purity. HRMS: m/z: 722.3227 $[M+H]^+$ (calcd. m/z: 722.3221; Δ 0.8 ppm).

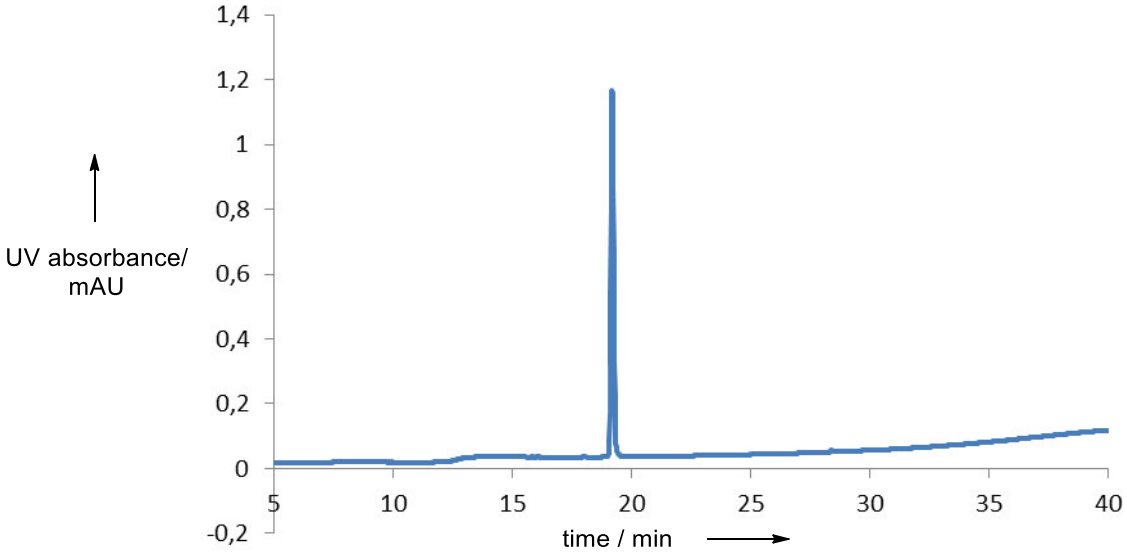

Figure 50. HPLC-UV chromatogram of isolated **72** using a gradient of 0 % to 100 % acetonitrile in water (with 0.1 % TFA) over 30 min.

6.5.2 Multivalent GFP-Mutants by AG Budisa

GFP mutants used in this study were provided by Nina Bohlke of AG Budisa, TU Berlin.

Bivalent GFP. The plasmid used for expression encoded a mutated variant of GFP containing two methionines at positions 134 and 143 in the loop regions, a serine at the N-terminus as well as an N-terminal HisTag and a Tobacco Etch Virus (TEV) protease recognition site to allow for purification of a homogenous protein after expression in a methionine auxotrophic E. coli strain in

homopropargylglycine containing medium. Incorporation of HPG in trivalent GFP was confirmed *via* ESI-MS (Exactive ESI-Orbitrap-MS, Thermo Fisher Scientific, US): found 26642 Da, calculated 26643 Da.

Trivalent GFP. The plasmid used for expression encoded a mutated variant of GFP containing tree methionines at positions 50, 134 and 143 in the loop regions, a serine at the N-terminus as well as an N-terminal HisTag and a Tobacco Etch Virus (TEV) protease recognition site to allow for purification of a homogenous protein after expression in a methionine auxotrophic E. coli strain in homopropargylglycine containing medium. Incorporation of HPG in trivalent GFP was confirmed *via* ESI-MS (Exactive ESI-Orbitrap-MS, Thermo Fisher Scientific, US): found 26650 Da, calculated 26651 Da.

7 REFERENCES

(1) Sood, A.; Panchagnula, R. *Chem. Rev. (Washington, D. C.)* **2001**, *101*, 3275.

(2) Sedelmeier, G.; Weber, F. *Nachrichten aus der Chemie* **2014**, *62*, 997.

(3) Werle, M.; Bernkop-Schnuerch, A. *Amino Acids* **2006**, *30*, 351.

(4) Kalia, J.; Raines, R. T. *Curr. Org. Chem.* **2010**, *14*, 138.

(5) Stephanopoulos, N.; Francis, M. B. *Nat. Chem. Biol.* **2011**, *7*, 876.

(6) Montalbetti, C. A. G. N.; Falque, V. *Tetrahedron* **2005**, *61*, 10827.

(7) Isidro-Llobet, A.; Alvarez, M.; Albericio, F. *Chem. Rev.* **2009**, *109*, 2455.

(8) Merrifield, R. B. *J. Am. Chem. Soc.* **1963**, *85*, 2149.

(9) Valeur, E.; Bradley, M. *Chem. Soc. Rev.* **2009**, *38*, 606.

(10) Wong, C. H.; Zimmerman, S. C. *Chem. Commun.* **2013**, *49*, 1679.

(11) Carpino, L. A.; Han, G. Y. *J Org. Chem.* **1972**, *37*, 3404.

(12) Atherton, E.; Fox, H.; Harkiss, D.; Logan, C. J.; Sheppard, R. C.; Williams, B. J. *J. Chem. Soc. Chem. Comm.* **1978**, 537.

(13) Alberts, B.; Johnson, A.; Lewis, J.; Raff, M.; Roberts, K.; Walter, P. *Molecular Biology of the Cell*; 4th ed.; Garland Science: New York, 2002.

(14) Takaoka, Y.; Ojida, A.; Hamachi, I. *Angew. Chem. Int. Edit.* **2013**, *52*, 4088.

(15) Dawson, P. E.; Muir, T. W.; Clark-Lewis, I.; Kent, S. B. *Science* **1994**, *266*, 776.

(16) Hackenberger, C. P. R.; Schwarzer, D. *Angew. Chem. Int. Edit.* **2008**, *47*, 10030.

(17) Muir, T. W.; Sondhi, D.; Cole, P. A. *Proceedings of the National Academy of Sciences of the United States of America* **1998**, *95*, 6705.

(18) Siman, P.; Brik, A. *Org. Biomol. Chem.* **2012**, *10*, 5684.

(19) Kochendoerfer, G. G.; Chen, S. Y.; Mao, F.; Cressman, S.; Traviglia, S.; Shao, H. Y.; Hunter, C. L.; Low, D. W.; Cagle, E. N.; Carnevali, M.; Gueriguian, V.; Keogh, P. J.; Porter, H.; Stratton, S. M.; Wiedeke, M. C.; Wilken, J.; Tang, J.; Levy, J. J.; Miranda, L. P.; Crnogorac, M. M.; Kalbag, S.; Botti, P.; Schindler-Horvat, J.; Savatski, L.; Adamson, J. W.; Kung, A.; Kent, S. B. H.; Bradburne, J. A. *Science* **2003**, *299*, 884.

(20) Pattabiraman, V. R.; Bode, J. W. *Nature* **2011**, *480*, 471.

(21) Saxon, E.; Armstrong, J. I.; Bertozzi, C. R. *Org. Lett.* **2000**, *2*, 2141.

(22) Nilsson, B. L.; Kiessling, L. L.; Raines, R. T. *Org. Lett.* **2000**, *2*, 1939.

(23) Levary, D. A.; Parthasarathy, R.; Boder, E. T.; Ackerman, M. E. *Plos One* **2011**, *6*.

(24) Mao, H. Y.; Hart, S. A.; Schink, A.; Pollok, B. A. *J. Am. Chem. Soc.* **2004**, *126*, 2670.

(25) Budisa, N. *Angew. Chem. Int. Edit.* **2004**, *43*, 6426.

(26) Kiick, K. L.; Saxon, E.; Tirrell, D. A.; Bertozzi, C. R. *Proceedings of the National Academy of Sciences of the United States of America* **2002**, *99*, 19.

(27) Tang, Y.; Tirrell, D. A. *Biochemistry* **2002**, *41*, 10635.

(28) Kast, P.; Hennecke, H. *Journal of molecular biology* **1991**, *222*, 99.

(29) Kirshenbaum, K.; Carrico, I. S.; Tirrell, D. A. *Chembiochem* **2002**, *3*, 235.

(30) Lepthien, S.; Merkel, L.; Budisa, N. *Angew. Chem. Int. Edit.* **2010**, *49*, 5446.

(31) Wang, L.; Schultz, P. G. *Angew. Chem. Int. Edit.* **2005**, *44*, 34.

(32) Noren, C. J.; Anthonycahill, S. J.; Griffith, M. C.; Schultz, P. G. *Science* **1989**, *244*, 182.

(33) Bain, J. D.; Glabe, C. G.; Dix, T. A.; Chamberlin, A. R.; Diala, E. S. *J. Am. Chem. Soc.* **1989**, *111*, 8013.

(34) Wang, L.; Brock, A.; Herberich, B.; Schultz, P. G. *Science* **2001**, *292*, 498.

(35) Chin, J. W.; Santoro, S. W.; Martin, A. B.; King, D. S.; Wang, L.; Schultz, P. G. *J. Am. Chem. Soc.* **2002**, *124*, 9026.

(36) Chin, J. W.; Cropp, T. A.; Anderson, J. C.; Mukherji, M.; Zhang, Z. W.; Schultz, P. G. *Science* **2003**, *301*, 964.

(37) Srinivasan, G.; James, C. M.; Krzycki, J. A. *Science* **2002**, *296*, 1459.

(38) Hao, B.; Gong, W. M.; Ferguson, T. K.; James, C. M.; Krzycki, J. A.; Chan, M. K. *Science* **2002**, *296*, 1462.

(39) Kaya, E.; Gutsmiedl, K.; Vrabel, M.; Muller, M.; Thumbs, P.; Carell, T. *Chembiochem* **2009**, *10*, 2858.

(40) Mukai, T.; Kobayashi, T.; Hino, N.; Yanagisawa, T.; Sakamoto, K.; Yokoyama, S. *Biochemical and biophysical research communications* **2008**, *371*, 818.

(41) Neumann, H.; Peak-Chew, S. Y.; Chin, J. W. *Nat. Chem. Biol.* **2008**, *4*, 232.

(42) Liu, C. C.; Schultz, P. G. *Annu. Rev. Biochem.* **2010**, *79*, 413.

(43) Xie, J. M.; Schultz, P. G. *Nat. Rev. Mol. Cell Bio.* **2006**, *7*, 775.

(44) Hoesl, M. G.; Budisa, N. *Chembiochem* **2011**, *12*, 552.

(45) Wan, W.; Huang, Y.; Wang, Z.; Russell, W. K.; Pai, P. J.; Russell, D. H.; Liu, W. R. *Angew. Chem. Int. Edit.* **2010**, *49*, 3211.

(46) Kolb, H. C.; Finn, M. G.; Sharpless, K. B. *Angew. Chem. Int. Edit.* **2001**, *40*, 2004.

(47) Prescher, J. A.; Bertozzi, C. R. *Nat. Chem. Biol.* **2005**, *1*, 13.

(48) Sletten, E. M.; Bertozzi, C. R. *Angew. Chem. Int. Edit.* **2009**, *48*, 6974.

(49) Ramil, C. P.; Lin, Q. *Chem. Commun.* **2013**, *49*, 11007.

(50) Patterson, D. M.; Nazarova, L. A.; Prescher, J. A. *ACS chemical biology* **2014**, *9*, 592.

(51) Lang, K.; Chin, J. W. *ACS chemical biology* **2014**, *9*, 16.

(52) Yang, M. Y.; Li, J.; Chen, P. R. *Chem. Soc. Rev.* **2014**, *43*, 6511.

(53) Boger, D. L. *Chem. Rev.* **1986**, *86*, 781.

(54) Devaraj, N. K.; Weissleder, R.; Hilderbrand, S. A. *Bioconjugate Chem* **2008**, *19*, 2297.

(55) Patterson, D. M.; Nazarova, L. A.; Xie, B.; Kamber, D. N.; Prescher, J. A. *J. Am. Chem. Soc.* **2012**, *134*, 18638.

(56) Yang, J.; Seckute, J.; Cole, C. M.; Devaraj, N. K. *Angew. Chem. Int. Edit.* **2012**, *51*, 7476.

(57) Blackman, M. L.; Royzen, M.; Fox, J. M. *J. Am. Chem. Soc.* **2008**, *130*, 13518.

(58) Song, W. J.; Yu, Z. P.; Madden, M. M.; Lin, Q. *Mol. Biosyst.* **2010**, *6*, 1572.

(59) Song, W.; Wang, Y.; Qu, J.; Madden, M. M.; Lin, Q. *Angew. Chem. Int. Edit.* **2008**, *47*, 2832.

(60) Song, W.; Wang, Y.; Qu, J.; Lin, Q. *J. Am. Chem. Soc.* **2008**, *130*, 9654.

(61) Wang, Y. Z.; Song, W. J.; Hu, W. J.; Lin, Q. *Angew. Chem. Int. Edit.* **2009**, *48*, 5330.

(62) Lallana, E.; Riguera, R.; Fernandez-Megia, E. *Angew. Chem. Int. Edit.* **2011**, *50*, 8794.

(63) Michael, A. *J. prakt. Chem.* **1893**, *48*, 94.

(64) Huisgen, R. *Angew. Chem. Int. Edit.* **1963**, *75*, 604.

(65) Rostovtsev, V. V.; Green, L. G.; Fokin, V. V.; Sharpless, K. B. *Angew. Chem. Int. Edit.* **2002**, *41*, 2596.

(66) Tornoe, C. W.; Christensen, C.; Meldal, M. *J. Org. Chem.* **2002**, *67*, 3057.

(67) Meldal, M.; Tornoe, C. W. *Chem. Rev.* **2008**, *108*, 2952.

(68) Lewis, W. G.; Magallon, F. G.; Fokin, V. V.; Finn, M. G. *J. Am. Chem. Soc.* **2004**, *126*, 9152.

(69) Chan, T. R.; Hilgraf, R.; Sharpless, K. B.; Fokin, V. V. *Org. Lett.* **2004**, *6*, 2853.

(70) Hong, V.; Presolski, S. I.; Ma, C.; Finn, M. G. *Angew. Chem. Int. Edit.* **2009**, *48*, 9879.

(71) Besanceney-Webler, C.; Jiang, H.; Zheng, T. Q.; Feng, L.; del Amo, D. S.; Wang, W.; Klivansky, L. M.; Marlow, F. L.; Liu, Y.; Wu, P. *Angew. Chem. Int. Edit.* **2011**, *50*, 8051.

(72) del Amo, D. S.; Wang, W.; Jiang, H.; Besanceney, C.; Yan, A. C.; Levy, M.; Liu, Y.; Marlow, F. L.; Wu, P. *J. Am. Chem. Soc.* **2010**, *132*, 16893.

(73) Worrell, B. T.; Malik, J. A.; Fokin, V. V. *Science* **2013**, *340*, 457.

(74) Zhang, L.; Chen, X. G.; Xue, P.; Sun, H. H. Y.; Williams, I. D.; Sharpless, K. B.; Fokin, V. V.; Jia, G. C. *J. Am. Chem. Soc.* **2005**, *127*, 15998.

(75) Rasmussen, L. K.; Boren, B. C.; Fokin, V. V. *Org. Lett.* **2007**, *9*, 5337.

(76) Boren, B. C.; Narayan, S.; Rasmussen, L. K.; Zhang, L.; Zhao, H. T.; Lin, Z. Y.; Jia, G. C.; Fokin, V. V. *J. Am. Chem. Soc.* **2008**, *130*, 14900.

(77) Agard, N. J.; Prescher, J. A.; Bertozzi, C. R. *J. Am. Chem. Soc.* **2004**, *126*, 15046.

(78) Codelli, J. A.; Baskin, J. M.; Agard, N. J.; Bertozzi, C. R. *J. Am. Chem. Soc.* **2008**, *130*, 11486.

(79) Baskin, J. M.; Prescher, J. A.; Laughlin, S. T.; Agard, N. J.; Chang, P. V.; Miller, I. A.; Lo, A.; Codelli, J. A.; Bertozzi, C. R. *Proceedings of the National Academy of Sciences of the United States of America* **2007**, *104*, 16793.

(80) Sletten, E. M.; Bertozzi, C. R. *Org. Lett.* **2008**, *10*, 3097.

(81) Jewett, J. C.; Sletten, E. M.; Bertozzi, C. R. *J. Am. Chem. Soc.* **2010**, *132*, 3688.

(82) Dommerholt, J.; Schmidt, S.; Temming, R.; Hendriks, L. J. A.; Rutjes, F. P. J. T.; van Hest, J. C. M.; Lefeber, D. J.; Friedl, P.; van Delft, F. L. *Angew. Chem. Int. Edit.* **2010**, *49*, 9422.

(83) Ning, X.; Guo, J.; Wolfert, M. A.; Boons, G.-J. *Angew. Chem. Int. Edit.***2008**, *47*, 2253.

(84) Debets, M. F.; van, B. S. S.; Schoffelen, S.; Rutjes, F. P. J. T.; van, H. J. C. M.; van, D. F. L. *Chem. Commun. (Cambridge, U. K.)* **2010**, *46*, 97.

(85) Leunissen, E. H. P.; Meuleners, M. H. L.; Verkade, J. M. M.; Dommerholt, J.; Hoenderop, J. G. J.; van Delft, F. L. *Chembiochem* **2014**, *15*, 1446.

(86) van Geel, R.; Pruijn, G. J. M.; van Delft, F. L.; Boelens, W. C. *Bioconjugate Chem.* **2012**, *23*, 392.

(87) Staudinger, H.; Meyer, J. *Helv. Chim. Acta* **1919**, *2*, 635.

(88) van Berkel, S. S.; van Eldijk, M. B.; van Hest, J. C. *Angew. Chem. Int. Edit.* **2011**, *50*, 8806.

(89) Schilling, C. I.; Jung, N.; Biskup, M.; Schepers, U.; Brase, S. *Chem. Soc. Rev.* **2011**, *40*, 4840.

(90) Saxon, E.; Bertozzi, C. R. *Science* **2000**, *287*, 2007.

(91) Tam, A.; Soellner, M. B.; Raines, R. T. *Org. Biomol. Chem.* **2008**, *6*, 1173.

(92) Tam, A.; Raines, R. T. *Methods in Enzymology: Non-Natural Amino Acids* **2009**, *462*, 25.

(93) Soellner, M. B.; Nilsson, B. L.; Raines, R. T. *J. Am. Chem. Soc.* **2006**, *128*, 8820.

(94) Gololobov, Y. G.; Zhmurova, I. N.; Kasukhin, L. F. *Tetrahedron* **1981**, *37*, 437.

(95) Kabachnik, M. I.; Gilyarov, V. A. *Russ. Chem. Bull.* **1956**, *5*, 809.

(96) Gololobov, Y. G.; Kasukhin, L. F. *Tetrahedron* **1992**, *48*, 1353.

(97) Chaturve.Rk; Pletcher, T. C.; Zioudrou, C.; Schmir, G. L. *Tetrahedron Lett.* **1970**, 4339.

(98) Bohrsch, V.; Serwa, R.; Majkut, P.; Krause, E.; Hackenberger, C. P. R. *Chem. Commun.* **2010**, *46*, 3176.

(99) Cooper, D.; Trippett, S.; White, C. *J. Chem. Res.* **1983**, 234.

(100) Boehrsch, V.; Mathew, T.; Zieringer, M.; Vallee, M. R. J.; Artner, L. M.; Dernedde, J.; Haag, R.; Hackenberger, C. P. R. *Org. Biomol. Chem.* **2012**, *10*, 6211.

(101) Serwa, R.; Majkut, P.; Horstmann, B.; Swiecicki, J.-M.; Gerrits, M.; Krause, E.; Hackenberger, C. P. R. *Chem. Sci.* **2010**, *1*, 596.

(102) Serwa, R.; Wilkening, I.; Del, S. G.; Muehlberg, M.; Claussnitzer, I.; Weise, C.; Gerrits, M.; Hackenberger, C. P. R. *Angew. Chem. Int. Edit.* **2009**, *48*, 8234.

(103) Serwa, R. A.; Swiecicki, J.-M.; Homann, D.; Hackenberger, C. P. R. *J. Pept. Sci.* **2010**, *16*, 563.

(104) Mathew, T.; Hackenberger, C. P. R. *unpublished results*.

(105) Bertran-Vicente, J.; Serwa, R. A.; Schumann, M.; Schmieder, P.; Krause, E.; Hackenberger, C. P. *J. Am. Chem. Soc.* **2014**, *136*, 13622.

(106) Vallee, M. R. J.; Artner, L. M.; Dernedde, J.; Hackenberger, C. P. R. *Angew. Chem. Int. Edit.* **2013**, *52*, 9504.

(107) Vallee, M. R.; Majkut, P.; Krause, D.; Gerrits, M.; Hackenberger, C. P. *Chemistry* **2015**, *21*, 970.

(108) Casey, P. J. *Science* **1995**, *268*, 221.

(109) Resh, M. D. *Bba-Mol. Cell Res.* **1999**, *1451*, 1.

(110) Resh, M. D. *Nat. Chem. Biol.* **2006**, *2*, 584.

(111) Ward, B. P.; Ottaway, N. L.; Perez-Tilve, D.; Ma, D.; Gelfanov, V. M.; Tschop, M. H.; Dimarchi, R. D. *Molecular metabolism* **2013**, *2*, 468.

(112) Yu, Y. C.; Tirrell, M.; Fields, G. B. *J. Am. Chem. Soc.* **1998**, *120*, 9979.

(113) Knudsen, L. B.; Nielsen, P. F.; Huusfeldt, P. O.; Johansen, N. L.; Madsen, K.; Pedersen, F. Z.; Thogersen, H.; Wilken, M.; Agerso, H. *J. Med. Chem.* **2000**, *43*, 1664.

(114) Bellmann-Sickert, K.; Elling, C. E.; Madsen, A. N.; Little, P. B.; Lundgren, K.; Gerlach, L. O.; Bergmann, R.; Holst, B.; Schwartz, T. W.; Beck-Sickinger, A. G. *J. Med. Chem.* **2011**, *54*, 2658.

(115) Frokjaer, S.; Otzen, D. E. *Nat. Rev. Drug Discovery* **2005**, *4*, 298.

(116) McGregor, C. L.; Chen, L.; Pomroy, N. C.; Hwang, P.; Go, S.; Chakrabartty, A.; Prive, G. G. *Nat. Biotechnol.* **2003**, *21*, 171.

(117) Smith, R. H.; Powell, G. L. *Arch. Biochem. Biophys.* **1986**, *244*, 357.

(118) Hamley, I. W. *Soft Matter* **2011**, *7*, 4122.

(119) Kokkoli, E.; Mardilovich, A.; Wedekind, A.; Rexeisen, E. L.; Garg, A.; Craig, J. A. *Soft Matter* **2006**, *2*, 1015.

(120) Brunsveld, L.; Kuhlmann, J.; Alexandrov, K.; Wittinghofer, A.; Goody, R. S.; Waldmann, H. *Angew. Chem. Int. Edit.* **2006**, *45*, 6622.

(121) Hang, H. C.; Linder, M. E. *Chem. Rev.* **2011**, *111*, 6341.

(122) Brock, R. *Bioconjug. Chem.* **2014**, *25*, 863.

(123) Heitz, F.; Morris, M. C.; Divita, G. *Brit. J. Pharmacol.* **2009**, *157*, 195.

(124) Torchilin, V. P. *Biopolymers* **2008**, *90*, 604.

(125) Wagstaff, K. M.; Jans, D. A. *Curr. Med. Chem.* **2006**, *13*, 1371.

(126) Erazo-Oliveras, A.; Najjar, K.; Dayani, L.; Wang, T. Y.; Johnson, G. A.; Pellois, J. P. *Nature methods* **2014**, *11*, 861.

(127) Ter-Avetisyan, G.; Tunnemann, G.; Nowak, D.; Nitschke, M.; Herrmann, A.; Drab, M.; Cardoso, M. C. *J. Biol. Chem.* **2009**, *284*, 3370.

(128) Futaki, S.; Hirose, H.; Nakase, I. *Current pharmaceutical design* **2013**, *19*, 2863.

(129) Futaki, S. *Adv. Drug Deliver. Rev.* **2005**, *57*, 547.

(130) Futaki, S.; Suzuki, T.; Ohashi, W.; Yagami, T.; Tanaka, S.; Ueda, K.; Sugiura, Y. *Journal of Biological Chemistry* **2001**, *276*, 5836.

(131) Delaroche, D.; Aussedat, B.; Aubry, S.; Chassaing, G.; Burlina, F.; Clodic, G.; Bolbach, G.; Lavielle, S.; Sagan, S. *Anal. Chem.* **2007**, *79*, 1932.

(132) Schmidt, N.; Mishra, A.; Lai, G. H.; Wong, G. C. L. *Febs Lett.* **2010**, *584*, 1806.

(133) Wender, P. A.; Mitchell, D. J.; Pattabiraman, K.; Pelkey, E. T.; Steinman, L.; Rothbard, J. B. *Proceedings of the National Academy of Sciences of the United States of America* **2000**, *97*, 13003.

(134) Saleh, A. F.; Arzumanov, A.; Abes, R.; Owen, D.; Lebleu, B.; Gait, M. J. *Bioconjugate Chem.* **2010**, *21*, 1902.

(135) Swiecicki, J. M.; Bartsch, A.; Tailhades, J.; Di Pisa, M.; Heller, B.; Chassaing, G.; Mansuy, C.; Burlina, F.; Lavielle, S. *Chembiochem* **2014**, *15*, 884.

(136) Herce, H. D.; Garcia, A. E. *Journal of biological physics* **2007**, *33*, 345.

(137) Herce, H. D.; Garcia, A. E.; Litt, J.; Kane, R. S.; Martin, P.; Enrique, N.; Rebolledo, A.; Milesi, V. *Biophysical journal* **2009**, *97*, 1917.

(138) Herce, H. D.; Garcia, A. E.; Cardoso, M. C. *J. Am. Chem. Soc.* **2014**, *136*, 17459.

(139) Sakai, N.; Matile, S. *J. Am. Chem. Soc.* **2003**, *125*, 14348.

(140) Ziegler, A.; Seelig, J. *Biochemistry* **2011**, *50*, 4650.

(141) Inomata, K.; Ohno, A.; Tochio, H.; Isogai, S.; Tenno, T.; Nakase, I.; Takeuchi, T.; Futaki, S.; Ito, Y.; Hiroaki, H.; Shirakawa, M. *Nature* **2009**, *458*, 106.

(142) Takeuchi, T.; Kosuge, M.; Tadokoro, A.; Sugiura, Y.; Nishi, M.; Kawata, M.; Sakai, N.; Matile, S.; Futaki, S. *ACS chemical biology* **2006**, *1*, 299.

(143) Nakase, I.; Takeuchi, T.; Tanaka, G.; Futaki, S. *Adv. Drug Deliver Rev.* **2008**, *60*, 598.

(144) Saar, K.; Lindgren, M.; Hansen, M.; Eiriksdottir, E.; Jiang, Y.; Rosenthal-Aizman, K.; Sassian, M.; Langel, U. *Analytical biochemistry* **2005**, *345*, 55.

(145) Zorko, M.; Langel, U. *Adv. Drug Deliver. Rev.* **2005**, *57*, 529.

(146) El-Andaloussi, S.; Jarver, P.; Johansson, H. J.; Langel, U. *The Biochemical journal* **2007**, *407*, 285.

(147) Cardozo, A. K.; Buchillier, V.; Mathieu, M.; Chen, J.; Ortis, F.; Ladriere, L.; Allaman-Pillet, N.; Poirot, O.; Kellenberger, S.; Beckmann, J. S.; Eizirik, D. L.; Bonny, C.; Maurer, F. *Biochimica et biophysica acta* **2007**, *1768*, 2222.

(148) Torchilin, V. *Drug discovery today. Technologies* **2008**, *5*, e95.

(149) Muller, S.; Zhao, Y. F.; Brown, T. L.; Morgan, A. C.; Kohler, H. *Expert Opin. Biol. Th.* **2005**, *5*, 237.

(150) Harris, J. M.; Chess, R. B. *Nat. Rev. Drug Discovery* **2003**, *2*, 214.

(151) Monfardini, C.; Schiavon, O.; Caliceti, P.; Morpurgo, M.; Harris, J. M.; Veronese, F. M. *Bioconjugate Chem.* **1995**, *6*, 62.

(152) Veronese, F. M.; Caliceti, P.; Schiavon, O. *J. Bioact. Compat. Polym.* **1997**, *12*, 196.

(153) Fee, C. J. *Biotechnol. Bioeng.* **2007**, *98*, 725.

(154) Pinholt, C.; Bukrinsky, J. T.; Hostrup, S.; Frokjaer, S.; Norde, W.; Jorgensen, L. *Eur. J. Pharm. Biopharm.* **2011**, *77*, 139.

(155) Haag, R. *Angew. Chem. Int. Edit.* **2004**, *43*, 278.

(156) Tunnemann, G.; Martin, R. M.; Haupt, S.; Patsch, C.; Edenhofer, F.; Cardoso, M. C. *Faseb J.* **2006**, *20*, 1775.

(157) Lattig-Tunnemann, G.; Prinz, M.; Hoffmann, D.; Behlke, J.; Palm-Apergi, C.; Morano, I.; Herce, H. D.; Cardoso, M. C. *Nature communications* **2011**, *2*, 453.

(158) Fried, W. *Exp. Hematol.* **2009**, *37*, 1007.

(159) Narhi, L. O.; Arakawa, T.; Aoki, K. H.; Elmore, R.; Rohde, M. F.; Boone, T.; Strickland, T. W. *J. Biol. Chem.* **1991**, *266*, 23022.

(160) Takeuchi, M.; Takasaki, S.; Miyazaki, H.; Kato, T.; Hoshi, S.; Kochibe, N.; Kobata, A. *J. Biol. Chem.* **1988**, *263*, 3657.

(161) Sasaki, H.; Bothner, B.; Dell, A.; Fukuda, M. *J. Biol. Chem.* **1987**, *262*, 12059.

(162) Kajihara, Y.; Yamamoto, N.; Okamoto, R.; Hirano, K.; Murase, T. *Chem. Rec.* **2010**, *10*, 80.

(163) Brailsford, J. A.; Danishefsky, S. J. *Proceedings of the National Academy of Sciences of the United States of America* **2012**, *109*, 7196.

(164) Wang, P.; Dong, S. W.; Brailsford, J. A.; Iyer, K.; Townsend, S. D.; Zhang, Q.; Hendrickson, R. C.; Shieh, J.; Moore, M. A. S.; Danishefsky, S. J. *Angew. Chem. Int. Edit.* **2012**, *51*, 11576.

(165) Nischan, N.; Hackenberger, C. P. *J. Org. Chem.* **2014**, *79*, 10727.

(166) Majkut, P.; Boehrsch, V.; Serwa, R.; Gerrits, M.; Hackenberger, C. P. R. *Methods Mol. Biol. (N. Y., NY, U. S.)* **2012**, *794*, 241.

(167) Nischan, N.; Chakrabarti, A.; Serwa, R. A.; Bovee-Geurts, P. H. M.; Brock, R.; Hackenberger, C. P. R. *Angew. Chem. Int. Edit.* **2013**, *52*, 11920.

(168) Cho, H.; Daniel, T.; Buechler, Y. J.; Litzinger, D. C.; Maio, Z.; Putnam, A.-M. H.; Kraynov, V. S.; Sim, B.-C.; Bussell, S.; Javahishvili, T.; Kaphle, S.; Viramontes, G.; Ong, M.; Chu, S.; Becky, G. C.; Lieu, R.; Knudsen, N.; Castiglioni, P.; Norman, T. C.; Axelrod, D. W.; Hoffman, A. R.; Schultz, P. G.; DiMarchi, R. D.; Kimmel, B. E. *Proc. Natl. Acad. Sci. U. S. A.* **2011**, *108*, 9060.

(169) Veronese, F. M. *Biomaterials* **2001**, *22*, 405.

(170) Eckl, K. M.; Weindl, G.; Ackermann, K.; Kuchler, S.; Casper, R.; Radowski, M. R.; Haag, R.; Hennies, H. C.; Schafer-Korting, M. *Experimental dermatology* **2014**, *23*, 286.

(171) Kuchler, S.; Abdel-Mottaleb, M.; Lamprecht, A.; Radowski, M. R.; Haag, R.; Schafer-Korting, M. *Int. J. Pharmaceut.* **2009**, *377*, 169.

(172) Kuchler, S.; Radowski, M. R.; Blaschke, T.; Dathe, M.; Plendl, J.; Haag, R.; Schafer-Korting, M.; Kramer, K. D. *Eur. J. Pharm. Biopharm.* **2009**, *71*, 243.

(173) Wolf, N. B.; Kuchler, S.; Radowski, M. R.; Blaschke, T.; Kramer, K. D.; Weindl, G.; Kleuser, B.; Haag, R.; Schafer-Korting, M. *Eur. J. Pharm. Biopharm.* **2009**, *73*, 34.

(174) Doherty, G. J.; McMahon, H. T. *Annu. Rev. Biochem.* **2009**, *78*, 857.

(175) Schmid, S. L. *Annu. Rev. Biochem.* **1997**, *66*, 511.

(176) Takei, K.; Haucke, V. *Trends Cell Biol.* **2001**, *11*, 385.

(177) Olesen, L. E.; Ford, M. G. J.; Schmid, E. M.; Vallis, Y.; Babu, M. M.; Li, P. H.; Mills, I. G.; Mcmahon, H. T.; Praefcke, G. J. K. *Journal of Biological Chemistry* **2008**, *283*, 5099.

(178) Wieffer, M.; Maritzen, T.; Haucke, V. *Cell* **2009**, *137*.

(179) von Kleist, L.; Haucke, V. *Traffic* **2012**, *13*, 495.

(180) von Kleist, L.; Stahlschmidt, W.; Bulut, H.; Gromova, K.; Puchkov, D.; Robertson, M. J.; MacGregor, K. A.; Tomilin, N.; Pechstein, A.; Chau, N.; Chircop, M.; Sakoff, J.; von Kries, J. P.; Saenger, W.; Krausslich, H. G.; Shupliakov, O.; Robinson, P. J.; McCluskey, A.; Haucke, V. *Cell* **2011**, *146*, 841.

(181) Stahlschmidt, W.; Robertson, M. J.; Robinson, P. J.; McCluskey, A.; Haucke, V. *Journal of Biological Chemistry* **2014**, *289*, 4906.

(182) Smith, C. M.; Haucke, V.; McCluskey, A.; Robinson, P. J.; Chircop, M. *Mol. Cancer* **2013**, *12*.

(183) Benmerah, A.; Begue, B.; DautryVarsat, A.; CerfBensussan, N. *Journal of Biological Chemistry* **1996**, *271*, 12111.

(184) Henegouwen, P. M. P. V. E. *Cell Commun. Signal*. **2009**, *7*.

(185) Slepnev, V. I.; Ochoa, G. C.; Butler, M. H.; De Camilli, P. *Journal of Biological Chemistry* **2000**, *275*, 17583.

(186) Stahlschmidt, W.; Haucke, V. *unpublished results*.

(187) Russell, M. A.; Laws, A. P.; Atherton, J. H.; Page, M. I. *Org. Biomol. Chem.* **2008**, *6*, 3270.

(188) Alford, R.; Simpson, H. M.; Duberman, J.; Hill, G. C.; Ogawa, M.; Regino, C.; Kobayashi, H.; Choyke, P. L. *Mol. Imaging* **2009**, *8*, 341.

(189) Fischer, R.; Mader, O.; Jung, G.; Brock, R. *Bioconjugate Chem.* **2003**, *14*, 653.

(190) Ilia, G.; Iliescu, S.; Macarie, L.; Popa, A. *Heteroat. Chem.* **2008**, *19*, 360.

(191) Caron, N. J.; Torrente, Y.; Camirand, G.; Bujold, M.; Chapdelaine, P.; Leriche, K.; Bresolin, N.; Tremblay, J. P. *Molecular therapy : the journal of the American Society of Gene Therapy* **2001**, *3*, 310.

(192) Richard, J. P.; Melikov, K.; Vives, E.; Ramos, C.; Verbeure, B.; Gait, M. J.; Chernomordik, L. V.; Lebleu, B. *J. Biol. Chem.* **2003**, *278*, 585.

(193) Nischan, N.; Herce, H. D.; Natale, F.; Bohlke, N.; Budisa, N.; Cardoso, M. C.; Hackenberger, C. P. *Angewandte Chemie* **2014**.

(194) Meier, C.; Muus, U.; Renze, J.; Naesens, L.; De Clercq, E.; Balzarini, J. *Antiviral chemistry & chemotherapy* **2002**, *13*, 101.

(195) Lawson, C. L.; Hanson, R. J. *Solving Least Squares Problems*; Society for industrial and applied mathematics (SIAM): Philadelphia, U.S., 1995.

(196) Mie, G. *Ann. Phys. (Weinheim, Ger.)* **1908**, *25*, 377.

8 APPENDIX

8.1 PEGylation of Polyglycerols

PEG200-hPG1

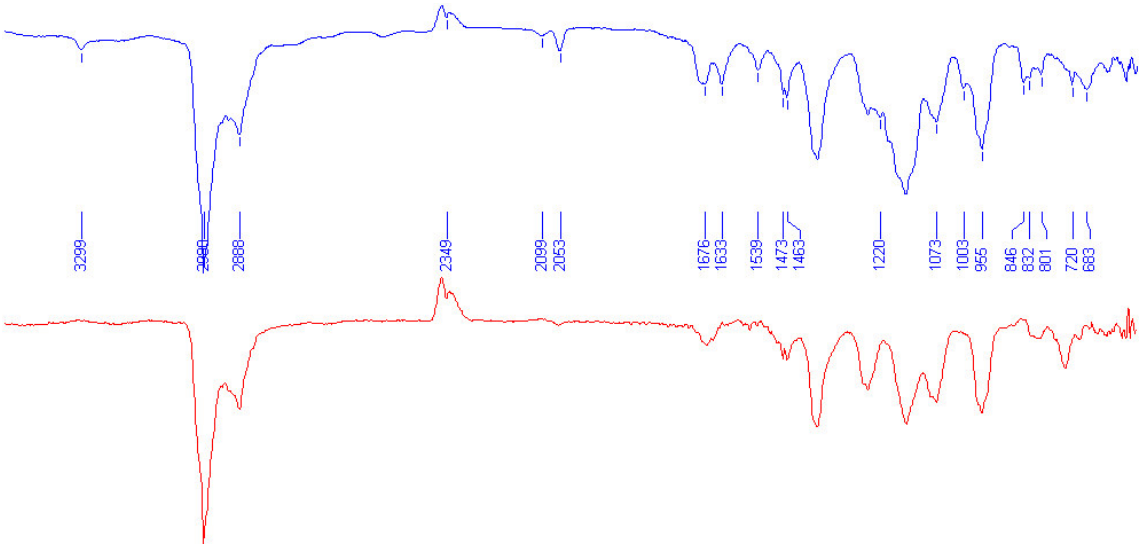

Figure 51. IR spectra of starting material **hPG1** (top) vs. product **PEG200-hPG1** (bottom).

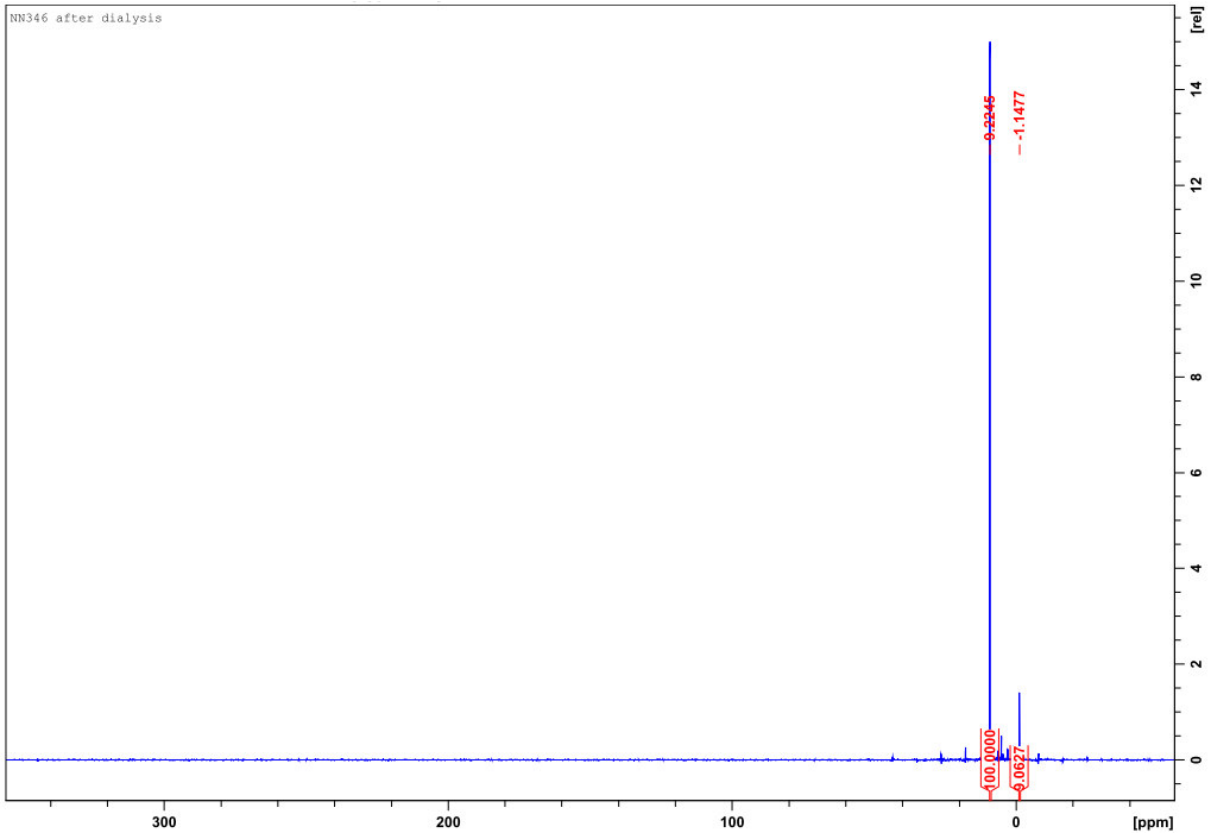

Figure 52. ^{31}P-NMR spectrum of **PEG200-hPG1**.

PEG200-hPG2

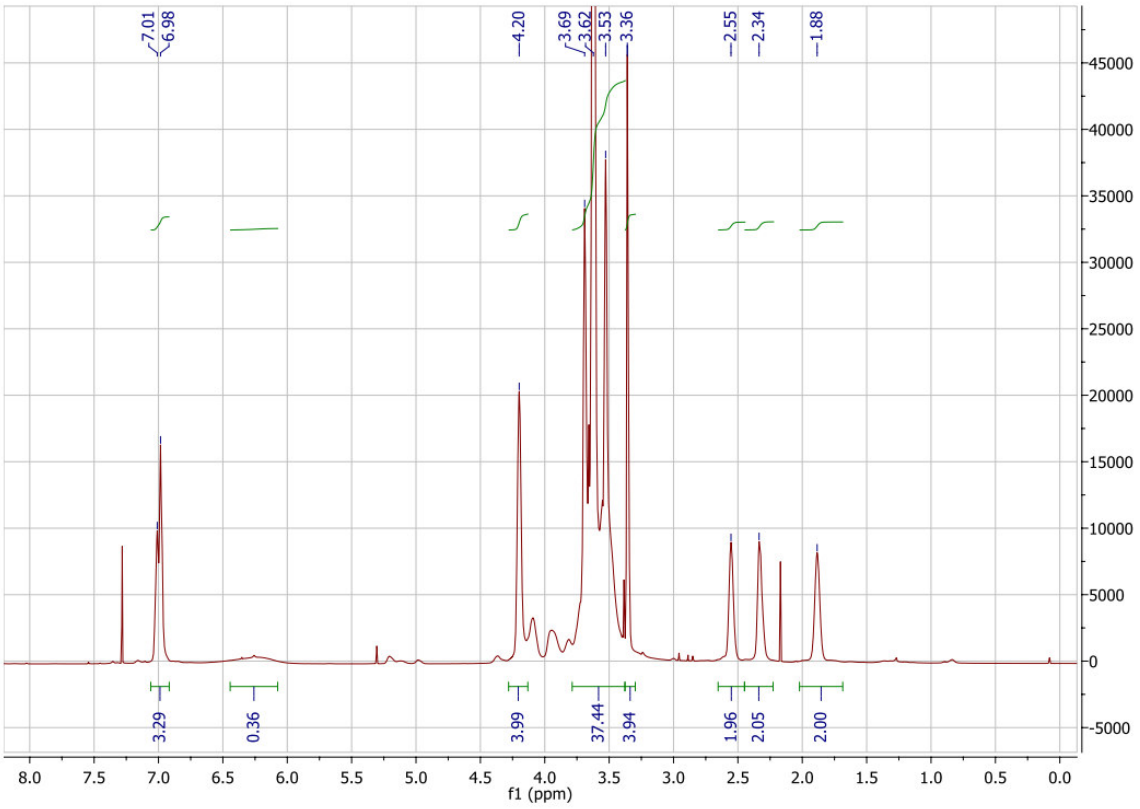

Figure 53. ^{1}H-NMR spectrum of **PEG200-hPG2**

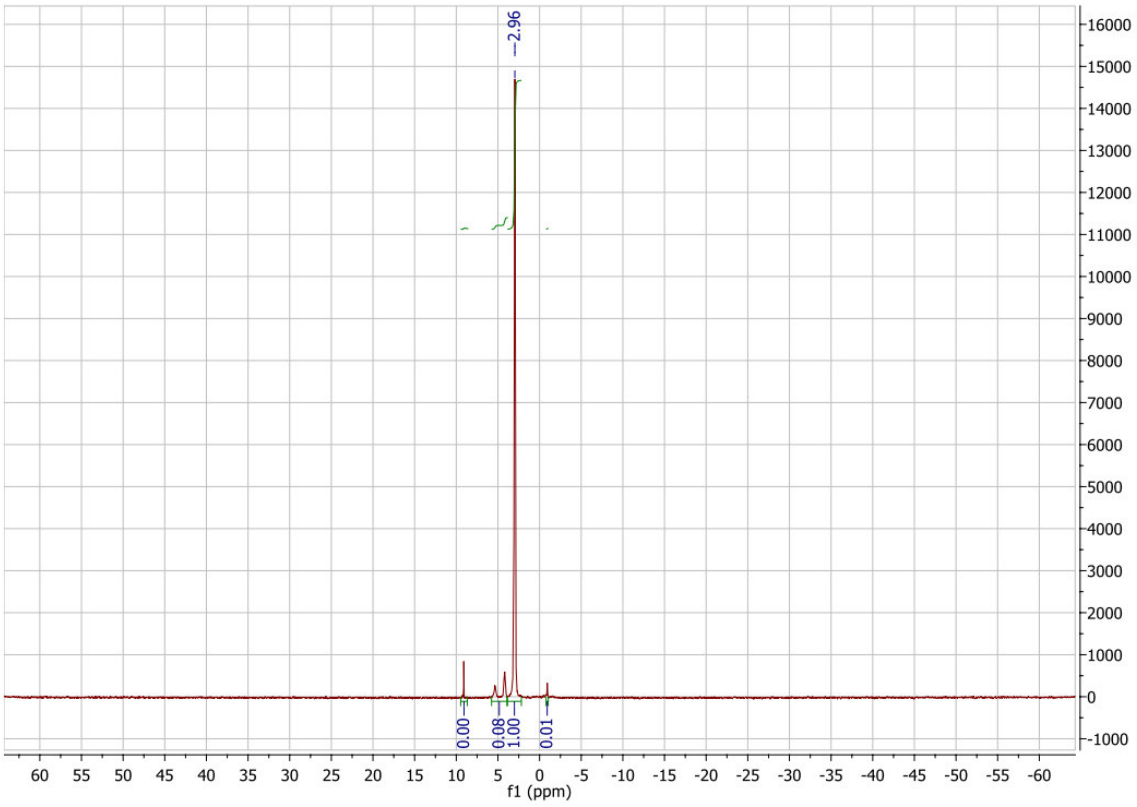

Figure 54. ^{31}P-NMR spectrum of **PEG200-hPG2**.

8.2 Lipidation

8.2.1 Spectra of Unsymmetrical Phosphites

Bis(pyridyl)-*N*,*N*-diisopropylphosphoramidite (51)

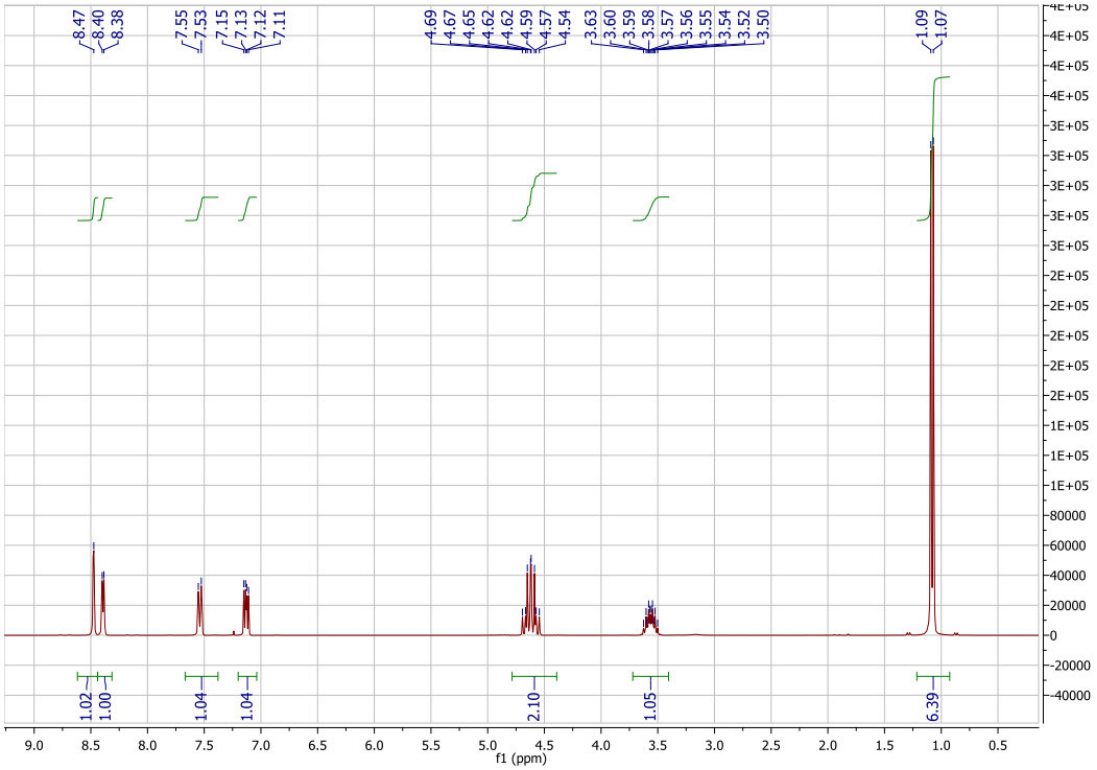

Figure 55. ^{1}H-NMR spectrum of bis(pyridyl)-*N*,*N*-diisopropylphosphoramidite (**51**) (300 MHz, $CHCl_3$).

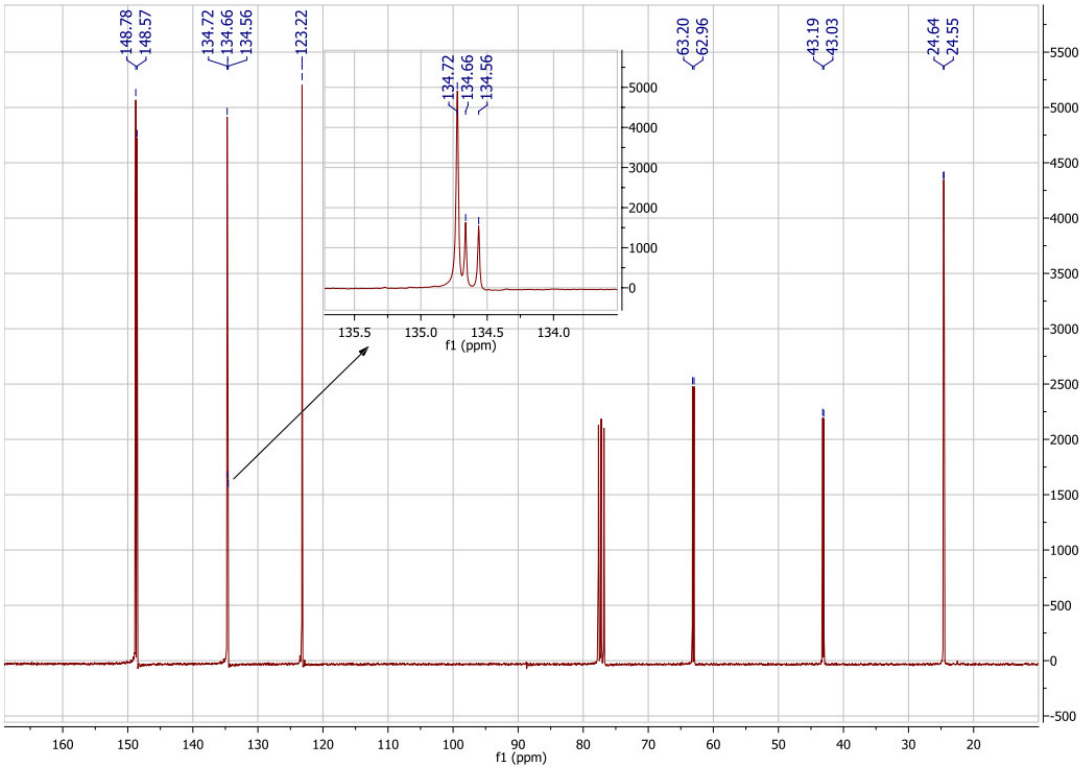

Figure 56. ^{13}C-NMR spectrum of bis(pyridyl)-*N*,*N*-diisopropylphosphoramidite (**51**) (300 MHz, $CHCl_3$).

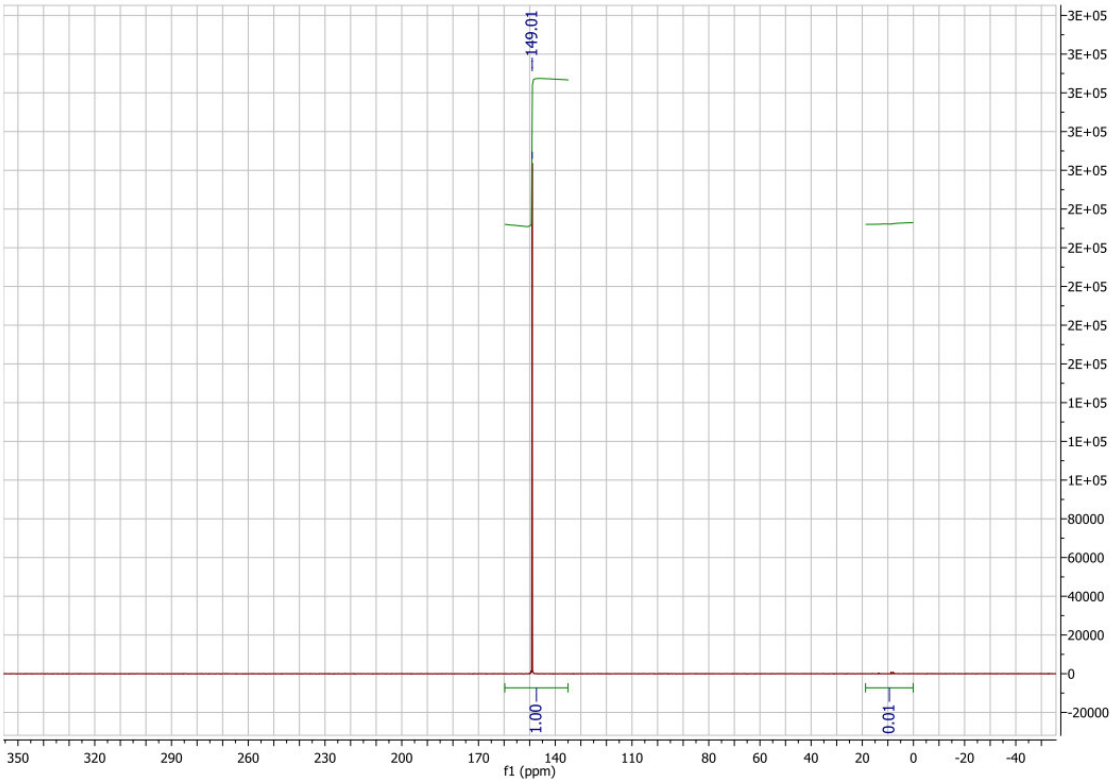

Figure 57. ^{31}P-NMR spectrum of bis(pyridyl)-*N*,*N*-diisopropylphosphoramidite (**51**) (300 MHz, $CHCl_3$).

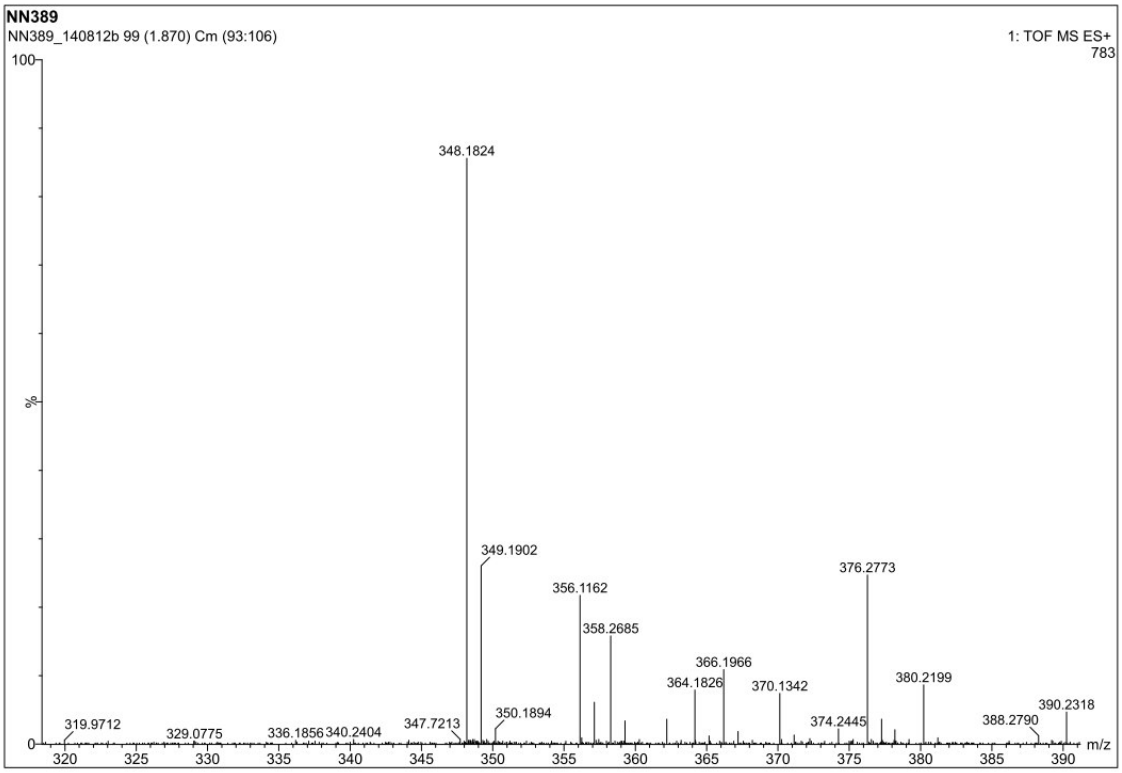

Figure 58. ESI-MS spectrum of bis(pyridyl)-*N*,*N*-diisopropylphosphoramidite (**51**).

Decyl bis(pyridin-3-ylmethyl) phosphite (**52**)

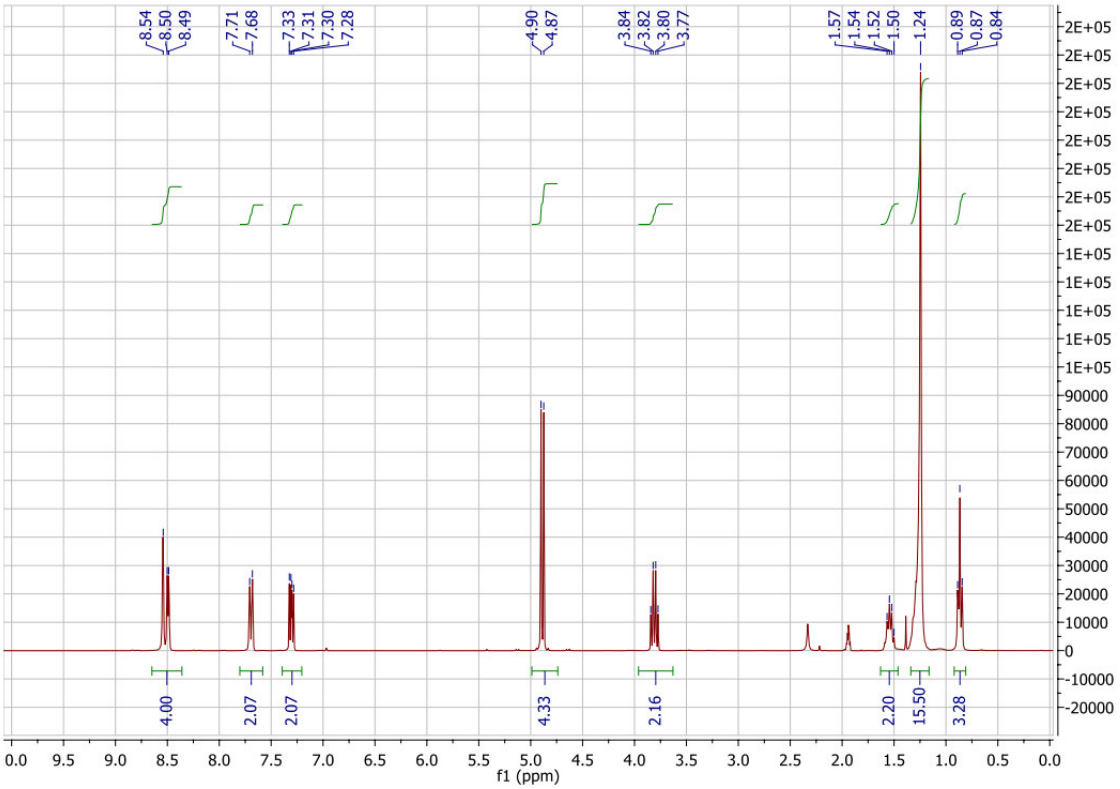

Figure 59. ^{1}H-NMR spectrum of decyl bis(pyridin-3-ylmethyl) phosphite (**52**) (300 MHz, CD_3CN).

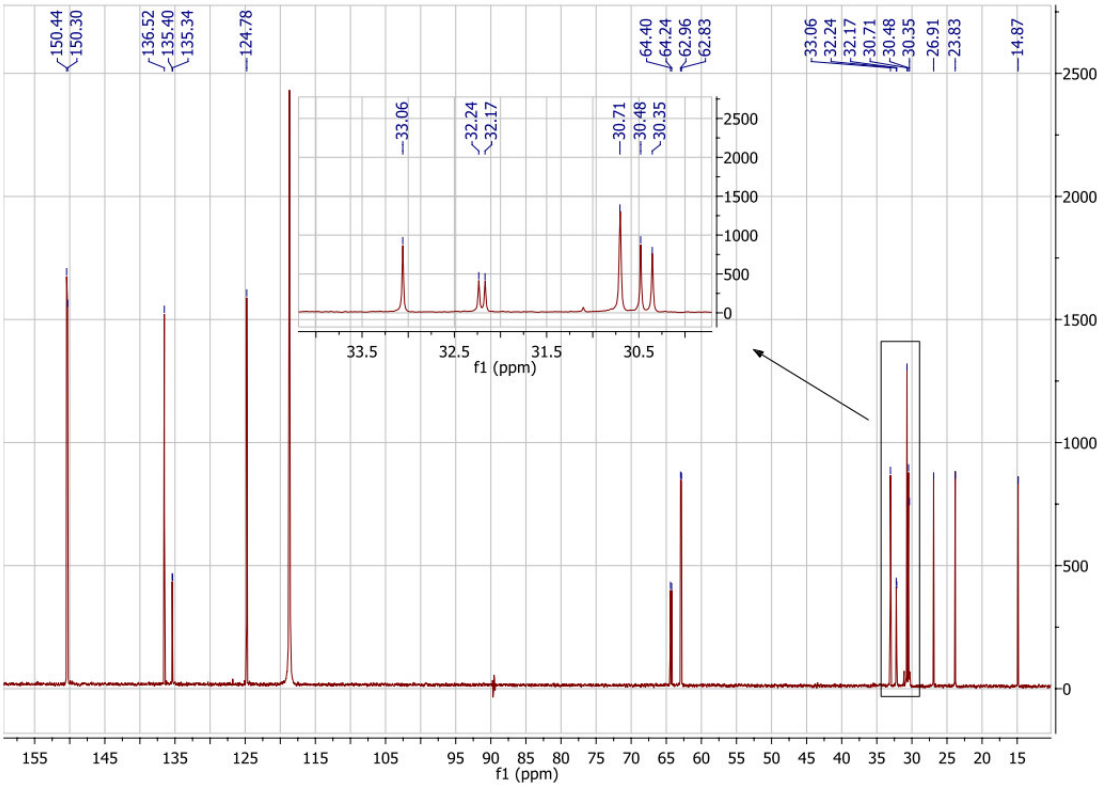

Figure 60. ^{13}C-NMR spectrum of decyl bis(pyridin-3-ylmethyl) phosphite (**52**) (300 MHz, CD_3CN).

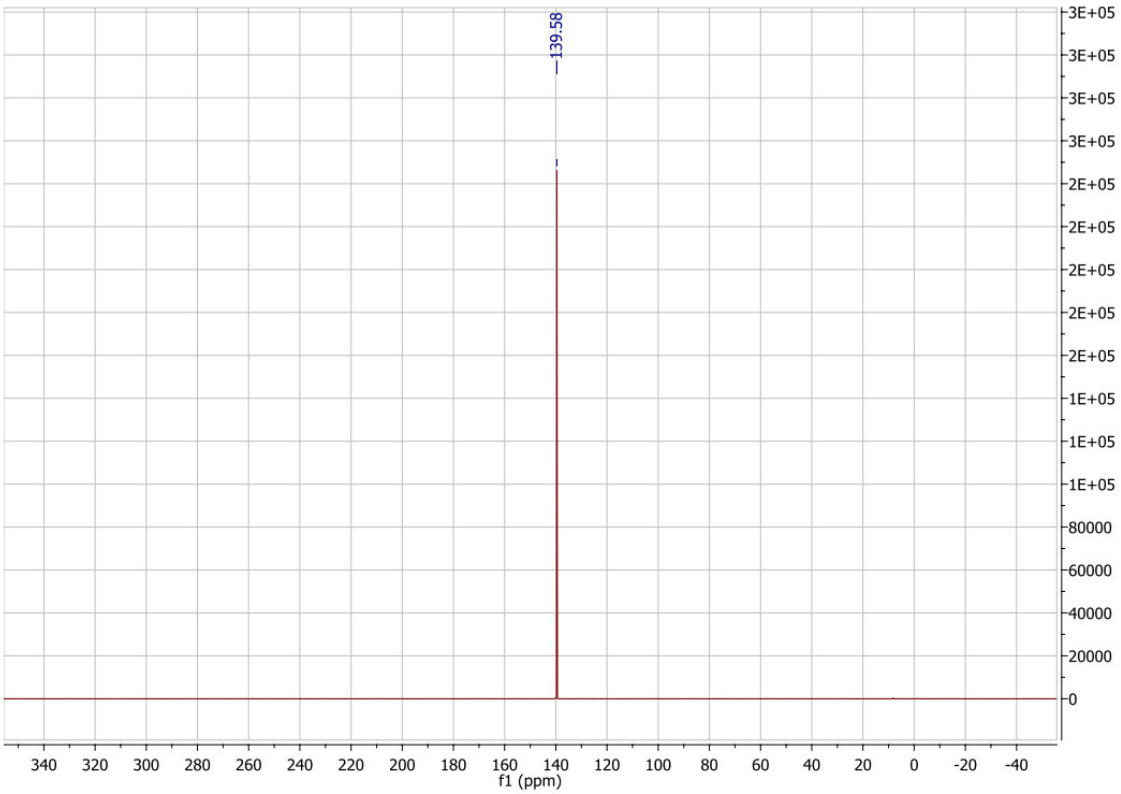

Figure 61. ^{31}P-NMR spectrum of decyl bis(pyridin-3-ylmethyl) phosphite (**52**) (300 MHz, CD_3CN).

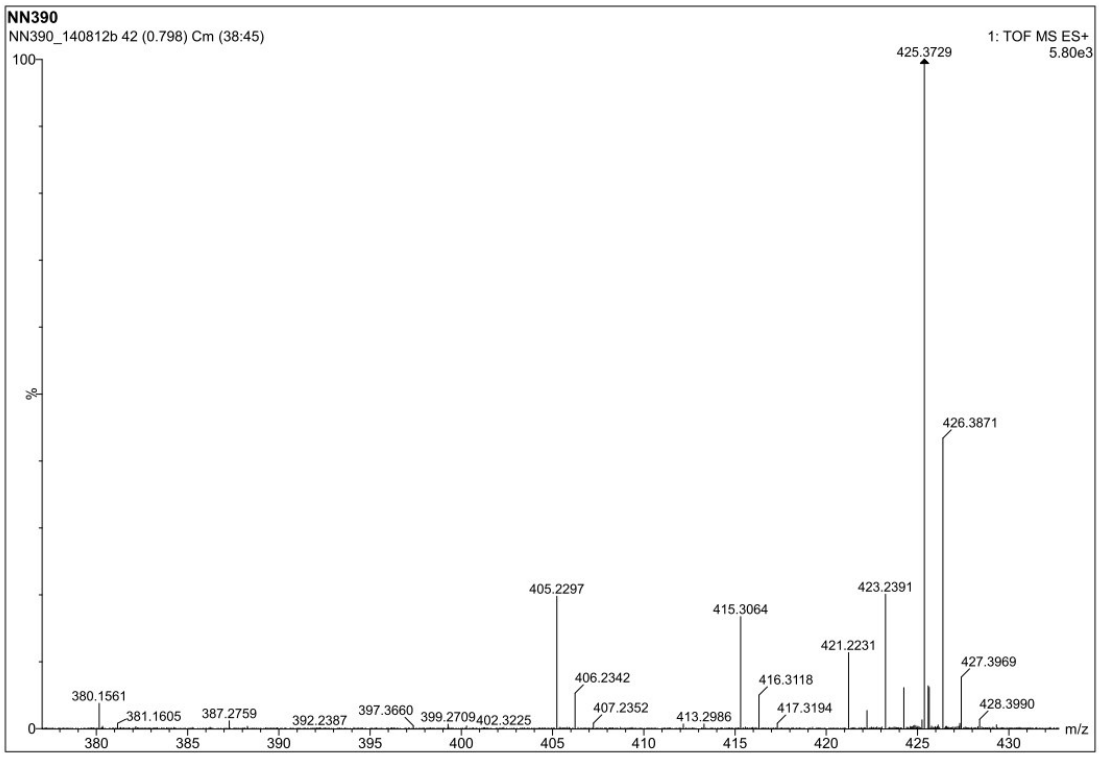

Figure 62. ESI-MS spectrum of decyl bis(pyridin-3-ylmethyl) phosphite (**52**).

Tetradecyl bis(pyridin-3-ylmethyl) phosphite (53)

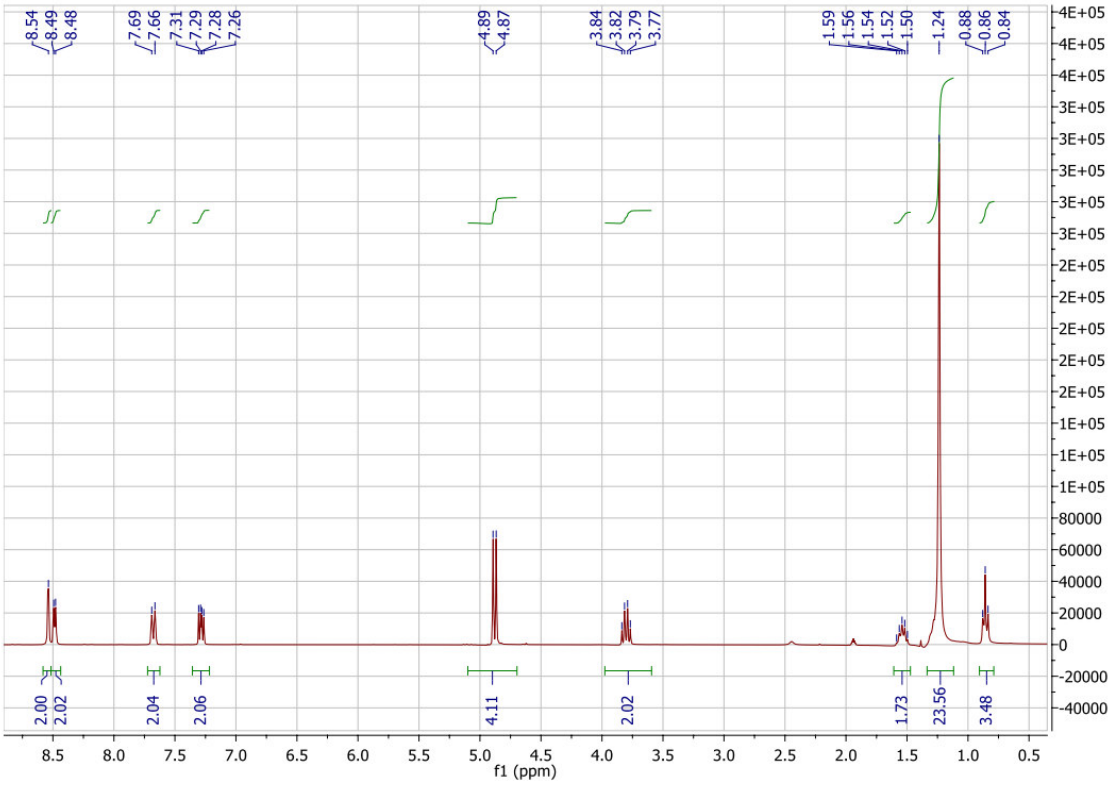

Figure 63. ^{1}H-NMR spectrum of tetradecyl bis(pyridin-3-ylmethyl) phosphite (**53**) (300 MHz, CD_3CN).

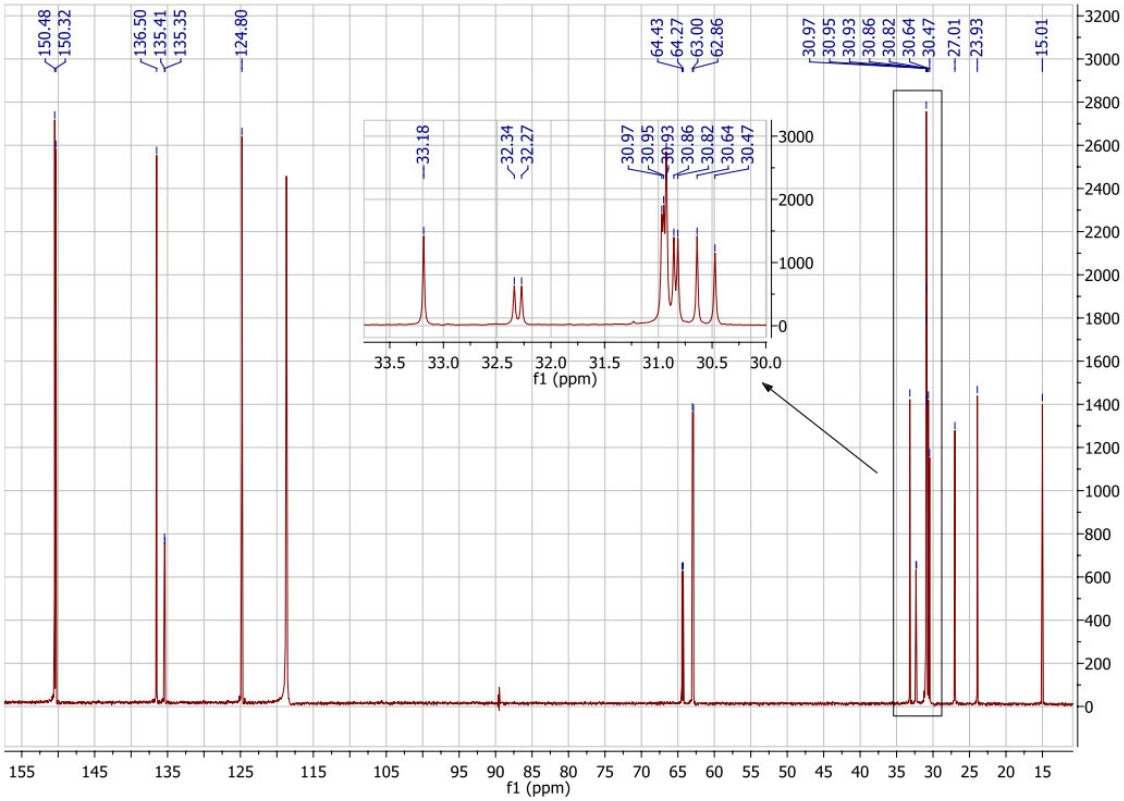

Figure 64. ^{13}C-NMR spectrum of tetradecyl bis(pyridin-3-ylmethyl) phosphite (**53**) (300 MHz, CD_3CN).

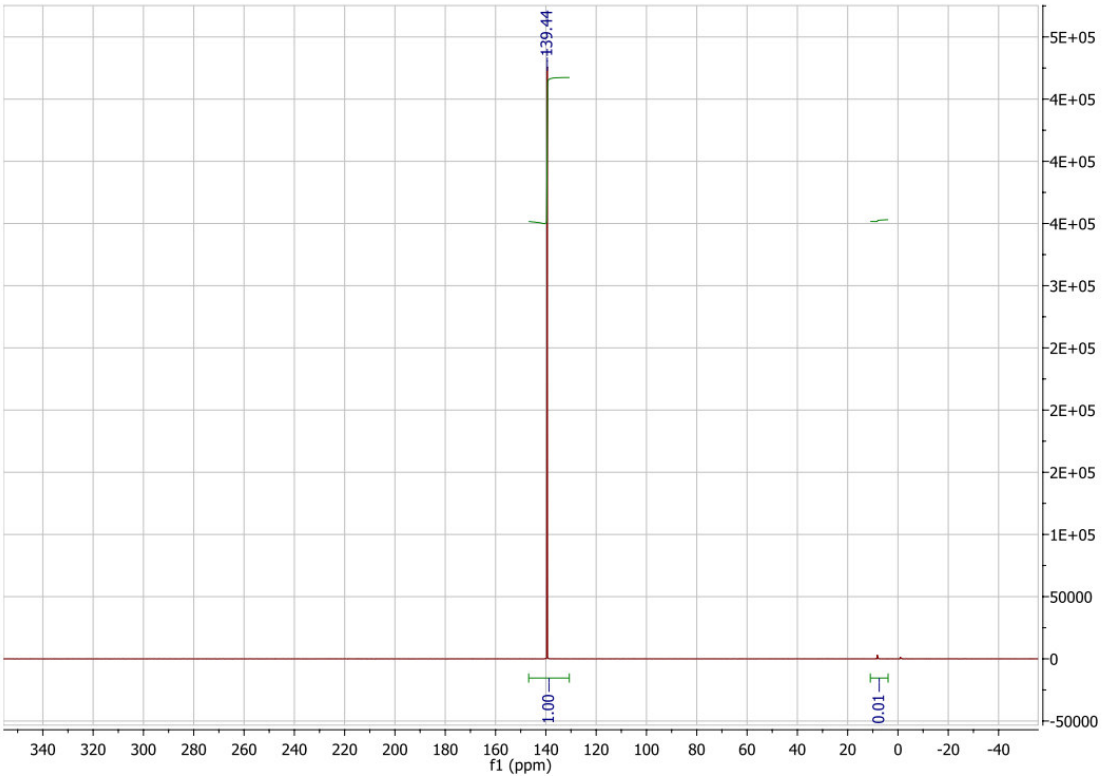

Figure 65. ^{31}P-NMR spectrum of tetradecyl bis(pyridin-3-ylmethyl) phosphite (**53**) (300 MHz, CD_3CN).

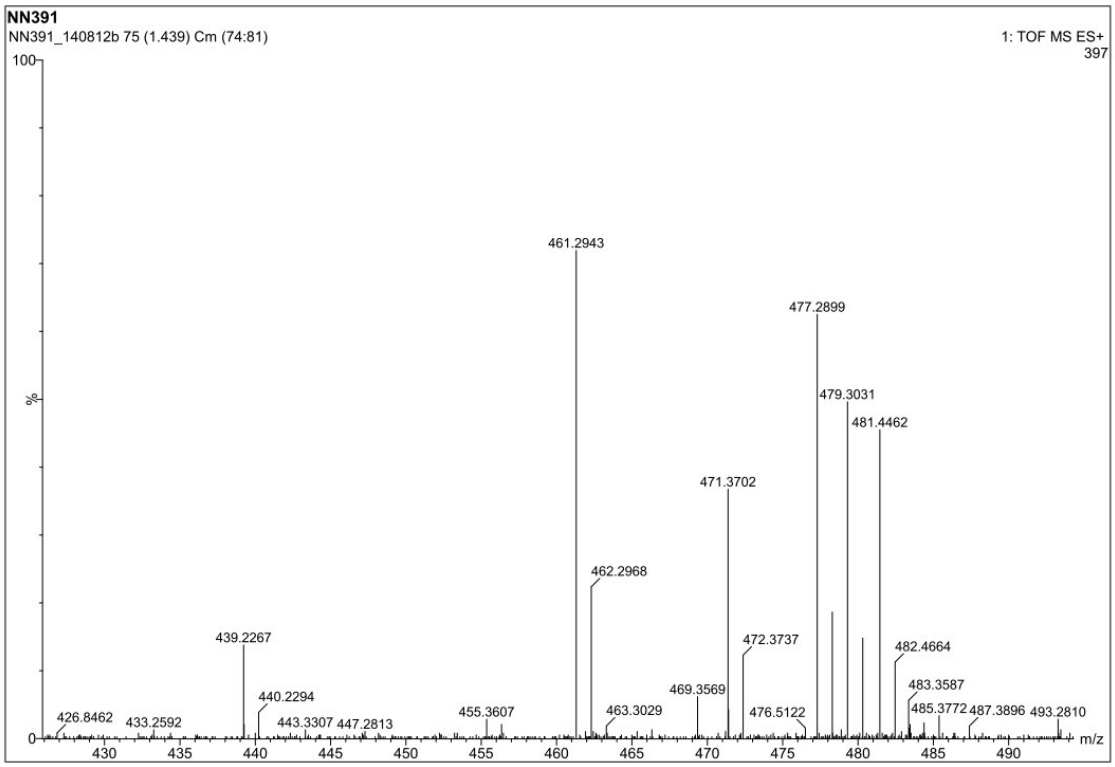

Figure 66. ESI-MS spectrum of tetradecyl bis(pyridin-3-ylmethyl) phosphite (**53**).

Octadecyl bis(pyridin-3-ylmethyl) phosphite (54)

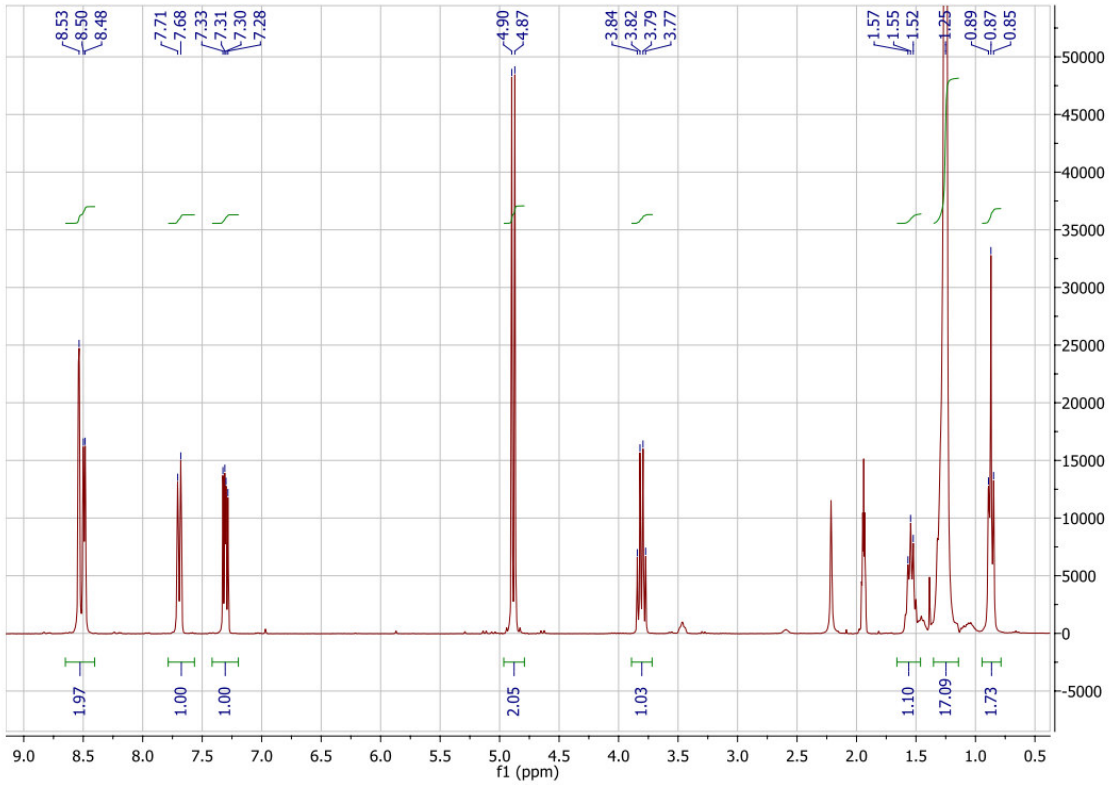

Figure 67. ^{1}H-NMR spectrum of octadecyl bis(pyridin-3-ylmethyl) phosphite (**54**) (300 MHz).

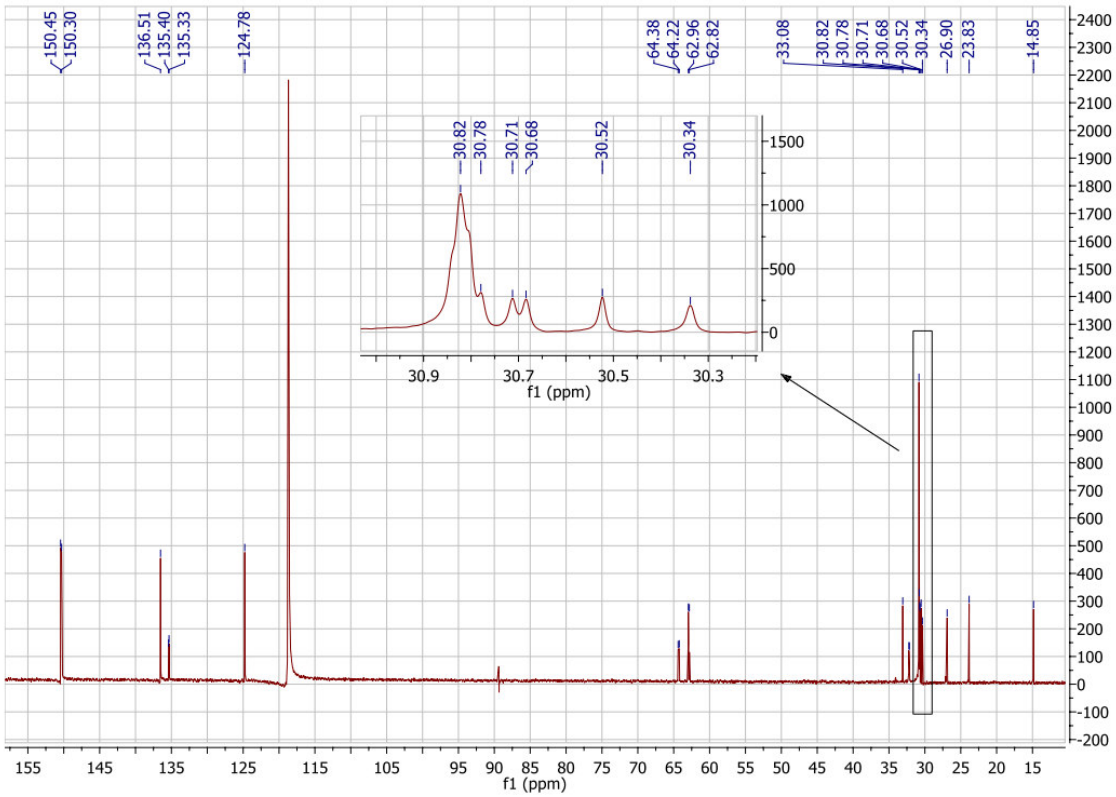

Figure 68. ^{13}C-NMR spectrum of octadecyl bis(pyridin-3-ylmethyl) phosphite (**54**) (300 MHz).

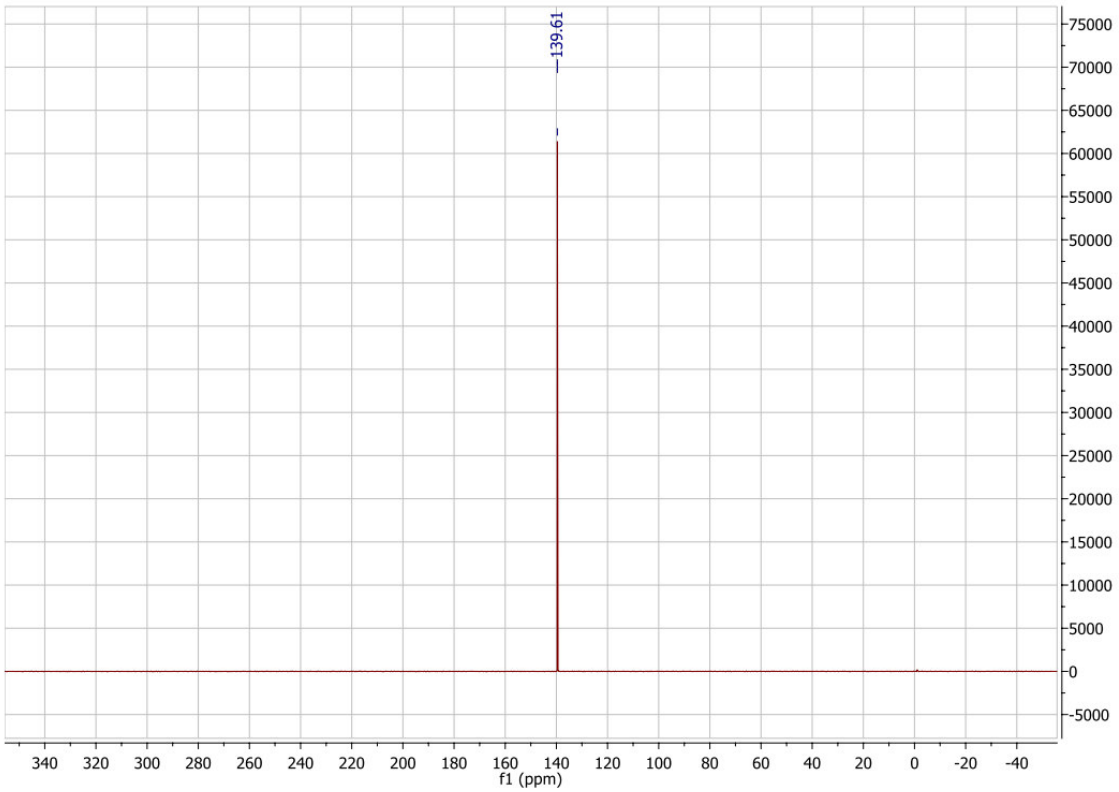

Figure 69. ^{31}P-NMR spectrum of octadecyl bis(pyridin-3-ylmethyl) phosphite (**54**) (300 MHz).

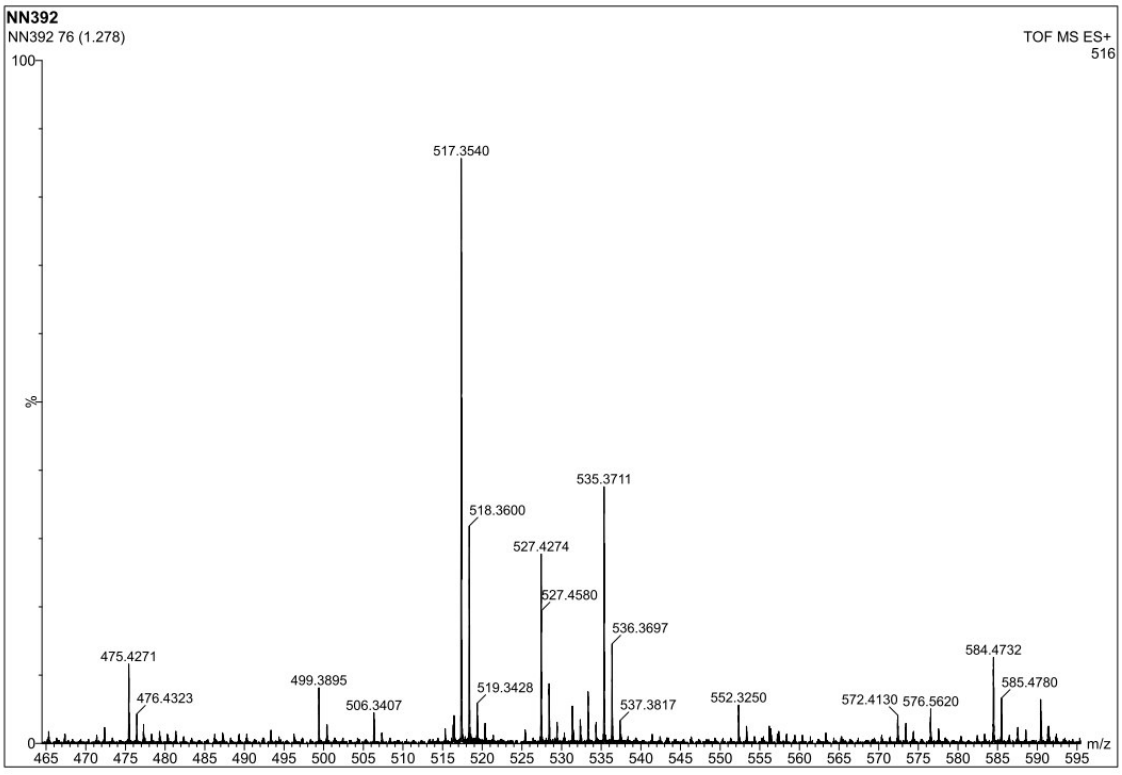

Figure 70. ESI-MS spectrum of octadecyl bis(pyridin-3-ylmethyl) phosphite (**54**).

Octadecyl bis(pyridin-3-ylmethyl) phosphite (56)

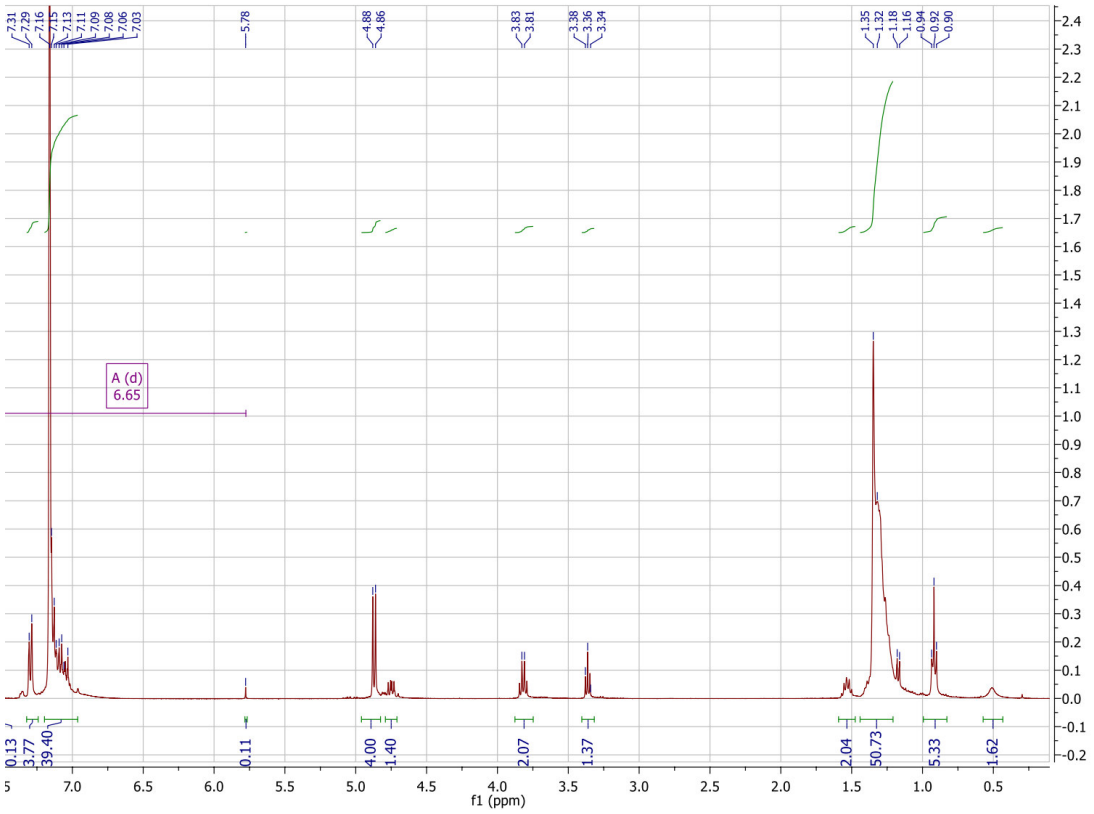

Figure 71. ^{1}H-NMR spectrum of octadecyl bis(benzyl) phosphite (**56**) (400 MHz).

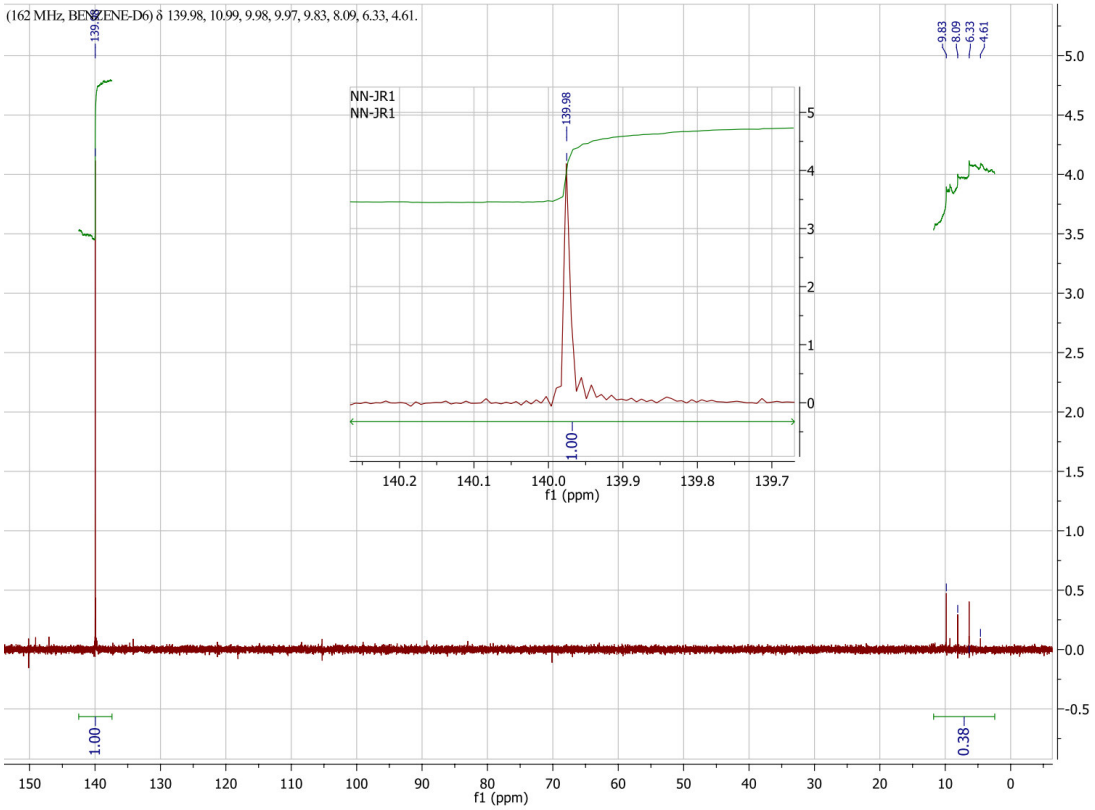

Figure 72. ^{31}P-NMR spectrum of octadecyl bis(benzyl) phosphite (**56**) (400 MHz).

8.2.2 Spectra of Mono-Lipidated EPS15-Peptides

azidobenzoic acetylated EPS15-peptide (61)

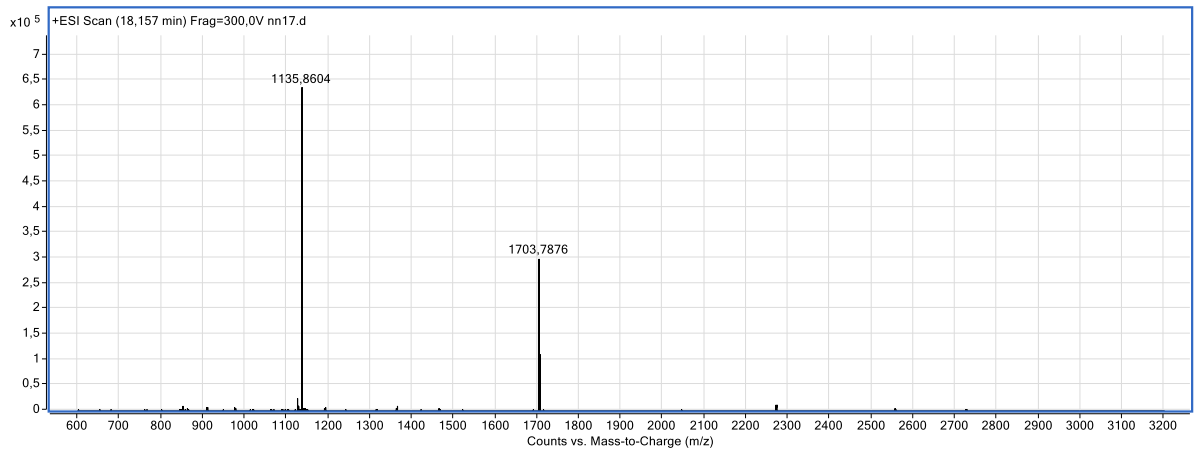

Figure 73. ESI-MS spectrum of azidobenzoic acetylated EPS15-peptide (**61**).

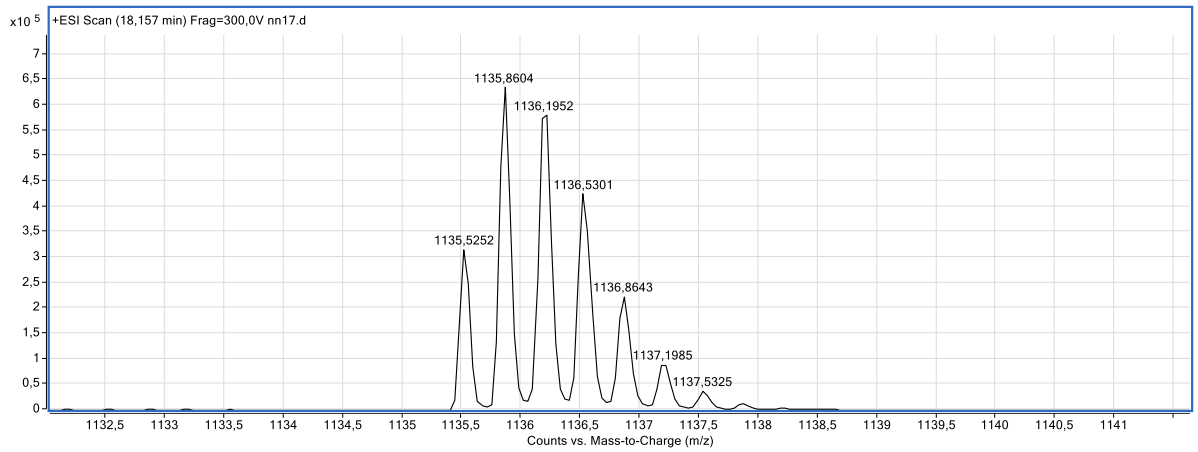

Figure 74. ESI-MS spectrum of azidobenzoic acetylated EPS15-peptide (**61**).

Decyl-pyridyl-phosphoramidate-EPS15-peptide (57)

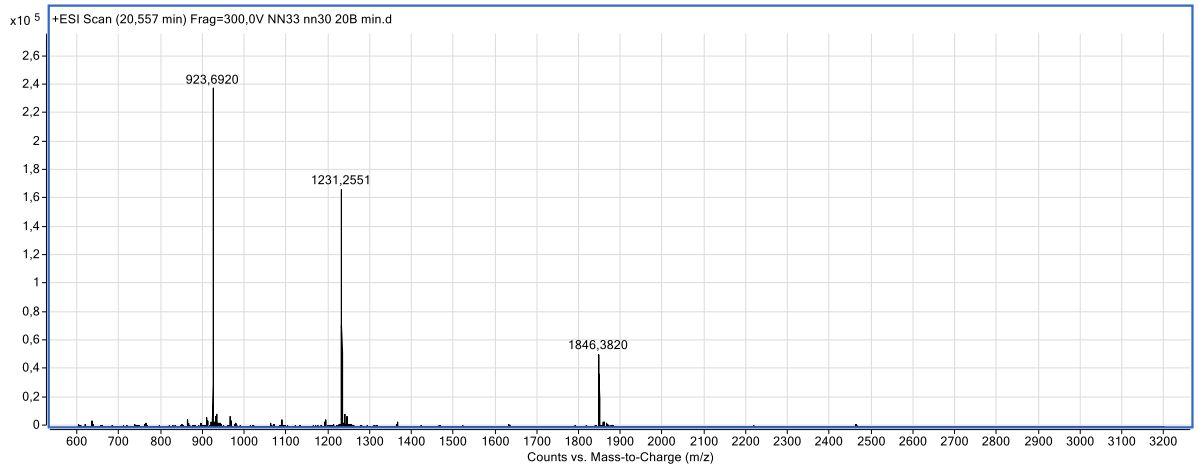

Figure 75. ESI-MS spectrum of decyl-pyridyl-phosphoramidate-EPS15-peptide (**57**).

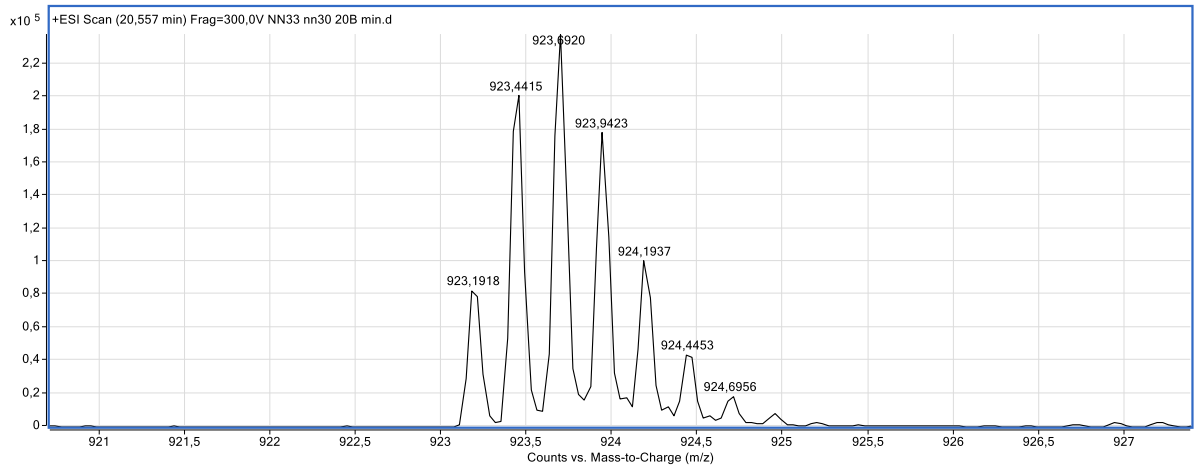

Figure 76. ESI-MS spectrum of decyl-pyridyl-phosphoramidate-EPS15-peptide (**57**).

Tetradecyl-pyridyl-phosphoramidate-EPS15-peptide (58)

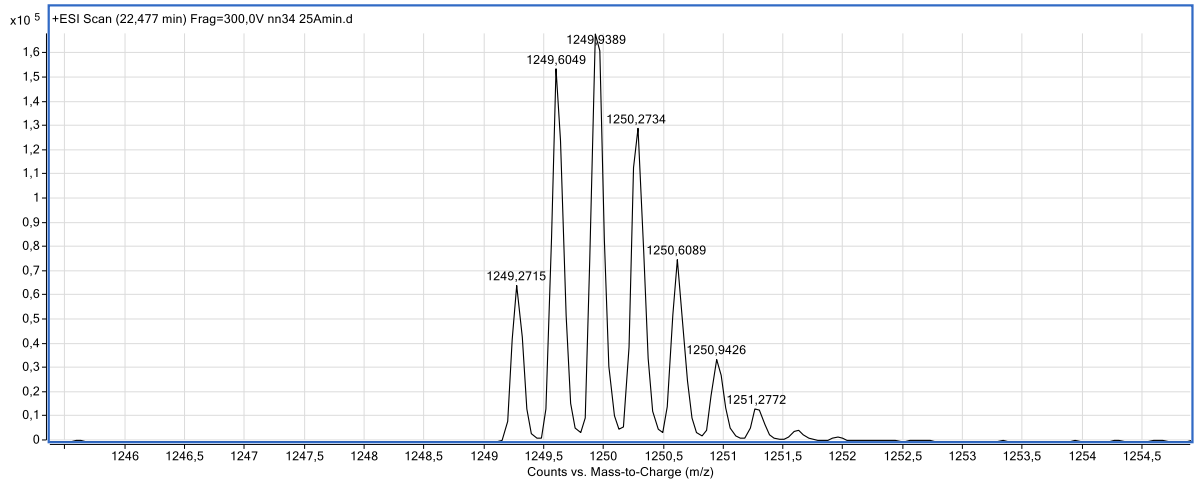

Figure 77. ESI-MS spectrum of Tetradecyl-pyridyl-phosphoramidate-EPS15-peptide (**58**).

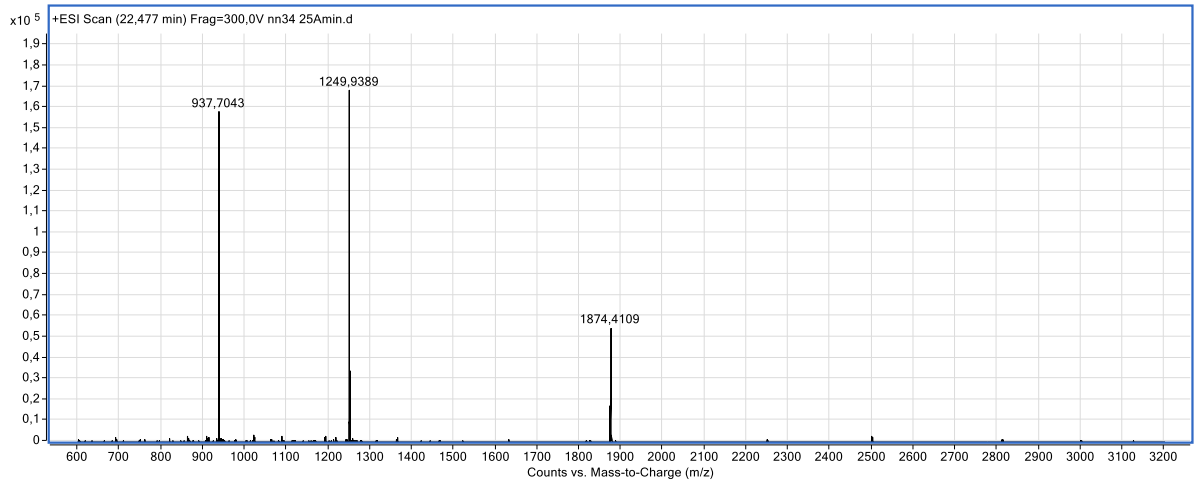

Figure 78. ESI-MS spectrum of Tetradecyl-pyridyl-phosphoramidate-EPS15-peptide (**58**).

Octadecyl-pyridyl-phosphoramidate-EPS15-peptide (**59**)

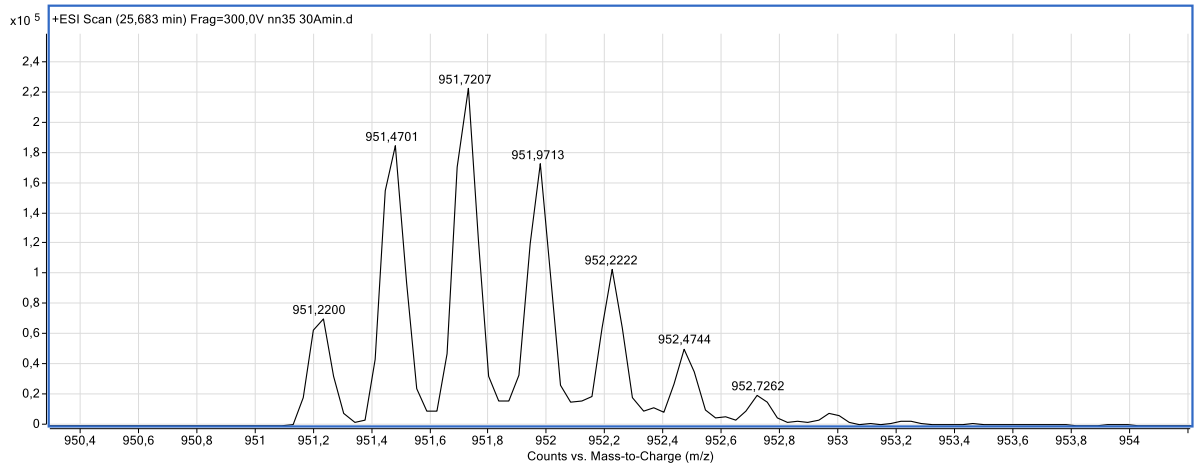

Figure 79. ESI-MS spectrum of octadecyl-pyridyl-phosphoramidate-EPS15-peptide (**59**).

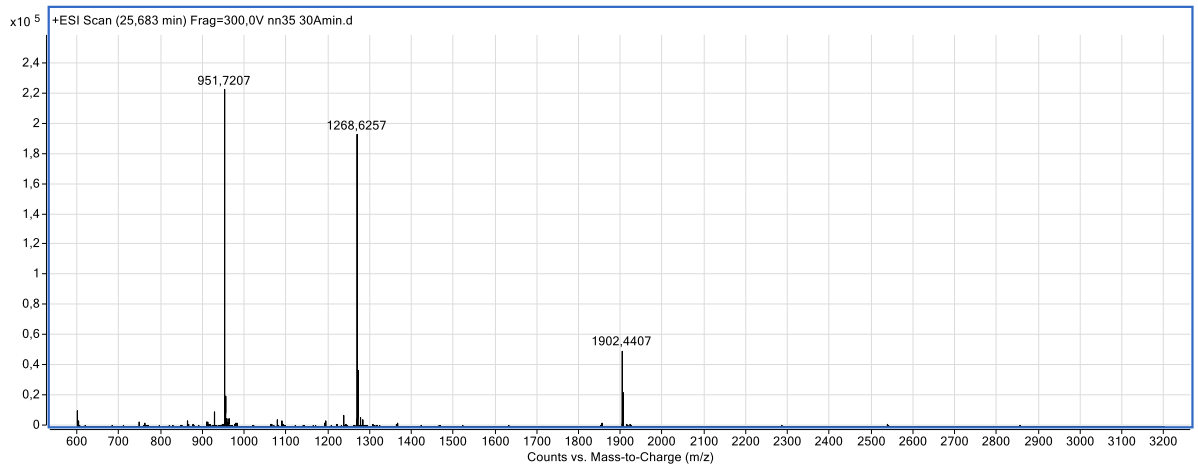

Figure 80. ESI-MS spectrum of octadecyl-pyridyl-phosphoramidate-EPS15-peptide (**59**).

Octadecyl-benzyl-phosphoramidate-EPS15-peptide (**62**)

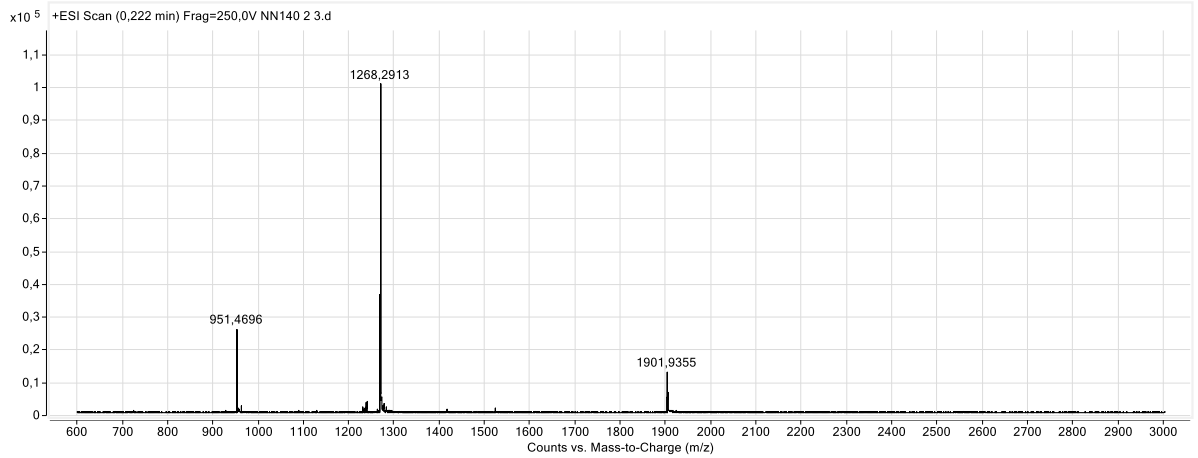

Figure 81. ESI-MS spectrum of octadecyl-benzyl-phosphoramidate-EPS15-peptide (**62**).

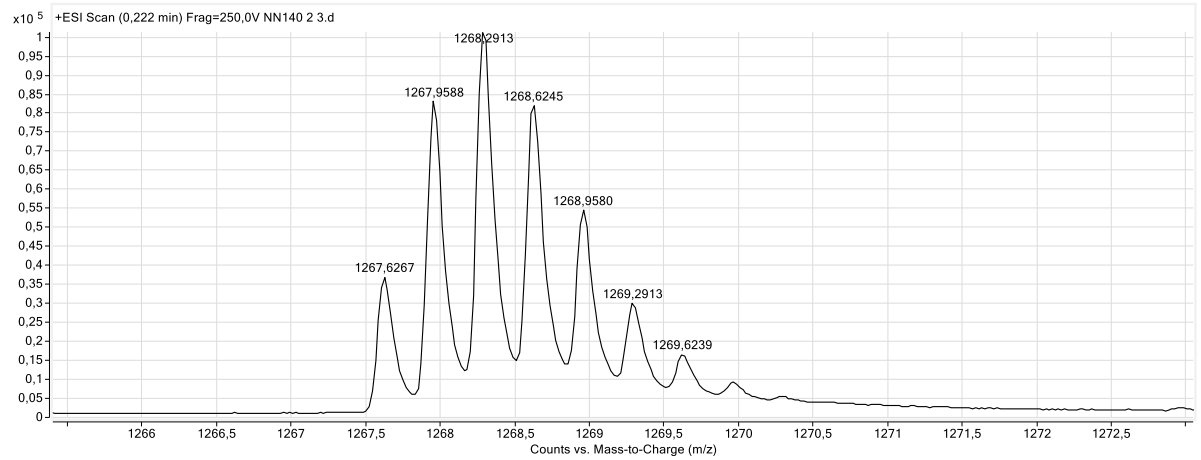

Figure 82. ESI-MS spectrum of octadecyl-benzyl-phosphoramidate-EPS15-peptide (**62**).

8.2.3 Spectra of Fluorescein-Labelled EPS15-Peptides

Fluorescein labelled octadecyl-pyridyl-phosphoramidate-EPS15-peptide (63)

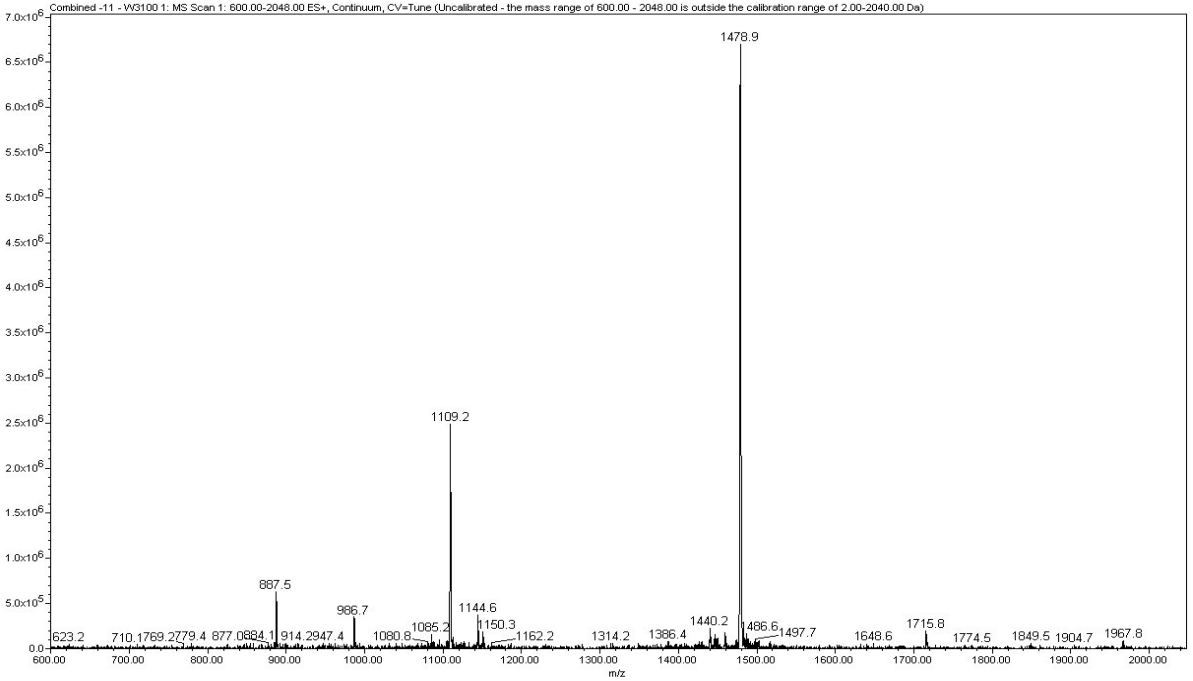

Figure 83. ESI-MS spectrum of fluorescein labelled octadecyl-pyridyl-phosphoramidate-EPS15-peptide (**63**).

Stearic acid coupled EPS15-azidopeptide (**64**)

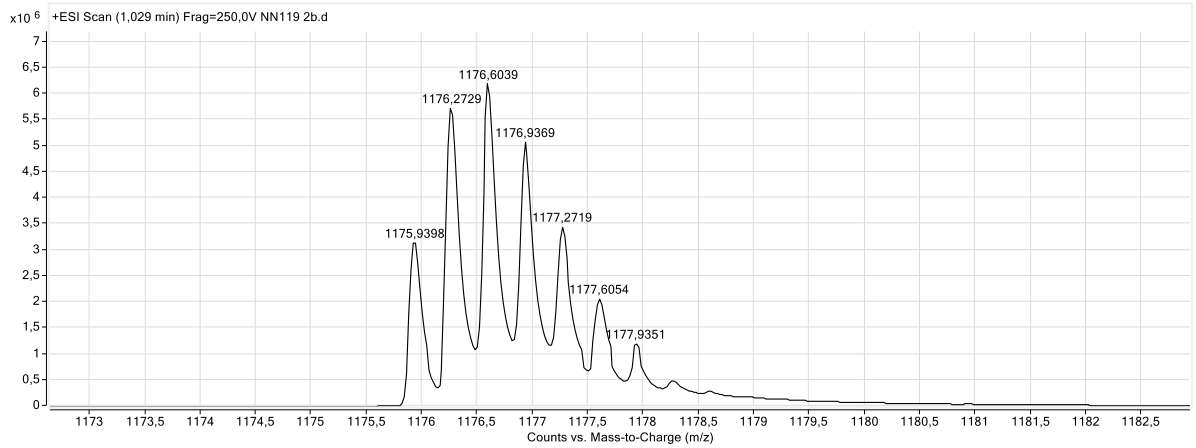

Figure 84. ESI-MS spectrum of stearic acid coupled EPS15-azidopeptide (**64**).

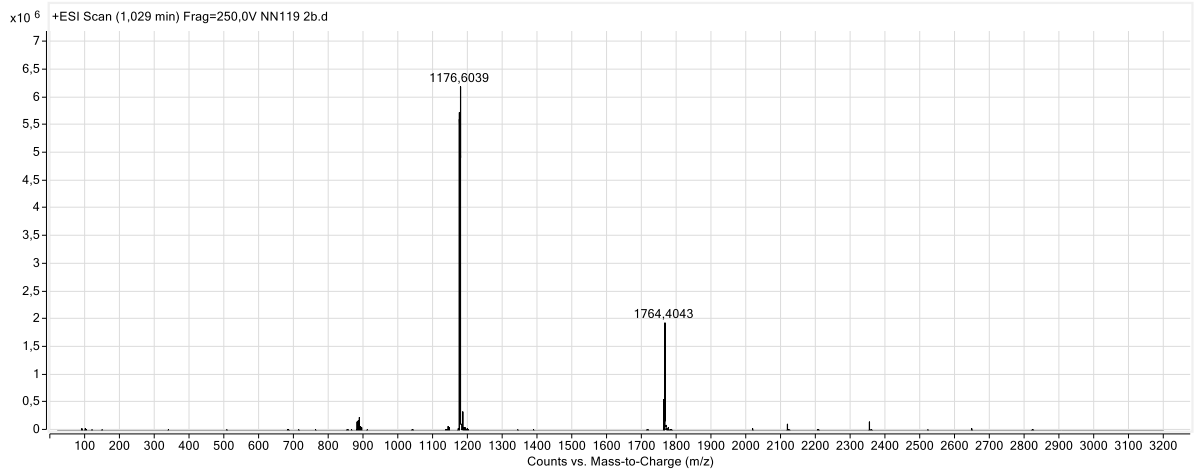

Figure 85. ESI-MS spectrum of stearic acid coupled EPS15-azidopeptide (**64**).

Fluorescein labelled stearic acid coupled EPS15-peptide (**65**)

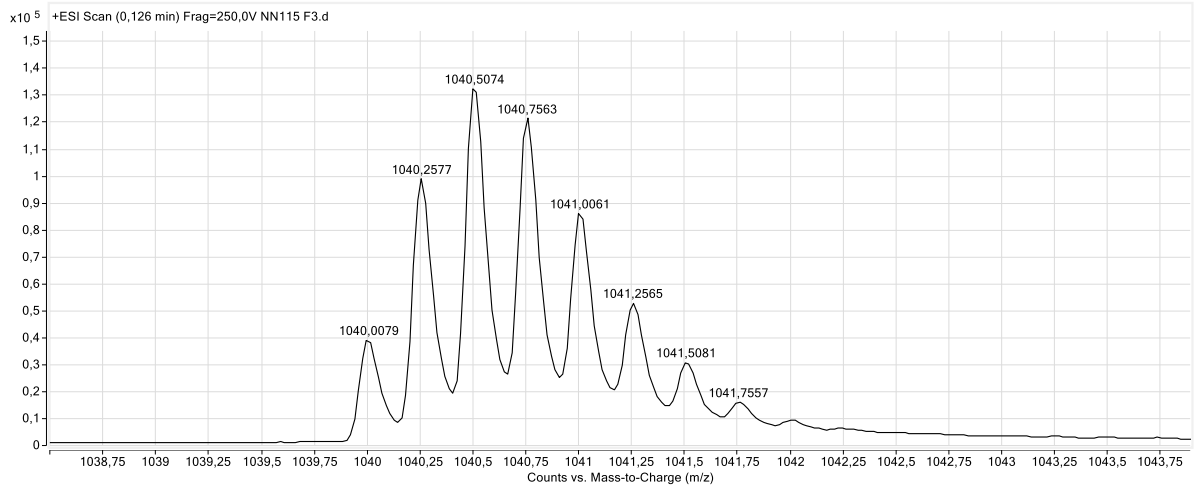

Figure 86. ESI-MS spectrum of fluorescein labelled stearic acid coupled EPS15-peptide (**65**).

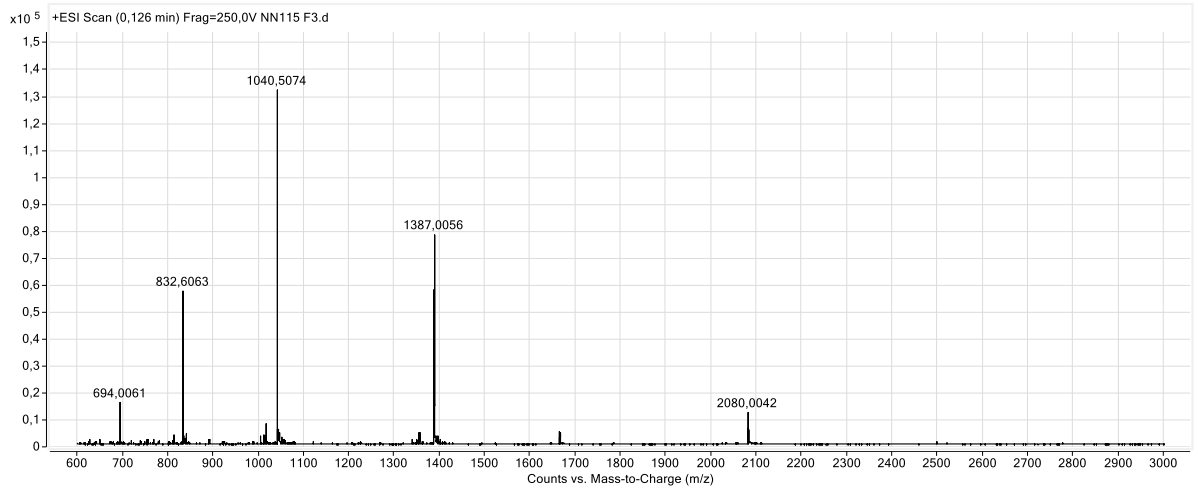

Figure 87. ESI-MS spectrum of fluorescein labelled stearic acid coupled EPS15-peptide (**65**).

8.2.4 Spectra of Bis-Lipidated EPS15-Peptides

Bis(decyl)-phosphoramidate-EPS15-peptide (66)

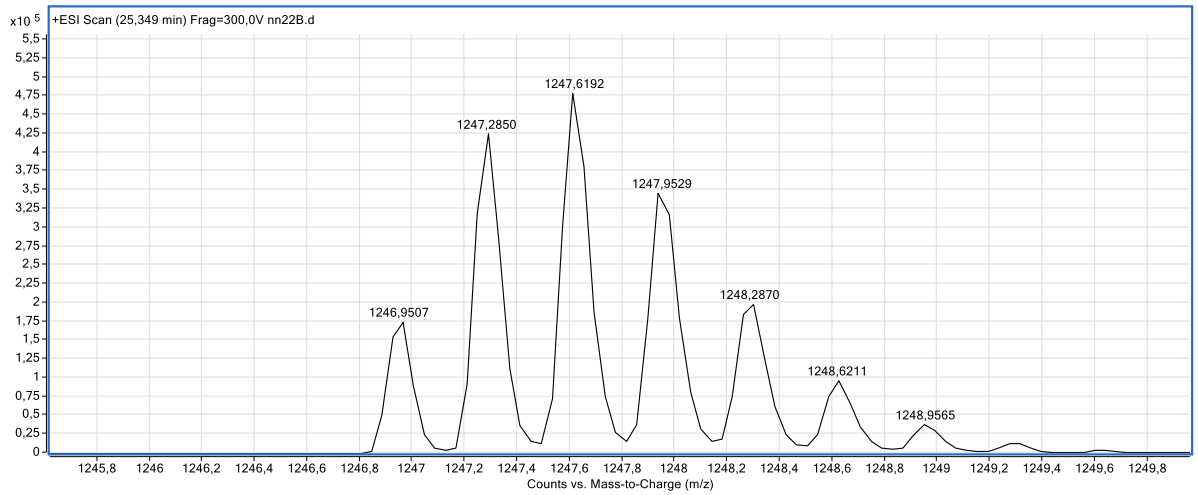

Figure 88. ESI-MS spectrum of bis(decyl)-phosphoramidate-EPS15-peptide (**66**).

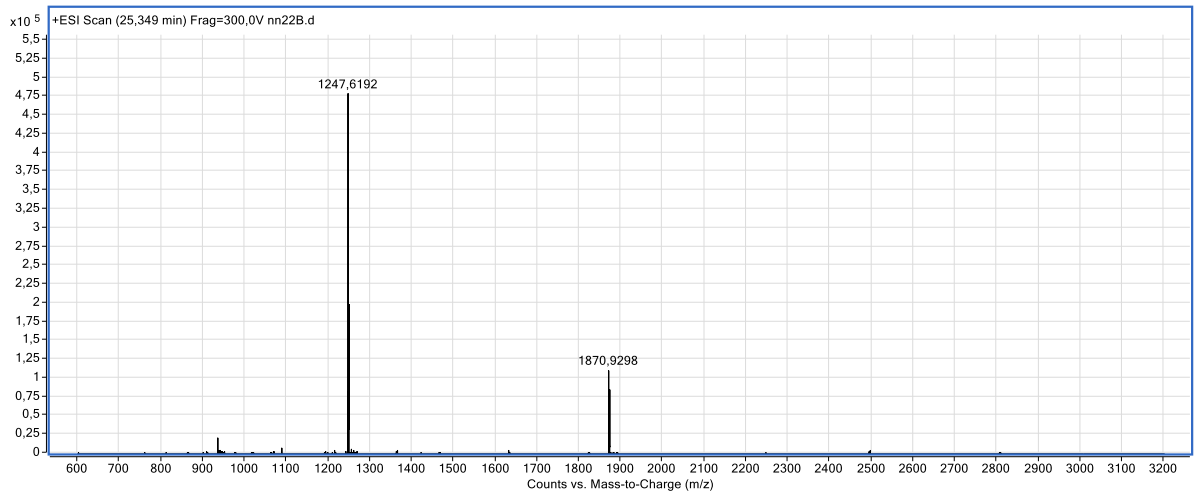

Figure 89. ESI-MS spectrum of bis(decyl)-phosphoramidate-EPS15-peptide (**66**).

Bis(tetradecyl)-phosphoramidate-EPS15-peptide (**67**)

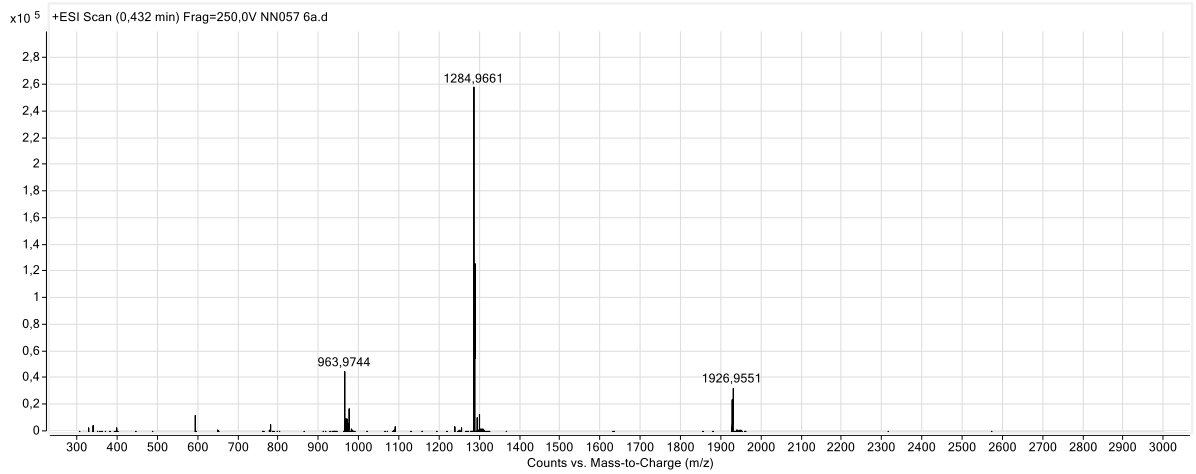

Figure 90. ESI-MS spectrum of bis(tetradecyl)-phosphoramidate-EPS15-peptide (**67**).

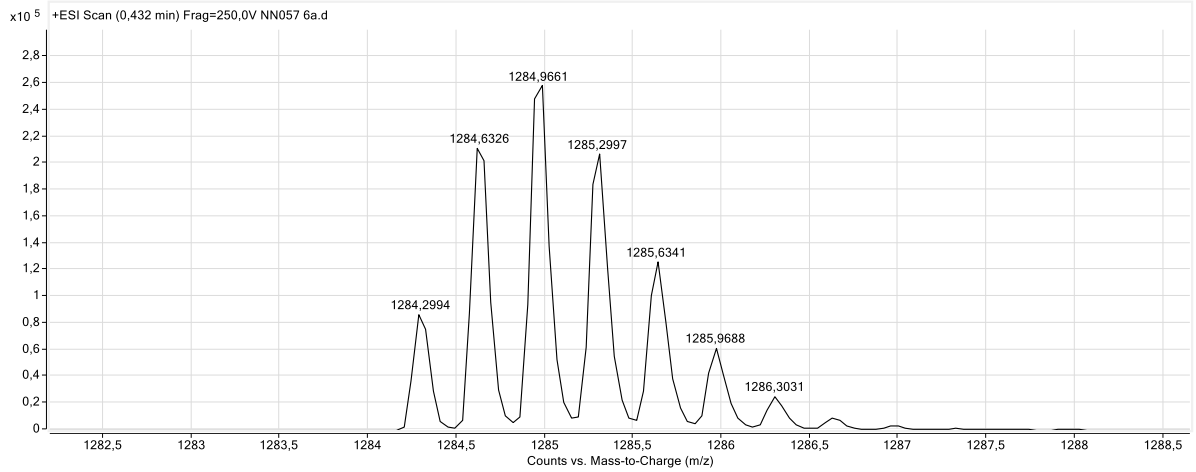

Figure 91. ESI-MS spectrum of bis(tetradecyl)-phosphoramidate-EPS15-peptide (**67**).

8.2.5 Spectra of Bivalent Peptides

Octadecyl-pyridyl-phosphoramidate bivalent FEDNFVPG peptide (69)

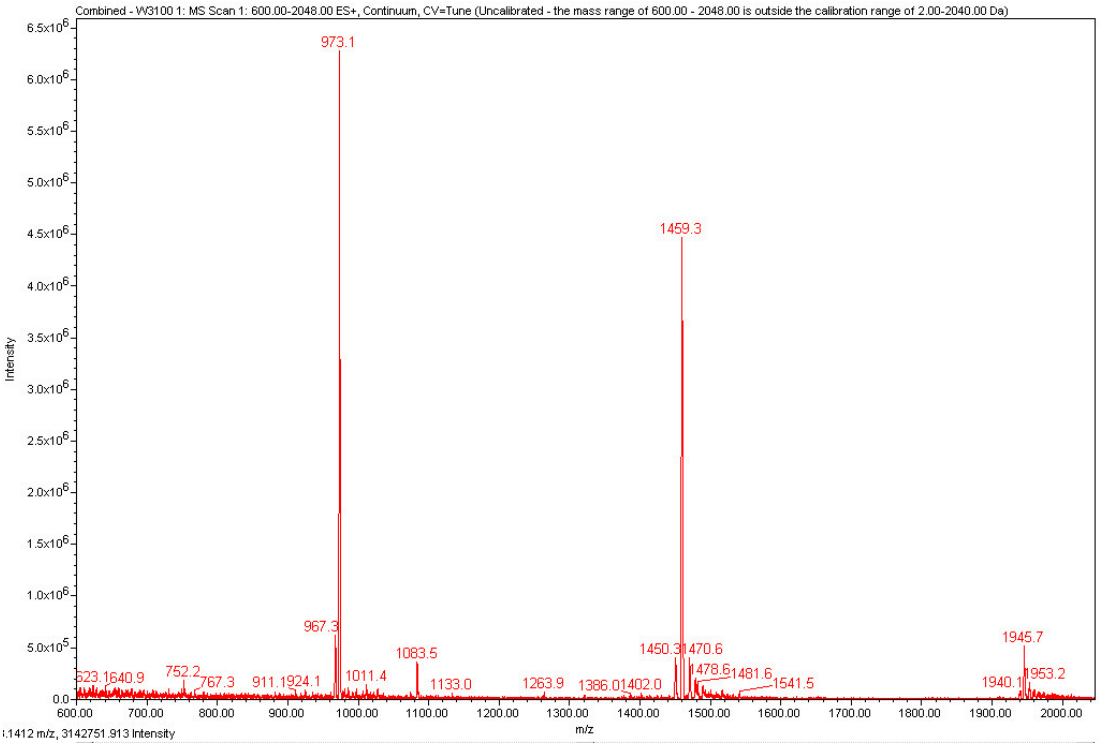

Figure 92. ESI-MS spectrum of octadecyl-pyridyl-phosphoramidate bivalent FEDNFVPG peptide (**69**).

Octadecyl-pyridyl-phosphoramidate bivalent INFFEDNFVPEIG peptide (70)

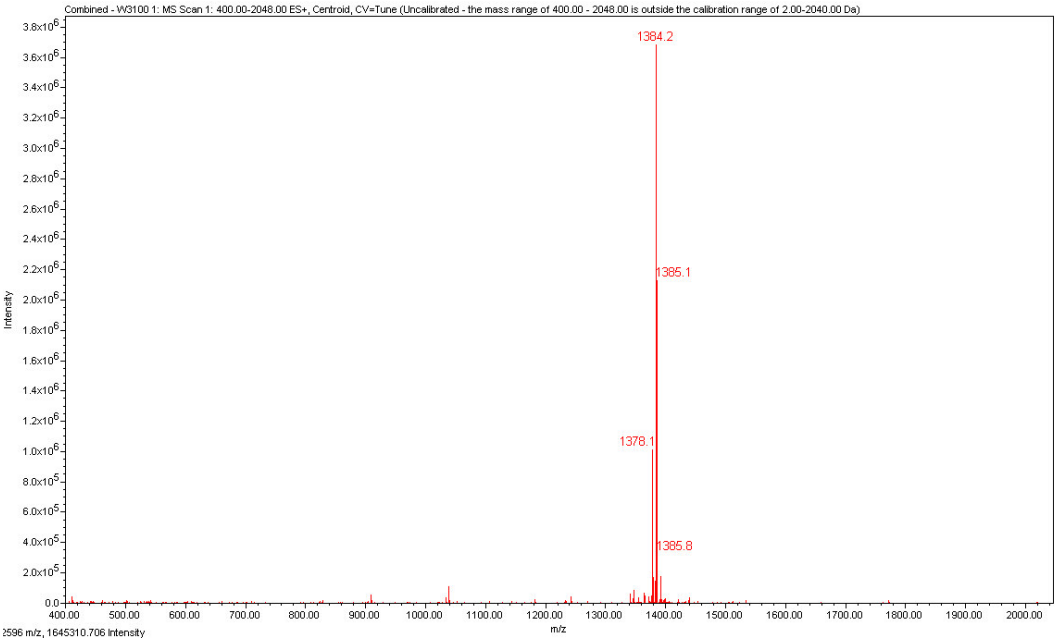

Figure 93. ESI-MS spectrum of octadecyl-pyridyl-phosphoramidate bivalent INFFEDNFVPEIG peptide (**70**).

8.3 Covalent Attachment of Cyclic TAT Peptides to GFP

Peptide with PEGlinker and Azidoglycine (**71**)

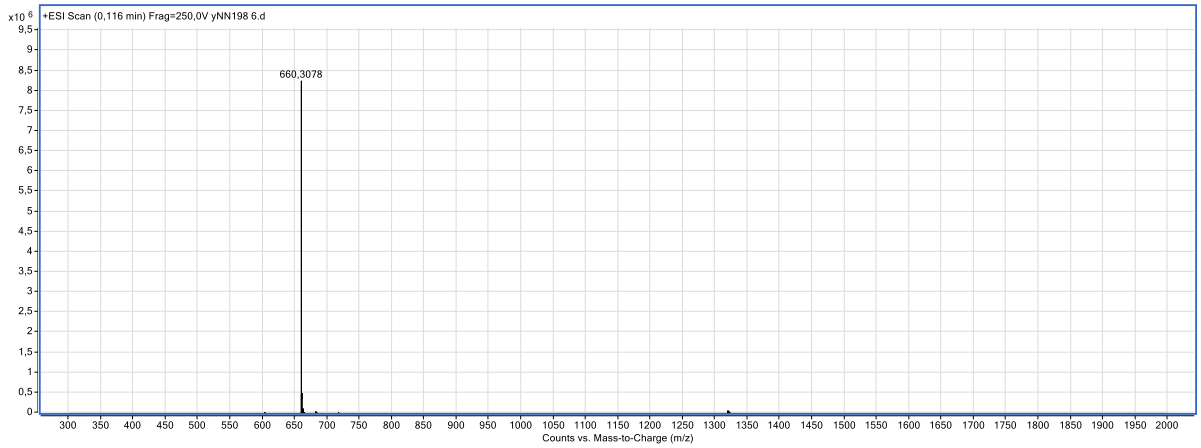

Figure 94. ESI-MS spectrum of peptide with PEGlinker and azidoglycine (**71**).

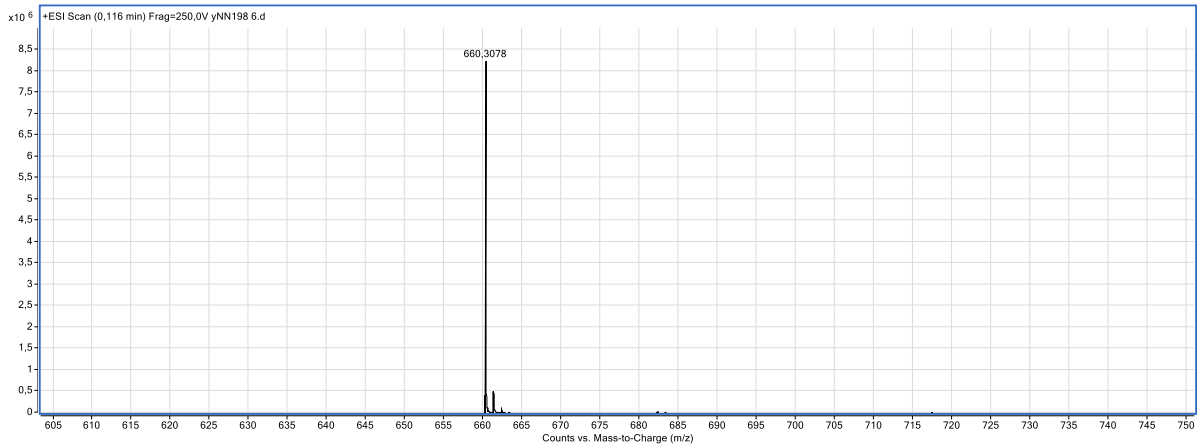

Figure 95. ESI-MS spectrum of peptide with PEGlinker and azidoglycine (**71**).

Peptide with PEGlinker and *para*-Azidobenzoic acid (**72**)

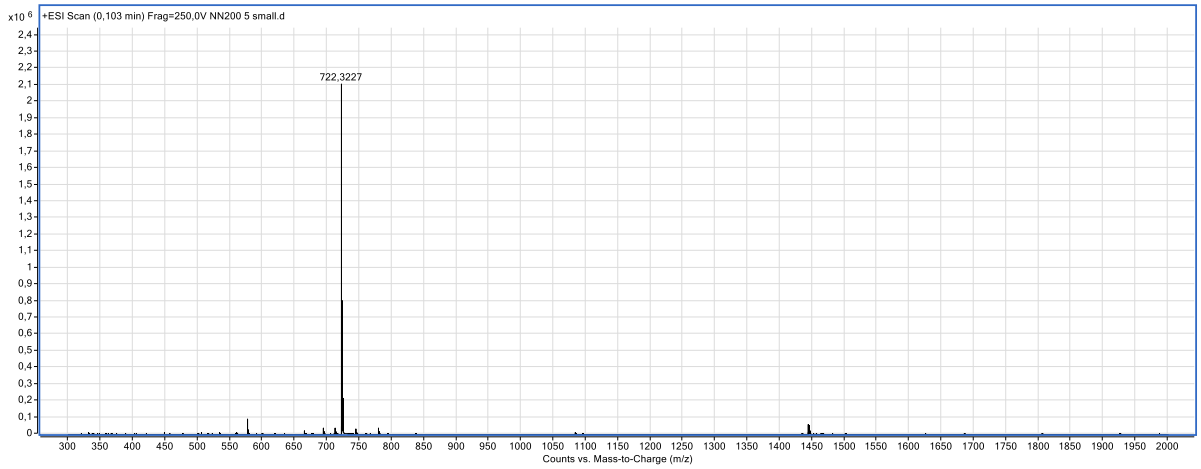

Figure 96. ESI-MS spectrum of peptide with PEGlinker and *para*-azidobenzoic acid (**72**).

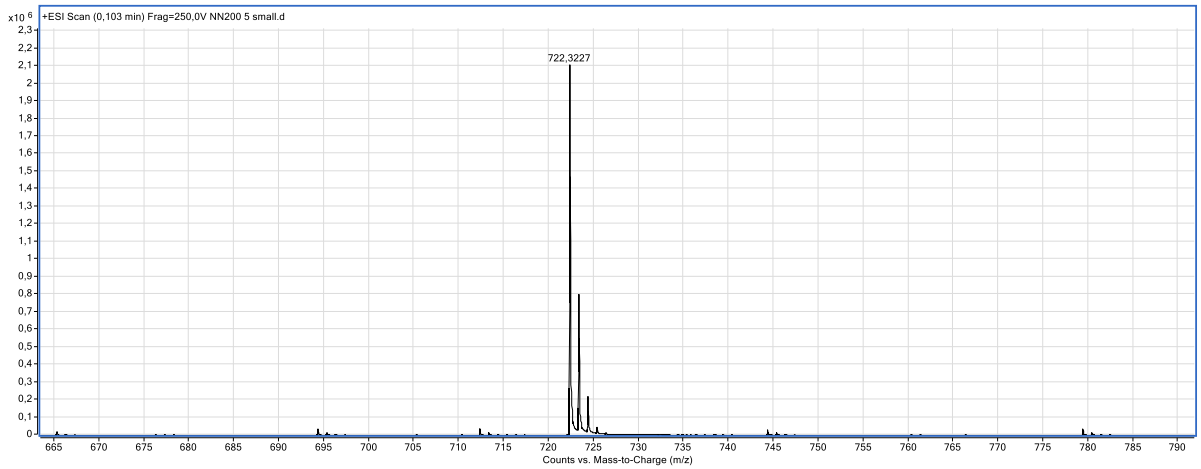

Figure 97. ESI-MS spectrum of peptide with PEGlinker and *para*-azidobenzoic acid (**72**).

9 CURRICULUM VITAE

Der Lebenslauf ist in der Online-Version aus Gründen des Datenschutzes nicht enthalten.